

University of Southampton Research Repository ePrints Soton

Copyright © and Moral Rights for this thesis are retained by the author and/or other copyright owners. A copy can be downloaded for personal non-commercial research or study, without prior permission or charge. This thesis cannot be reproduced or quoted extensively from without first obtaining permission in writing from the copyright holder/s. The content must not be changed in any way or sold commercially in any format or medium without the formal permission of the copyright holders.

When referring to this work, full bibliographic details including the author, title, awarding institution and date of the thesis must be given e.g.

AUTHOR (year of submission) "Full thesis title", University of Southampton, name of the University School or Department, PhD Thesis, pagination

UNIVERSITY OF SOUTHAMPTON

FACULTY OF ENGINEERING AND THE ENVIRONMENT

Civil and Environmental Engineering

Understanding Defence Failures and Coastal Flood Events: a Case Study Approach

by

Matthew Wadey

Thesis submitted for the degree of Doctor of Philosophy

October 2013

UNIVERSITY OF SOUTHAMPTON

UNIVERSITY OF SOUTHAMPTON

ABSTRACT

FACULTY OF ENGINEERING AND THE ENVIRONMENT

Civil and Environmental Engineering

Doctor of Philosophy

**UNDERSTANDING DEFENCE FAILURES AND COASTAL FLOOD EVENTS: A CASE
STUDY APPROACH**

By Matthew Wadey

Extreme sea level events are a current global threat, whilst sea-level rise (SLR) and climate change over the 21st century will increase the frequency and severity of flooding in most coastal regions. Numerical model simulations can help to understand and predict coastal floods (e.g. flood mapping and forecasting) but in comparison to flood sources (waves and water levels) coastal flood pathways (defence failures and inundation) are presently less integrated within these models. This thesis develops and demonstrates a methodology to rapidly simulate and understand the consequences of coastal flood events, with an emphasis upon regions where the risks of flooding are not well understood and could change quickly with SLR. The Solent on the south coast of England is the case study, and is prone to frequent flooding. This region is currently differentiated from the UK east and west coasts by experiencing smaller storm surges, and is characterised by undefended sections of shoreline and small floodplains. Within the Solent is Portsmouth, a city of national flood significance (only London and Hull contain more people considered at risk of coastal flooding in the UK). However, life threatening floods have not occurred in living memory. An integrated modelling approach is developed, coupling loads and defence failures with two-dimensional simulations of floodplain inundation. Observations collated from a real storm surge and flood event are shown to generate a validation data set, which indicates that this model can predict floodplain water levels to a good level of accuracy, whilst highlighting implications of such data collection. Solent-wide analysis includes simulations of hypothetical coastal flood events based upon scenarios that cover the full range of coastal loadings (realistic waves and water levels) and defence failures (overflow, outflanking, overtopping and breaching). More detailed case-studies are also applied at two sites within the region (including Portsmouth). This analysis generates peak flood water depths and an overview of impacts across this spectrum of possible floods.

This research improves the existing knowledge of coastal flooding in the case study, and highlights a number of generic concepts that should be applied to others. For example the combination of flood simulation methods with real flood event analysis is essential for optimising the interpretation of model outputs whilst supporting inferences about flood consequences associated with extreme loading events (including how these may change with SLR). Simple methods estimated that >24,000 properties are within a 1 in 200 year flood event outline; and incorporating defence failures, flood dynamics, validation and detailed case studies substantially refine the assessment of places likely to experience damages. Breach defence failures generate the worst flood impacts, although in the Solent this failure mechanism is presently less of a threat than outflanking, overflow and wave overtopping. The modelling system includes easily interpreted outputs, whilst being computationally fast; therefore with potential applications including supporting land-use and defence planning, and real-time flood forecasting and warning.

Contents

LIST OF FIGURES	7
LIST OF TABLES	8
DECLARATION OF AUTHORSHIP	10
ACKNOWLEDGEMENTS	11
ABBREVIATIONS AND DEFINITIONS	12
DEFINITIONS/GLOSSARY	13
1. INTRODUCTION	18
1.1 Coastal flood events	18
1.2 Role, timeliness and relevance of this research	19
1.3 Aims and objectives	20
1.4 The Solent case-study	21
1.5 Thesis structure	23
2. LITERATURE REVIEW	25
2.1 Coastal flood sources	25
2.2 Coastal flood pathways	34
2.3 Receptors and consequences	46
2.4 Understanding and forecasting coastal flooding	52
2.5 Changes to coastal flood risk	59
2.6 Summary	62
3. COASTAL FLOODING CASE STUDY: THE SOLENT	65
3.1 Regional overview	65
3.2 Description of the detailed case study sites	70
3.3 Summary	75
4.1. Overview of the hydraulic flood simulations	77
4.2. Data sources and integration	78
4.3. Integrating loads, defence failures and inundation modelling	87
4.4. Numerical simulations of floodplain flow	99
4.5. Surface features and receptors	100
4.6. Scenarios for coastal flood simulations	101
4.7. Summary	105
5. MODEL VALIDATION & UNDERSTANDING COASTAL FLOOD EVENTS	109
5.1. The 10 March 2008 Storm Surge	111
5.2. The 14 and 17 December 1989 West Solent floods	120
5.3. Historic water levels & flood events in the Solent	124
5.4. Summary	126
6. COASTAL FLOOD SIMULATIONS: HYPOTHETICAL EVENTS IN THE SOLENT	131
6.1. Solent-wide coastal flood simulations	132
6.2. Detailed case study 1: Portsmouth	138
6.3. Detailed case study 2: the Pennington flood compartment	150

6.4.	Summary	154
7.	DISCUSSION	161
7.1.	Overview of the methodological position	161
7.2.	Review of flood simulation methods	165
7.3.	Historic floods, data sets and validation	167
7.4.	Detailed analysis and higher resolution studies: findings and applications	171
7.5.	Coastal flood events in the Solent	172
8.	CONCLUSIONS	181
8.1.	Achievement of aims and objectives	181
8.2.	Recommendations for further research	186
7.	REFERENCES	191
	APPENDICES	210
	Appendix A – Additional information of case study datasets	210
	Appendix B - Exposure to coastal flooding in the Solent	212
	Appendix C - Breach analysis - Fragility curves	214
	Appendix D – Evaluation of the 10 March flood event photo data set	222
	Appendix E – Wave Overtopping	234

List of Figures

Figure 1.1 Position of this research within the well-known ‘source-pathway-receptor’ model	19
Figure 1.2 Coastal floodplain and sub-regions used to describe flood modelling	22
Figure 2.1 Coastal sea level effects caused by tides, storm surge and wave processes	26
Figure 2.2 The global distribution of tropical cyclones	27
Figure 2.3 (a) UK Environment Agency regional divisions and ‘Class A’ tide gauges, the Solent case study area is highlighted; (b) example visual output of a numerical storm surge simulation	29
Figure 2.4 Wave transformation at the coast	31
Figure 2.5 Sea level analysis using the skew surge joint probability method	33
Figure 2.6 Sea wall failure modes	35
Figure 2.7 A breach in the defences in the southwest Netherlands, 1953	38
Figure 2.8 A typical breach outflow hydrograph	40
Figure 2.9 Example of a sea defence’s fragility	41
Figure 2.10 Inundation map example (location: Towyn, Wales)	44
Figure 2.11 Coastal flood mortality based upon large-scale events	48
Figure 2.12 The main components of a flood risk assessment methodology	54
Figure 2.13 Example of UK Depth-Damage-Duration Data for Residential Properties (sector mean) ..	55
Figure 2.14 Example of spatial distribution of EAD in the Thames Estuary	55
Figure 2.15 Stages within the flood forecasting and warning process	57
Figure 3.1 The Solent case study region	66
Figure 3.2 The city of Portsmouth; (a) key locations; (b) floodplain topography	67
Figure 3.3 Sea level time-series recorded at three locations across the Solent during a spring tide	68
Figure 3.4 Flooding in Old Portsmouth on the 16 th December 1989	72
Figure 3.5 The Pennington detailed case study site, showing defence types and key locations	74
Figure 4.1 Method overview	77
Figure 4.2 Hydraulic flood modelling method flow diagram	78
Figure 4.3 Two methods for spatially prescribing SWL (to simulate uniform water level events)	80
Figure 4.4 Sea level time-series used in the Solent-wide coastal flood simulations	80
Figure 4.5 Overflow duration associated with negative freeboards & regional storm-tidal variations ..	81
Figure 4.6 Selection of significant wave height return periods in the Solent	82
Figure 4.7 DEM of the defences and floodplain surrounded by 10 m spaced inflow points	84
Figure 4.8 Defence data processing	85
Figure 4.9 Solent defence types, which correspond to descriptions in table 4.2	87
Figure 4.10 Model inflow boundary conditions	88
Figure 4.11 Crest-dependent duration of overflow and overtopping inflows for all failure events.	88
Figure 4.12 Overtopping and flooding caused by swell waves, Hayling Island, 3 November 2005	90
Figure 4.13 Floodplain configurations, water level event scenarios and limits set to the overtopping ..	91
Figure 4.14 Expected changes in water level in a 50 m ² boundary cell filled by overtopping event	94
Figure 4.15 Tidal curve segment plotted with the corresponding wave overtopping rate	95
Figure 4.16 Peak values for modified water level time-series (10 m resolution overtopping inflows) ..	96
Figure 4.17 Fragility curves for overflow-overtopping induced damage	97
Figure 4.18 Representation of flow between raster cells in LISFLOOD-FP	99
Figure 4.19 Land-use and building polygons and aerial photography	101
Figure 4.20. (a) The A27 embankment, and (b) Hilsea Lines	104
Figure 4.21 Locations of potentially compromised section of flood defences in north Portsmouth	104
Figure 4.22 (a) Breach locations selected for the additional scenario at Pennington, and sub-compartments which contain topographic break-lines which may restrict hydraulic connectivity; (b) defence weak spots and approximate locations of 17 th December 1989 breaches	105
Figure 5.1 Methodology outline: floods were modelled and compared to observations	109
Figure 5.2 Application of flood event photos to verify inundation area and characteristics	110

Figure 5.3 Atmospheric pressure at 1200 h on the 10 March 2008 over the British Isles.....	111
Figure 5.4 Still water level time series across the Solent on 10 March 2008	113
Figure 5.5 Flooding at Selsey 10 March 2008.....	115
Figure 5.6 Example of utilisation of photos to approximate observed inundation extent.	116
Figure 5.7 Locations of wave, water level and flooding observations during the 10 March 2008.....	117
Figure 5.8 The 17 December 1989 flood simulation and observed flood outline.	122
Figure 5.9 (a) Highest annual still water levels recorded (a) at Portsmouth (b) Southampton.	124
Figure 5.10 High sea level event at Southampton docks (photo taken 10 March 2008).	126
Figure 6.1 Inundation modelling results: total number of properties	135
Figure 6.2 Inundation modelling results: total number of properties inundated to >1m	136
Figure 6.3 Land area inundated by the Solent-wide coastal flood simulations	137
Figure 6.4 (a) Peak flood depths from the breach simulation for the 50 m resolution model, and (b) the 10 m resolution model	140
Figure 6.5 (a) The 50 m, and (b) the 10 m resolution models; both showing peak flood depths for simulations of a 1 in 200 year SWL combined with maximum waves.	141
Figure 6.6 (a) Properties flooded in Portsmouth (10 m and 50 m resolution simulations)	143
Figure 6.7. Water depth distribution for a 1 in 200 year SWL flood (and maximum waves) in northern Portsmouth, at present-day and with 0.5 m SLR.....	147
Figure 6.8 Flood event map of Portsmouth.	149
Figure 6.9 Flood simulation output at Pennington	151
Figure 6.10 (a) Flood modelling results for Pennington by the total number of properties flooded....	152
Figure 6.11 Flood compartments in the Solent (for use alongside Tables 6.5a, b and c).	155
Figure 6.12 Example model output showing: grid of (peak) floodplain water depths for a 1 in 200 year SWL and full breach simulation, and probability of breach for each defence section	159
Figure 6.13 Flood outlines and depth distribution for a 1 in 200 year SWL and full breach event	160

List of tables

Table 2.1 Flood inundation characteristics and their relevance to flood damage.....	47
Table 2.2 Basic definitions of local scale flood map.....	52
Table 2.3 UKCP09 relative sea-level rise projections over the 21 st century for London.	60
Table 3.1 Data from the 2001 Census relevant to the Solent case study area	70
Table 3.2 Extreme water levels and flood events in Portsmouth.....	73
Table 3.3 Extreme sea levels and flood events at Pennington.	75
Table 4.1 Return still water levels at Portsmouth in 2008.....	79
Table 4.2 Solent defence types	86
Table 4.3 Values used to assign resistance to breach by overflow/overtopping mechanisms	98
Table 4.4 Typical friction values applied to flood modelling.....	100
Table 4.5 Selection of floodplain volumes	106
Table 5.1 Measured peak water levels and waves on 10 March 2008.....	114
Table 5.2 Summary of flood locations and mechanisms on 10 March 2008.....	118
Table 5.3 Summary of the observational data and modelling used to reconstruct the 10 March 2008 coastal flood event in the Solent.....	120
Table 5.4 (a) Properties counted as flooded on 14 December 1989 (hydraulic model simulations)....	123
Table 5.5 The ‘depth criteria’ required to evaluate the model’s predictions of flood depth at properties. Based on locations in Table 2 where photographs depicting the event are available.....	129
Table 6.1 Properties and land area in the Solent affected by a 1 in 200 year SWL coastal flood simulation.	132

Table 6.2 Summary of properties inundated by the 1 in 200 year SWL plus full breaching simulation. Results are segregated by Portsmouth's flood compartments as shown in Figure 6.4	139
Table 6.3 Coastal flood simulations with 1 in 200 year still water level for Portsmouth.....	141
Table 6.4 Number of properties inundated at Pennington by a 1 in 200 year SWL	150
Table 6.5 The top 10 Solent coastal flood compartments according to the total number of properties potentially within a full breach and overtopping flood outline	156
Table 6.6 The top 10 Solent coastal flood compartments according to the number of properties flooded to >1 m depth (with an additional of 0.5 m SLR compared to a present day 1 in 200 year still water level event).....	158
 Table 7.1 Summary of the model scale and run-time.	167
Table 7.2 A selection of flood events in the UK and coastal floods in the Solent.....	174
Table 7.3 Summary of method decisions and uncertainties in the case study flood simulations	178

Declaration of authorship

I, Matthew Wadey declare that the thesis entitled ‘**Understanding Defence Failures and Coastal Flood Events: a Case Study Approach**’ and the work presented in the thesis are both my own, and have been generated by me as the result of my own original research. I confirm that:

- This work was done wholly or mainly while in candidature for a research degree at this University;
- Where any part of this thesis has previously been submitted for a degree or any other qualification at this University or any other institution, this has been clearly stated;
- Where I have consulted the published work of others, this is always clearly attributed;
- Where I have quoted from the work of others, the source is always given. With the exception of such quotations, this thesis is entirely my own work;
- I have acknowledged all main sources of help;
- Where the thesis is based on work done by myself jointly with others, I have made clear exactly what was done by others and what I have contributed myself;
- Parts of this work have been published as:

Published Journal Article:

Wadey, M.P.; Nicholls, R.J. & Hutton, C., Coastal Flooding in the Solent: An Integrated Analysis of Defences and Inundation. *Water* 2012, 4, 430-459.

Wadey, M.P., Nicholls, R.J. & Haigh, I., Understanding a coastal flood event – the 10th March 2008 storm surge event in the Solent, UK. *Natural Hazards* (2013): 1-26.

Ruocco, A., Nicholls, R., Haigh, I. & Wadey, M.P. Reconstructing coastal flood occurrence combining sea level and media sources: a case study of the Solent, UK since 1935. *Natural Hazards* (2011), 59, 1773-1796.

Conference Proceedings:

Wadey, M.; Nicholls, R.; Hutton, C., Threat of Coastal Inundation in the Solent: Real-time forecasting. In: *ICE Coastal Management. Innovative Coastal Zone Management: Sustainable Engineering for a Dynamic Coast*, Belfast, UK, 2011.

Signed:

Dated:

Acknowledgements

I am thankful for all of the insightful advice, support, and opportunities provided by my supervisors Professor Robert Nicholls and Dr Craig Hutton. I also am grateful for the funding that was provided by the EPSRC and the 'SemSorGrid4Env' (SG4E) EU research project.

The LISFLOOD-FP flood inundation model was an essential tool in this research – I would like to express my thanks for the help and provision of this model by Paul Bates (model founder) and Jeffrey Neal (model developer), both of the University of Bristol.

The Channel Coastal Observatory (CCO)/New Forest District Council (NFDC) provided key data sets (LiDAR floodplain and defence survey data, wave and water level observations, photos etc.). I have always appreciated the support of my former CCO/NFDC colleagues; in particular Andrew Bradbury and Travis Mason who provided me with my first coastal science job. Andrew Colenutt, Samantha Cope, Stuart McVey, and other staff at CCO have also been instrumental in generating vital background information – including the North Solent Shoreline Management Plan and survey data. I am thankful to friends and staff at the University of Southampton for their help & friendship during this period of research – especially all those from Building 22 all of whom I cannot list here. In relation to work, this thanks in particular goes to Ivan Haigh who provided valuable water level analysis, data, and advice.

The Environment Agency (EA) Data Team provided return period sea level data, and reports of flood events; and the EA's Charlotte Creswell provided key flood extent & event datasets, and hosted a meeting about flood forecasting, warning and management in the Solent region. The Portsmouth and Havant Coastal Partnership (including Lyall Cairns, Matt Hosey, Brett Davis and Caroline Barford) provided defence data set and advice. Photos (and their permissions) for the 10th March 2008 flood were provided by the Yarmouth Coastal Defence Partnership, Emsworth Residents Association, Trevor Price of Dinosaur Island (Sandown) and Jenny Jakeways (Isle of Wight Council); and water level datasets were sent from William Heaps (ABP) and Barry Blaydes (Solentmet Support Group).

I sincerely apologise to anyone I have missed from these acknowledgements.

The greatest thanks are to my family – Mum, Dad, Joe, Toby, and of course my amazing wife Rebecca, who have been loving and supportive (and tolerant) throughout.

Abbreviations and Definitions

Abbreviations

ABP	Associated British Ports
CCO	Channel Coastal Observatory
CHIMET	chimet.co.uk
CHM	Cowes Harbour Master
CPU	Central processing unit
DEFRA	Department for Environment Food and Rural Affairs
DEM	Digital elevation model
DTM	Digital Terrain Model
EA	Environment Agency
EAD	Expected Annual Damages
EU	European Union
FC	Flood compartment
FE	Flood extent
FEMA	Federal Emergency Management Agency
GIS	Geographical Information Systems
GPU	Graphics processing unit
HRW	Hydraulics Research Wallingford
Mb	Millibars (pressure)
mODN	metres above Ordnance Datum (Newlyn)
MDSF	Multi-Disciplinary Support Framework
MoD	Ministry of Defence
MSL	Mean sea level
NAFRA	National Flood Risk Assessment
NFCDD	National Flood and Coastal Defence Database
NFFS	National Flood Forecasting System
NRA	National Rivers Authority (forerunners of the EA)
OS	Ordnance Survey
PPG25	Planning Policy Guidance 25 (UK Government paper on ‘Development and flood risk’ for England)
RASP	Risk Assessment for Strategic Planning (an integrated flood modelling method which underpinned the Nafra and Foresight studies)
RMSE	Root mean square error
SEPA	Scottish Environmental Protection Agency
SLOSH	Sea Lake and Overland Surges from Hurricanes
(R)SLR	(Relative) Sea level rise
SMP	Shoreline Management Plan
STFS	Storm Tide Forecasting Service (now UKCMF)
SWL	Still water level
UKCMF	UK Coastal Monitoring and Forecasting (formerly STFS)

Definitions/Glossary

Assimilation Data assimilation is frequently used in meteorological, wave, and water level predictions forecasting (e.g. Horsburgh and Flowerdew, 2009) to adjust the appropriate variables in the model to match the measured data, and hence provide a more accurate set of initial conditions for the forecast run. For each analysis cycle of a numerical model run, results are analysed alongside observations of the current (and sometimes past) state of the system to balance the uncertainty in the data and the forecast. The model is then advanced in time, and its result becomes the forecast in the next analysis cycle.

Bimodal sea This term describes a sea state at any given location where there are distinctly present (but separate) components in a wave spectrum, including (1) longer period ‘swell’, and (2) locally generated, shorter period ‘wind’ waves.

Constituents One of the harmonic elements in a mathematical expression for the tide producing force and in corresponding formulas for the tide or tidal current. Each constituent represents a periodic change or variation in the relative positions of the Earth, Moon, and Sun (*also see ‘tide tables’*)

DEFRA UK Government department tasked with issues such as the environment

Dike Another word for sea wall; although usually refers to wide embankment structures constructed on mainland European North Sea coastlines.

Discount (rate) Concept typically used by accountants, that income in the future is worth less than income now.

Ensemble Instead of providing a single forecast, this approach runs a model many times from slightly different starting conditions. The complete set of forecasts is referred to as an ensemble, with each ensemble ‘member’ associated with a probability. These quantify uncertainty by making many numerical simulations using different choices of initial states and key parameters.

Environment Agency (EA) are a British non-departmental public body of DEFRA and an Assembly Government Sponsored Body of the Welsh Government that serves England and Wales. The EA is the principal flood risk management operating authority; and as of 2008 have a strategic overview role for all flood and coastal erosion risk management. The EA has the power (but not the legal obligation) to manage flood risk from designated main rivers and the sea; and is responsible for increasing public awareness of flood risk, flood forecasting and warning and has a general supervisory duty for flood risk management.

Exposure This term in this thesis, describes a quantity of land or people that could theoretically be flooded by a specified return period of water level or other load conditions. In this work this typically refers to non-hydraulic or non-numerical modelling methods (planar water level or ‘bath-tub method’) which assume that for a given sea level all areas below the elevation on the adjacent land are

submerged. It is a worst-case possible interpretation and in real floods only part of this area is submerged (refer to Section 2.2.2).

Extreme value theory A statistical discipline which uses the concepts of return level and return period to convey information about the likelihood of rare events such as floods (refer to Section 2.1.4).

Failure mode Description any mechanisms that allows a defence or defence system to provide a flood pathway (potentially progressing to flooding).

Flood drivers Any phenomenon that may change the state of the flooding system. In Evans et al (2004) these are also implied as potential responses to flood risk.

Flood compartment (also see ‘exposure’) In Chapter 4 it is explained how hypothetical water levels (representative of extremes including combined tide and surge) can be layed across a digital representation of the floodplain land surface (a DEM), to define areas that could theoretically be flooded. Using a DEM, if cells below the given water level are joined (‘hydraulically connected’) they form part of the flood compartment. As explained in Chapter 4, because of the uncertainty in flood prediction parameters, large extremes are used to broadly define hydraulically discrete flood compartments.

Fragility curve (or fragility function) A probabilistic (and usually graphical) representation of the relationship between load and resistance; gained from a limit state equation (see below) and a form of reliability analysis to determine the probability of failure (usually of the y-axis) from each incremental load increases (usually along the x-axis) – see Figure 2.9.

Harmonics See ‘*tide tables*’

Iribarren number Parameter for describing wave behaviour on a slope, also known as the ‘surf similarity parameter’ (refer to Equation 17).

Kelvin wave A low-frequency non-dispersive gravity wave (in the ocean or atmosphere) that balances the Earth's Coriolis force against a boundary such as a coastline.

Limit state equation Defines the ‘limit state’ (or structural threshold of failure) as defined by ‘Z’. Resistance (or strength) ‘R’ is compared to the stress (load) ‘S’. ‘R’ represents the gathering of all terms or parameters which relate to the strength of the defence. ‘S’ represents all terms or parameters that relate to the loading applied. Z = the limit state function. The equation is applied, $Z = R - S$. If $Z \geq 0$ the defence does not fail, if $Z \leq 0$ (i.e. the load exceeds the resistance strength) the limit state is exceeded and the defence fails. In a quantitative flood risk assessment reliability theory is usually applied to calculate a probability of failure.

Mesh refers to a geometry-based analysis technique that requires the geometry to be broken into a discrete representation of shapes or cells (also known as a grid).

Monte Carlo analysis is one type of ensemble prediction system comprising a class of computational algorithms which rely on repeated, random sampling. This term describes a large number of

approaches, which are considered forms of stochastic simulation, aimed at solving problems where there are uncertain inputs. These tend to include: (1) generating inputs randomly from a given domain by using a specified probability distribution, (2) performing a deterministic computation from these inputs, (3) aggregating the results of the individual computations into a final result.

Numerical model is a computer simulation (or model, program, network of computers) that attempts to simulate an abstract model of a particular system; using for example fundamental hydrodynamic equations.

Phase-averaging are types of model which reconstruct the sea surface elevation in space and time while accounting for such effects as refraction, diffraction, and, in some models various forms of wave-wave interactions.

Real time In terms of data transfer applications, the term ‘real-time’ relates to computer systems that update information at a similar rate to which they receive data, enabling them to direct or control a process (such as information suitable for flood warnings). Hence in relation to forecasting and warning, the term real-time in this thesis may refer to a rapid computational model which can complete its objective (i.e. a flood simulation) fast enough so offer a real-time response to wave and water level inputs. Alternatively (and where clearly stated), for the simulation of physical phenomena such as flood spreading, real-time can refer to how temporally comparable the model simulation is to reality of flood wave propagation.

Reliability analysis A measure of consistency within a set of measurements (analogous to precision). For an engineered component such as a flood defence, reliability can refer to how many times the component is expected to fail given a series of tests.

Risk In a quantitative analysis, risk usually refers to the product of probability and consequence (e.g. expected losses) of particular undesired event (e.g. a coastal flood).

Root mean square error is a statistical measure of accuracy for measured data of a varying quantity, also known as the quadratic mean. In the case of elevation data, this is calculated by taking the square root of the average set of squared differences between dataset values (e.g. modelled flood water surface elevations versus surveyed or observed elevations).

Seiches are oscillatory motions that can originate in any body of water (Proudman, 1953) with periods dependent on the horizontal dimensions of the water body and the depth of the water (which can be many hours for the seas and oceans). For an enclosed body of water the seiche motion can be considered as a standing wave with a node of no vertical motion at the centre and maximum vertical displacement alternately at opposite ends. In many locations, small seiches result from wind stress and tidal resonance and appear as small oscillations in a tidal signal; for example oscillations related to wind stress and with periods of the order of ten minutes have been observed at tide gauges around Britain (Pugh, 1987).

Sea wall Man-made structure (usually concrete or masonry) that is built along a shoreline to block erosion or prevent flooding or resist erosion Where necessary, different geometries (e.g. vertical or sloping are distinguished).

Sensors (e.g. wave and tide) record a change in pressure or spatial position in response to water level variations. Tide gauges rely upon elevation calibration against a geodetic datum; wave buoys often use a GPS receiver to record movement, with readings dependent upon knowledge of local water depth. The current Portsmouth tide gauge is a pneumatic bubbler system with two full-tide and mid-tide sensors, and is currently the only gauge in the Solent which is part of the UK's National Tide and Sea level Facility (refer to Figure 2.3).

Shallow water equations (also called the Saint Venant equations when in one-dimensional form). These are a set of hyperbolic partial differential equations that describe the flow below a pressure surface in a fluid (sometimes, but not necessarily, a free surface). The shallow water equations are derived from equations of conservation of mass and conservation of momentum (the Navier–Stokes equations), which are valid even when the assumptions of shallow water break down, such as across a hydraulic jump. These form the basis for most numerical modelling of flow hydrodynamics relating to flooding.

Shoreline Management Plan (SMP) These studies are large-scale assessments of the risks associated with coastal processes. SMPs provide a framework for dealing with flooding and erosion by dividing sections of shoreline on the basis of coastal processes (Motyka and Brampton, 1993) and related defence systems; to provide advice that may help to reduce these risks to people and the developed, historic and natural environments.

Significant wave height is the averaged highest third of wave heights recorded over a specified time interval and location.

Skew surge is the difference in level between peak observed tide and peak predicted tide (Figure 2.5).

Storm surge is a rise above normal water level on the open coast due to the action of wind stress and atmospheric pressure upon the water surface, sometimes known as the (meteorological) residual, or surge component of a water level. This is usually defined as the difference between observed water levels and tidal predictions. At any point along the coast a representation of how the observed sea level varies with time may be expressed by:

$$X(t) = Z_0(t) + T(t) + S(t) + \text{non-linear interactions} \quad (\text{Pugh, 1987})$$

Where $X(t)$ is the observed sea level variation in time, $Z_0(t)$ is mean sea level (MSL), $T(t)$ is the astronomical tide and $S(t)$ is the non-tidal component of sea level, often called the meteorological or surge residual. Other components could be added to the equation (waves, seiche, river discharge and tsunamis). Surges at the coast may be positive or negative, the latter of which are relevant to coastal flooding. The two main physical processes responsible for the generation of storm surges are atmospheric pressure and wind stress. Atmospheric pressure has an inverse relationship with sea level

by exerting a vertical force; whereas wind stress transfers energy and momentum to the water column. The largest surges occur when winds blow for a long time over large expanses of shallow water (refer to Section 2.1).

Tide tables can be generated using harmonic analysis, which accounts for the main influences the time and elevation of tidal water levels (Earth's rotation, the positions of the Moon and the Sun, the Moon's elevation above the equator, and ocean/shelf bathymetry). Variations with periods of less than half a day are referred to as *harmonic constituents* whereas cycles of days, months, or years are known as *long period* constituents.

Wave set-up occurs when waves break on a beach, water can pile up and produce a rise in still water level. Unlike a storm surge, this effect only occurs in the surf zone. Hence, wave set-up is the super-elevation of mean water level at the coast as caused by breaking incident waves.

Wave run-up is the vertical displacement of water above the still water level. This is from the effects of swash (residual wave energy at the shoreline) and asymmetrical wave motion; that overall enables water to propagate onto 'dry' areas of a beach or defence. This effect can be substantial under energetic conditions, and can cause flooding by overtopping or by causing rapid foreshore erosion.

Wave spectra are plot(s) of wave energy versus frequency (or period).

1. Introduction

1.1 Coastal flood events

Coastal floods are usually caused by storm surges, in combination with the effects of tides and waves. These forces can push sea water onto land, into estuaries (and adjacent rivers), and overload defences. Society adapts to flooding (VanKoningsveld et al., 2008; Dawson et al., 2011b) although often in response to significant events which can include a range of losses (e.g. economic, environmental, and cultural) and even deaths. In Europe, developments in flood risk¹ management accelerated following the 1953 North Sea floods which killed 1836 people in the Netherlands, 307 people in the UK and 17 people in Belgium (Gerritsen, 2005; Baxter, 2005; McRobie et al., 2005) and floods on the German Bight in 1962 when more than 300 people lost their lives (Bütow, 1963; von Storch and Woth, 2006). In comparison to understanding at the time, coastal planners now benefit from a more developed understanding of the nature and degree of exposure to flooding due to advances in modelling of waves and water levels (Battjes and Gerritsen, 2002), numerical simulations of inundation (Bates et al., 2005; Brown et al., 2007; Gallien et al., 2011; Smith et al., 2012b), and flood risk assessment methodologies (Hall et al., 2003; Dawson and Hall, 2006; Gouldby et al., 2008b; EA, 2009a). Real-time coastal flood forecasting (Flather, 2000; Horsburgh and Flowerdew, 2009) and flood warning systems also provide means for preparation with or without defences.

Sea-level rise (SLR) is increasing the probability of extreme water levels in most coastal regions (Church et al., 2006; Menéndez and Woodworth, 2010; Haigh et al., 2011; Wahl et al., 2011), and it is recognised that improvements to flood management should include further integration of defence failures and inundation within coastal flood maps and forecasting. For example on the French Atlantic coast in February 2010 more than 40 people died following failure and outflanking of coastal defences during the well forecast storm Xynthia (Lumbroso and Vinet, 2011; Pineau-Guillou et al., 2012). This disaster was exacerbated by a lack of awareness of the underlying coastal flood risks, which left authorities incapable of planning and management before and during the event (Kolen et al., 2010).

This research aims to develop a coastal flood modelling approach that can improve the understanding of coastal flood events, with a particular focus upon the application of these methods in regions where sea-level rise threatens to substantially change the frequency and nature of coastal flooding and coastal management practices.

¹ Defined by the product of probability and consequence

1.2 Role, timeliness and relevance of this research

An illustration of the well-known source-pathway-receptor-consequence (SPRC) (DETR and EA, 2000) flood ‘system’ concept (with relevance to coastal flooding) is shown in Figure 1.1. This is often referred to in flood modelling studies (HRW, 2004b; Evans et al., 2004) to acknowledge interacting flood system components. *Sources* include wind, waves and coastal still water levels (tide and storm surge) which exert loadings across the sea-land interface. *Pathways* include foreshore responses, defence failures, and floodplain flows, which connect the *sources* to *receptors*. *Receptors* include any entity that can undergo damage as a result of flooding (people, livestock, property etc.), leading to *consequences* which are usually categorised as direct/indirect damages, and tangible/intangible effects. Uncertainties and practical constraints are often encountered within hydraulic and numerical modelling and poorly understood links and sensitivities are inherent in coastal flood analyses across the SPRC model (Narayan et al., 2012). Coastal flood mapping and forecasting methods suggest that pathways in particular tend to be less studied in numerical modelling of coastal flood events (Wadey et al., 2011), and these are the main focus within this research.

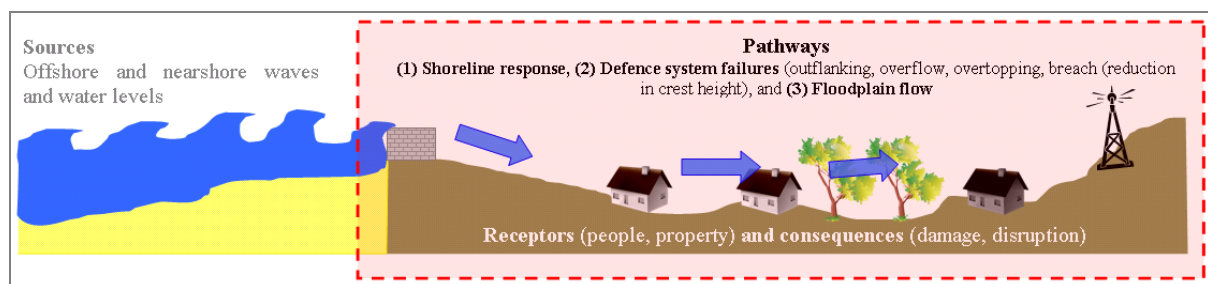


Figure 1.1 Position of this research within the well-known ‘source-pathway-receptor’ model

The EU Flood Directive (2007/60/EC) has determined that frameworks are required to assess flood risk, including emphasis upon the frequency, magnitude and consequences of flooding. Many datasets and numerical tools are already available for this type of analysis EA (EA, 2010b), although the pathways component of the aforementioned conceptual SPRC coastal flood system often lacks integration within coastal flood management operations and planning. For example, within real-time flood forecasting, the modelling of processes landward of the nearshore zone is not yet well combined or commensurate with the more detailed knowledge of sources and receptors (DEFRA and EA, 2004; Wadey et al., 2011), whilst few flood maps contain information on consequences (de Moel et al., 2009). Often there is a lack of inundation detail specific to coastal defence failures such as wave overtopping (Kortenhaus and Kaiser, 2009) or breach (collapse of reduction in height of a defence) (Brown et al., 2007; Morris et al., 2008).

Practical considerations within flood modelling include achieving a suitable compromise between spatial resolution and computational run-time. Highly simplified models are usually insufficient to resolve floodplain details and simulate flood event flows, whilst very detailed approaches may be too slow or costly for analysis over areas of the scale at which coastal floods are managed. Previous studies highlight the issues of the large uncertainties with flows into coastal flood models (e.g. defence failure and coastal water levels), and parallel to this problem is a lack of information to validate these models (Bates et al., 2005; Smith et al., 2012b).

1.3 Aims and objectives

Sea-level rise threatens to rapidly change the nature of coastal flooding in many coastal regions. To allow society to adapt quickly, methods are required to generate a flexible and practical approach for a realistic understanding of individual coastal flood events, by incrementally describing the link between loadings (wave and water levels), defence failures, and inundation. To achieve this, and to be commensurate with existing technologies, this must provide simulations of the dynamics of coastal flooding at relatively high spatial resolution. Furthermore, to be effective for coastal flood management, the approach should generate outputs rapidly, and in a manner that is accessible to planners, government, and the wider public. Ultimately, such a model would aim to provide the capacity to prevent disasters such as Xynthia, by complimenting existing coastal flood analysis and management techniques (such as real-time flood forecasting, warning and risk assessment). The principal theme of this research is that by conducting a detailed case-study of coastal flood events that new concepts and insights can be obtained of common interest to coastal flood analysis.

Therefore the aim of this research is to **“develop and apply a case study methodology to simulate coastal flood events, whilst producing accessible results and showing potential for a range of applications”**. The objectives to achieve this are to:

- Develop an integrated method (inclusive of loadings, defence failures, floodplain flows and validation) to simulate coastal flood events;
- Apply the method regionally for a series of synthetic coastal flood events across a range of defence failures and loadings;
- Using a ‘hotspot’ analysis, select locations within the case-study region for more detailed assessment. The basis for the selection of these locations will be their importance in the context of regional flooding, including their contribution to regional flood risk and/or historical flood events;

This method will allow the impacts of extreme present day coastal flood events and sea-level rise (SLR) to be considered, as discussed in later chapters. This research aims towards improving the understanding of many types of coastal flood events within the case study. This is in a manner that

acknowledges increasingly important tools for the successful management of extreme present day flood events and the effects of SLR. This includes the communication and visualisation of complex information relating to coastal change is (e.g. Jude et al., 2013), and stakeholder engagement which is an integral aspect of coastal management, including preparation for the potential impacts of future climate change (Tompkins et al., 2008). The interface between science and social dimensions is essential for flood management (Brown and Damery, 2002); and with much at stake the public can be mistrustful of measures proposed by practitioners (Myatt et al., 2003). Coastal managers often prefer to utilise specific and transparent information (Tribbia and Moser, 2008), an outcome which is targeted in the flood event analysis and case-study modelling approach developed within this thesis (e.g. flood simulation results that enable the translation of SLR predictions to the remapping of flood zones). Following the floods which impacted the UK in the summer of 2007, an independent review which followed (Pitt, 2008) included recommendations which highlighted the importance of visualising flood hazards. This is also likely to have direct implications for the effectiveness of flood warning dissemination particularly when targeting the vulnerable and difficult to persuade (Twigger-Ross et al., 2009; EA and DEFRA, 2009). Therefore this case-study's consolidation of data, methods and analysis, is relevant to a wide-range of research-concepts that aim towards an improved understanding of coastal inundation events.

1.4 The Solent case-study

This method is developed using a case study approach, with the Solent selected due to it being a region² on the UK south coast where coastal inundation risks are heterogeneous and poorly understood, and where impacts and risk will increase with sea-level rise. The modelling approach developed is demonstrated to offer an improvement to the current understanding of coastal flood events.

The UK has a long history of flooding from marine sources (Lamb, 1991; Zong and Tooley, 2003); with large storm surges and floods well documented on the east coast (Wolf and Flather, 2005; RMS, 2003a) and west coast (Horsburgh and Horritt, 2006; RMS, 2007). However, meteorologically-induced sea level effects on the south coast are generally less severe, although surge events (Wells et al., 2001; Haigh et al., 2011) and Atlantic swells (Lewis, 1979; Mason et al., 2009) have been associated with coastal flood events. A national assessment of flood risk (Evans et al., 2004) identified that the South coast would experience some of the largest increases in flood risk during the 21st century. The Solent is already subject to frequent coastal flooding (Ruocco et al., 2011) with hotspots at Portsmouth, Hayling Island, Cowes, Southampton and Fareham (refer to Figures 1.2 and 3.5 for maps that show these locations).

² By definition the Solent is an Environment Agency sub-region which forms a large proportion of flood-threatened shoreline and property in the Southern Region.

The Solent comprises more than 500 km of shoreline inclusive of tidal rivers, estuaries harbours and open coast. Previously published estimates suggest that at least 24,000 properties in the Solent are exposed to a 1 in 200 year coastal flood (NFDC, 2009; Wadey et al., 2012); the city of Portsmouth containing more than 15,000 of these properties alone. After London and Hull, Portsmouth is identified as the city containing the greatest coastal flood risk in the UK (RIBA and ICE, 2009), whilst it has also been estimated that 25 per cent of the city's coastal defences provide less than a 1 in 200 year level of protection (which is the indicative standard of protection for urban coastal areas in the UK) (Atkins, 2007). The region's other city, Southampton, may also be susceptible to the effects of sea-level rise because there is currently no formal flood defence system in place (Atkins, 2007).

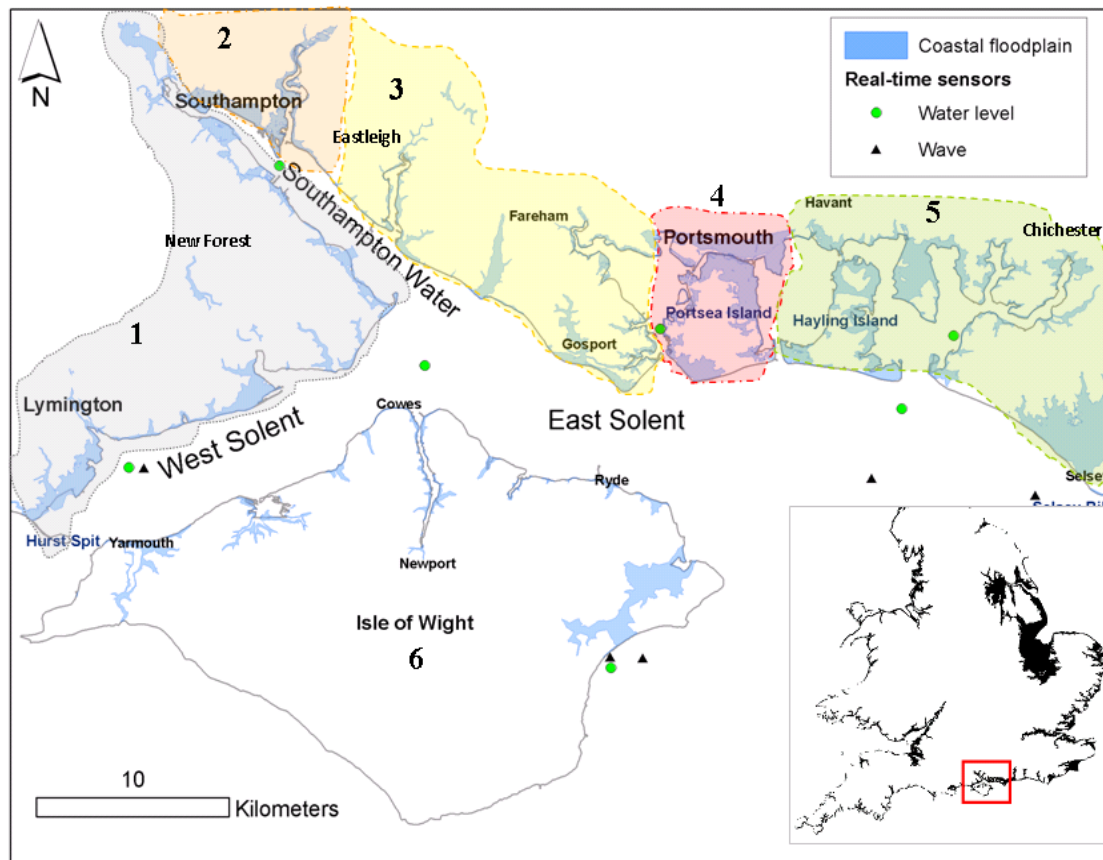


Figure 1.2 Coastal floodplain and sub-regions used to describe flood modelling.

1. New Forest. 2. City of Southampton. 3. Boroughs of Eastleigh, Fareham and Gosport. 4. City of Portsmouth. 5. Boroughs of Havant and Chichester. 6. The Isle of Wight. The base map (lower right) is the 1 in 1000 year indicative coastal floodplain of England and Wales (DEFRA and EA, 2004).

The body of available research is understandably smaller for regions such as the Solent where storm surges are not large and where under present conditions, including sea level, severe defence failures such as breaching are less prevalent. Literature relating to coastal flooding in the Solent itself is not extensive and coastal flood analysis that has combined a large number of defence failures and inundation modelling was not available prior to the start of this thesis. Therefore, the Solent provides a suitable case study, with a growing threat of flooding along a long and varied shoreline (which contains

a mixture of defended and undefended floodplains and property) with flood protection and land-use planning likely to become growing issues. Previous to this study, there is not a source of information available to indicate the likelihood and nature of individual extreme coastal flood events in the Solent, in particular relating to the effects of different types of defence failures.

1.5 Thesis structure

Chapter 2 provides a review of the literature necessary to understand the aims of this thesis. This follows the order of sources, pathways, receptors and consequences, and provides a background to coastal flood events and modelling. Due to the location of the case study, much of the reviewed literature centres upon UK examples. Chapter 3 describes the Solent case study in more detail; Chapter 4 outlines the available datasets and modelling methodology. Chapter 5 provides a background to extreme sea level events, and validation results for actual flood events in the Solent. Chapter 6 presents results for the regional flood event simulations, and the hotspot analysis at two locations within the Solent. Chapter 7 is a discussion of how chapters 2 to 8 have addressed the aims and objectives of this research. Conclusions are drawn in Chapter 8. The Appendices include an overview of calculated exposure to flooding in the Solent, and information about methods for approximating breaching probabilities. Whilst important, the available data and methods for specifying breaching were too uncertain to be fully integrated with the chosen methods and analysis, whilst repeating techniques which have already demonstrated in flood risk assessments (Gouldby et al., 2008b). Appendix D includes photos taken during a storm surge and flood event that was used to validate the model (Wadey et al., 2013).

2. Literature Review

This chapter provides a background to the information required to understand this research, firstly by continuing in greater detail from Section 1.2 an explanation of the relevant coastal flood sources, pathways, receptors and consequences. This includes a background to the mechanisms and consequence of coastal flood events, alongside the knowledge available to analyse and predict them. Following this an overview is provided of some of the applications of flood modelling and analysis, and subsequently a summary of the role of this research.

2.1 Coastal flood sources

The main coastal flood sources are depicted in Figure 2.1, and described in more detail in the following sub-sections. These include: (1) tides, which are generated by gravitational forces (primarily the differential pull of the moon and sun) acting over the whole water column in the deep ocean; (2) meteorological surges, which are the sea-level response to wind stress and the horizontal atmospheric pressure gradient at the sea surface, and (3) gravity waves. Tsunamis (caused by underwater landslides, earthquakes, volcanic activity and asteroid impacts) are also a source of coastal flooding; although the processes and probabilities of this event category are markedly different to the aforementioned sources, and are not covered here.

With the exception of bores and currents, the effects of tides and surges generally appear at the coast as a slowly fluctuating still water level. Surges and tides move across the ocean predominantly as Kelvin waves or ‘long waves’ whose propagation is dissipated by bottom friction in shallow water on continental shelves. Motion can be understood on the fundamental assumption that wavelengths are large (hundreds of kilometres) compared with the water depth (Gill, 1982; Bode and Hardy, 1997). Tidal propagation is modified in the presence of a surge, and nonlinear interactions between tide and surge have been observed to produce a negative feedback resulting in the peak surge being shifted away from high tide (Horsburgh and Wilson, 2007). Local enhancements can occur due to resonance producing large tidal ranges (Pugh, 1987) and in such situations the relative timing of a surge peak and tidal high water is critical to coastal flooding.

Higher frequency waves, in the form of wind-sea or swell and whose primary restoring force is gravity, are the dominant source of energy in the nearshore zone. The magnitude of these waves is dependent upon wind strength; fetch length and the track of the driving low-pressure pattern. Upon generation they propagate in a spread of directions with wavelengths small or comparable to offshore water depth. The characteristics of gravity waves are generally divided into three main zones:

- *Offshore*: wave generation and the interaction of waves with each other;

- *Nearshore*: where the seabed influences wave propagation and includes shallow water effects such as shoaling, depth refraction, interaction with currents and depth-induced wave breaking;
- *Shoreline response*: responses and interactions of waves with beaches and structures. Here there can be some overlap with definitions of flood pathways.

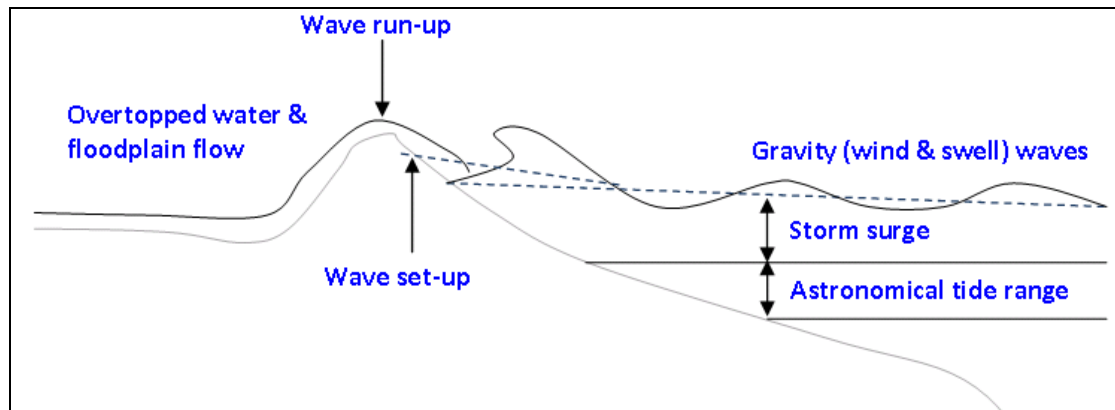


Figure 2.1 Coastal sea level effects caused by tides, storm surge and wave processes

2.1.1 Still water levels: storm surges and tides

Wind stress over shallow water is the most influential of surge formation processes, whilst in deep water surge elevations are approximately hydrostatic, with a 1hPa decrease in atmospheric pressure giving about 1 cm increase in surge elevation (Flather, 2000). The increase of wind stress as the square of the wind speed causes most numerical models of storm surges to be sensitive to errors in the wind forecasts (Pugh, 1987) with the actual process of transfer of momentum and energy from the atmosphere to the sea to form surges and waves not fully understood (Wolf, 2009). Storm surges can be generated from mid-latitude depressions known as extra-tropical cyclones (ETCs), or smaller and more intense tropical storms (hurricanes, cyclones and typhoons). In comparison to tropical storms, ETCs are usually relatively slow moving and tend to have a sprawling geometry (hundreds of kilometres around the central region of low atmospheric pressure) and generate surges up to 5 m in height (von Storch and Woth, 2008). Storm surge water levels can be particularly large when magnified in enclosed seas (Pugh, 1987), although smaller surges can be associated with flooding, particularly when persistent for several tidal cycles (Wells et al., 2001).

Tropical storms produce more extreme water level elevations, frequently exceeding 5 m, and which move in an unpredictable manner until they meet the coast where they produce extreme water levels within a confined region (tens to hundreds of km) (Pugh, 1987). The Bay of Bengal is notorious for large surges and dangerous coastal floods, with surge heights frequently exceeding 10 m. Surges are amplified by the time they reach the northern tip of the bay where they encounter a long continental

shelf, shallow bathymetry, and complex coastal geometry, before impacting expansive, flat, and highly populated deltaic land surfaces along the coastlines of India and Bangladesh.

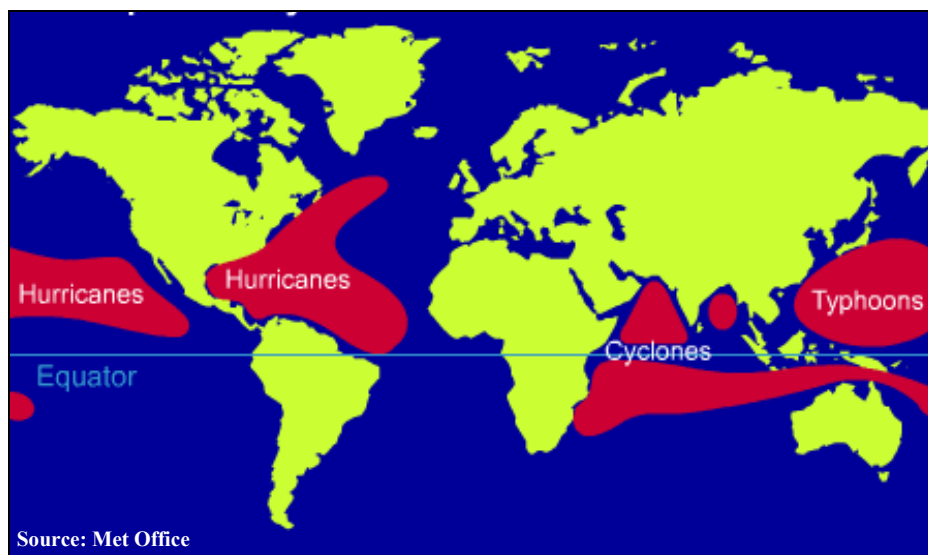


Figure 2.2 The global distribution of tropical cyclones

Still water levels can be understood by analysing time series of water level heights. For example the first fully automated tide gauge was introduced at Sheerness in the Thames Estuary which made it possible to record the full tidal curve (Palmer, 1831; Woodworth et al., 2009). If determined to be a vertically accurate and consistent dataset (e.g. covering all stages of the tide), such a long time series provides useful information to understand past water levels, and determine the nature of future extremes. However, often much shorter time spans are available, and datasets are spatially and temporally extended by numerical model simulations (Flather, 2000). Numerical modelling of storm surges, tides and waves, has been integral to the development operational coastal flood forecasting systems.

It is generally viewed that available theory and empirical models allow wind-surge processes to be successfully modelled at scales which are well resolved by current ensemble systems (Golding, 2009a). Separate tide-surge and wave models have long been in operation at many forecasting centres, with global and regional wave models and national surge and tide models applied in limited areas (Wolf, 2009). Models are usually supplemented with real-time sea surface sensors, which provide validation and the opportunity for data assimilation techniques to improve starting conditions for model runs and the accuracy of forecasts (e.g. Horsburgh and Flowerdew, 2009). In the UK, the Storm Tide Forecasting Service (STFS), since 2009 known as the UK Coastal Monitoring and Forecasting Service (UKCMF) was initiated as a direct result of the North Sea 1953 floods (refer to sections 1.1 and 2.3.2). This protects communities at risk of coastal flooding by providing coastal water levels and storm tide alerts to the Environment Agency (EA) and the Scottish Environment Protection Agency (SEPA). The UKCMF use the CS3 model which was developed by the Proudman Oceanographic Laboratories (POL)

and is run by the Met Office. This is deployed at approximately 12 km horizontal resolution across the entire northwest European shelf, although finer models nest within this domain. This is driven by surface boundary condition inputs of sea level pressure and 10 m resolution wind fields from an atmospheric model, which are at a similar resolution to the surge-tide model. The prediction of surges and wind driven currents using two-dimensional depth-averaged models has generally been successful in shelf seas (Horsburgh and Flowerdew, 2009; Wolf, 2009), although most coastal flood forecasting systems incorporate harmonic generated tides (subtracted from modelled water surface elevations) for greater accuracy. Predictions by this method are considered good although errors in elevation and timing of tidal amplitudes near the coast generally greater increase proportionally with tidal range (Horsburgh and Flowerdew, 2009). Typical monthly mean root mean square (RMS) errors for sea level are within the order of 10 cm although rare instantaneous errors of 60 cm can occur (Horsburgh and Flowerdew, 2009; Wolf, 2009). In the UK, forecasts are generated four times a day, covering 48 hour duration; and during recent storm surge events models have predicted coastal still water levels to within 20 cm (Horsburgh and Flowerdew, 2009; Horsburgh et al., 2008).

Similar systems to the UK are in place in the Netherlands (Verlaan et al., 2005) and other European countries (Flather, 2000); although in tropical regions (where surge development can be more rapid) surge forecasts are generally less reliable (Pugh, 1987). Shallow coastal bays or estuaries prone to flooding from tropical storms require smaller grid sizes to represent the relevant physical processes, for example the US operational model known as SLOSH (Jeslesnianski et al., 1992) has similar capabilities to European models although is configured to forecast the movement of surges from tropical cyclones close to the coast, using highly variable grid cell sizes to resolve flow through barriers, gaps, deep passes between bodies of water, and coastal reflections of surges such as coastally trapped Kelvin waves. Other abilities include modelling of inundation and the overtopping of barrier systems, levees, and roads, although often at too coarse a resolution to enable useful forecasts of inland flooding (Zhang et al., 2008). The operational forecast system for Venice is notably different to many others, and is based on statistical models since their skill is not yet matched by hydrodynamic models (Lionello et al., 2006).

Previously alleged as the largest of its kind and allowing water to penetrate 5 kilometres inland, was a 14 m storm surge at Bathurst Bay in Queensland, Australia, on 5th March 1899, generated by Cyclone Mahina (Whittingham, 1958). This claimed surge height is now questionable following surveys of storm-deposited debris and numerical simulations (Nott and Hayne, 2000), which indicated that this event is a world record holder for a high water mark set by a tropical cyclone rather than the largest known storm surge. Hence, the surge itself may have been as small as 3 m and accompanied by extreme large wave run-up, a process which is described in the following section.

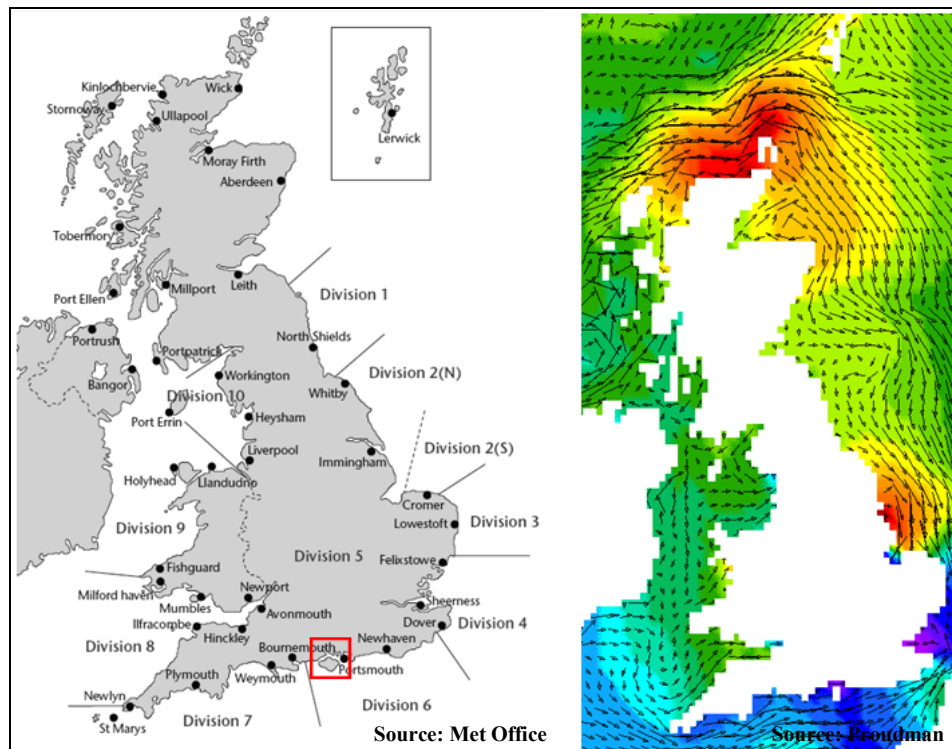


Figure 2.3 (a) UK Environment Agency regional divisions and the location of approximately 44 'Class A' tide gauges, the Solent case study area is highlighted; **(b)** example visual output of a numerical storm surge simulation

2.1.2 Gravity waves

When ocean waves approach a coast, the majority of wave energy is dissipated across the surf zone by wave breaking. In some cases, wave 'set-up' occurs as waves cause water to pile up in the surf zone, causing water level increases at the coast. Setup and longshore currents are also modified by the presence of currents generated by tides and surges, and can contribute to water level and mean circulation via radiation stresses in shallow water, (Longuet-Higgins and Stewart, 1964). The contribution of wave set-up to water level is generally included within definitions of wave run-up which is collectively the vertical displacement of water at the shoreline caused by swash combined with set-up (Figure 2.1). Gravity waves at the coast can be classified according to their provenance, as is usually indicated by wave period. Locally generated components containing higher frequencies (and smaller periods) are known as 'wind-sea', whereas 'swell' is generated when non-linear interactions among wave components results in the transfer of energy from high to lower frequencies, allowing waves to travel large distances and impact coasts far from the site of generation, and with larger periods of between 10 and 30 seconds.

For some coastal areas in northwest Europe, swell generated in the Arctic and western or tropical Atlantic can be an important consideration for coastal flood forecasting (Flather, 2000) because of the effect of longer periods upon wave run-up (Pullen et al., 2007). In deep and intermediate water depths

these are successfully modelled due to approximately linear behaviour, allowing for a theoretically sound statistical description of wave characteristics (DEFRA and EA, 2004). This is usually based on a Gaussian distribution of instantaneous values of surface elevation, resulting in a Rayleigh distribution of (crest-to trough) wave heights that is fully determined by local wave energy (Battjes and Groenendijk, 2000). Numerical phase-averaging models usually determine the sea state at any point in the model domain by summing many individual waves, each of a particular direction and frequency. The resultant plot of wave energy against frequency can be used to partition distinct frequency bands to indicate the relative presence of swell or wind-wave dominated seas. Typically, spectral wave-by-wave (statistical) analysis of offshore wave fields can yield parameters relevant for coastal engineering applications (e.g. significant wave height, mean period). Offshore waves can be monitored by wave buoys and satellite altimeters, which can provide wave spectra for further analysis or forecasting.

As waves approach the coast there is a continuum of transition once shoaling occurs and wave orbital velocities reach the seabed (Figure 2.4). Between coastal shelves and shoreline; transformation processes such as depth-limited wave breaking and wave refraction cause marked changes in wave height and distribution (Battjes and Groenendijk, 2000). Generally wave heights reduce as they propagate over shallow water towards the shore; with the wave heights at shallow coastal foreshore much smaller than in deep water situations. Larger waves tend to break first and small waves remain unchanged, which generates a non-homogeneous set of wave heights, of broken waves and non-broken waves. Battjes and Groenendijk (2000) developed the composite Weibull distribution for characterising wave heights in shallow water; as opposed to deep water wave heights which tend to have a Rayleigh distribution, characterised by a spectral wave height that is close to the statistical wave height. The influence of wave breaking has predictable and quantifiable effects on wave height predictions over foreshore slopes from 1:10 to 1:100; with conversion rules (e.g. Equation 1) generally indicating a reduction factor in wave height of up to a half (from deep water to shallow water), although with increases to the average wave period (Pullen et al., 2007). In the majority of instances, significant wave heights reduce by a third, although when the steepest of waves (i.e. steepness can be defined by the deep water wave height divided by deep water wavelength) cross the steepest gradient foreshores, wave heights may increase by up to twenty per cent; and decrease by more than thirty per cent when crossing the shallowest foreshores.

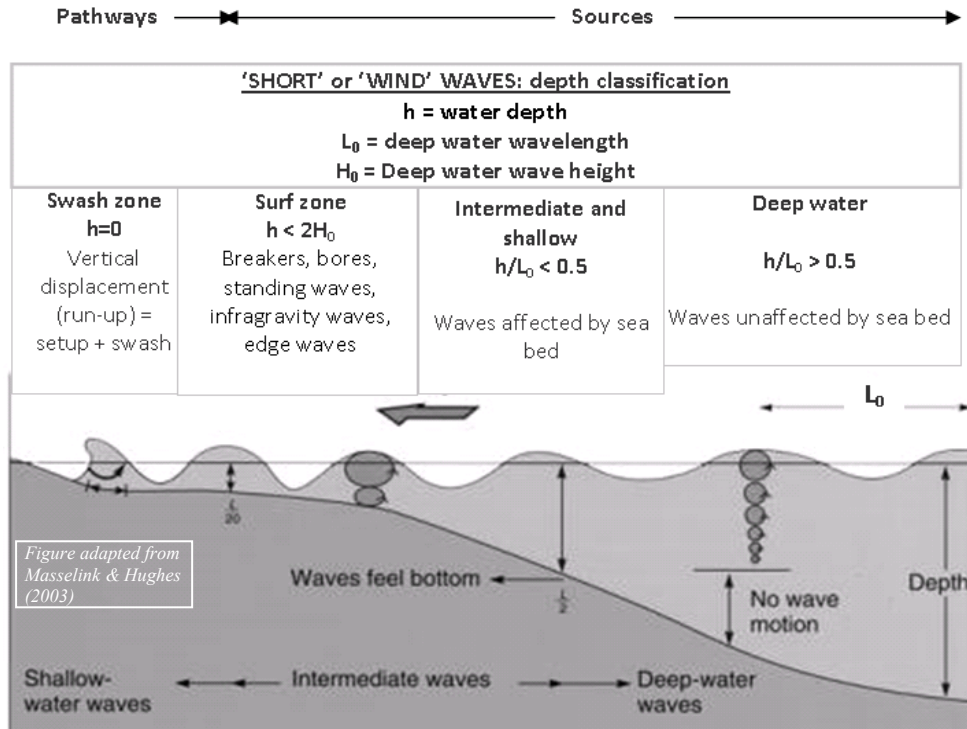


Figure 2.4 Wave transformation at the coast

Wave characteristics in shallow water are usually calculated from deep-water data with a wave energy model, although behaviour is more complicated than in deep water and the knowledge of statistical wave field characteristics more limited. Depth-induced breaking can cause the distribution of wave heights to differ considerably from a Rayleigh distribution to a manner that is not well known (Battjes and Groenendijk, 2000). Simple rules exist for determining a wave shoaling coefficient based on linear wave theory. For example the nearshore wave height (H_n) can be, defined in terms of offshore wave heights (H_0) by the coefficient $K_s = H_n/H_0$ which usually in reality varies between 0.7 and 1.4. This can be derived using the relationship:

$$K_s = 1 \div \left[\left(1 + 2kh \div \sinh(2kh) \right) \tanh(kh) \right]^{0.5} \quad (1) \quad \text{Kamphuis (2000)}$$

where h = water depth and $k = 2\pi/L$ (L = wavelength). For coastal engineering applications third-generation numerical wave model are often used to compute random, short-crested waves in coastal regions with shallow water and ambient currents, a widely applied example being the SWAN (Simulating Waves Nearshore) model (Booij et al., 1999).

2.1.3 Seiches and infragravity waves

Seiches can exacerbate coastal flooding, particularly where tide and surge are small; for example 0.2 m amplitude seiching in the Adriatic Sea is significant because it being twice the elevation of tidal oscillations (Ivica, 2006). Seiching can be activated by a sudden wind event. Resulting water level

oscillations may have periods of about 21 hours and persist for several days (Cerovečki et al., 1997), such as the three day seiche event associated with the great Venice flood of November 1966 (Ivica, 2006). Coastal seiches have been noted to contribute water level changes of order 1 m at some locations (Thompson et al., 2009), although are usually of much lower elevation than this (Pugh, 1987). Seiching is most often observed in harbours and lakes, although a storm surge event in the English Channel which persisted for several days was associated with seiching of period 3–4 hours that may have exacerbated flooding on the northern coast of France and the south coast of the UK (Wells et al., 2001).

Infragravity waves are a sea level effect present in the surf zone and characterised at lower frequencies than swell and wind waves; with periods of 20 seconds to several minutes. Certain types of infragravity waves (e.g. edge waves) may be significant to formation of nearshore morphological features (Holman and Bowen, 1982) and incident wave energy (Guza and Thornton, 1985). Studies have indicated that such sea surface resonance can both slightly exacerbate the peak of the surge, and make some aspects of surge propagation less predictable (Gönnert et al., 2001) although the inclusion of these processes within coastal flood modelling is not well developed.

2.1.4 Return periods of waves and water levels

To approximate how often an extreme sea level or wave conditions may be expected to occur, ‘return periods’ are often generated using probabilistic calculations applied to observations (or model simulations) that span a number of years. Return periods estimate the probability that a given water level or wave height will occur in any one year. For example an extreme event (e.g. the peak elevation of a still water level) defined as having a 1 in every 200 year return period may be considered as having a 0.05% chance of occurring in any given year (it is actually possible that extremes may actually occur more closely together in time than expected, due to the random variability inherent in climate driven processes). Knowing the return periods of water levels and waves is vital for assessing threats to coastal communities, and for indicating costs of protection. For example an uncertainty of 1m in setting defence crest levels might cost £1500–2000 per metre length (Allsop et al., 2005). To derive return periods, analysis of sea level or wave data has often been undertaken using extreme value theory (Coles et al., 1999). This is often combined with joint probability analysis, which can be used to assess the likelihood of two (or more) partially related environmental variables occurring simultaneously to produce a response of interest (Hawkes et al., 2002; DEFRA and EA, 2005b).

Haigh et al (2010b) summarise the main methods that can be applied for return period analysis of still water level. These include direct methods that analyse the extremes of observed sea-levels (Gumbel, 1958); indirect methods where tide-driven (deterministic) and storm-driven (stochastic with strong seasonal patterns) components are modelled separately (Davidson and Smith, 1990; Tawn, 1992); and ‘spatial methods’ where any form of extremes analysis from individual sites is extended along a stretch

of coastline (Dixon and Tawn, 1994; Dixon and Tawn, 1995; Dixon and Tawn, 1997). Different techniques have different sensitivities to the quality and length of the data record, and the ratio of tidal to non-tidal variability at a given site. For example the revised joint probability method has been shown to provide the lowest prediction errors at sites analysed on the UK south coast (Haigh et al., 2010b). The most recent national guidance in the UK is based upon this method, using the Skew Surge Joint Probability Method (SSJPM) (Figure 2.5) (McMillan et al., 2011). This considers the difference between the predicted high tide level and the highest tide level observed over the period of the semi-diurnal tide (Horsburgh and Wilson, 2007). Its value is therefore not affected by time differences between the observed and predicted tidal values, unlike in the calculation of the non-tidal residual.

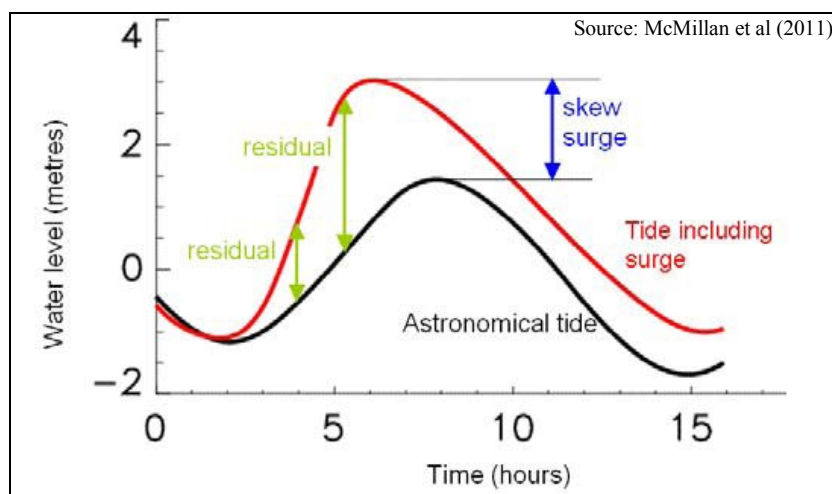


Figure 2.5 Sea level analysis using the skew surge joint probability method. The skew surge is defined as the difference between predicted and observed high water

Quantifying the combined effects and likelihood of still water levels and waves, is important for assessing coastal defences and flood risk (Hawkes et al., 2002). Often these are referred to as ‘loads’ (a term which tends to refer to waves, water levels, and their combined effects such as overtopping rates at defences, rather than traditionally defined units of force such as Newtons). Wave overtopping rates and run-up, which are described in the following section, are loadings associated with the combined effects of waves and sea levels.

In the UK, return period analysis is often used in conjunction with indicative targets set for flood protection. For example the Environment Agency aims to manage urban coastal defences in England and Wales so that they can protect against a 1 in 200 year storm event (a 1 in 100 year standard is used for river flood defences, reflecting the greater consequences associated with large coastal flood events). Lower indicative standards are generally accepted for rural areas and higher targets for important infrastructure (e.g. nuclear power stations). In terms of regional coastal defence characteristics in the UK, the largest structures are usually seen upon the east coast to protect large low-lying floodplains against extreme North Sea storm surges.

2.2 Coastal flood pathways

Failure or gaps in coastal flood defences can allow seawater or tidally-locked freshwater, to propagate landward of the shoreline and come into contact with receptors. This section explains defence failures and floodplain flow, and provides an overview of the current knowledge of these processes and methods used to simulate or predict them.

2.2.1 Defence failures – an overview

Flooding can arise from ‘functional’ failures when wave and water level conditions exceed those for which the defence is designed, or structural failure where some element or components of the defence do not perform as intended under the design conditions (Reeve et al., 2009). Functional failures arise from society’s need to compromise between the cost of the defence and the consequences of a flood, and can feature waves overtopping or still water levels overflowing defences. These may progress to structural failures known as breaching, where the crest of the defence is lowered or an aperture forms. Once other processes (such as overtopping) become replaced by significant breaching; the volume of water that passes onto the floodplain can increase by several orders of magnitude, and this can be dangerous to floodplain inhabitants. Most sea defences are now designed to accommodate a tolerable amount of overtopping during storms, although wave overtopping at seawalls has been known to disrupt transport infrastructure, and cause structural damage to roads and railway track. The causes of structural defence failure in the UK can be due to direct damage caused by water levels and waves, or may be exacerbated by weaknesses such as toe scour, geotechnical loads, and local irregularities. Currently, coastal and flood defences in England and Wales are routinely inspected and maintained to reduce the risk of breaching, although localised flooding quite frequently occurs due to overtopping.

In this study, overflow, wave overtopping and breaching are considered as separate types of defence failure. Defence failures can also be broadly classified as either ‘passive’ or ‘breaching’ responses. Passive responses include still water levels flowing over (overflow), around (outflanking), or wave action propelling water over the crest (overtopping). Few defences remain undamaged under heavy overtopping, and as already mentioned this can result in the initiation and subsequent development of a breaching response (Figures 2.6 and 2.7), which is defined as a reduction in crest height or an aperture forming in a defence. Failure to close flood gates, mobile barriers, and sluices can also cause severe flooding, and are mainly caused by errors in human operation.

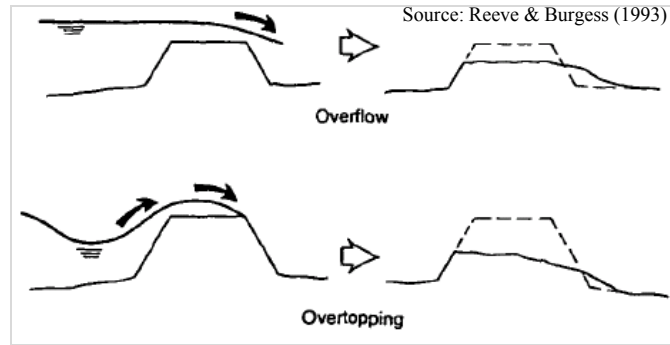


Figure 2.6 Sea wall failure modes

Natural features may directly or indirectly provide flood protection. Beaches and dunes can attenuate wave effects prior to contact with structural defences, or act as a line of defence in their own right; whilst offshore barriers, breakwaters, reefs, saltmarshes and mudflats may dissipate wave energy further away from the floodplain. The unmanaged breaching of barrier beaches is noted to increase water levels and wave heights in estuarine environments (Cope, 2004; Stripling et al., 2008) and subsequently flood risk. Hence beaches are often managed by artificial recharge and sediment retaining structures (such as groynes). The presence of a wide inter-tidal flat and marsh system is also considered extremely effective for the dissipation of the hydrodynamic energy available for erosion and sediment transport, as well as influencing tidal currents and incident waves; which may in turn influence refraction and shoaling patterns (Möller and Spencer, 2002).

Overflow failure: this occurs when the still water level is above the defence and flows onto the floodplain. In coastal environments, the duration of this process is controlled by the rise and fall of the tide over the crest of the defence. Previous flood modelling studies (Dawson et al., 2005b) have quantified volumetric overflow discharges from overflow failures using a broad-crested weir formula. One version of a weir formula, from EurOtop (Pullen et al., 2007) is shown:

$$q = 0.61 * \sqrt{g * h} \quad (2)$$

Where h is the height of the still water level over a defence. More complex variants exist, for example Chadwick et al (2009) consider an ideal fluid (i.e. ignoring frictional resistance) and allowing energy losses to be varied by a coefficient accounting for different weir geometries. The formulation by Poleni (Rouse and Ince, 1963) accounts for all energy losses, and has been previously been applied to quantifying flood inflows for breach analysis studies (Kamrath et al., 2006; D'Eliso, 2007). Over the course of numerical flood event simulations comprising a full tidal cycle; substantial variations in discharge have been observed between each type of weir formula for flood modelling (Marshman, 2010). This suggests that although an accurate method of flow calculation, it is significant for flood event analysis that weir calculations can be sensitive to parameterisation based upon knowledge of the structure that is being analysed, and with uncertainties that are potentially magnified over time.

Where substantial historic water level datasets exist for a good quality extremes analysis, most urban areas or locations with vulnerable infrastructure have sufficiently high defences to prevent overflow. The effect of waves in combination with still water levels generally exerts a more frequently occurring (but complex to quantify) contribution to flooding, as explained below.

Wave run-up and overtopping: coastal flooding due to overtopping is caused by the combined effects of water levels and waves allowing water to enter a floodplain at a faster rate than it can drain away. This mode of failure can occur when the still water level is below the height of the defence crest or floodplain. Where waves break onto a seawall, ‘green water’ can result in a relatively continuous overtopping volume, whereas if the crest is high in relation to wave height ‘splash’ overtopping occurs, which relies upon the water’s own momentum or wind to be transmitted landward of the crest. Splash overtopping is less well understood due to model scale effects in laboratory tests (Pullen et al., 2007). Overtopping rates generally increase with larger wavelengths, incidence of attack, and with decreasing freeboard (the distance between the crest and still water level) and the structure’s width (Schüttrumpf and Oumeraci, 2005) although combinations of wave frequency, water depth and structural configurations can be highly complex influences. The relationship between incident wave steepness and slope is important for sloping defences (beaches, embankment sea walls); whereas wave size and water depth are more significant influences upon overtopping behaviour for vertical structures.

Wave overtopping onto a floodplain is a more intermittent process than overflow, and can be described by a Weibull distribution (Pullen et al., 2007) comprising a sharply upward bounded curve illustrating how only a few large overtopping waves account for most of the overtopping discharge. For example, the number of incoming waves (N_w) during a wave overtopping event can be approximated by dividing the overtopping duration by the wave period. For example, if a wave with a mean period (T_{m0}) of ten seconds persisted at the coast for three hours, 1080 waves would impact the shoreline.

$$N_w = \frac{D}{T_{m0}} \quad (3)$$

The amount of waves actually likely to overtop (N_{ow}) can then be estimated by multiplying N_w by the probability of overtopping (P_{ov}). For slopes, the probability of overtopping (at a given still water level) is directly linked to wave run-up, whilst at vertical walls is related to a Rayleigh-distributed set of incident wave heights.

$$N_{ow} = P_{ov} \cdot N_w \quad (4)$$

Where:

$$P_{ov} = \exp \left[- \left(\sqrt{-\ln 0.02} \frac{R_c}{R_{U2\%}} \right)^2 \right] \quad (5)$$

The ratio of overtopped waves to the total number of incoming waves is subsequently:

$$Q_{OT\%} = N_{ow} / N_w \quad (6)$$

Where R_c is the freeboard between the crest and still water level, and the wave run-up value ($RU_{2\%}$) is explained by Equation 8. Predictions of specific wave run-up and overtopping values are available from empirical and numerical models. However, in reality these are complicated by nearshore water level predictions, and also feedbacks between water level, wave action, sediment movement and beach erosion; studies of these processes are not yet considered mature with sensitivities yet to be determined (Horrillo-Caraballo and Reeve, 2008). Various methods are used to approximate wave overtopping (e.g. for coastal engineering design or flood analysis) although the two main methods are: (1) empirical formulae which provide simple approximations of overtopping rates, or (2) numerical models which can be configured for a variety of structures and generate realistic simulations of overtopping processes (e.g. shoaling, breaking on or over the structure, and overturning of waves). Recording detailed flow fields associated with wave overtopping and hence derivation of values such as pressure, flow velocity and shear stress) are not usually feasible along large shorelines (Schüttrumpf and Oumeraci, 2005); whilst theoretical approaches to wave overtopping are not well developed (due to the complexity of fluid motion at structures) (e.g. Pullen et al., 2007). Therefore the most widely used tools for predicting wave overtopping rates at seawalls are empirical or semi-empirical formulae based on hydraulic model (e.g. flume) tests (Pullen et al., 2007; Reis et al., 2008), using relatively simple equations to describe wave overtopping discharges in relation to defined wave and structure parameters. Rather than providing accurate values they provide an order of magnitude approximation (e.g. Pullen et al., 2007). A typical wave overtopping formula is that used in British overtopping guidelines (Owen, 1980):

$$q = (T_m \cdot g \cdot H_s) \cdot A \cdot \exp\left(-b \cdot \frac{R_c}{t_m \sqrt{g \cdot H_s}}\right) \quad (7)$$

Where H_s is the significant wave height; T_m is the mean wave period; A and b are parameters for the slope of the front of the structure. Empirical run-up calculations can also indicate if waves can exceed the crest of a defence, and is mainly a function of the wave breaking process on the seaward slope; affected by berms, roughness elements, wave walls and obliquity of wave attack. Armoured features (rubble slope, concrete blocks etc.), and shingle beaches are characterized by some porosity or permeability which can usually reduce run-up. For example, this is expressed in standard empirical formulae which are based upon tests which quantify exceedance of the run-up two per cent level. The choice of the two per cent threshold is now considered quite an arbitrary value although still adhered to in empirical formulations (Pullen et al., 2008).

$$\frac{R_{u2\%}}{H_{m0}} = 1.65 \cdot y_b \cdot y_f \cdot y_\beta \cdot \zeta_{m-1.0}$$

$$\text{With a maximum of } \frac{R_{u2\%}}{H_{m0}} = 1.00 \cdot y_b \cdot y_f \cdot y_\beta \left(4.0 - \frac{1.5}{\sqrt{\zeta_{m-1.0}}}\right) \quad (8)$$

Y_b , Y_f and Y_B are coefficients for the berm, slope angle of the defence and obliquity of wave attack; $\zeta_{m-1.0}$ (the Irrabean number or surf similarity parameter). H_{m0} is the significant wave height at the toe of a structure.

For vertical structures run-up is not a measure of physical importance, with up-rushing jets of water more influential upon overtopping rates (Allsop et al., 2005; Pullen et al., 2007). At vertical walls, when waves are small compared to water depth (not often the case for urban frontages); ‘pulsating’, as opposed to wave breaking conditions prevail, which generates smoothly varying loads. When waves are larger compared to water depth, ‘impulsive’ waves are expected, influenced by bathymetry and the defence toe. These sometimes break violently against the wall, associated with short-duration forces that are 10 – 40 times greater than for pulsating conditions (Allsop et al., 2005).

Breaching: once other processes become replaced by significant breaching, the volume of water that passes onto the floodplain can increase by several orders of magnitude (Muir Wood and Bateman, 2005). Approximately 84 per cent of the volume of water that entered the Greater New Orleans flood perimeter during the floods caused by Hurricane Katrina in August 2005 was through breaches (Van Heerden, 2007). The most concentrated casualty locations during the 1953 North Sea floods were associated with closeness to breach sites (DEFRA and EA, 2003), for example 56 out of the 58 people who died on Canvey Island were near a significant breach (Baxter, 2005). This is because of high flow velocities immediately behind breaches which are associated with much greater floodplain dangers such as instability, drowning and building collapse (Jonkman et al., 2009).

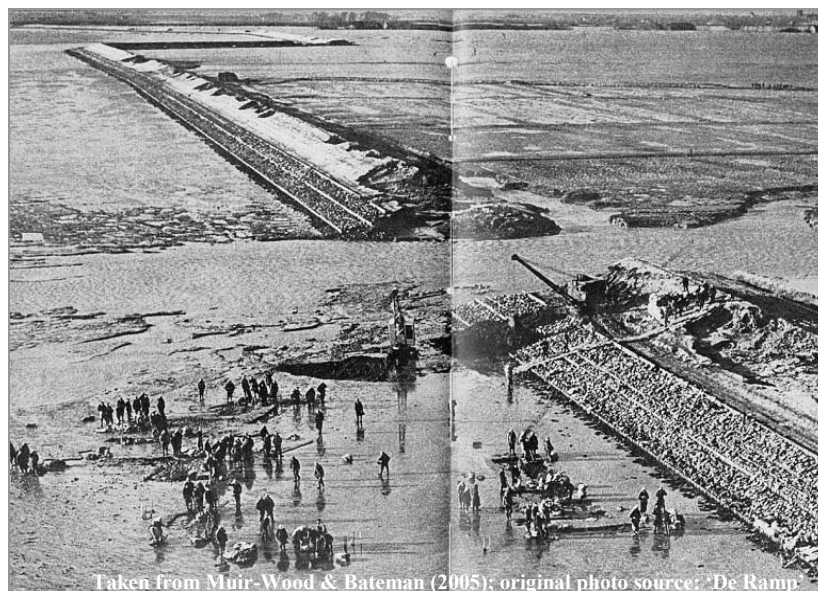


Figure 2.7 A breach in the defences in the southwest Netherlands, 1953

Statistics indicate that excessive overtopping is the most common breach initiation mechanism (Kanning et al., 2007; Vorogushyn et al., 2009), although there are numerous other process types that

can weaken a defence. Breach triggering mechanisms generally fall into three main groups (Vorogushyn et al., 2009):

- Hydraulic failure: erosion or scour via overtopping damage to the landward side;
- Geo-hydraulic failure such as piping (seepage through foundations or dike body to erode the internal structure) and other pore water related effects; and
- Global static failure: pressure forces (ice, wind, waves) or the structures own weight may exceed resistance. Includes breaking waves damaging the seaward face of a structure.

There has been much research into the dynamics of breaching, which is characterised by initiation followed by a growth. Both phases are significant to the rate of water release onto a floodplain, although the processes of breaches and their influence upon flood wave propagation generally lacks a comprehensive view (e.g. Morris et al., 2008). Consequences of breaching may be affected by interventions such as timely evacuation of people, or repairs near the time of initiation or when the tide has retreated (to prevent multiple tidal cycle inflows). Some features of breach growth behaviour can be roughly characterised by material type, although more cohesive and heterogeneous constituent materials generally make breach prediction increasingly uncertain.

Once a breach is initiated; growth can be rapid depending upon subsequent hydraulic processes and construction and/or design of the defence. The larger and lower the floodplain, the larger the breach because this allows a steep hydraulic gradient to persist (Muir Wood and Bateman, 2005). The tidally controlled water level elevation outside a defence can be considered infinite, hence the elevation and extent of the floodplain into which the water can flow is a major constraint upon the final size.

Figure 2.8 shows a generic ‘breach flow hydrograph’ (Morris et al., 2008) with a series of time markers indicating stages of breach activity. T0–T1 is the stage of stability; T1 is the start of breach initiation via seepage through, or flow over the defence. T1–T2 is an interval that may represent minutes, hours, days or months where initiation progresses as flow removes material. T2–T3 is the transition to breach formation where steady erosion cuts through to the landward face of the defence initiating relatively rapid and often unstoppable breach formation. T3–T5 is the completion of breach formation. Rapid erosion of the embankment vertically is followed by continued erosion of the embankment vertically and laterally. Extent and rate is dependent upon the volume of available flood water and the design and condition of the embankment. At T4: The peak discharge (Q_p) is a function of factors including available flood water and embankment design and condition, whilst T4 and T5 mark continued breach growth, when one erosion of the embankment vertically has terminated (to or beyond the embankment bed) a continued supply of water will continue eroding the breach laterally.

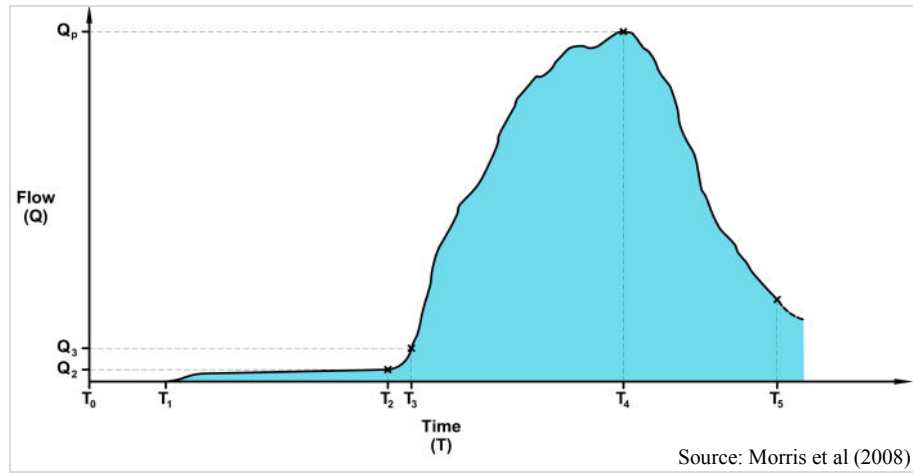


Figure 2.8 A typical breach outflow hydrograph

Over 1200 defence breaches occurred on the east of coast of England as a result of the 1953 storm surge (RMS, 2003a). Observations during the 1953 North Sea floods describe the largest breach in the Netherlands as 520 m wide and 36 m deep with a cross section of 10 000 m² (Muir Wood and Bateman, 2005). The largest in England were around 100 m width and eroded to approximately 12 m below sea level (600 m²), although many did not erode below low water level. The order of magnitude in cross-sectional area reflects the hydraulic gradient at breach initiation and the more rapid reductions in hydraulic gradient owing to ponding (Muir Wood and Bateman, 2005). Neighbouring breaches also appeared to compete; possibly due to the water that arrives behind the defence from the initial breach reducing the hydraulic gradient and hence erosion rates of subsequent breaches. For this reason, the first breach to form in a section of defence will tend to be the largest (Muir Wood and Bateman, 2005). A section of 26 breaches of between 9 m and 622 m in length (although some merged into others) occurred in the New Orleans East Back Levee area during Hurricane Katrina, some of the largest believed to have occurred rapidly at peak overtopping loads (Bernitt and Lynett, 2010).

Models have attempted to analyse the dynamics of breach initiated from the landward side (D'Eliso, 2007) and repeated wave impacts on the seaward slope (Stanczak, 2008); although runtimes and inherent uncertainties are still inhibitive for inclusion within integrated flood prediction models (Morris et al., 2008). Furthermore, predictive tools are almost non-existent for masonry structures (Brown et al., 2007). Breach dimensions are considered a key determinant for flood outcome in flood risk analysis studies (Dawson et al., 2005a; Nicholls et al., 2005) hence even the application of simplified rules is considered appropriate, for example final breach width (B_w) can be estimated by:

$$B_w = \min(10h.a, B) \quad (9)$$

Where B is the dike/defence length, h is the overflow depth and a is the material type; which can be as little as 3 for cohesive materials (HRW, 2004a), and as great as 15 for non-cohesive materials according to (Visser, 1998). The application of existing models for dam engineering (Wahl, 2004) has been

proposed for flooding studies, although relevance to coastal defences is questionable because of the difference in the coastal loadings and defences; and for coastal flood risk analysis, breaching remains the most critical uncertainty (e.g. Muir Wood and Bateman, 2005).

Prediction of breach locations is sensitive to the interaction of seaward loads (waves, water levels), geotechnical loads (e.g. pore pressure) and local irregularities (e.g. animal burrows; internal concrete damage). In parts of Europe (e.g. Netherlands) structural and geotechnical data is recorded for safety monitoring; and sometimes real-time sensors within sea defences are integrated with flood simulation tools (Pyayt et al., 2011; Gouldby et al., 2010; Krzhizhanovskaya et al., 2011) to warn of the initiation of instability (e.g. using measurements of pressure, temperature and inclination). These systems are currently at trial stage, and aim to offer risk management opportunities in large and deep floodplains where inundation is almost inevitably catastrophic (hence pre-emptive defence repairs are vital).

In the UK, the Environment Agency allocate condition grade scores, of between 1 for excellent and 5 for poor, during routine inspections. These and other defence asset information (e.g. crest height and structure type) are stored in the National Flood and Coastal Defence Database (NFCDD) and have been used for flood modelling and risk analysis, such as that within the Risk Assessment for Strategic Planning (RASP) project (Sayers et al., 2002). In most countries the collection of datasets to indicate the resistance defences and likelihood of breaching tends to involve less structurally specific parameters than for the Netherlands. Probabilistic approaches have been developed to express a conditional relationship between loads and strength parameters (Dawson and Hall, 2002), by expressing structural reliability concepts in the form of fragility functions (Casciati and Faravelli, 1991). Reliability analysis used to build fragility functions in flood risk assessment studies (Hall et al., 2003; Dawson et al., 2005a; Dawson and Hall, 2006; Gouldby et al., 2008a) combines random sampling techniques (e.g. Monte Carlo analysis) with knowledge of failure thresholds (limit state functions). This allows an expression of failure probability against a single load type (e.g. still water level) or as a three dimensional surface to define response to more than one load variable (Dawson and Hall, 2006) (Figure 2.9).

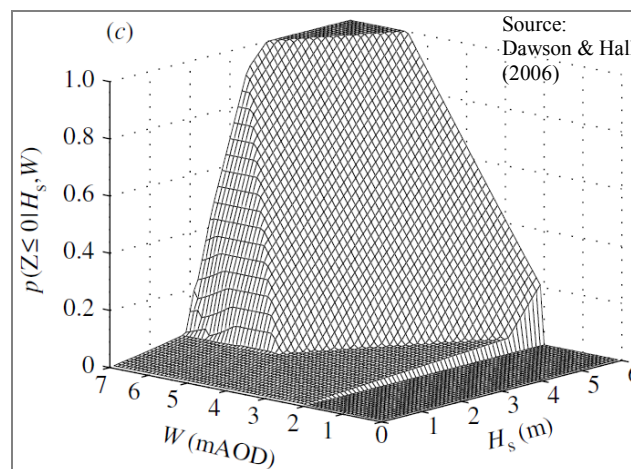


Figure 2.9 Example of a sea defence's fragility plotted over loading space: increased loads (water level and significant wave height) increase the probability of defence failure

The determination of structural failure probabilities can be further extended, for example structures of a fault tree representing the different chains of events leading to an overall failure of the flood defence structure (the top event usually comprising flooding of the hinterland) (Naulin et al., 2011). However, actual probabilities of failure in response to specific loads can be quite inaccurate where a lack of data on real events exists (Reeve and Burgess, 1993) although combined with uncertainty analysis may form a robust approach to understanding flood systems within a system-wide flood risk analysis (Flikweert and Simm, 2008) (as further explained by risk analysis, in Section 2.4.2). It has been proposed that the most poorly understood aspects of breaching are transitions between defence types and ‘point structures’ (e.g. outfalls and jetties) both observed as starting points for erosion and subsequent failure in the New Orleans flood system during Hurricane Katrina (Kanning et al., 2007), whilst other not well understood factors include the relationship between peak loadings and their variation over the times scales during storms, as well as intra-storm loadings or longer term deterioration (Allsop et al., 2007).

2.2.2 Floodplain inundation

Once water enters land due to a combination of extreme sea levels and exceedance of defence systems, inundation characteristics are primarily dependent upon the type of defence failure(s) and the floodplain topography (e.g. gradient, barriers, and obstacles). Water levels and flow patterns are also influenced by features that accelerate, obstruct or retain water (e.g. buildings, vegetation, walls, fences and drainage features). Urban floodplains are highly complex to model due to many interacting variables (Dawson et al., 2008), containing hard structures, surfaces, people and debris. Urban floodplain processes are also characterised by turbulence, inertia, and flow transitions due to the spatially dense presence of obstacles, obstructions and features that cause rapid flow constrictions and variations in floodplain friction. Also, most cities also have a sewer network for the removal of storm water rather than relying on natural channels alone; hence interaction of overland flows with subsurface drainage networks (mainly sewerage related) can be an important influence upon the spatial and temporal dynamics, and final consequences of urban floods. Structures such as pipes and culverts have a finite hydraulic capacity; hence flooding can arise due to limitations of a system’s design specifications, or incidents such as blockage or sedimentation, e.g. if the hydraulic gradient line is too high, sewers may surcharge (when the water level rises above the crown of the sewer conduit). In rural floodplains, natural topography is likely to be the predominant influence upon flow characteristics; although frictional resistance may also be critical and be dominated by drag due to vegetation. These complexities are represented to varying degrees by numerical models, which are described in the following subsection.

As explained further in Section 2.4, variants of flood map are an important component of flood risk analysis and management. These may be generated by inundation analysis, which can be used to spatially express flood risk, or emphasise different types of consequence. Flood maps can be used for operational flood warning management or planning. For example, the Environment Agency in England

and Wales publish and provide maps such as the ‘Flood Zone 3’ maps which shown an outline of sea floods which have a 0.5 per cent (1 in 200) or more chance of occurring annually. Often taking a cautious approach to capture the full potential flood outline, flood maps consider inundation to be directly related to a specific boundary water level using, the ‘planar water level method’ described below, or inundation patterns produced by hydraulic models but without considering specific defence failures. Described in the following sub-section is the use of methods which consider the effects of pathways and receptors to generate flood risk outputs.

Advances in geographical information systems (GIS) and high resolution topographic floodplain data have benefited the analysis and visualisation of inundation. A form of floodplain elevation data considered effective for flood modelling is airborne topographic Light Detection and Ranging (LiDAR). This is an implementation of laser ranging incorporating the representation of the ground surface at high resolutions, which increases the ability to predict flood inundation extent and depths more precisely (Marks and Bates, 2000). Such systems are capable of providing elevations of the earth’s surface to decimetre-level precision or better. In coastal environments, the root mean square error (RMSE) is dependent on slope and has been noted to yield points that are ± 0.3 m of reality (Xharde et al., 2006; Webster et al., 2006). Such data can be used to construct a digital elevation model (DEM) and subsequently generate flood maps if combined with other layers such as boundary water levels and features such as roads, building etc.

One of the simplest forms of inundation map is to lay a return period planar still water level³ across a DEM and generate a flood outline, to determine what is within or beneath this theoretical flood extent. Although capable of providing a quick overview of land that could be affected by flooding, this method can significantly over-predict the spatial extent of inundation; and it is often preferable to use methods which account for hydraulic connectivity and mass conservancy (Bates et al., 2005; Gallien et al., 2011), particularly for complex or low gradient floodplains, and where defences play a significant role (Nicholls et al., 2005; Dawson et al., 2005a).

Relatively recent advances in flood propagation algorithms and collection and processing of topographic elevation data have supported the widespread application of hydraulic models to aid flood prediction (Brown et al., 2007); by defining a computational domain, boundary conditions and using a two-dimensional solver to simulate the free surface elevation of floodplain flow (depending on the complexity of the 2D model an initial condition, and depth-averaged velocity vector may also be incorporated). The application of more complex models which solve the three-dimensional Reynolds-averaged Navier Stokes equations (Cugier and Le Hir, 2002) is rare due to computational cost and lack of necessity, whereas one dimensional modelling is more suited to problems where there are well-defined channels or subsurface flow networks; and nowadays rarely used for coastal flooding

³ This is method is referred to by different terms including the ‘bathtub method’, ‘equilibrium flood mapping’, and the ‘planar GIS method’.

predictions due to the supremacy of 2D codes. Hence 2D models are now widely used; by coupling coastal boundary conditions and such models to allow numerical simulation of floodplain flow processes and propagation of the flood wave. 2D hydraulic numerical modelling of inundation can also allow analysis of a wide range of scenarios (Bates et al., 2005).

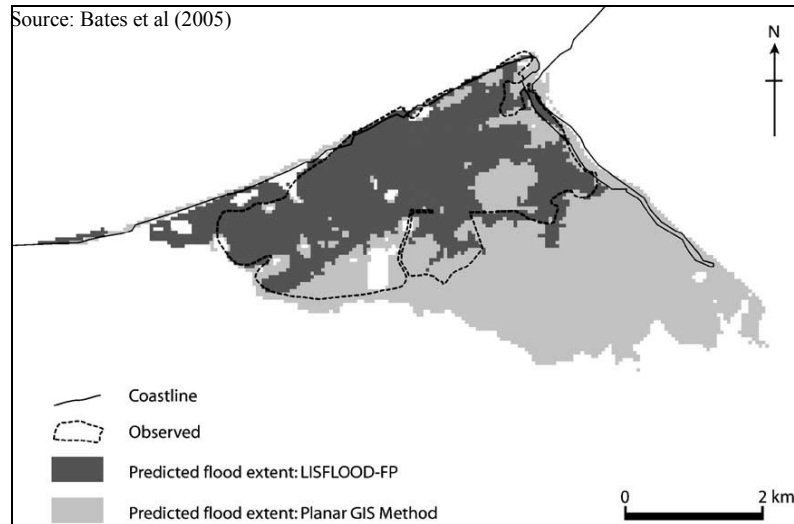


Figure 2.10 Inundation map example (location: Towyn, Wales), illustrating: (1) an observed flood extent (event: February 1990), (2) an output from a hydraulic model, and (3) the usually over-predictive method of using a planar water level placed across a DEM

Classifications of 2D modelling range in complexity and configurations. For example some models use a simplified version of the shallow water equations by neglecting certain terms and utilising the DEM in the form of a grid with square cells (Bates and De Roo, 2000) with the main limitations to this approach noted to include the simpler representation of hydrodynamics which can break down in deep water (Bates et al., 2005) and predictions of actual flood water velocity that tends to be less accurate than ‘full’ 2D methods (Néelz et al., 2009). Full 2D models can simulate flow constrictions and trans-critical flows (Syme, 2008), whilst flexible meshes (using an optimised and heterogeneous spatial schematisation of the floodplain topography as opposed to a regular spaced grid interpolation) are more easily optimised to the level of detail required. Generally, greater spatial sampling of the actual topography can benefit all model types although at greater computational cost; and models may attempt to attain a balance between resolution and computational resources by interpolating the original data, and in some examples manually incorporating narrow, linear, flood diverting landscape elements (Vanderkimpfen et al., 2008). Aside from grid cell size, the choice to include/exclude surface items (e.g. buildings) on the DEM used for urban flood modelling can result in substantial differences in final flood extents and depths (Fewtrell et al., 2008b). For these reasons, modelling of urban inundation is highly uncertain, particularly if using grids with coarser than 10 m spatial resolution (Fewtrell et al., 2008a). Subsurface drainage applications such as linkage of 1D pipe networks with 2D surface model schemes may have further potential to improve accuracy of flood simulations (Syme, 2008), although

attempts to address this aspect mostly concur that there is a lack of established methodology and minimal validation (Coulet et al., 2008).

The use of numerical models to simulate coastal flooding has so far been less prolific and more of a recent development than for fluvial inundation modelling, although proven to be achievable (Bates et al., 2005) and used for analysis of flood risks (Dawson et al., 2009). An essential aspect of coastal inundation modelling is the assignment of still water level and wave boundary conditions and defence failures. A variety of approaches are used across different studies to derive and schematise boundary conditions, and defence and floodplain datasets. Gallien et al (2011) describe and demonstrate a framework for regional, and high resolution (approximately 3 m cells) mapping of tidal flooding impacts in urbanized embayments for the case study of Newport Beach, California. This study focused upon issues of hydraulic connectivity and the significance of crest height variations and intricate defence (outer and inner floodplain) details for case-studied urbanised embayments in California; and included the development of tidal curves and the comparison of numerically modelled flood extents with constraining intra-floodplain factors (largely based upon the planar water level). In view of their own work and previous studies, Gallien et al (2011) recognised four key requirements for effective coastal flood modelling. These included that:

1. Models must account for the full inventory of flood defences;
2. Resolution and vertical accuracy must be focused in areas where elevation error and flood depth are similar orders of magnitude (e.g. uncertainty in overtopping thresholds must be considered, whereas offshore bathymetry effects are small);
3. Uncertainty in still water level boundary conditions must be considered;
4. Detailed site specific information about hydraulic connectivity is important.

The UK Environment Agency's inundation maps which are published online and used for flood warning and planning purposes are derived from a variety of methods. They often use cautious approaches (to include as much possible of the floodplain theoretically at risk) although maps have been developed to prioritise locations where flooding is more likely (e.g. Ray et al., 2011), including coupling overtopping and breach input scenarios to inundation modelling on floodplains on the English east coast (MottMacDonald and EA, 2010). Flood maps were derived by linking a full 2D inundation with empirical overtopping predictions and breach scenarios. However, these methods have not been compared to actual flood events, because such datasets are rarely available. The issue of validation of coastal flood models is explained in Section 2.4.3.

2.3 Receptors and consequences

Fatalities are widely viewed as the worst type of impact of a flood event; and analysis of a global database has suggested that large scale coastal flood events are associated with greater mortality⁴ than for inland floods (Jonkman and Vrijling, 2008). Alongside the numerous detrimental societal effects, loss of life has significant economic implications, e.g. a human flood fatality in England and Wales has been associated with a reference valuation of £1,144,890 (in June 2000) for flood management appraisal studies (DEFRA, 2008).

Direct damages refer to harm caused by contact between flood water and receptors, and are usually measured as damage to stock values, whereas indirect flood damages are usually disruption to linkages of the economy, and the extra costs of emergency and other actions taken to prevent flood damage and other losses. Tangible damages can easily be specified in monetary terms, such as damages to assets, loss of production etc.; whereas intangible damages such as casualties, health effects, and ecological effects are far more difficult to assess in monetary terms (Messner et al., 2007). Significant damages to a local or national economy can result from loss of agricultural land or livestock. The most severe damage type is direct loss of life. This has been approximately related to the number of people exposed to flood waters (Jonkman and Vrijling, 2008), and is caused by multiple factors such as the physical flood hazard (table 2.1) and human vulnerability (e.g. age, wealth, pre-existing health or mobility problems).

Rise rate of the water is an important determinant of loss of life because it influences the possibilities to find shelter on higher ground or floors of buildings. Danger to people is also influenced by how buildings respond to the floodwaters. Generally in the case of breaching, the severity of flood hazards is often dominated by distance from the breach site. Death rates in floods are high where buildings fail to provide a safe refuge; and dwellings that are fragile or temporary (mobile homes, caravans, tents etc.) may give rise to significant losses; whilst people can get trapped in underground cellars or car parks. People may also be unaware of the speed and power of floodwaters, and simply be swept away whilst on foot or in their vehicle. Exposure problems related to lack of water, food or temperature may occur due to duration of entrapment on a roof or in a building. Debris or pollution from the release of dangerous chemicals can be hazardous, perhaps long after the flood, whereas discoloured floodwaters may exacerbate unseen underwater hazards such as manholes.

⁴ Number of deaths per population exposed to the flood in one event

Table 2.1 Flood inundation characteristics and their relevance to flood damage (DEFRA and EA, 2003; DEFRA and EA, 2006; Messner et al., 2007)

Inundation characteristics	Relevance
Area	Determines which elements at risk will be affected If extensive areas are affected, escape and rescue is difficult
Depth	Often the strongest influence on loss of life and the amount of damage
Duration	Special influence on damages to building fabric Long flood duration and/or severe climatic conditions cause death from exposure
Floodplain flow velocity	Implications for human stability ($0.6 \text{ m}^2/\text{s}$ to about $2 \text{ m}^2/\text{s}$ considered critical). Only very high velocities wash buildings away (relevant in flash flood areas or areas near breaches).
Rise rate	Significant to warnings and evacuation
Time of occurrence and warning	Sudden onset flooding minimises escape chances. No warning (a rough guidance is less than 60 minutes) is significant to loss of life
Debris, contaminations, other hazards	Contamination may significantly increase risk of disease and damages Debris in the floodwater can crush or injure people; or damage buildings Electrocution
Salt-/freshwater	Saltwater may increase damages

People may also be curious to see floods, with flood tourism a recognised problem in parts of Europe (DEFRA and EA, 2003). The long term effects of flooding on psychological health may perhaps be even more important than illness or injury (Ohl and Tapsell, 2000), with physical or psychological problems, or even premature deaths known to occur long after floodwaters have receded. Fatalities may also occur due to adverse health conditions associated with extended exposure of those in shelters.

2.3.1 Coastal flood events – global overview

Globally, it has been estimated that in excess of 150 million people live within 1 m of high tide level and a further 100 million live within 5 m of high tide (Anthoff et al., 2006), although estimates vary according to DEM and population datasets, and other components of the methods of assessment (Lichter et al., 2010).

Figure 2.11 is derived from global datasets, and indicates coastal flooding mortality. This study indicated that approximately one per cent of people exposed to these coastal floods lost their lives. Already mentioned in Section 2.1.1 as a hotspot for large and frequent storm surges was the Bay of Bengal, a region which accounts for approximately five per cent of global tropical cyclones, and 80 per cent of the global storm surge casualties (Ali, 1999). Bangladesh alone has experienced 53 per cent of all global fatalities from coastal flooding (Debsarma, 2009). Notable events were 1970 with between 300,000 and 500,000 people killed, April 1991 when 138,882 were killed, and the most recent major cyclone in Orissa, India in 1999 with over 10,000 fatalities (UNEP, 2002; Dube et al., 2009).

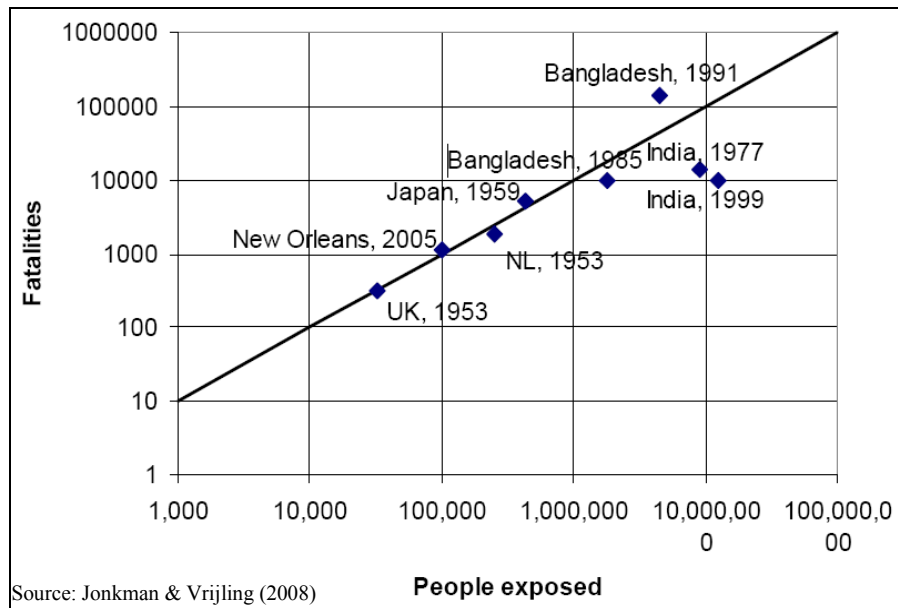


Figure 2.11 Coastal flood mortality based upon large-scale events

Generally, the largest numbers of coastal flooding fatalities occur in regions exposed to tropical cyclones (refer to Figure 2.2) especially when large storm surges combine with weaker defences, a lack of forecasting and human vulnerability. However, wealthy countries with forecasting and defence systems are still subject to coastal flooding disasters. For example, a 4.5 m storm surge was responsible for the greatest loss of life in any natural disaster in US history; when in September 1900 flood waters drowned 6,000 – 12,000 people in Galveston, Texas (Blake and Landsea, 2011). Developments in construction followed, although did not prevent the flooding caused by Hurricane Katrina in August 2005. This storm surge was extreme, peaking to the east of the hurricane's path with consistent recordings between 7 and 10 meters along a 60 km stretch of Mississippi coastline; and 2 metre surge heights 240 km east of the Katrina's track along Florida's panhandle (Fritz et al., 2007). Clear weather warnings had indicated the location and timing of the hurricane's landfall two days before the event (McCallum and Heming, 2006), and eighty per cent of the population (of approximately one million people) of the city of New Orleans acted on these warnings. However, various societal issues meant that many did not evacuate and remained in the path of the floods; whilst the main evacuation centre (the Superdome) was not suitably placed and surrounded by floodwater. Furthermore, inaccurate flood maps meant that 34,000 – 35,000 of the flooded homes did not have flood insurance, as they had not been defined in flood zones according to the Flood Insurance Rate Maps developed by FEMA (Muir-Wood and Grossi, 2006). The final overall death toll has not been finalised but may exceed 1500 (Van Heerden, 2007) with 1100 reported killed in Louisiana. Over 800 of these deaths are associated with the effects of flooding (Jonkman et al., 2009). This was the costliest natural disaster in US history with total damages of around US \$ 81 billion (Pielke et al., 2008), with parts of the city of New Orleans requiring complete reconstruction.

In Europe, the largest storm surges, and historically the greatest casualties have occurred on the North Sea coastlines. The North Sea is relatively shallow and prone to large externally generated surges; and records suggest that North Sea surges may have killed 100,000 people in the UK in 1099, with similar death tolls (from surges) in the 1421 and 1446 (Gönnert et al., 2001). Historically the Netherlands, Belgium (De Kraker, 2006), German Bight (A Plüß et al., 2001) and Denmark (Gönnert et al., 2001) have all repeatedly suffered terrible human and agricultural losses from such surges. Observations and model simulations suggest that the notorious 31st January – 1st February 1953 surge reached amplitudes of 3 m along areas of the UK east coast and closer to 4 m at the Netherlands (Wolf and Flather, 2005). This flood event killed 1836 people in the Netherlands, 307 in the UK, and 17 in Belgium (Gerritsen, 2005; Baxter, 2005; McRobie et al., 2005; RMS, 2003a), and is generally viewed as a pivotal time in European risk management. Also significant were floods on 16th-17th February 1962 when a 4 m surge hit the German Bight including the city of Hamburg which lies more than 100 km from the coast on the River Elbe, killing 315 people (Bütow, 1963; von Storch and Woth, 2006).

However, despite developments in defences and forecasting, as mentioned in Section 1.1, a lack of information of flood extent and depth was apparent prior to the 1.5 m surge and large waves which struck the French Atlantic coast on the 28th February 2010 caused by Storm Xynthia, killing between 40 (Lumbroso and Vinet, 2011) and 65 people (Kolen et al., 2010) in the Vendee and Charente-Maritime compartments. Water entered floodplains due to ancient sea walls being overtopped, outflanked and damaged; despite that weather and sea level forecasts were timely and accurate (Pineau-Guillou et al., 2012). However, flood-specific dangers were not clearly known and flood warnings were not disseminated. Some victims were trapped in buildings, due to failed electric shutters that had been closed in response to generic warnings of bad weather, rather than being specific to coastal flooding (Kolen et al., 2010). Shortly after the event a politician in the Vendee was quoted: “where would we evacuate 400,000 people at 4 am?” despite that moving only couple of thousand people a relatively short distance would have saved most lives (Kolen et al., 2010).

The following section focuses upon coastal flood events and risk in the UK, where despite advanced defence systems and flood forecasting, faces many coastal and flood management challenges over the 21st century. These sections also set the context for the selection of the Solent as the case-study region for this research, and the research requirements for further understanding of coastal flooding.

2.3.2 Coastal flood events – UK perspective

Since at least Roman times the British coast has been heavily modified by flood and coastal defences to protect human activities, and land has been reclaimed for agricultural, industrial, port and residential development. The UK now has around 2300 km of artificially protected coast, the longest in Europe (Eurosion, 2004) with approximately 1300 km sea defences aimed at protection against coastal flooding

in England and Wales (Madrell et al., 1998). However, maintenance costs are high, with a legacy of seawalls and drainage systems built more than a century ago (Allsop et al., 2005).

With a history of North Sea floods, storm surges, and the presence of the UK capital city; the east coast is a focal point for coastal flooding in the United Kingdom. The UK has also experienced severe coastal flood events on the south and west coasts (Lamb, 1991; Zong and Tooley, 2003). Notable storms on the south coast include the December 7th -8th 1703 (or November 26th-27th 1703 on English calendars at that time). This windstorm is reported to have washed away the lowermost houses of Brighthelmstone (Brighton) (RMS, 2003b). Surges of between 1 m – 2 m occur quite frequently in the Bristol Channel, although timing with high astronomical tide is critical to flooding, due to a mean spring range of 12.2 m (the world's second largest) (Horsburgh and Horritt, 2006). Surge and tide combined to devastating effect on January 30th 1607 to drown between 500 and 2,000 people, inundating more than 500 km² of land covering villages and isolated farms on low-lying coastlines around the Bristol Channel and Severn Estuary (RMS, 2007; Horsburgh and Horritt, 2006). The coastlines of Devon and Dorset were devastated by a storm surge on November 22nd 1824 (Le Pard, 1999; West, 2010) where overtopping waves drowned 26 people in the Dorset Village of Chiswell (Lewis, 1979) which is amongst historically flood-prone communities in the vicinity of Chesil Beach (Stripling et al., 2008).

The floods of January 31st-1st February 1953 (and the German Bight floods of 1962) are for many in living memory, and mark pivotal changes in UK, and European flood risk management. The loadings on defences (see previous Section 2.3.1) caused more than 1200 defence breaches on the UK east coast; killing 307 people, flooding 647 square kilometres of land, damaging more than 24,000 houses, and killing over 46,000 livestock (RMS, 2003).

Many North Sea coast communities are sufficiently protected for extensive flooding to be considered an infrequent phenomenon. For example the Thames Barrier and associated defences are designed to protect London from a 1 in 1000 year (0.1 per cent annual probability) combined tidal-fluvial event, whilst high standards are also maintained for sensitive infrastructure and locations where the physical flood hazard is likely to be exceptionally high (e.g. nuclear power stations). For example, similar water levels to those of the 1953 storm surge impacted the UK east coast 8th-9th November 2007 with relatively minor flooding (Horsburgh et al., 2008); whilst a larger surge and water level than 1962 hit Hamburg in 1976 with no serious impact (von Storch and Woth, 2006). In most UK coastal areas, defences are now designed to prevent flood events with a return period of 50-200 years (Zou and Reeve, 2009) with the higher end of these targets set for urban areas.

There have not been any direct coastal flooding fatalities (drowning etc.) in the UK since 1953⁵, but notable events have occurred on the west coast, including a 1.2 m surge and wave overtopping at Fleetwood on the Fylde peninsula on 11th November 1977 which flooded 1800 homes, many to depths of more than 1 m (Posner, 2004). On 13th December 1981 a storm surge in the Bristol Channel, overtopped and damaged 11 km of coastal defences, causing flooding in Avon and Somerset (EA, 2011b). These floodwaters reached the M5 motorway, and encroached over 1000 properties, 50 km² land and drowned 2,500 livestock (sheep, cattle and pigs) and more than 20,000 chickens (EA, 2011b). Towyn in Kimmel Bay on the north-east Wales coast was impacted by a 1.3 m surge and 4.5 m waves on the 26th – 27th February 1990 which breached 467 m of Network Rail owned sea wall, inundating 10 km² of land and 2800 properties (Bates et al., 2005; EA and DEFRA, 2009).

Relatively recent defence improvements are associated with the paradox of risk growth. For example UK flood damages in the 1953 North Sea floods equate to approximately £1 billion from 2003 values (de la Vega-Leinert and Nicholls, 2008) whereas an equivalent flood could now cause £10 billion damage due to the increased assets at risk and impacts such as disruption (Muir Wood et al., 2005). Amongst the strongest defence structures in the UK protect Canvey Island which saw the largest UK cluster of flood deaths in the 1953 North Sea event (58 fatalities) (Baxter, 2005). The population on low-lying Canvey is now even more reliant on defences and flood warnings. In 1953 there were 12,000 residents on Canvey (Baxter, 2005), and there are now nearly 40,000 (UK Census, 2001). On the west coast, Bristol, Gloucester, Cardiff and Swansea are within floodplains containing a total of £32 billion worth of property threatened by a repeat of the 1607 surge event (RMS, 2007) although defences and warning systems would now play a much greater role.

Although protected by defences and flood forecasting and warning systems, approximately 6 million people in the UK (about 10 per cent of the population) are presently considered at risk of combined of tidal and fluvial flooding (DEFRA, 2012). The total numbers of properties within this broad definition of flood risk are:

- 2.4 million in England (EA, 2009a);
- 220,000 in Wales (EA, 2009b);
- 125,000 in Scotland (SEPA, 2011);
- 46,000 in Northern Ireland (HRW, 2007).

Currently 560,000 properties are viewed as exposed to a significant risk (an annual probability of 1.3 per cent or 1 in 75 years on average of flooding). These amalgamated numbers (inclusive of river and

⁵ There are incidents of people being killed by wave overtopping in the vicinity of sea walls, whilst premature deaths resulting from illness of distress linked to the floods are likely to have occurred, but are difficult to quantify.

coastal flooding) can be appropriate to mention from a coastal perspective, because fluvial and coastal flood sources can interact, for example due to tide-locking of rivers or the convergence of overland flows from each source. However, specific to tidal flood risk, it has been estimated that 2.5 million people live in coastal areas below 5m Ordnance Datum (approximately mean sea level) in England and Wales, including one million in London (de la Vega-Leinert and Nicholls, 2008) which approximates to between 1 - 1.5 million UK properties at risk of tidal flooding alone. Defra (2012) suggests that 170,000 properties in England and Wales are at significant risk of an exclusively tidal (i.e. storm surge) flooding event; and SEPA (2011) approximate that approximately 21,000 properties are at risk of tidal flooding in Scotland.

2.4 Understanding and forecasting coastal flooding

This section extends upon explanations of some of the modelling techniques and datasets mentioned in sections 2.1, 2.2 and 2.3, and how these may be used for understanding and mitigating flood risks. It has become increasingly important and expected by society that there should be knowledge of where and how flooding can occur in any given location. Earlier sections have introduced methods such as return period analysis and inundation modelling, and as explained these can be used to illustrate the spatial distribution of past floods or flood scenarios. For example these are useful when integrated with other information to generate flood maps such as the types listed in table 2.2, statistics of flood damages, or real-time information to warn of flooding. Modelling may form the basis for understanding flood risk (the product of probability and consequences) of flooding over any given interval of time.

Meteorological and oceanographic forecasting methods mentioned in Section 2.1 may also be linked to systems which disseminate and allows warnings of risks near to the time of potential flooding.

Table 2.2 Basic definitions of local scale flood map (Merz et al., 2007)

Type of flood map	Spatial distribution definition
Danger	Flood dangers without exceedance probability
Hazard	Information on flood intensity and probability for several scenarios.
Vulnerability	Exposure and /or susceptibility of flood prone elements (population, buildings, natural environment).
Damage risk	Expected damage risk for single or several events with an exceedance probability.

2.4.1 Flood risk assessment

This research is not aimed at generating flood risk calculations, but for completeness, flood risk assessment is briefly considered since this has been widely used to determine flood probabilities and characteristics, whilst invoking use of the tools mentioned earlier in this chapter, such as extremes

analysis and hydrodynamic models. Flood risk assessment methodologies (Reeve and Burgess, 1993; Hall et al., 2003; Dawson and Hall, 2006; Gouldby et al., 2008b) have been developed to allow planning of coastal defences, land-use, insurance and flood event management.

Risk assessments can consider to a varying degree, the combined effects of sources, pathways and receptors; often to approximately quantify the potential for spatially varying impacts across a floodplain, and over a given period of time. The emphasis of outputs may focus upon direct flood impacts such as loss of human life, damage to property or other potential impacts, by using values and inventories of floodplain contents. Other categories like impacts of flooding to traffic infrastructure, cars, agricultural products or even indirect impacts such as disruption tend to be investigated by other approaches.

Prediction of flood risk R_{fc} is usually attained by combining flood occurrence probabilities P_{fc} (which to varying detail can incorporate sources such as return periods, and pathways that may link sources to the receptor) with expected damages and losses $E(D)$ so that:

$$R_{fc} = P_{fc} \cdot E(D) \quad (10)$$

A variation upon this mathematical expectation of risk (R) and damage is also described by Dawson and Hall (2006):

$$R = \int p(x)D(x)dx \quad (11)$$

Where x is a vector of variables that describe the properties of the system such as the strength of flood defences or the loading upon them; $p(x)$ is a joint probability density function of x , whilst $D(x)$ is a quantified measurement of impact (often expressed in economic terms), which is a function of x . This risk calculation provides a snapshot of risk at any instance in time. As shown in Figure 2.12, this can be used to evaluate the following aspects of flood risk:

- **Tolerable risk:** this is viewed as difficult to assess (Kortenhaus and Kaiser, 2009) due to being subject to a range of parameters, including revisions of return periods and public perceptions of risk.
- **Residual risk:** can be calculated by comparing predicted and tolerable risk.
- **Management of residual risk:** by defences, planning, or measures for flood event management.

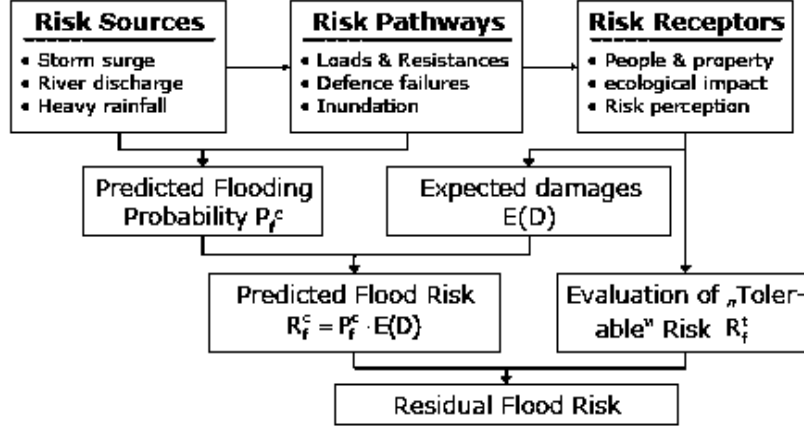


Figure 2.12 The main components of a flood risk assessment methodology

In general, risks will be changing through time due to various natural and socio-economic processes, and flood defence changes, and equation 11 can be extended accordingly:

$$R(t) = \int p(x, t) D(x, t) dx \quad (12)$$

Described in Dawson et al (2011b), these equations provide a general framework for quantifying risk and to compare the net benefits of all costs for each year of different adaptation strategies, discounted back to the present date the present value of risk (PVR) over an year time period (with discount rate d) calculated using:

$$PVR = \sum_{t=1}^n \frac{R(t)}{(1+d)^t} \quad (13)$$

Also described in Dawson et al (2011b), equation 13 can be extended to a spatial analysis of flood risk over a given segment of time; by using water level and wave (and sometimes river flow) joint probabilities and their spatial distribution. These can be integrated with fragility functions and inundation calculations to generate a spatial distribution of flood depths for each loading condition.

Risk or inundation maps can be intersected with the spatial distribution of information about floodplain assets. For example, in the UK this is often according to information on property type (from the National Property Database). For residential properties an inventory of residential property types has been compiled by means of expert judgement and relevant datasets (type, age and social status); with each of the building fabric and household inventory components assessed with its depreciated (average remaining) value. A similar approach is carried out for non-residential properties; with the approximate value per square metre of building fabric, fixture and fittings, moveable equipment and inventories for each economic branch derived from surveys. Subsequently, flood data combined with property dependent depth-damage curves which are contained in the Multi Coloured Manual (MCM) (Penning-

Rowse et al., 2005) enables functions describing damage in the floodplain conditional on flood depth. This can show either the damaged share or the absolute monetary amount of damages per property or square metre of a certain group of elements at risk as a function of the magnitude of certain inundation characteristics. Currently, the main inundation parameter considered in these damage functions is water depth, whilst velocity, duration and time of occurrence are rarely taken into account (Messner et al., 2007). As the susceptibility of elements at risk depends on their type and attributes (e.g. mode of construction), properties of similar type are often grouped and expressed by one approximate damage function (although the extent of this aggregation and categorisation varies among the different approaches).

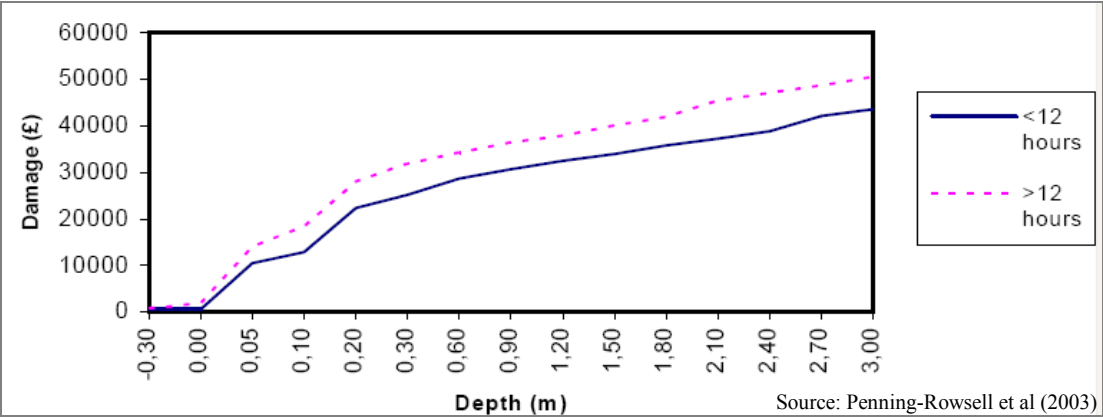


Figure 2.13 Example of UK Depth-Damage-Duration Data for Residential Properties (sector mean)

In development and application of a regional flood risk assessment methodology, Gouldby et al (2008b) evaluate residual risk attributed to defences and flood-spreading, from multiple simulations. An example output is shown in Figure 2.14, which is a spatial evaluation of expected annual damage (EAD) in the Thames Estuary.

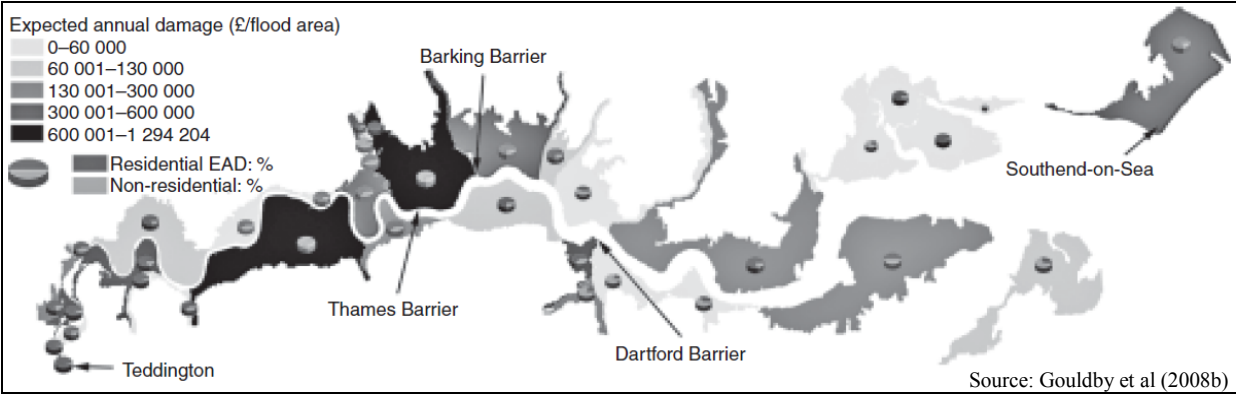


Figure 2.14 Example of spatial distribution of EAD in the Thames Estuary derived from a risk assessment

Empirical data and/or flood models can also be used to map where the physical inundation impacts are likely to be worst for people. For example, this may provide estimates of fatalities from a modelled

flood which can be plotted against flood probability (e.g. the area under the curve may then be used to determine the annual average number of fatalities for different flood risk scenarios). More sophisticated approaches combine dynamic computational simulations of receptors ('agents') and the flood wave (using a numerical inundation model), known as agent based modelling. As demonstrated by Di Mauro and Lumbroso (2008) and Dawson et al (2011a) this enables flood event simulations to indicate likely areas of trapped roads, congestion, and movement of people; which can be used to optimise evacuation and plan the location of shelters.

Jonkman et al (2008) consider methods to predict mortality using empirical models, mostly for hydraulically extreme flood events (e.g. tsunamis, dam breaks, storm surges and breaching), and suggest that loss of life prediction methods may provide an indicative estimate of the loss of life from a flood. In the UK, related research has included the 'Risks to People' project (DEFRA and EA, 2003; DEFRA and EA, 2006) describes methods to assess and map the risk of death or serious harm to people caused by flooding. For example a method to generate hazard maps combines: (1) flood hazard (depth and velocity of water, and a debris factor), gained from hydraulic modelling and classification of the potential for an area to contain debris during a flood (e.g. whether an urban or rural area); (2) area vulnerability, from scores for the availability and performance of flood warnings, the likely speed of onset of a flood, and the nature of buildings, and (3) people vulnerability (percentage of residents aged 75 years or over, and the percentage of residents suffering from long-term illness). However, the outcomes of flood events are difficult to simulate and predict due to the complex chain of events and responses across the SPRC model, including flood management. Methods for real-time forecasting of wind, waves and water levels can be combined with preparatory measures (such as flood mapping and contingency plans). An essential part of flood incident management is flood warnings, which are now described.

2.4.2 Coastal flood forecasting and warning systems

Coastal flood forecasting and warning processes can be differentiated, but are part of the overall flood forecasting, warning and action process (Figure 2.15). Noted in Section 2.1 in the UK, each coastal flood warning division (Figure 2.2) has a reference port, and each of these has predefined danger levels ('trigger levels') derived from the knowledge of conditions likely to cause flooding, often evolving from experience. When this level is forecast to be reached, the Met Office then alerts the EA or the Scottish Environmental Protection Agency (SEPA). Beyond this, further examination of the weather and sea conditions may be applied within each division before the decision is given to administer warnings. Information from the UKCMP is usually provided 12 to 36 hours before a significant event (EA, 2009), whilst according to the EA Customer Charter, this information is used to provide a minimum of 2 hours warning prior to flooding. The EA often use the National Flood Forecasting System (NFFS) (an open architecture system with many different types of model running concurrently)

to develop warnings, although a consistent approach is not applied nationally (DEFRA and EA, 2004), partly due to the diversity and scale of the UK's coastline and levels of risk. Warnings are usually generated from look-up tables which use fixed conversions between offshore and nearshore waves combined with deterministic water level predictions (best estimate predictions at 15 minute intervals updated four times daily). Flood warning delivery may be via the EA website, media, fax, text message or phone. Flood warning statuses are regularly updated: categories range from 'Flood Watch' (e.g. farmers would probably move their animals from low-lying) to 'Severe Flood Warning' (where a serious situation is anticipated). An 'All Clear' status is issued when the threat has passed.

Numerical models linking atmospheric and offshore processes to wave run-up predictions have also been demonstrated in regions exposed to tropical cyclones (Cheung et al., 2003); although in many parts of the world the majority of real-time operational forecasting systems rely upon relatively coarse resolution meteorological and sea-surface forecasts with some diversity that reflects how they have evolved to address the needs of their own coastal and marine environments (Flather, 2000).

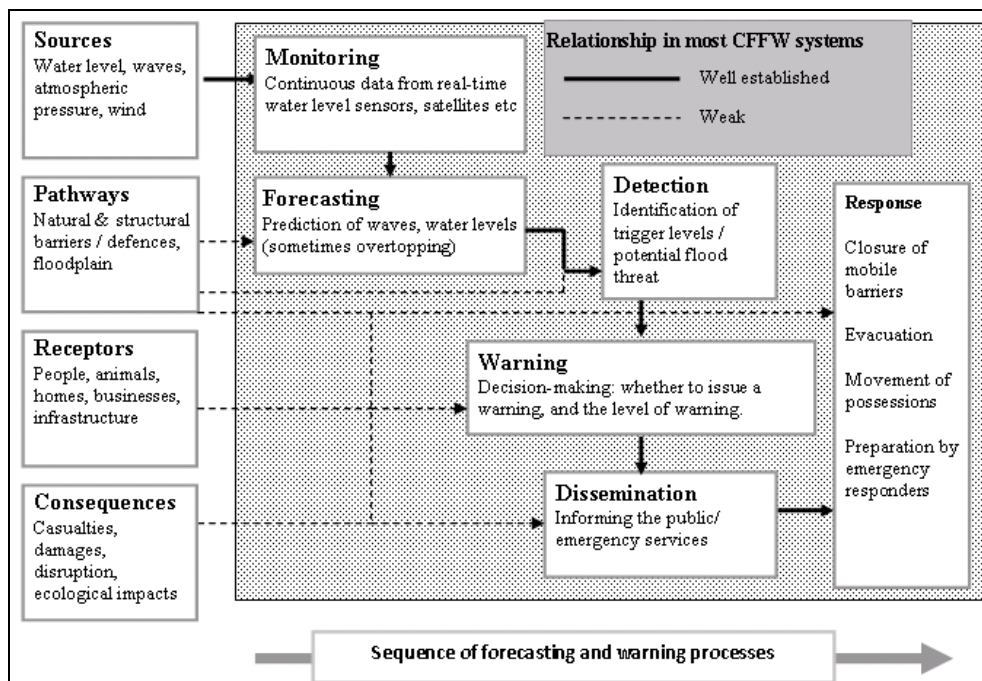


Figure 2.15 Stages within the flood forecasting and warning process

Look-up tables have been extended to predictions of wave overtopping rates and volumes in the northeast of England, from Berwick-on-Tweed to the Humber Estuary where a semi-numerical wave overtopping model (Hedges and Reis, 1998) is used for a dual-trigger warning system (Lane et al., 2008; EA, 2007a). The northwest region of England has a well-established model of this kind using a module in NFFS known as TRITON (EA, 2007a). This has an interface which includes a colour coded list of sites indicating whether threshold levels have been exceeded by forecasts; based upon hydraulic models. Overtopping is quantified by the spectral nearshore wave model SWAN linked to a numerical overtopping model known as AMAZON. However, as implied in Figure 2.15, in most circumstances

numerical models used for real-time coastal flood forecasting and warning systems currently provide a more comprehensive understanding of offshore processes, grading into more empirical modelling approaches between the nearshore zone and floodplain (DEFRA and EA, 2004; Hu and Wotherspoon, 2007). Amongst limitations are that inaccurate, vague or poorly delivered flood warnings may not interface closely enough with social science due to a lack of ability (from the available modelling approaches) to target and prioritise warnings for certain receptors (e.g. those untrusting of, or with experience or inaccurate or unspecific warnings, or in need of particular assistance to respond – elderly, long-term illness, disabled etc.) (Twigger-Ross et al., 2009).

2.4.3 Model validation

Amongst the main methods to handle links between data and model uncertainty is to use calibration and validation. A simple interpretation of *calibration* is to adjust a set of parameters associated with a model, so that the model agreement is maximised with respect to a set of experimental data; whereas a model is said to be *validated* if its accuracy and predictive capability in the validation period are proven to lie within acceptable limits or errors for a particular purpose (Hunter et al., 2007). Related topics are verification and sensitivity analysis, which are different to validation, but in modelling exercises have similar objectives: to improve the model itself, and/or to improve understanding of the models outputs. Dual use of calibration and validation are well-known for meteorological and oceanographic modelling where actual real-time recorded measurements such as water level can be assimilated with numerical modelling, which is essential to attain the accuracy required for flood forecasting (e.g. Horsburgh and Flowerdew, 2009). For fluvial inundation modelling, benchmarking studies have proved highly beneficial in determining the best modelling approaches for use in given situations and their potential prediction accuracy (Hunter et al., 2008). Formal hydraulic model calibration procedures such as the generalised likelihood uncertainty estimation (GLUE) methodology have been applied to fluvial flood models, with considerable success (Beven and Freer, 2001; Aronica et al., 2002; Hall et al., 2005). However, in most coastal areas validation data is rarely available (Bates et al., 2005).

To develop and test coastal flood models, observations of interest are the flood inundation extent (Bates et al., 2005). These datasets are rarely available or compiled, partly due to the infrequency of large coastal floods, and the fact that collecting scientific data can be low on the list of priorities during or in the aftermath of a flood. Coastal flood model evaluation can comprise a compilation of hard data (i.e. tide gauge measurements, surveying of debris lines, geo- and time-referenced aerial photography) or soft data (i.e. photos, TV coverage and eye witness descriptions) to approximately reconstruct events (Bates et al., 2005; Gallien et al., 2011; Smith et al., 2012b). Literature relating to this topic is surprisingly sparse, despite the recognised requirement for more widespread and comprehensive validation (Brown et al., 2007; Smith et al., 2012b). Smith et al (2012) describe a coastal modelling validation study combining empirical wave overtopping and the resultant inundation predictions, using

a mixture of hard and soft data to validate simulations of floods on 13th December 1981 in the Bristol Channel, UK; and discussed the known uncertainty in empirical overtopping predictions, as otherwise only discussed in overtopping-focussed studies such as Pullen et al (2009) who compare between measured and calculated wave overtopping discharges. Flood event data collection is undertaken to varying degrees in other coastal areas. For example, the U.S Federal Emergency Management Agency (FEMA) have a rapid response capacity to document the effects of coastal and inland flood events and provide a historical perspective on planning decisions and assessment of other events (FEMA, 2011). Such data collection exercises provide a timeline of data that can indicate the severity of hazards that can be expected due to a complex combination of factors involved in flooding (e.g. characteristics of inundation, sequences of events, hazard hotspots, and human responses). Numerical flood simulations are also more plausible and accurate if validated. Validation of breach defence failure analysis is also uncommon; Flikweert and Simm (2008) compare real defence breaches (in the UK 2007 river floods) to fragility curves, demonstrating a high degree of uncertainty when attempting to predict geotechnical failures using simplified structural strength data.

2.5 Changes to coastal flood risk

An extensive and growing body of literature indicates the large potential impacts of sea-level rise (Nicholls, 2011). It is clear that coastal flooding is already a significant global threat to human populations (McGranahan et al., 2007), which is growing due to climate and socio-economic changes (Nicholls, 2010). Coastal areas and the distribution of risks are also changing due to the impacts of human developments, such as urbanisation, port and industrial expansion, and the drainage of coastal wetlands. Analysis of historic water level datasets suggests that sea-level rise is increasing the probability of extreme events in a number of coastal regions (Church et al., 2006; Menéndez and Woodworth, 2010; Haigh et al., 2011; Wahl et al., 2011). Sea-level rise is mainly caused by eustatic effects (which include the amount of water in the oceans, water temperature, and oceanic circulation patterns), although isostatic effects (vertical land movements caused by compression and decompression of the Earth's crust) can be important. In some regions deltaic subsidence is the largest contributor to relative sea-level rise (Nicholls et al., 1999; Syvitski et al., 2009). For example, during the twentieth century, Tokyo subsided by 5 m, Shanghai by 3 m, and Bangkok by 2 m (Nicholls and Cazenave, 2010; Hanson et al., 2011).

The United Kingdom Climate Change Impact Programme (UKCP09) based on climate modelling from the Intergovernmental Panel for Climate Change's 4th Assessment Report (IPCC AR4) (Lowe et al., 2009) presents what is considered to be the current best understanding of how the climate system operates and might change in the future around the UK. Isostatic effects are considered likely to be small in comparison to the absolute sea level rise estimates over the 21st century in the UK; and some studies have suggest that uplift rates are now modest and are less than eustatically-driven rising sea

levels (Rennie and Hansom, 2011). However, glacial isostatic adjustment is responsible for spatially variable rates of SLR: southeast England is associated with downwards vertical land movement, and the north upwards vertical land movement (in particularly the northwest of Scotland) (Shennan and Horton, 2002). The vertical land movement velocities used in UKCP09 projections are taken from Bradley et al (2009) and are assumed to be constant for the 21st century projections.

The mean estimates of sea-level rise have remained steady over the past decade, and medium emission climate change scenarios suggest approximately half a metre can be expected by the end of the 21st century. However, the original UKCP09 work was based upon estimates which excluded climate-carbon cycle feedbacks and the possibility of future rapid dynamical changes in ice sheet flow. The biggest uncertainty in sea level projections is the response of the large ice sheets of Greenland and west Antarctica. Consequently the UKCP09 marine report provides an additional high-plus-plus (H++) scenario. The H++ scenario for possible SLR for 2100 (compared to 1990) gives a lower estimate (0.93m) obtained from the maximum global mean sea level rise value given by the Intergovernmental Panel for Climate Change's 4th Assessment Report (IPCC AR4), whilst the top of the range (1.9m) is derived from indirect observations of sea level rise in the last interglacial period. Whilst considered unlikely, other studies acknowledge even larger changes are theoretically possible (Rohling et al., 2008).

Table 2 3 UKCP09 relative sea-level rise projections over the 21st century for London (inclusive of eustatic and isostatic change) under three emission scenarios and with 5th to 95th percentile confidence intervals. The changes are amalgamated for the periods 1980–1999 to 2090–2099 (Millin, 2010).

Year/ Scenario	Relative SLR (m)		
	5 th percentile	Central estimate	95 th percentile
High emissions	0.154	0.456	0.758
Medium emissions	0.131	0.369	0.607
Low emissions	0.116	0.298	0.480

The Foresight national assessment of flood risk (Evans et al., 2004) approximated that, with no adaptation to increasing coastal flood risk, the expected annual damage due to coastal flooding in England and Wales could increase from the current £0.5 billion to between £1.0 billion and £13.5 billion. In terms of drivers of coastal flood risk, recent observed trends in storm surge frequency, magnitude, and wave climate, and changes to their effect upon extreme sea levels appear to be less important than changes in global mean sea level over the next 100 years (Horsburgh et al., 2011).

The Environment Agency (EA) have estimated that investment into the building and maintenance of flood defences, to maintain the flood threat to existing standards in England, will by 2035 need to almost double to £1billion a year (compared to £570million now). In Wales, the equivalent figure is

around £135 million a year (compared to the present value of approximately £44 million) by 2035. Non-structural measures such as changes to land use spatial planning, insurance and flood resilient construction may yet prove to reduce the burden of expectation placed upon traditional sea wall and embankment construction. Furthermore, efforts to reduce coastal squeeze and intertidal ecosystem loss may be increasingly used, although the success of natural systems response to rapid SLR is uncertain. Burgess and Townend (2004) estimated that by the 2080s the annual cost of coastal defence structures will be between 150 and 400 per cent of the current levels (depending on the emissions scenario). However, these estimates did not incorporate ‘non-structural’ flood risk reduction measures. Costs were less sensitive to geographic location than to emissions scenario, and predicted to increase because structures are vulnerable to increases in water depth (and wave heights reaching structures increase linearly with water depth). Raising crest levels may have to be accompanied by re-engineering of entire structures to mitigate scour around the toe, overall resulting in a substantial increase in costs (of two to four times the present cost to provide a similar level of performance).

A number of initiatives and studies aim to improve the understanding and management requirements for coasts, flood risk and climate change. These include:

- *Climate Change Risk Assessment (CCRA)*: this study has quantified the possible impacts of climate change, published by the UK Government on 25 January 2012 and is the first assessment of its kind for the UK and the first in a 5 year cycle. The CCRA reviewed the evidence for over 700 potential impacts of climate change in a UK context. Detailed analysis was undertaken for over 100 of these impacts across 11 key sectors (including coasts and flooding) on the basis of their likelihood, the scale of their potential consequences and the urgency with which action may be needed to address them (Defra, 2012);
- *Shoreline Management Plans (SMPs)*: SMPs provide large-scale assessments of coastal processes over the coming century for the coastline in England and Wales, and the framework for dealing with flooding and erosion. Many have completed a second review;
- *Living With Environmental Change (LWEC) and the National Flood and Coastal Erosion Risk Management (FCERM)*: the LWEC partnership coordinated a steering group (consisting of the main flooding research funding organisations) in March 2012 to oversee delivery of the FCERM strategy covering the whole of the UK (England, Wales, Scotland and Northern Ireland). This is intended to cover the period from 2011-2030, and aims to facilitate future research collaboration and exchange of knowledge between researchers and practitioners, and provide guidance to all organisations involved in flood and coastal erosion risk management (including local authorities, internal drainage boards, water and sewerage companies, highways authorities, and the Environment Agency). Some outcomes of the strategy may have implications for coastal flooding in the near future.

The changing drivers and consequences of coastal flooding provide a large uncertainty to what could happen in the future. Any evaluation of potential flood events associated with sea level rise encounters this uncertainty, alongside a range of complex (e.g. development, land-use planning) scenarios. The Defra (2012) Climate Change Risk Assessment (CCRA) estimates that a coastal flooding event of 1 in 75 year probability could affect 170,000 properties in England and Wales, increasing to between 500,000 and 1.25 million properties likely to be affected by 2080 using the full range of UKCP09 scenarios. This highlights large potential changes in flood risk, and uncertainty. Flood warning and defence strategies, flood managers and communities would benefit from more specific and accurate estimates of flooding consequences. Hence flood event analyses should aim to achieve this, whilst also capable of being rapidly updated, because so many components of flood risk are changing (e.g. non-stationarity of still water level return periods due to SLR) alongside revisions to data and analysis techniques.

2.6 Summary

Technology and theory have progressed to enable various forms of coastal flood modelling, analysis and prediction. Weather and water level forecasts are available in most regions at least a day in advance of a given coastal flood event; whilst land and defences heights can be surveyed at high spatial resolution and sub-decimetre levels of vertical accuracy. There is however an emphasis upon flood sources within numerical coastal flood forecasting models, with pathways (defences and floodplains) less integrated. Meanwhile, modelling of defence failures and coastal inundation has been demonstrated and applied for several case studies (e.g. Bates et al., 2005; Nicholls et al., 2005; Dawson et al., 2005b; Dawson et al., 2009), including detailed reviews of uncertainty e.g. (Brown et al., 2007; Gallien et al., 2011). Defence failure models and inundation mapping have also been demonstrated for flood forecasting (Golding, 2009b; Ray et al., 2011). However, integrated coastal flood modelling, where (to varying degrees of detail) inundation simulations are linked to coastal processes and defence failures, has not yet progressed far in terms of operational use; mainly because model outputs are widely acknowledged as highly uncertain for depicting specific event scenarios. Many uncertainties propagate through coastal flood modelling, from the oceanographic boundary conditions, coastal defence failures, floodplain DEM. Flood risk assessments have included the development of now well-established methods to provide scientifically robust estimates of flood probability and consequence (e.g. Dawson and Hall, 2006). However, there remains a shortage of literature that scrutinises and demonstrates an understanding of individual coastal flood events and their potential impacts across a spectrum of loadings and floods. A lack of validation data is one of the most frequently encountered problems to assess events and model outputs, partly due to the rarity and large consequences of coastal floods.

The case of Storm Xynthia in France, 2010 (Section 2.3.1) demonstrated how a lack of understanding of coastal flood events can be catastrophic; and this is a recent and stark reminder that methods to predict

inundation will become increasingly important to understand the impacts of extreme events.

Simulations of synthetic events can determine coastal flood event impacts where extreme loading events have not yet been realised (e.g. due to centennial-scale probabilities of extreme weather events, accompanied by the relative recentness of much coastal development), especially where extreme water level events gradually become more likely due to climate change and SLR.

Broad-scale impact assessments of regions exposed to storm surges and sea-level rise (e.g. Hanson et al, 2011) have estimated economic risks and generated scenarios for adaptation; whilst detailed modelling (e.g. Brown et al, 2007; Gallien al, 2011) provides a localised (e.g. street level) view of flow routes and depths, to allow interpretation of potential flood consequences. However, regional case-studies that integrate detailed modelling of loads, defence failure, hydraulic modelling and consequences are lacking. In particular, the generation and analysis of multiple inundation simulation scenarios from different failure mechanisms and loading conditions is not widely demonstrated and potentially beneficial to regions where floods are quite small and threaten to grow with SLR (Wadey et al., 2012). Hence in view of existing research and the need for the development of methods to improve the understanding of coastal flooding, this thesis presents a case-study approach to assess coastal flood events. This includes:

- Simulating theoretical coastal floods and indicating the consequences that could occur, as a result of water levels, wave loadings, and defence failures. Suggested by the literature, the fundamentals for this type of flood modelling are to compile and integrate detailed information about the defence systems, loadings and floodplain topography.
- Infrequently carried out within coastal flood research is to integrate flood simulation methodologies with observational flood event data sets. This thesis describes a reconstruction and validation of a coastal flood event by compiling quantitative and qualitative data (Wadey et al., 2013). Such post-event ‘forensic’ style analysis and collation of datasets to validate coastal flood models and evaluate events is currently rare, but important to understand facts about these events (e.g. flood extents, water depths, number of properties impacted). This is considered essential in other locations and activities: the U.S Federal Emergency Management Agency (FEMA) collect information about natural hazard events soon after they occur, whilst systematic and critical incident reporting has been notoriously progressive in high risk industries such as aviation and health-care (Mahajan, 2010).

The development and evaluation of coastal flood modelling on a case-study basis could offer new generic insights to flood analysis (*c.f.* Hall, 2010). In relation to coastal management, new and useful insights are likely to be more generically relevant if the case study is a large and varied region. Also, to demonstrate the benefits of this proposed new type of study, the geographic area selected should be a location where a thorough understanding of present and future coastal flood event impacts is currently limited. The literature suggests that new modelling studies need to contribute to knowledge for both

research and practical applications, e.g. shoreline management, flood forecasting, warning, planning, and as scenario-development tools to enable imaginative thinking about extreme events and the impacts of climate change. Currently the monitoring and modelling of coastal flooding tends to focus more upon regions where coastal flooding is well-known to have the potential to be catastrophic to life and property (refer to Sections 2.1 and 2.3.1), although in many countries data sets can exist which have potential to be utilised for coastal flood analysis at greater detail than present. Such data sets and tools may for example include defence surveys, floodplain LiDAR data, and non-commercial inundation models. Furthermore, with the possibility of accelerated climate change and SLR, coastal flood event analyses and the aforementioned methodological approaches should also be able to adapt and remain applicable to changing coastal boundary condition definitions (e.g. updated return period analysis, defence data, methods to simulate and predict failure). Subsequently, a region suitable for this case study is the Solent on the UK south coast, which was introduced in Section 1.4 and is described in more detail in the following chapter.

3. Coastal Flooding Case Study: The Solent

This chapter provides an overview of the relevant characteristics (e.g. sources, pathways and receptors, and a background to past flood events) of the Solent case study area, which is introduced in Section 1.5. This includes two more detailed case study sites within this region (Portsmouth and Pennington).

3.1 Regional overview

The Solent case-study is within the Environment Agency's Southeast Region. Alongside the South Downs, the Solent is a sub-region for which defences and flood warnings are managed by the EA (and local councils). The Solent contains two shoreline management plan (SMP) (Defra, 2006) areas: the mainland Solent, and the Isle of Wight. Figure 1.1 introduces the location of the Solent case study area, the areas broadly at risk of coastal flooding, and six 'sub-regions' for analysis that are described in Section 6.1. Figure 3.1 is a map which shows locations around the Solent in greater detail, including urban areas and rivers (which are shown because these may exacerbate and provide pathways for tidal flooding).

Prior to inundation by the sea after the last ice age, the Solent was a river system. Marine conditions are likely to have reached the outer part of Southampton Water in the early Holocene after rapid sea level rise around 7,000 years before present. The form and extent of the Solent estuary has largely been controlled by changes in sea level until progressive development and land reclamation began in the 18th century. This was most significant around Southampton Water and Portsmouth; the two cities having grown together to form an urban area containing over one million inhabitants. The Solent-Southampton Water estuarine system is the largest estuary on the UK south coast (Levasseur et al., 2007). From north to south, the estuary is defined by Southampton Water, a 2 km wide and 10.3 km long meso-tidal spit with an artificially deepened channel. It is fed by the rivers Test, Itchen and Hamble which drain catchments of over 1500 km² (Townend, 2008).

The tidal range increases from approximately 2 m at Hurst to 5 m at Selsey; and the region is internationally renowned for its complex tides (Pugh, 1987). The amplitudes of tidal components which are influenced by resonance in the English Channel and more localised shallow water effects (M_4 and M_6 constituents) are relatively large in the region, compared to the amplitude of the main semidiurnal lunar (M_2) tidal constituent. This results in double high waters in Southampton Water (which are particularly pronounced during large spring tides and at mid-flood) and extended high waters in the eastern Solent. Typical semi-diurnal lunar spring tidal cycles for three locations across the region are shown in Figure 3.3. The Solent's defences are frequently subjected to hydraulic action which due to the double high tides can be prolonged during storms. This effect is most prevalent in the central and eastern area of the region.

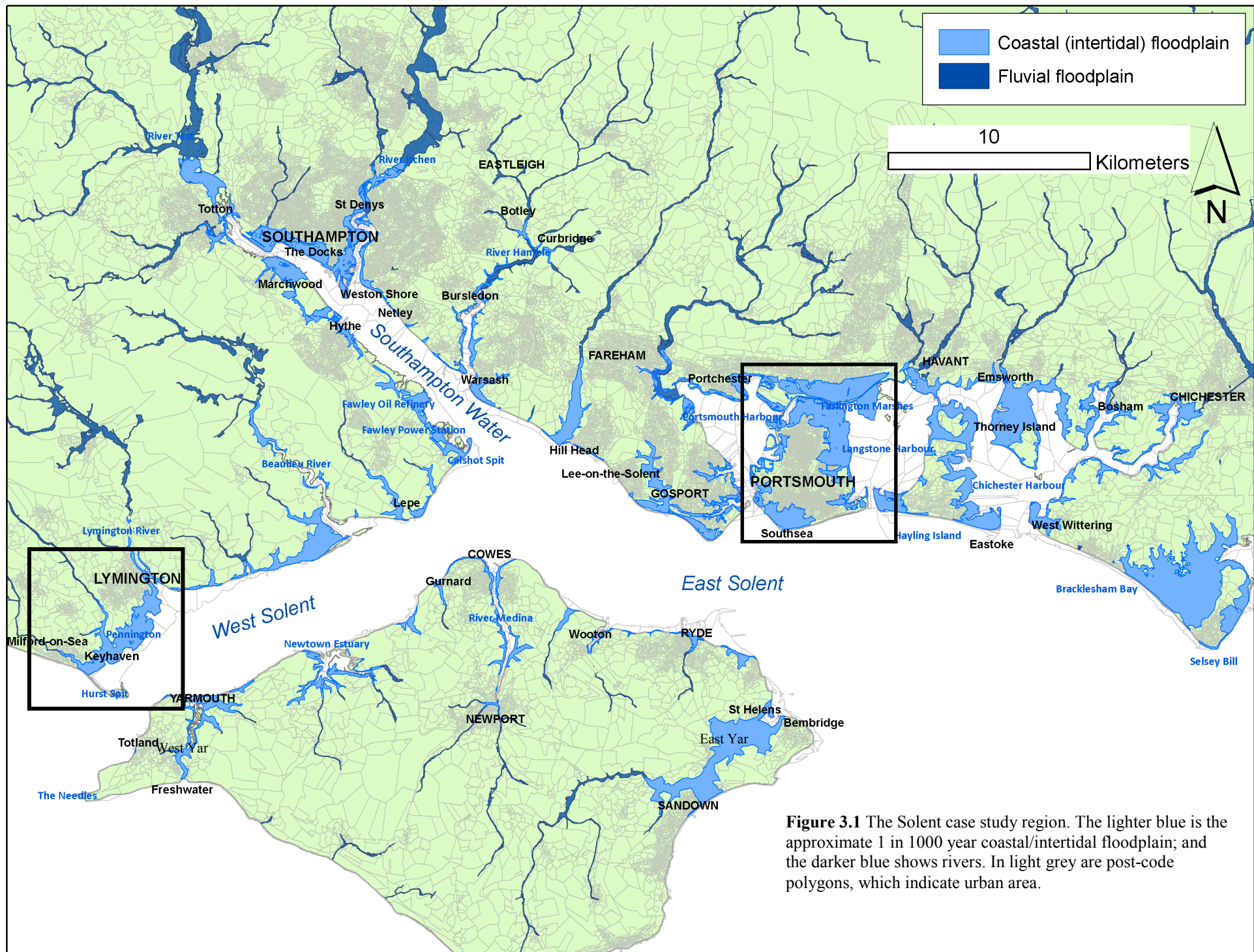


Figure 3.1 The Solent case study region. The lighter blue is the approximate 1 in 1000 year coastal/intertidal floodplain; and the darker blue shows rivers. In light grey are post-code polygons, which indicate urban area.

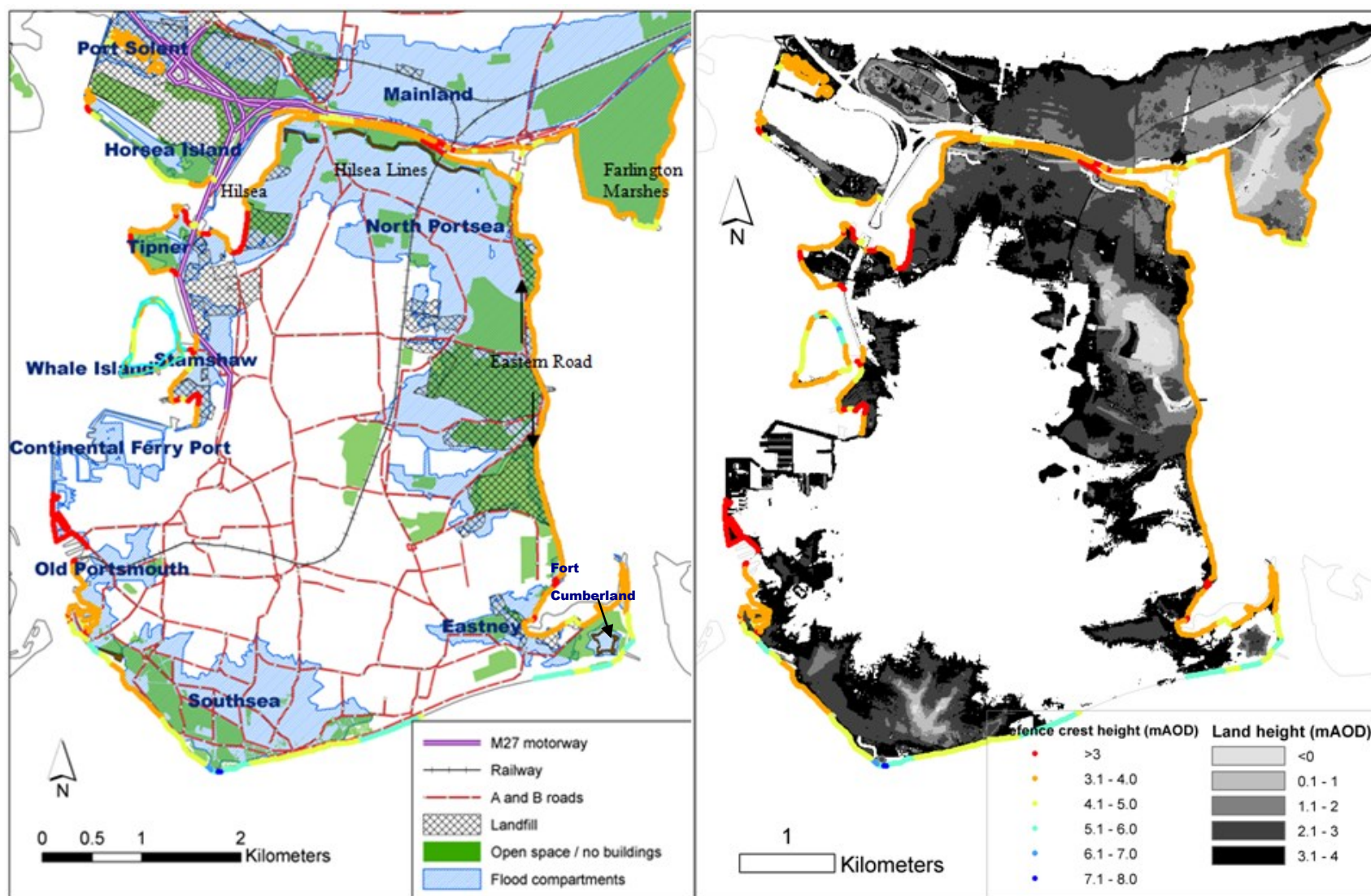


Figure 3.2 The city of Portsmouth; (a) key locations, urban area and main roads (the city is densely urbanised hence non-urban land is shown); (b) floodplain topography – note that parts of the Southsea Morass, Eastern Road (Saltern's) Golf Course, and Farlington Marshes contain areas below normal high tide levels.

Much of the Solent is sheltered from south-westerly Atlantic waves by the Isle of Wight, and a managed shingle barrier at the western end known as Hurst Spit (Bradbury and Kidd, 1998). Storm surges in the Solent mainly occur as a result of low pressure systems that move from the Atlantic eastward over southern England (Haigh et al., 2004) whilst smaller surges also occur as a result of large North Sea storm surge events transmitted into the English Channel through the Dover Strait (Law, 1975). Tidal residuals rarely exceed 1 m; with only a 0.33 m difference between a 1 in 10 and 1 in 1000 year water-level (Haigh, 2009).

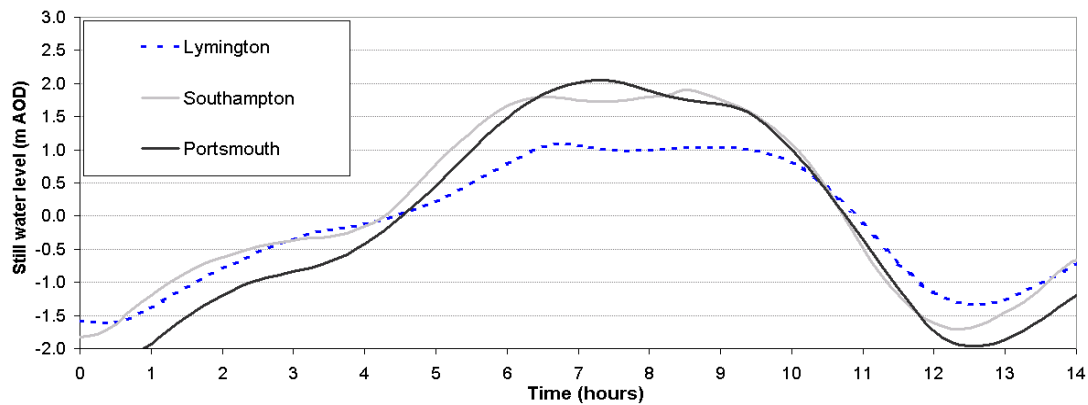


Figure 3.3 Water level time-series recorded at three locations across the Solent (refer to Figure 1.2) during a typical spring tide

Meteorological induced sea level effects on the UK south coast are generally less severe than on the east and west coasts; although surge events (Wells et al., 2001; Haigh et al., 2011) and Atlantic swell waves have been associated with coastal flooding (Mason et al., 2009). Historical associations with flooding in the region date to the legend of King Canute commanding the retreat of the sea at Bosham in Chichester Harbour more than a thousand years ago. Later accounts of pre-20th flooding include descriptions of storms which breached defences and caused flood water depths to exceed five feet (approximately 1.5 m) in south Portsmouth 4th-5th March 1818, washing away entire houses and drowning livestock (Davison et al., 1993). On the First of January, 1877, a south-westerly storm associated with an exceptionally high tide caused a storm surge that flooded parts of Southampton (Davison et al., 1993). In the early to mid-20th century, water levels were formally recorded at several tide gauges, which is discussed further in relation to storm surge and flood events in Chapter 5. Coastal floods in the Solent during the 20th and early 21st centuries have been frequent but usually involving small water depths, and with no recorded loss of human life (Ruocco et al., 2011).

From Calshot and northwards, the Southampton Water estuary is flanked by land which rises rapidly from the high water mark to over 10 m ODN, although narrow strips of coastal floodplain exist. Fawley Power Station and Oil Refinery are within the Environment Agency Flood Zones but are protected to a high standard (to withstand an approximately 1 in 1000 year event) (EA, 2010a). Since the start of construction in the early 20th century Southampton docks have served inadvertently as flood defences to

the city. Flood defences are otherwise not present, which could leave the city susceptible to the effects of sea-level rise (Atkins, 2007). To the east, the shingle beach at Weston Shore is susceptible to overtopping (SCC, 2010) and there are coastal floodplains along the tidal reaches of the River Hamble (Atkins, 2007).

On the Isle of Wight flooding in the town of Cowes is quite frequent due to a lack of flood defences, with notable events during the extreme water levels of 13-18 December 1989 and 10 March 2008. Several locations were flooded during 10 March 2008, including Yarmouth which was flooded without warning. The Yar floodplains that bisect the east and west sides of the Island are by far the most expansive areas of hinterland at risk of flooding on the Island, although have not been severely flooded in recent years. For both, tidal inflows are prevented by sluice gates which protect freshwater marshes and habitats. Lamb (1991) describes floods from a south-westerly storm during 9-11th November 1931 which covered the flood plain between Yarmouth and Freshwater Bay cutting off the area to the west. More frequently, tide locking is a problem for the numerous fluvial outflows on the Island (Entec, 2007).

East of Portsmouth, sections of open coast are exposed to Atlantic swell waves, for example long period waves overtopped defences and caused flooding at Eastoke on Hayling Island on 3 November 2005 (Ruocco et al., 2011). This event was associated with a lack of warning, attributed to bimodal swell wave conditions, which exposed a weakness in the trigger levels for flood forecasting and warning in this part of the region (Mason et al., 2009). Further east, the shingle ridge at Selsey protects low-lying land from being flooded, and is prone to breaching (Cope, 2004; Stripling et al., 2008). Within the large 'Broad Rife' floodplain is grazing pasture, West Sands Caravan Park, and residential and commercial property. The western end of the barrier protects the village of Bracklesham from flooding.

The population density in the Solent is relatively high in comparison with other areas of the UK (Table 3.1), particularly within the cities of Portsmouth and Southampton. At the time of writing, datasets to describe the susceptibility of receptors to the effects of flooding are not available, although Portsmouth is considered to contain pockets of deprivation and human vulnerability (PCC and Halcrow, 2008); and a relatively high proportion of elderly people reside in some parts of the region.

Table 3.1 Data from the 2001 Census relevant to the Solent case study area

Area	Total (1000s)	Residents aged 75+ (%)	Residents permanent sick/disabled	Average household size	People per km ²
New Forest	169.3	11.49	2.43	2.31	220
Southampton	217.4	7.39	3.76	2.31	4360
Eastleigh	116.2	6.98	2.27	2.45	1460
Fareham	108.0	7.98	2.02	2.43	1450
Gosport	76.4	7.65	3.80	2.36	3020
Portsmouth	186.7	7.99	3.37	2.30	4640
Havant	116.8	8.49	3.38	2.39	2110
Chichester	106.5	11.59	2.09	2.26	140
Isle of Wight	132.7	11.44	4.05	2.24	350
Solent total	1230.1	8.98	3.08	2.33	N/A
England & Wales	52084.5	7.60	5.5	2.30	370

The following sections describe two study sites which are considered in greater detail for the flood simulations described in Chapter 6.

3.2 Description of the detailed case study sites

The city of Portsmouth and a single west Solent flood compartment in the New Forest (named Pennington) are the focus of two case studies for more detailed flood analysis. The reasons are that Portsmouth is recognised as a city of national coastal flooding significance whilst containing a high proportion of the Solent's property at risk of coastal flooding. Pennington is mostly rural, although contains the town of Lymington and other settlements. Both case-studies sites contain properties and landfill sites which are at risk of flooding from both breaching and overtopping. Coastal flood events are documented at both sites, although in particular detail at Pennington when sea defences breached on the 17th December 1989. The location of these areas is highlighted in Figure 3.1, and further information about them is summarised below.

3.2.1 Portsmouth

Portsmouth's shoreline is surrounded by two harbours and open sea coast. With approximately 45 km of open coast frontage, 32 km of which is around Portsea, the main source of flood risk to the city is from the sea (Atkins, 2007). Most of the city lies on Portsea Island, one of the most heavily urbanised and densely populated areas of the UK, containing major residential, commercial, military and historical assets. Despite being low-lying, densely populated and with pockets of human vulnerability (PCC and Halcrow, 2008), 25 per cent of the city's sea defences were considered to lie below a 1 in 200 water level (Atkins, 2007). Development pressure within the floodplain is also high (Atkins, 2007; PCC, 2009). The legacy of intense urban development, contaminated land and coastal landfill has meant that future development on the floodplain is generally considered unavoidable; yet the current standard

of flood risk management is not considered sufficient to cater for rises in sea level predicted over the next 100 years (PCC and Halcrow, 2008). After London and Hull, Portsmouth is believed to contain the greatest coastal flood risk for any city in the UK (RIBA and ICE, 2009). Only a relatively small area of the city is more than 5 m above mean sea level. Portsmouth contains approximately half of the Solent region's property at risk of coastal flooding with more than 15,000 properties exposed to a 1 in 200 year coastal flood (PCC, 2004; NFDC, 2009). The main areas of interest within the city, and their coastal flooding characteristics are summarised:

South Portsmouth open coast originally comprised a gravel barrier beach fronting saltmarshes and creek systems before these were drained in the early 19th century, and reclaimed for development in 1885-6. Old Portsmouth is historically flood-prone, although now protected by armoured concrete sea walls and flood gates which are closed in response to warnings. These structures are structurally robust and in good condition, hence breach is unlikely. Southsea adjoins Old Portsmouth, and is exposed to a larger wave fetch of 155 km from the south. Southsea's defences are regularly overtopped by waves, but it has been many years since seawater⁶ has flooded the low-lying central area known as the 'Morass', although a significant event inundated Southsea Common in 1912 (Section 6.2.4). The land in this former ancient waterway rapidly falls away from the coast, and consequently the coastal defences fronting Southsea are relatively substantial compared to the other areas of the region. On the southeast coast at Eastney, residential and MoD properties on the open coast adjoin an old landfill site inside the shelter of Langstone Harbour entrance.

Northeast Portsea contains defence sections with relatively low crest heights and deep floodplains. A golf course, suburban housing estates (including Anchorage Park) and Eastern Road are within the EA flood zones. Eastern Road flooded during the December 1989 storm surges, and has closed due to overtopping several times since (PCC, 2008; Ruocco, 2009).

West Portsea includes the ferry port and naval dockyards on the coast of Portsmouth Harbour. Historic flood events in these compartments are not documented. Tipner is an area of landfill with only a few properties at risk of flooding, whilst the Whale Island Military base is mostly above extreme sea levels and surrounded by sea walls.

Mainland, Horsea Island and Port Solent: Farlington Marshes' defences are currently in poor condition. On the urbanised mainland, the motorway and main road are protected by a substantial embankment, fronting an expansive and low-lying floodplain. To the west, Port Solent is a recent development comprising a marina and luxury housing estate built on former landfill, although is quite well protected from coastal flooding (Atkins, 2007).

Section 4.6.2 describes in greater detail several of the flood walls and features which protect the Mainland and Northeast Portsea floodplains either side of Port Creek.

⁶ Over 750 properties flooded on the 15th September 2000 due to failure of pumping systems (Halcrow, 2011)

Table 3.2 provides a selection of water level return periods and flood incidents in Portsmouth. A fuller compilation of media records of flood events is provided by Harlow (2012). Old Portsmouth has historically been the most frequently flooded area during high tides, but the installation of new defences over the last decade has proved beneficial and the 10 March 2008 floods causing insignificant flooding compared to the lesser water levels and floods of December 1989.



Figure 3.4 (a) Flooding in Old Portsmouth on the 16th December 1989, (b) the same location when not flooded (taken 5 October 2009).

Table 3.2 Extreme water levels and flood events in Portsmouth.

Level (metres)		Date	Return periods and description of events	Information about flooding
CD	OD			
6.23	3.50	1 in 10 000 year return period water level		
5.90	3.20	1840	Highest alleged water level, flooding reported in Southsea	Sherwood and Backhouse (2012)
5.85	3.12	1 in 200 return period water level		
5.57	2.84	27 Feb 1990	Highest water level recorded in the period 1961 – 2012. No serious flooding, although overtopping reported on the open coast	<i>The Portsmouth News</i> , 27-28 February 1990
5.50	2.77	10 Mar 2008	0.85 m surge; widespread flooding in the Solent region; minor flooding in Old Portsmouth.	EA (2010c)
5.48	2.75	7 Dec 1994	0.78 m surge. Minor flooding in Old Portsmouth and Southsea (although pumping required).	PCC (2008); Ruocco (2009); Ruocco et al. (2011)
5.48	2.75	11 Jan 1993	0.64 m surge, severe flooding in Old Portsmouth	
5.44	2.71	25 Dec 1999	0.69 m storm surge. Portsmouth escapes flooding, although incidents occur elsewhere in the Solent.	
5.42	2.69	19 Jan 1995	0.82 m surge. Overtopping and minor flooding at Southsea. Langstone Harbour worst affected (road closure on the east coast).	
5.40	2.67	13 Dec 1981	0.57m surge. At Hilsea (north Portsea) the fishing lake was contaminated with saltwater when Ports Creek’s defences overflowed.	<i>The Portsmouth News</i> , 14 th December 1981
5.29	2.56	1 in 1 return period water level		
5.18	2.48	13-17 Dec 1989	Prolonged high water levels in the English Channel and widespread flooding (Wells et al., 2001). Surges of 0.45 – 0.65 m; severe flooding in Old Portsmouth, and breach of an embankment at Eastney causing flooding of a caravan park (PCC, 2009).	PCC (2008)
5.08	2.35	Highest astronomical tide		
4.66	1.93	Mean high water spring tides		
3.86	1.13	Mean high water neap tides		
2.73	0.00	Ordnance Datum (mean sea level at Newlyn, Cornwall)		
1.87	-0.86	Mean low water neap tides		
0.72	-2.01	Mean low water spring tides		
0.00	-2.73	Chart datum at Portsmouth		

Event sea levels are provided by Haigh (2009), and the British Oceanographic Data Centre, with the exception of the 1840 sea level (Easterling, 1991). Tidal Levels are from the National Tide and Sea Level Facility (www.pol.ac.uk), return periods are for the year 2008, from (McMillan et al., 2011).

3.2.2 Pennington

This Pennington flood compartment (Figures 3.1 and 3.5) is situated at the western end of the Solent between Hurst Spit and the Lymington River. Most of the site is valuable grazing marsh, classified as a Site of Special Scientific Interest (SSSI). The town of Lymington and villages of Keyhaven and Milford-on-Sea are partly within the potential floodplain, as well as an area of gravel excavation east of Keyhaven (which is being filled with domestic and inert waste) and a historic landfill closer to the shoreline. Most of the compartment's shoreline is shielded by the Isle of Wight and Hurst Spit, with

wave climate controlled by predominantly south-westerly winds and locally-generated waves. In the lee of Hurst Spit, wave climate is mostly fetch limited to significant wave heights of between 0.3 and 0.8m (Halcrow, 1998), although south-east or south-south-east gale force winds operating over the deeper water of the east Solent can theoretically generate waves of up to 2 m. Lymington has experienced combined fluvial and coastal floods, with notable events occurring in December 1954, December 1989, and December 1999.

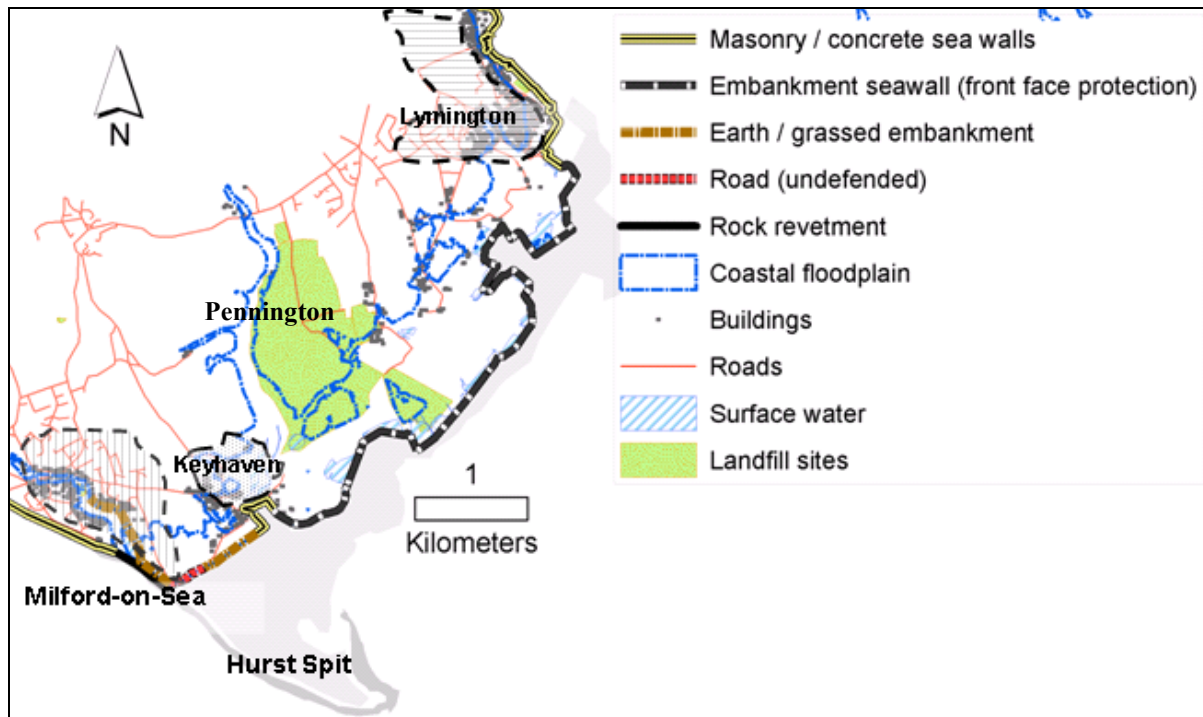


Figure 3.5 The Pennington detailed case study site, showing defence types and key locations

In the lee of Hurst Spit, earth and grassed embankment stretch approximately 1 km eastwards until meeting the village of Keyhaven which is mostly defended by a mixture of masonry and concrete sea walls. These adjoin the main coastal defence structure across the site, which stretches 8.1 km between eastern Keyhaven to Lymington; an embankment known as the Pennington sea wall. Along the central and eastern sections this is protected by interlocking concrete blocks on the front face, and is the main length of defence across the site protecting over 500 ha of land at mean high water spring tides (Martin, 1994). The Pennington sea wall was reconstructed soon after breaching during the storms of December 1989 (NRA, 1990), with the crest raised by up to half a metre (higher crest heights are required at the northeast end to accommodate wave run-up) to provide an approximately 1 in 25 year standard of protection.. However these defences are threatened by loss of mudflat and saltmarsh (increasing wave attack and erosion) over the coming century (Gardiner et al., 2007). Hurst Spit was also breached 16th-

17th December 1989 and since 1996 has been managed to maintain its stability (Bradbury and Kidd, 1998).

Table 3.3 Extreme sea levels and flood events at Pennington.

Level (metres)		Date	Relevance / description of event	Source
CD	OD			
4.38	2.40	1 in 200 return period water level (approx.)		
4.15	2.17	10 Mar 2008	Approx. 1 m storm surge in the Solent. Highest water level recorded since 1992 (recorded at Environment Agency tide gauge; although the water level was also recorded as 0.13 m less at an alternative gauge nearby (CCO, 2011).	EA (2010c)
4.08	2.10	17 Dec 1989	Storm surge of 1.1 m. Overtopping and overflow caused flooding to 50 houses and 10 commercial properties in the town of Lymington, some to a depth of 1.2 m. Submergence of railway line and electrical substations. Breaching and flooding of the rural site, damaging 10 houses and the hinterland marsh environment.	NRA (1990)
3.97	1.99	24-25 Dec1999	Flooding occurred in Lymington due to the river overtopping upstream of the Toll Bridge on the Lymington side and flowing on to the railway.	O'Connell (2000)
3.90	1.92	14 Dec 1989	Wave overtopping on the river estuary and open coast caused flooding in Lymington and the Pennington marshes.	NRA (1990)
	1.89	1 in 1 return period water level (approx)		
3.0	1.02	Mean high water spring tides		
2.60	0.62	Mean high water neap tides		
1.98	0	Ordnance Datum (mean sea level at Newlyn, Cornwall)		
1.40	-0.58	Mean low water neap tides		
0.70	-1.28	Mean low water spring tides		
0	-1.98	Chart datum at Lymington		

Tidal Levels in Table 3.3 are from the Channel Coastal Observatory (www.channelcoast.org), return periods water levels are for 2008 and from (McMillan et al., 2011).

3.3 Summary

The Solent is a populated coastal region with complex hydrodynamic conditions, variable (mainly small) sized floodplains and a range of potential coastal flood mechanisms. Historic accounts of coastal flooding portray more extreme events than have been seen in living memory. During the 20th and 21st centuries, although frequent, storm surges and flood events in the Solent are less severe than those on the UK east and west coasts. On-going defence improvements are partially attributable to this, and coastal flood forecasting and warning systems are also available.

Part of the region has undergone a strategic flood risk assessment (SFRA) (Atkins, 2007) which provides a useful background to this research; but includes inundation modelling with limited detail of defence failures and floodplain case-studies, and only a few specific flood simulations which are

referenced to (now outdated) still water level return period analysis. The Environment Agency (EA) have also generated flood zone maps, which provide a conservative flood outline for flood warning and planning purposes. This thesis differs from these sources of coastal flooding information, by providing a comprehensive and transparent coastal flood event simulation methodology and analysis of floodplain water depth distributions. The flood simulation results in this thesis are derived from specific loads and failure mechanisms, although generated and presented across a wide range of load and defence failure scenarios. The EA flood outlines are compared to the flood outlines generated in this work (and also as a partial verification of methods and datasets). Prior to this research, there is limited analysis of past coastal flood events. The 10 March 2008 event (Wadey et al., 2013) was reviewed in a regional assessment by the Environment Agency (EA, 2010c), a report which provides an essential foundation for this research, although as shown later a number of flooded sites were omitted. There is therefore a need to generate further datasets that could support model validation.

The small range of vertical differences within the return period water levels and past events (e.g. Tables 3.2 and 3.3) suggest some potential for more extreme coastal flood events than have been previously observed across the Solent. SLR and future development threaten further changes to coastal flood events and to escalate the probability of these occurring; hence for this Solent case study future decision-making would benefit from an improved understanding of the consequences of coastal flood events. The chosen detailed case studies of Portsmouth and Pennington encapsulate a range of coastal flooding issues, and analysis at a closer scale can better demonstrate the application of an improved understanding of coastal floods. Chapter 4 outlines the methods used to determine flood extents and depths via model simulations and analysis of floodplain topography and water level datasets. Chapter 5 outlines and summarises an approach and outcomes of collating coastal flood event datasets.

4. Datasets and Methodology

The modelling and analysis approach is summarised in Figure 4.1. Firstly an assessment of exposure to coastal flooding in the Solent was generated by combining planar water levels with a digital elevation model (DEM) to generate flood outlines and depths without considering defences or the dynamics of flooding. Secondly, flooding was simulated more realistically by using a hydraulic model combined with flood defence analysis, and wave and still water level time-series. The output grids of flood water depths were intersected with a database of properties, and viewed alongside other information (e.g. aerial photos and land-use maps) in geographical information systems (GIS). To check accuracy and enhance the understanding of the model outputs, validation case studies were applied (Chapter 5). Hydraulic modelling was also applied at two spatial resolutions of DEM: 50 m for fast Solent-wide modelling, commensurate with the level of data detail regionally available; and 10 m resolution for the two detailed sites (Portsmouth and Pennington).

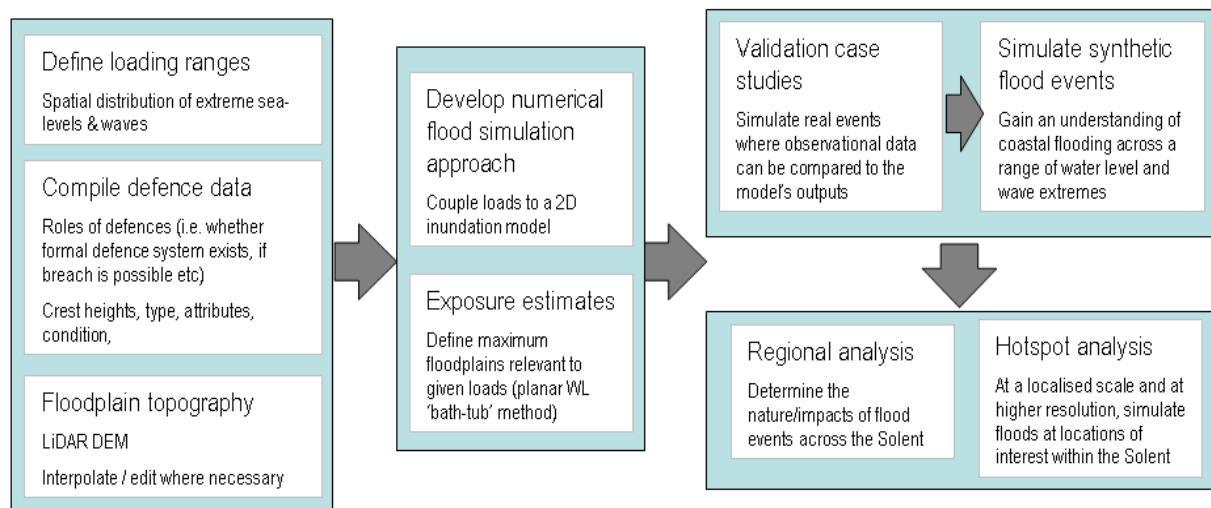


Figure 4.1 Method overview showing (1) inputs; (2) inundation simulation approaches; (3) outputs; and (4) example applications

4.1. Overview of the hydraulic flood simulations

Water is routed into the model domain via specified points which are representative of the sea-land boundary. These points are associated with storm-tide water levels and defence responses, and coupled to a numerical model which spreads the inflowing water in two dimensions, approximately simulating the real-time propagation of the flood wave. For Solent-wide flood simulations, this amounted to inflows from 5,000 shoreline locations (many of which represent sections of defence). Inflow time-series were determined by a database of shoreline information, observed storm-tide water level measurements, and defence failure calculations. The outcome of flood simulations is grids of water depths for various stages of the flood. Analysis here focuses upon the peak flood depths in each cell during each simulation of a dynamic coastal flood event.

The sequence of analysis and processing of results is depicted in Figure 4.2, which is explained in more detail in the subsequent sections. The numerical model used to simulate floodplain inundation from these inflows was LISFLOOD-FP. Variants of this model developed by the University of Bristol have previously been used to simulate coastal flooding (Bates et al., 2005; Purvis et al., 2008; Smith et al., 2012b). This model is described in further detail in Section 4.4. Importantly, when coupled to the defence response this allows for rapid regional simulations up to the peak water level, driven by applying water level time-series at the model boundary.

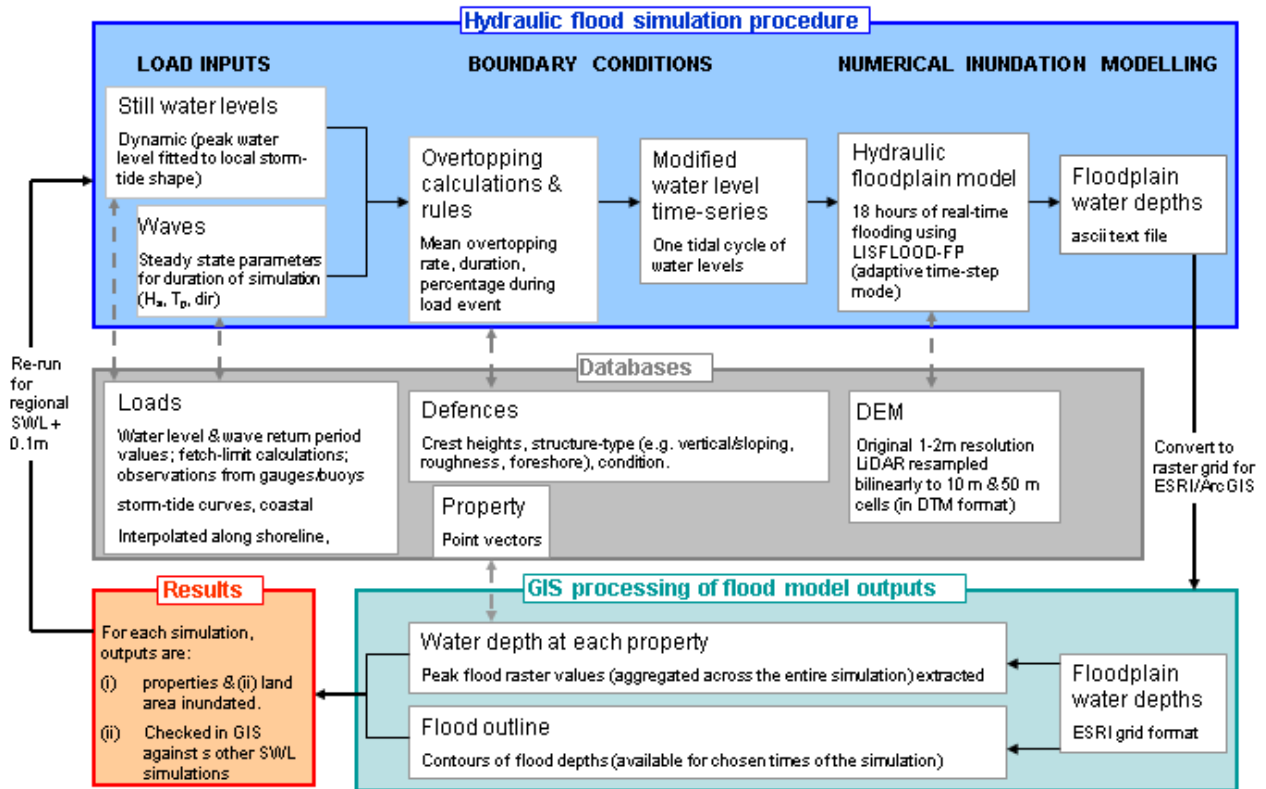


Figure 4.2 Hydraulic flood modelling method flow diagram

4.2. Data sources and integration

4.2.1. Still water levels and waves

To simulate flood events, required are still water level time-series and knowledge of their spatial variability in the case study region. Also, load observations and return period information is important to approximate the range of still water levels and waves to use as boundary conditions, and to indicate relevance of these loads to present-day or future flood events. Fortunately the UK benefits from a recently generated water level return period data set: Table 4.1 water levels at Portsmouth for the baseline year of 2008 derived from a national study which applied the Skew Surge Joint Probability Method around the UK coast (McMillan et al., 2011). These are the water return periods referred to

throughout this thesis. Regional sea-level rise in the past decade has been approximately 1.7 mm per year (Haigh, 2011) hence the recently derived return periods do not require significant adjustment.

Table 4.1 Return period still water (sea) levels at Portsmouth in 2008 (McMillan et al., 2011); the water level datum referred to throughout this thesis is mODN (metres above Ordnance Datum, which is approximately mean sea level)

Return period (years)	1	10	20	50	100	200	1000	MHWS	10 Mar 2008
Elevation (mODN)	2.56	2.81	2.88	2.98	3.05	3.12	3.28	1.97	2.77

Flood events associated with peak still water levels (SWLs) incorporate a combined scenario for storm surge and tide. These are applied as boundary conditions for flood simulations across a range of SWL increments, which cover normal tidal levels to greater than the present day extremes. Further details of the synthetic flood event scenarios are described in Section 4.6, and the validation case-study boundary conditions are explained in Chapter 5.

Peak water levels were prescribed spatially to simulate hypothetical uniform flood events by use of ‘tide zones’ illustrated in Figure 4.3. This method assumes spatial variations in still water level in the Solent are mostly influenced by tidal range, and subsequently a linear interpolation is applied between offshore nodes (some of which had return period information available). This method has previously been used for the Environment Agency’s (EA) flood zone mapping, and a flood risk assessment which covered part of the Solent (Atkins, 2007). In relation to the tide gauge at Portsmouth this method equates to extreme water levels that are approximately 0.8 m less at the western end of the region (Hurst) and 0.5 m greater at the eastern extent. Also shown in Figure 4.3 are points where specific extreme water levels have actually been calculated from modelling at higher spatial resolution, gained from the recent national still water level study by McMillan et al (2011). Variations in alongshore spatial water levels are very similar between methods, although the newer data does not include Southampton Water or the harbours. The tide zone method was used to generate the range of hypothetical still water level events for simulations of coastal inundation in the Solent-wide results (Chapter 6).

Water level time-series for inflows to the inundation model were obtained from observed storm-surge water level time-series, and simplified to hourly values (Figure 4.4, in which the four storm-tide curves are representative of the main storm-surge influenced water level characteristics across the Solent). The Lymington storm-tide water level time-series shown in Figure 4.4 was applied to inflows between Milford-on-Sea and Calshot Spit, and the adjacent areas on the Isle of Wight, including Cowes. The Southampton Water storm-tide was applied to the shoreline between the tip of Calshot Spit to northeast of Hill Head. The Portsmouth storm-tide was applied to inflows surrounding mainland areas between Hill Head and Selsey Bill, and the north of the Isle of Wight between east Cowes and Ryde; and the Bembridge storm-tide applied between Ryde and Sandown coast of the Isle of Wight.

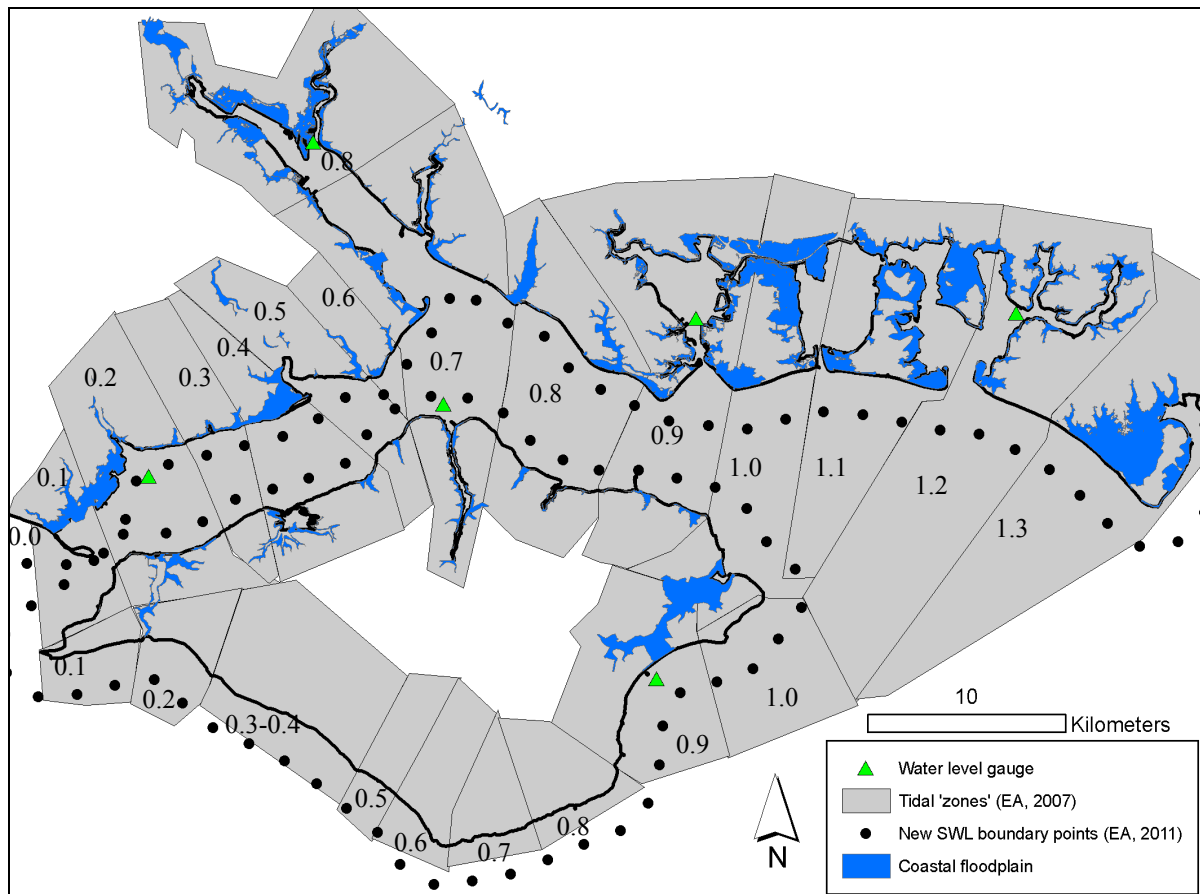


Figure 4.3 Two methods for spatially prescribing SWL (to simulate uniform water level events) are shown: (a) tide zones – each zone represents a 0.1m increase in peak SWL from west to east; and (b) 2 km spaced points generated by the POL CS3 hydrodynamic model (refer to McMillan et al., 2011 for more details)

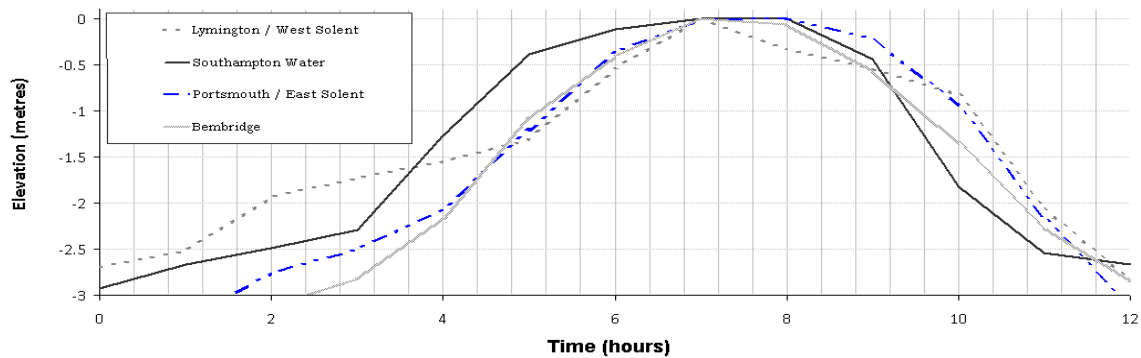


Figure 4.4 Water level time-series used in the Solent-wide coastal flood simulations (shown here as standardised to the same height, and as hourly-averaged versions of SWLs recorded during 10 March 2008 with the exception of Bembridge which is an averaged water level time-series for events between 13-18 December 1989)

The impact of spatially variable tidal characteristics and storm-surge interaction upon the duration of overtopping or overflow events in the Solent can be inferred from Figure 4.5; for example the pronounced double high water at Southampton can prolong inflows at small overflow heads. However,

different weather events and tide conditions will vary the shape of the storm-tide water level time series and should be a consideration for future work as discussed in Chapter 7.

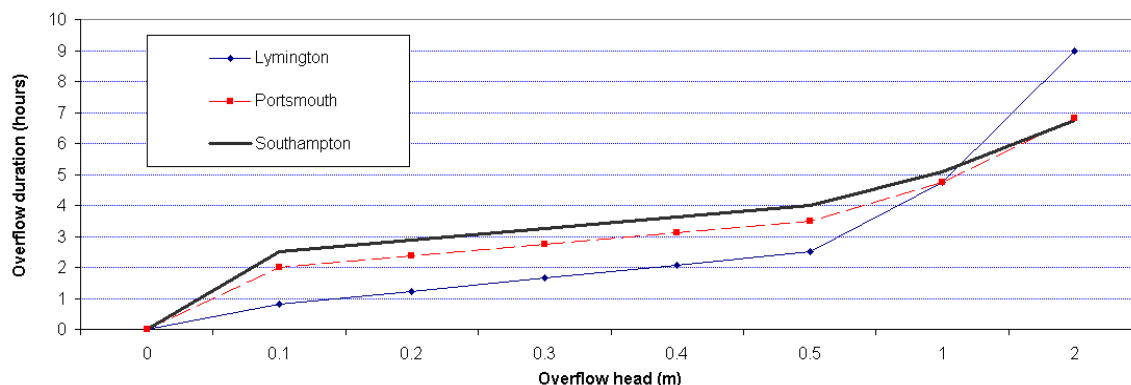


Figure 4.5 Overflow duration associated with peak negative freeboards & regional storm-tidal variations

For wave loading scenarios to be combined with regional still water level extremes and converted to overtopping rates, observed and return period wave data was compiled. Relative to the SWLs wave return period guidance is quite ad-hoc in the case study region, with shorter observation time-spans and spatial gaps (e.g. particularly in sheltered areas). However, relative to many other regions there is quite an abundance of data. For example archived data is available for the real-time nearshore observation sites shown in Figure 1.2, provided by the Southeast Strategic Regional Monitoring Programme (CCO, 2012). Return period analysis for different sites was amalgamated from various sources including two SMP studies which include analysis from modelling (HRW and HPR, 1997; NFDC, 2010) (refer to Appendix A). Summarised in Figure 4.6 are some of the spatially-varying significant wave heights across the Solent – gaps in the known return periods were filled by linear interpolation. Wave conditions in the harbours and rivers are less well known; although a regional sediment transport study by SCOPAC (2004) describes a selection of numerical modelling, hindcast methods, return periods and observations. Fetch-limited conditions were also calculated using a wave nomogram (CERC, 1984) to approximate the ‘fully arisen’ sea condition – in some situations this was confirmed by the background information, for example at the Portsmouth open coast the maximum theoretical waves (from the fetch analysis) are almost identical to 1 in 50 year return period waves (HRW and HPR, 1997). Records of the largest swell wave heights and periods were also noted from measurements. To obtain for example 1 in 1 year wave periods, observed 1 in 1 year H_s and wave period values were plotted against each other (using the CCO data sets summarised in Table 5.1); and from this the H_s values were matched to the corresponding wave periods in the observations (using the mean of the observations).

EurOtop (Pullen et al, 2007) overtopping formulae at beaches and vertical walls requires inputs which are specific to wave conditions at the toe of the structures (for use in equations 16-21, i.e. to convert the offshore H_s to the spectral wave height at the toe of the structure H_{m0}); because shoaling and refraction can significantly change H_s by the time waves reach the coast (refer to Section 2.1). Wave height (H_s)

recordings and return period analysis from the CCO wave buoys are at approximately 10 m water depth. The nearshore slope (or seabed gradient) and shoaling curve graphs (the latter contained in the EurOtop Manual) were used to generate a coefficient to convert the offshore wave height to a wave height at the toe of coastal defences. The nearshore slope was defined as the average slope between the run-up limit and twice the break point of H_s with the depth $h_b = H_b / k$. For wave conditions at beaches in the Solent a value of $k = 0.78$ was applied; this approximation of k is recommended in the absence of more detailed modelling, and resultant overtopping calculations are not considered overly sensitive to this parameter (*c.f.* Masselink and Hughes, 2003; FEMA, 2005) although this is acknowledged as an area of some uncertainty which justifies the approach of displaying results across a range of wave loads. The approximation of foreshore slope was obtained by merging freely available and recent topographic and bathymetric survey data (from www.chanelcoast.org), and gaps filled by a coarser bathymetry grid assembled by Quinn et al. (2012). In deep water, H_{m0} is approximately the same as H_s although at shallow water (i.e. mainly beaches fit this criterion during storm surges) H_{m0} is 10-15% smaller than H_s .

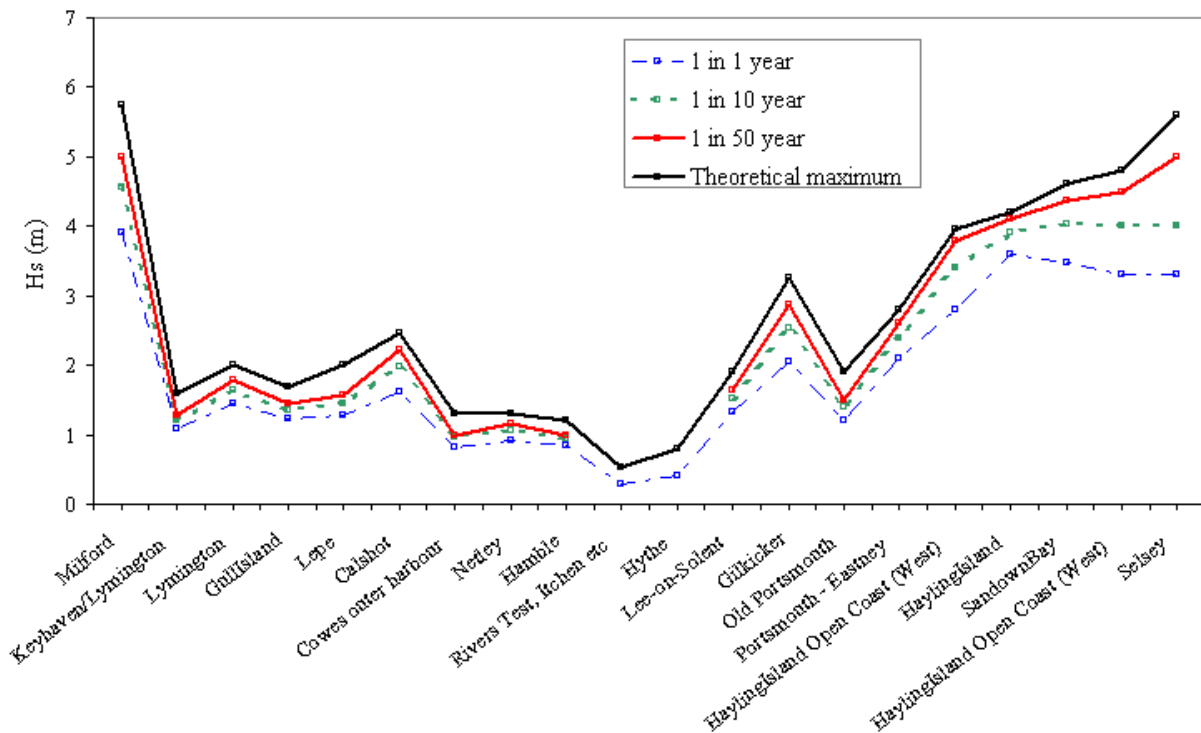


Figure 4.6 Selection of significant wave height (H_s) return period data in the Solent

4.2.2. Floodplain topography and defence heights

The DEM used to model floodplain inundation was mostly constructed from Light Detection and Ranging (LiDAR) surveys, processed in the format of a digital terrain model (a DTM, which has artefacts such as buildings removed). The LiDAR data was collected by the Environment Agency in 2007 and 2008 at 1 - 2 m spatial resolution. The resolution and accuracy of LiDAR is widely accepted as the best available topographic data set for flood modelling. The vertical root mean square error is

generally known to be within ± 0.3 m of the ground being measured (Xharde et al., 2006; Webster et al., 2006), although in the UK the Environment Agency (EA) attempt to obtain survey points within ± 0.15 m vertical accuracy. Accompanying survey reports suggest that the EA's LiDAR points collected in the Solent are within ± 0.10 m of the available ground-based check points (CCO, 2012). At the upper reaches of several tidal rivers and beyond the reaches of most of the present-day coastal floodplain, the LiDAR DEM was extended using a 10 m resolution topographic dataset derived from photogrammetry (Ordnance Survey Land-Form data) (OS, 2001) (refer to Appendix A). This land height dataset is surveyed at a scale of 1:10,000, with contours at 5 metre vertical intervals. This generates a 10 m resolution DTM, with accuracy of the order of ± 1.8 m RMSE. Visual comparisons made with the overlapping LiDAR showed agreement often better than 1 m. Despite the high resolution and good accuracy of the LiDAR surveys, there are accuracy implications with the use of the digital terrain model (DTM) product which is generated by 'cleaning' of the raw data (to remove cars, houses, vegetation such as trees and hedges, etc.) from the raw digital surface model (DSM). This is achieved via a combination of computational algorithms and manual editing to mask out items that may bias flood modelling. However a detailed description of the methods used by the EA for this process is not available. The cleaning process can introduce systematic errors, including objects incorrectly remaining in place (and hence leading to underestimations of inundation extent) whilst also masking too much elevation from the surface (potentially allowing for overestimation of floods) as highlighted by Liu (2008).

Hydraulic modelling for this research used two variants of DEM; one at 50 m spatial resolution and another at 10 m resolution. LiDAR survey points were interpolated to these resolutions by re-sampling the original data using a bilinear interpolation technique in ArcGIS™. This computes a new value for the larger grid cell based on the weighted average of the values of the four nearest input cell centres (DeMers, 2009); a suitable method for continuous data such as elevation since it produces more accurate and realistic surface for floodplain modelling than most other techniques (DeMers, 2009; Fewtrell et al., 2008b). The DEM was checked for spikes and holes; the latter found where water bodies were filtered by Environment Agency data processing procedures. These were filled using a function in ArcGIS ("nibble"), which processes cells of a raster corresponding to a mask with the values of the nearest neighbours. Defence datasets describing condition and structural elements (such as roughness, berms, and crest heights) were available across the region. Information about defence was also gained from the DEM, aerial photography, photos, literature and site visits. Essential, was the generation of a high resolution crest-height dataset, mostly gained from real-time kinematic (RTK) GPS surveys, collected between 2004-2009 and quoted to have a vertical accuracy of ± 0.03 m (CCO, 2012). Gaps in crest data were filled with Light Detection and Ranging (LiDAR) data.

4.2.3. Defence and floodplain data: preparation for inundation modelling

For the regional and hotspot analysis, 50 m and 10 m DEMs were generated by averaging the height values from the original LiDAR surveys (using the bilinear interpolation technique described above). The 50 m model is suitable for the Solent-wide flood analysis because this resolution is commensurate with the spatial detail of corresponding defence data; and offers practical benefits such as a fast computational run-time. Large areas of the region comprise rural floodplain, and this resolution has been considered suitable in previous flood modelling studies (Purvis et al., 2008). The 10 m resolution model is beneficial for inundation simulations in selected areas, and is noted in previous studies to be suitable for accurate representation of urban inundation (Fewtrell et al., 2008a; Fewtrell et al., 2008b).

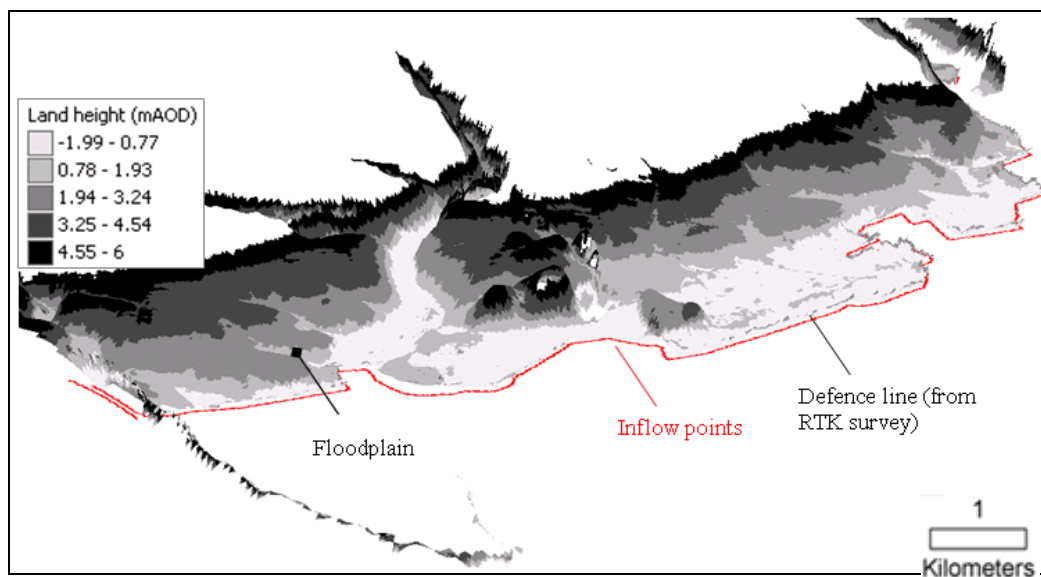


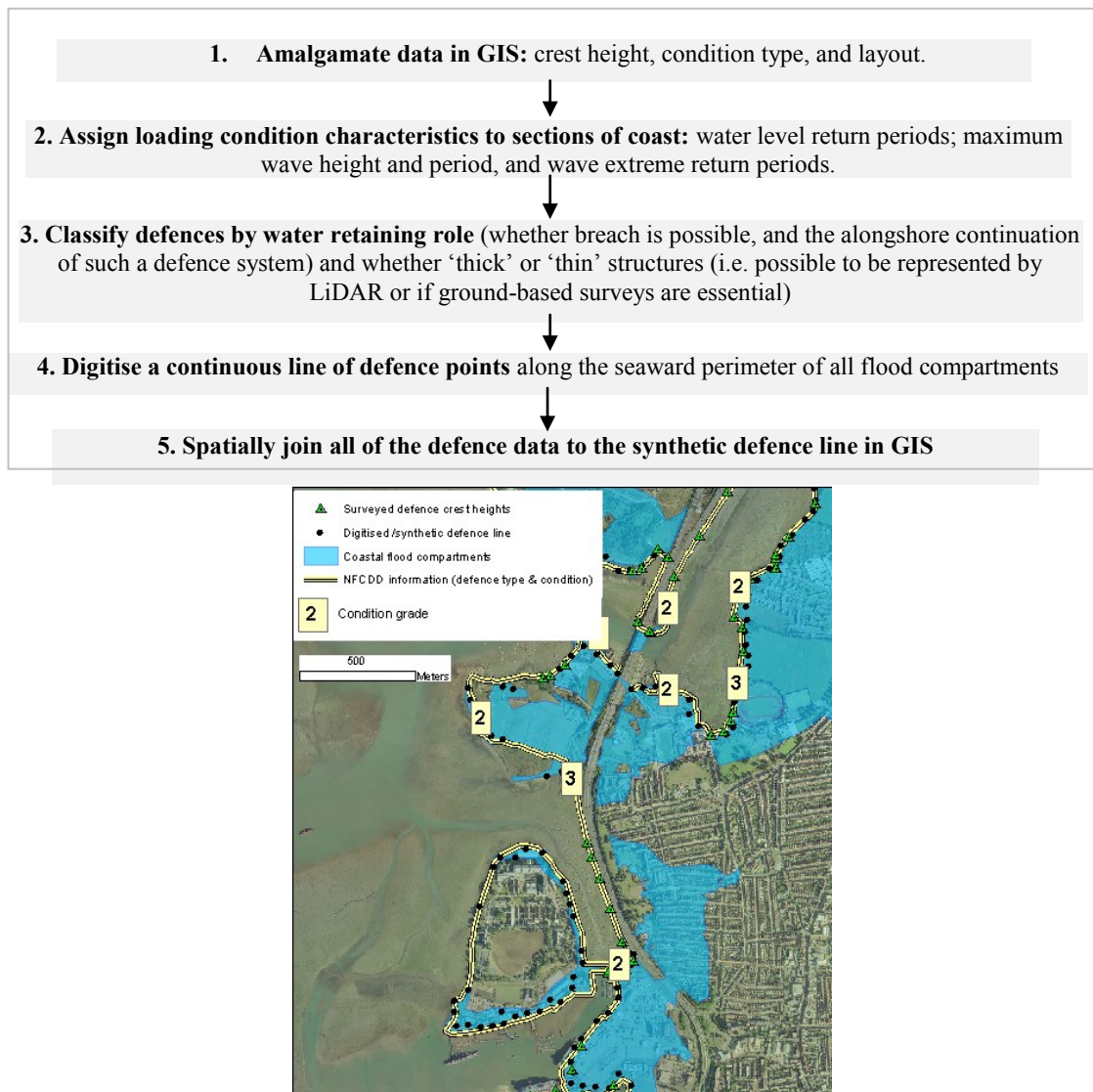
Figure 4.7 Digital elevation model of the defences and floodplain surrounded by 10 m spaced inflow points (Pennington)

For the Solent-wide model DEM point vectors were placed in cells corresponding to defence locations, to allow inflows from defence failures to be simulated. This resulted in almost 5000 potential inflow point locations along 246 km of intertidal shoreline. Defence datasets (e.g. crest heights, type and condition) were joined to these points so that any boundary conditions applied to these points would represent the relevant inflow along the shoreline. The procedure for processing defence data for the Solent-wide model is depicted in Figures 4.8a and 4.8b. For the hydraulic modelling, two variants of DEM were constructed:

1. **DEM with ground-surveyed defence crest heights appended onto the surface:** remotely sensed survey data can miss sharp edges of structures, therefore ground surveyed crest height data (which also has greater vertical accuracy) was attached to the floodplain DEM. This type of DEM was used for inundation simulations under ‘no wave’ scenarios, because it provides an accurate method of routing water level time-series over defences by allowing the crest heights to delimit the interval of

inflow. For the 10 m modelling method this was the only type of DEM used, and overtopping wave conditions were incorporated into water level time-series applied seaward of the DEM.

2. **DEM with shoreline flood defences masked:** the defence line was flattened to the level of the land immediately landward of the defence. For the Solent-wide 50 m resolution model with simulations inclusive of wave effects, inflows were generated immediately landward of the defence line. This was achieved by generating a new water level time-series in the cells landward of the defence based upon analysis of overflow and overtopping. For breach simulations, this type of DEM also allows the original still water level time-series to be routed into the model. The DEM was edited so that the seaward edge corresponded to the landward edge of the theoretical defence line; and the cells on the seaward edge were at the height of the land immediately in the lee of the defence.



Defining exposure with the planar water level ('bathtub') method

For any regional hypothetical water level event, the 10 m DEM and planar water levels were used to define maximum flooding for each scenario (using the distribution of water levels shown in Figure 4.3). At the Eastoke Peninsula on Hayling Island this method was supplemented with an additional 2 m to allow for wave run-up onto land above SWLs (this run-up value estimated by eq.8 with annual wave conditions, and supported by past observations of flooding. e.g. 3 November 2005 – Mason et al., 2009; Ruocco et al, 2011). Application of the 1 in 1000 year regional still water levels, plus 0.3 m allowance for vertical data errors identified 99 hydraulically separate flood 'compartments' covering 120 km² of land. These compartments were separate on the basis of topographic elevation only (which would allow connections between potential surface sea water). These planar water level flood outlines at the different increments of SWL were included alongside the equivalent hydraulic simulations, and also checked alongside the Environment Agency's tidal Flood Zone 3 data. This is explained further in Chapter 6 which discusses a Solent-wide 1 in 200 year flood event simulation.

Table 4.2 Solent defence types

Defence type	Defence description	Floodplain (immediately behind defences)	Floodplain (whole)	Defence failure modes	Inflow representation in model
0	Features/barriers detached from the floodplain	N/A	N/A	Could contribute to load increases elsewhere.	N/A
1	Natural topography / embankments	Low risk	Variable. Hydraulic consequences of failure near the defence (risk further inland affected by floodplain connectivity)	Flow over & around ad-hoc features	Activated in all simulations.
2	Structure at similar level to the floodplain; or with gaps.	Moderate urban or rural risk		Overflow/overtopping	Overflow / overtopping inflows processed separately
3	Above the floodplain.			Reduction in crest height can increase overtopping; although defence system not clearly defined for entire flood compartment	Breach scenarios also relevant
4	Defences prevent water from reaching low-lying land.			Moderate to high risk.	
5		Receptors would be severely affected if flooding occurs		High risk, deep, expansive: floodplain	

The main defence and floodplain types for the Solent-wide modelling are shown in Table 4.2 and Figure 4.9, which characterise areas by the basic type and potential consequence of defence failures. Some locations lack defences which in the hydraulic modelling method allows for the still water level time-series to simply be routed into the model; whereas most locations require water to be routed over defences and/or with calculations to determine overflow and overtopping inflows.

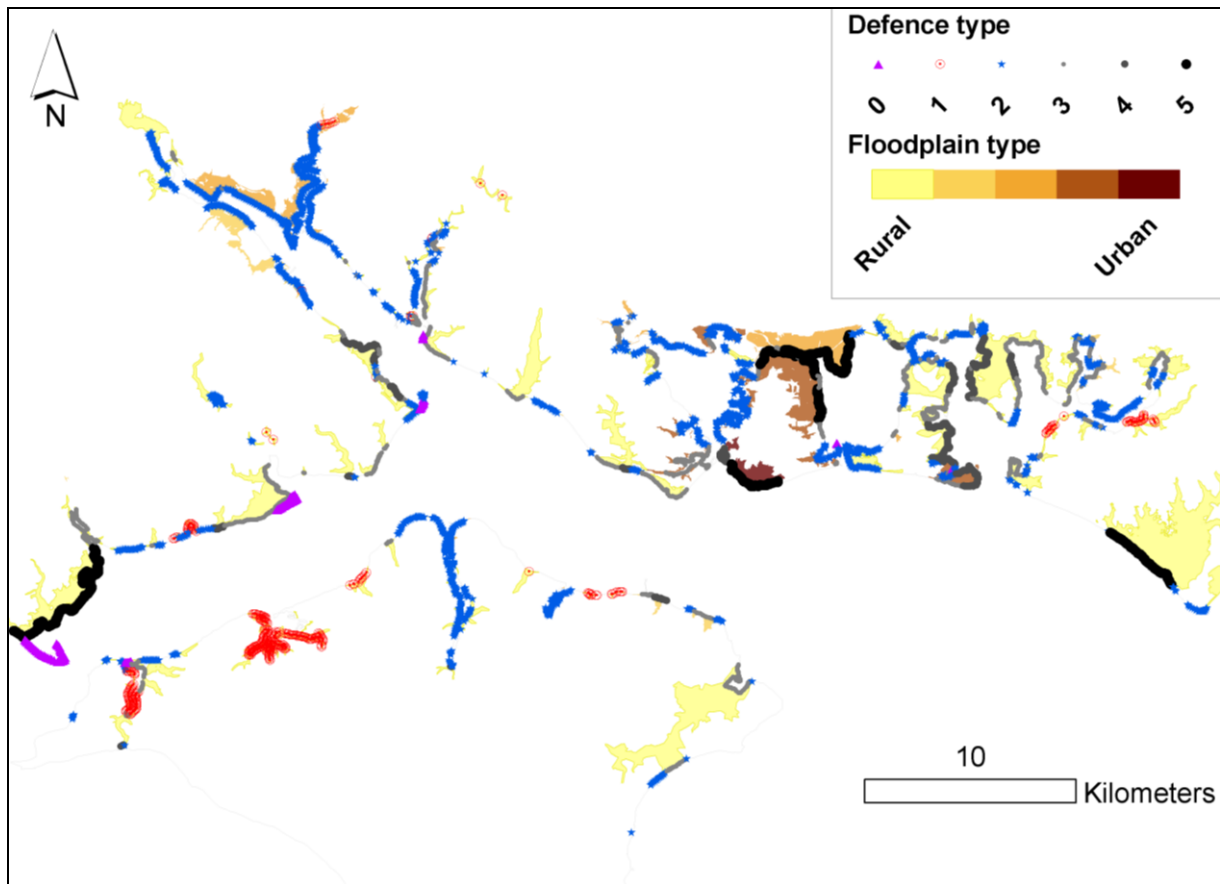


Figure 4.9 Solent defence types, which correspond to descriptions in table 4.2

4.3. Integrating loads, defence failures and inundation modelling

Inflows based upon the storm and tide still water level times series, crest heights, and wave parameters (e.g. significant wave height and period) are processed and applied to the inundation model boundary, where they form a starting point for further continuity of flow into adjacent cells and into the floodplain. Methodologies are described in this section for the 50 m and 10 m resolution versions of the model. Shown in Figure 4.11 the interval of overflow failure can be considered as bounded by the time that the SWL and/or wave overtopping inflow exceeds the crest height ('a' and 'b' are shown to depict an idealised water level time-series applied to the relevant boundary cell at the edge of the DEM). This concept is more uncertain and difficult to model when defining wave-influenced inflow scenarios. The choice of overtopping method is described further below and in Section 4.3.1 and discussed further in Chapter 7.

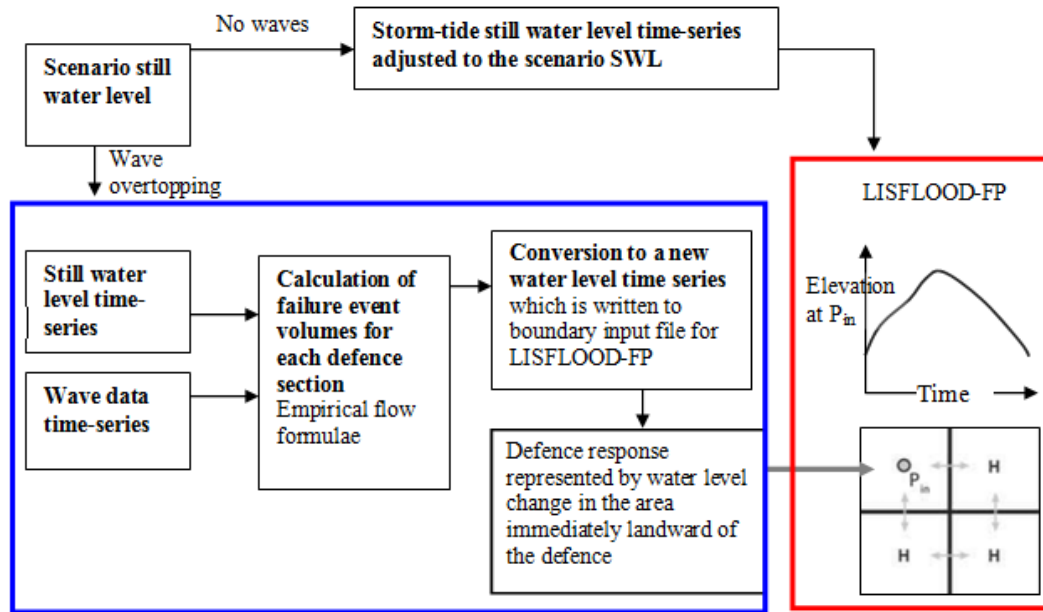


Figure 4.10 Model inflow boundary conditions for the inundation model (P_{in} denotes the inflow point and H denotes water heights)

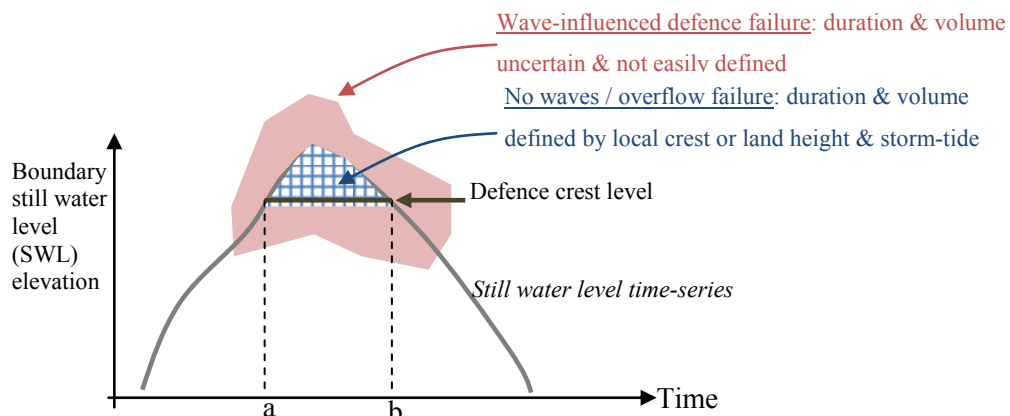


Figure 4.11 The crest-dependent duration of overflow and overtopping inflows for all failure events was determined at each defence section based upon the local storm tide water level time-series and nearest crest height value. Duration and volume of still water overflowing a defence can be delimited by crest height; wave-inclusive defence failures are less simple to quantify.

No wave scenarios: For coastal flood event simulations comprising conditions *without* waves, inflows representative of outflanking and overflow of defences are applied to the inundation model. The regionally variable still water level time-series (described by figures 4.3-4.5) are applied to the crest-height appended DEM. This automatically delimits inflows according to defence crest heights and the rise and fall of the scenario storm-tide.

Wave scenarios: to delimit an inflow interval and volume (e.g. Figure 4.11) for loading scenarios inclusive of waves and/or breach, this is more complicated than for overflow failures (refer to section 2.2.1). Wave parameters are combined with SWL time-series to calculate an event overtopping volume at each inflow location; which subsequently generates a series of water levels (based upon the rise and

fall of the original storm-tide curve) to apply to inflow cells at the DEM edge. The following approaches were applied in the simulations described in this thesis:

- *50 m resolution simulations*: inflows comprise rising/falling water levels in the DEM cells representative of the land area immediately landward of defences. These ‘wave modified’ water level time series were applied to inflow locations on the DEM with defences masked from it. This simplification is acceptable because the inflow is a rising water level in the lee of the defence generated by the overtopping calculations. Important to note is that the DEM cells in the coarsened DEM are a good representation of the land landward of the defence (as indicated by the finer DEM) so that flooding is accurately represented. For situations dominated by overflow, this gives a conservative approach to generate slightly larger inflows which implicitly allow for additional fluxes that may occur during an overflow event. This is also reflective of the wider-scale modelling requirements across the entire case-study area (i.e. this approach is commensurate with the detail and spatial resolution of the case study’s crest height and defence description database).
- *10 m resolution simulations*: as for the non-wave simulations, the versions of DEM with defence crest heights appended to the surface were used for wave-inclusive simulations. For breach scenarios defences were masked (so that inflows entered the model at the floodplain level immediately landward of defences).

4.3.1. Calculation of wave overtopping inflows

Overtopping methodology: overview and rationale

To simulate flood events caused by wave overtopping; water level times-series were generated to link wave overtopping discharge to the numerical inundation model. A method was developed which incrementally represents combined wave and water level loadings, and also allows a logical limit to the inflow. Wave overtopping inflows for the coastal flood simulations were generated using the following steps:

1. Calculate volumetric overtopping rates by applying formulae relevant to individual defence section configurations (e.g. sloping or vertical structures); and at different freeboards within the tidal cycle (at hourly intervals). This also includes estimation of the percentage of time that water passes over the defence during any given interval of time (eq. 3 to 6).
2. Determine times of onset, termination and duration of overtopping.
3. Generate a total inflow volume for each defence section.
4. Convert overtopped volumes to a series of water levels at the boundary cells of the inundation model.

Either volume time-series, or water level time-series are typically used to generate flood outlines via numerical coastal inundation models. Literature from other studies suggest that more often the time-series-volume approach is used to simulate flooding from wave overtopping calculations using empirical formulae (e.g. Mott MacDonald and EA, 2010), detailed numerical simulations (e.g. Chini and Stansby, 2012), or volume calculations accompanied with prior information of flood outlines and discharges (Bates et al., 2005; Smith et al., 2012b). In the Solent case-study, trialling direct volume vs. water level time-series input approaches indicated that the direct volume input to the boundaries of the inundation model over-predicted flooding; as indicated by comparison of these simulations with: (1) the maximum flood outline for a given SWL scenarios (i.e. by the planar water level or ‘bathtub’ flood outline), and (2) observed flood outlines (Chapter 5). Therefore, inflows to the inundation model for each flood event simulation comprised wave overtopping volumes (calculated for each section of defence) converted to water level time-series. The peak inflow water level (for any given simulation) could straightforwardly be set to a logical limit according to prior analysis of the floodplain configuration (Figure 4.13); although for the 50 m resolution model this overtopping-inflow method requires careful editing of the DEM to ensure that the grid cell in which the inflow point lay is representative of the ground surface lying landward of a defence structure. Within this cell, the overtopped water level rises and falls during an overtopping-induced coastal flood event, accompanied by subsequent continuity of flow into adjacent cells. For example, at Eastoke (Hayling Island, Havant) water has been noted to overtop the shingle beach and accumulate on a narrow strip of concrete walkway between the beach and the houses, before flowing into the streets behind (Figure 4.12). The original LiDAR DEM was edited and each inflow location checked to ensure that the landward inflow area remains well represented (e.g. after interpolation). For the 10 m resolution model, a detailed schematisation and DEM of the defences was constructed and appended to the floodplain DEM and wave inflows applied as water level time-series on the seaward side of defences.



Figure 4.12 Overtopping and flooding caused by long period (swell) waves at Eastoke (Hayling Island, Havant) on 3rd November 2005

For each overtopping simulation, the limits set for the peak water level in the boundary cells on the edge of the 50 m DEM are depicted in Figure 4.13. These prevent the inflow water surface elevation

and subsequent flood spreading becoming unrealistic (e.g. when the empirical calculations output very high volume discharges at small freeboards and/or extreme wave conditions). For example, for floodplains lying beneath the peak SWL of a tide-surge scenario it is intuitively possible that the peak inundation depth in any given flood compartment could theoretically reach the same height as the seaward SWL. However information to inform such limits is sparse particularly for floodplains lying above the SWL. Field tests by Pullen et al (2009) describe overtopping observations where instantaneous water depths of around 0.05 m to 0.075 m occur in the area immediately behind a sea wall (during heavy overtopping events). Alternatively, the RASP higher level plus flood risk assessment methodology (HRW, 2003; HRW, 2004b) as an approximation for a relatively low-resolution overview of flooding, suggests that wave overtopping discharges of 50 l/s/m to 250 l/s/m (0.05 to 0.25 m³/s/m) may cause 0.2 m water depth to accumulate in the lee of the overtopped defence (and a minimum depth of 0.2 m when overtopping has exceeded 250 l/s/m). Based upon this and flood event observations (e.g. Figure 4.12) a limit of 0.2 m was set for overtopping in situations where the floodplain is above the still water level. Water entering the model at the boundary cell can then escape to lower areas of floodplain behind. In most other circumstances, as shown in Figure 4.13, overtopped water levels may reach a similar level to the peak still water level. This method incorporates assumptions and simplifications about drainage and the interaction of flow across the boundary (which is most likely to overestimate inflow), as well as forcing of water further into the floodplain by the overtopping waves (which adds to momentum of inflowing water and may lead to under-estimation of inflow). Consequently, Section 8.2.1 makes recommendations for further work in this area.

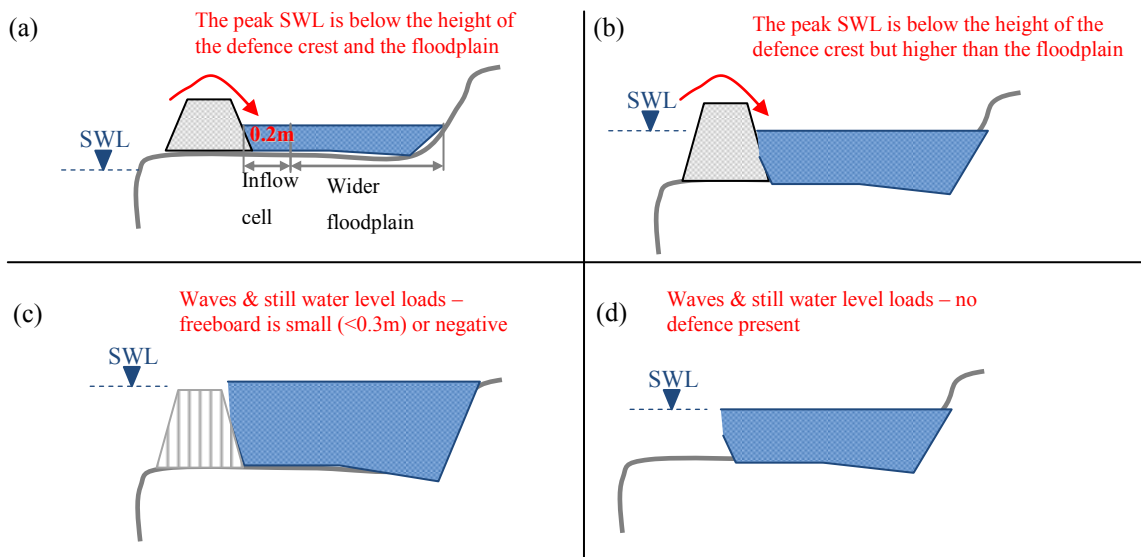


Figure 4.13 Floodplain configurations, water level event scenarios and limits set to the overtopping (OT) inflows at boundary cells (for inundation simulations); (a) the peak still water level (SWL) is below the height of the floodplain, OT volume converted to SWL time-series limited to 0.2m (b) OT volume across defences converted to SWL time-series which is limited to the peak (event) storm-tide SWL (c) Original SWL time-series routed into boundary cell (duration is dependent upon crest of defence but defence is removed from the DEM).

The model, as explained in this section, incrementally associates wave and SWL loadings to the inflow level and storm-tide SWL time-series applied to the model boundary. The following sections describe the methods for calculating the overtopping rates which are fundamental to the water level time-series that have been described in this section.

4.3.1.1 Overtopping rate calculations

Overtopping rates calculated by empirical formulae (and guidance) from the EurOtop Manual) (Pullen et al., 2007) yield overtopping discharges during a loading and flood event simulation. Three variants of overtopping formulae were used:

1. Sloping structures: The British Guidelines formula for sloping sea walls by Owen (1980) (Eq. 7) was applied to sloping structures (embankments and sloping sea walls). This utilises significant wave height (H_s) combined with the mean wave period (T_m);

2. Sloping foreshore (beaches): A similar formula to that of Owen (1980) was developed by TAW (2002), and is the advised method in the EurOtop Manual (Pullen et al., 2007) for calculating overtopping discharges on slopes. This formula was applied to the non-structural sloping defences in the Solent (e.g. open coast beaches of Portsea Island, Sandown, Ryde, Hayling Island and Selsey):

$$q = \sqrt{gH_{m0}^3} \cdot \frac{0.067}{\sqrt{\tan \alpha}} \cdot \gamma_b \xi_{m-1,0} \exp \left(-4.3 \cdot \frac{R_c}{\xi_{m-1,0} H_{m0} \gamma_h \gamma_f \gamma_\beta \gamma_v} \right)$$

With a maximum of

$$q = \sqrt{gH_{m0}^3} \cdot 0.2 \exp \left(-2.3 \cdot \frac{R_c}{H_{m0} \gamma_f \gamma_\beta} \right) \quad (16)$$

γ_b , γ_f , γ_β and γ_v are, respectively, factors to reduce the overtopping rate for the presence of berms, roughness elements, oblique wave attack and vertical walls on the slope. Within this formula is the Iribarren number (also known as the breaker and surf similarity parameter):

$$\zeta_{m-1,0} = \tan \alpha / (H_{m0} / L_{m-1,0})^{1/2} \quad (17)$$

where α is the slope of the front face of the structure and $L_{m-1,0}$ is the deep water wave length $gT_{m-1,0}^2 / 2\pi$. The other notable difference between this and the Owen (1980) formula is the use of the H_{m0} value (rather than H_s). This value accounts for a change in significant wave heights that have occurred by the time waves have reached the toe of the defence, due to shoaling and other depth-induced changes as wave cross the foreshore (refer to Section 4.2.1).

3. Vertical and composite structures: Formulae are described in the EurOtop Manual for calculating overtopping discharges at vertical walls (with slight variants for composite structures for which the emergent part of the structure is vertical, fronted by a modest berm). The approach for these structures is more iterative than for slopes. Firstly, it is determined whether the toe of the defence is submerged by

the still water level, and for submerged toes a wave breaking or “impulsiveness” parameter, h^* is defined which is based on depth at the toe of the wall (h_s), and incident wave conditions inshore:

$$h^* = 1.35 \frac{h_s 2\pi h_s}{H_{m0} g T_{m0}^2} \quad (18)$$

Non-impulsive (pulsating) conditions dominate at the wall when $h^* > 0.3$, and impulsive conditions occur when $h^* < 0.2$. The transition between conditions for which the overtopping response is dominated by breaking and non-breaking waves lies over $0.2 \leq h^* \leq 0.3$. In this region, overtopping was predicted for both non-impulsive and impulsive conditions, and the larger value assumed.

Consequently, for non-impulsive (pulsating) conditions ($h^* < 0.2$) the following formula was used:

$$q = \sqrt{g H_{m0}^3} \cdot 0.04 \cdot \exp\left(-2.6 \cdot \frac{R_c}{H_{m0}}\right) \quad (19)$$

For impulsive conditions ($h^* > 0.3$):

$$q = \sqrt{g H_{m0}^3} \cdot 0.04 \cdot \exp\left(-1.8 \cdot \frac{R_c}{H_{m0}}\right) \quad (20)$$

The transition between conditions for which the overtopping response is dominated by breaking and non-breaking waves lies over $0.2 \leq h^* \leq 0.3$. In this region, overtopping was predicted for both non-impulsive and impulsive conditions, and the larger value assumed. For broken waves (where $h^* < 0.2$) the following formula was used:

$$q = h^2 \sqrt{g h_s^3} \cdot 2.7 \times 10^{-4} \left(h^* \frac{R_c}{H_{m0}} \right)^{-2.7} \quad (21)$$

These calculations in this thesis assumed the following:

- Fixed wave conditions (significant wave height and period) for the entire duration of each event (hence the peak overtopping rate occurs at high water, according to the tidally-varying SWL);
- That overtopping occurs across the width of the entire defence section;
- Wave shoaling effects remain constant during the event (e.g. due to sediment movement);
- Waves approach the coast directly;
- The failure interval (used to amalgamate overtopping rates into a single ‘event overtopped volume’) is bounded by a mean overtopping rate of 10 l/s/m; i.e. hourly storm-tide SWLs and subsequent temporal freeboard variations generate overtopping rates and the duration for which discharge equals or exceeds 10 l/s/m was calculated (using interpolation where required) to subsequently generate the total overtopped volume ‘ Q_{TOTAL} ’ (eq. 22);

- The coefficient generated in eq. 6 ($Q_{OT\%}$) was used to approximate the ratio of overtopped waves to the total number of waves occurring during the overtopping interval, and reduce the total overtopped volume to incorporate the intermittency of overtopping wave inputs:

$$V_{event} = Q_{Total} \cdot Q_{OT\%} \quad (22)$$

The ' V_{event} ' value is then used to generate time-series water level inflows into the inundation model, as described in the following section.

Conversion of discharges to water level time-series:

For the **50 m resolution model**, conversion of the total overtopped volumes to inundation model boundary conditions/inflows is by associating event overtopped discharges V_{event} (eq. 22) to new flood depth time-series in the boundary cell of the inundation model. The total event overtopped volume for any section generates a peak water depth, which creates a modified storm-tide water level time series in the DEM cell immediately behind the overtopped defence. The principle is to determine the depth of water behind the overtopped defence by viewing an idealised segment of floodplain (which is equivalent to the area in which the inflow point lies). A prior dataset was generated which considers the water level change possible in a 50 m by 50 m area that would result from various wave overtopping events. Assuming that water surface elevation change in the overtopped area is driven by a continuous discharge (with no drainage from the cell during overtopping) a set of water levels is obtained, occurring simultaneously across the cell with the changing storm-tide. This linkage between volume input V_{event} (eq.22) and the flood event's change in water level in the boundary cell (H_{inflow}) is represented as a simple linear relationship:

$$H_{inflow} = f(V_{event}) \quad (23)$$

Subsequently, H_{inflow} is a height value which is added to the floodplain height in the corresponding cell of the DEM, and converted to generate a modified water level time series for the failure event inflow. The relationship between the event overtopped volume (V_{event}) and peak change in floodwater height in the inflow cell (H_{inflow}) is shown in Figure 4.15.

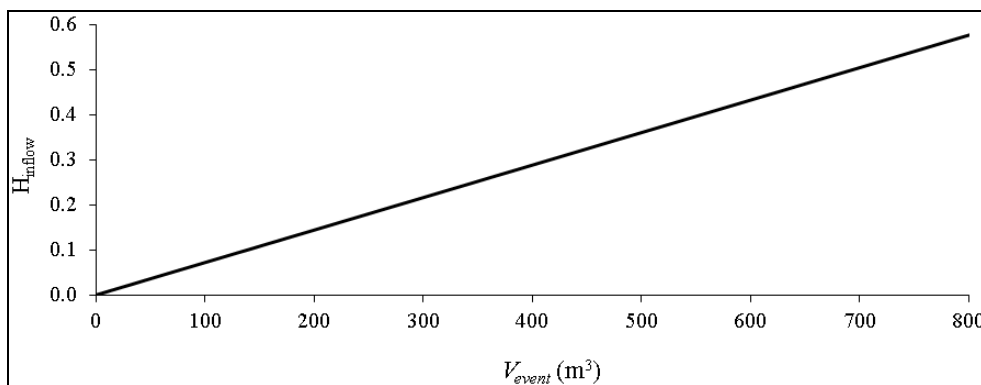


Figure 4.14 Expected changes in water level in a 50 m² boundary cell filled by overtopping event discharges (to generate water level time-series at the boundaries of the 50 m resolution version of the inundation model)

A summary of these methods is, with reference to Figure 4.15, to imagine an overtopping event peaking at more than 125 l/s/m ($0.125 \text{ m}^3/\text{s/m}$), with freeboard varying over time according to the Lymington storm-tide curve. Duration of the overtopping is delimited by rates which exceed 10 l/s/m, so that 4.5 hours of overtopping occurs. This event generates 356,000 litres (356 m^3) of overtopped water according to the sloping wall formulae and site specific parameters. Also calculated is a $Q_{OT\%}$ value (eq. 6) of 0.65, allowing a total discharge V_{event} of 231,660 litres (approx. 232 m^3). Using Figure 4.14, this generates a peak elevation change (H_{inflow}) of approximately 0.17 m in the lee of the defence. The local storm-tide water level time-series is then shifted as to add 0.17 m to the floodplain height in the corresponding boundary cell. The floodplain height is 1.80 mODN, hence generating an inflow level of 1.97 mODN for this simulation; and because the floodplain is below the scenario's peak SWL (2.5 mODN, Figure 4.15) a limit does is not invoked. Water is then spread into the surrounding cells as described in Section 4.4.

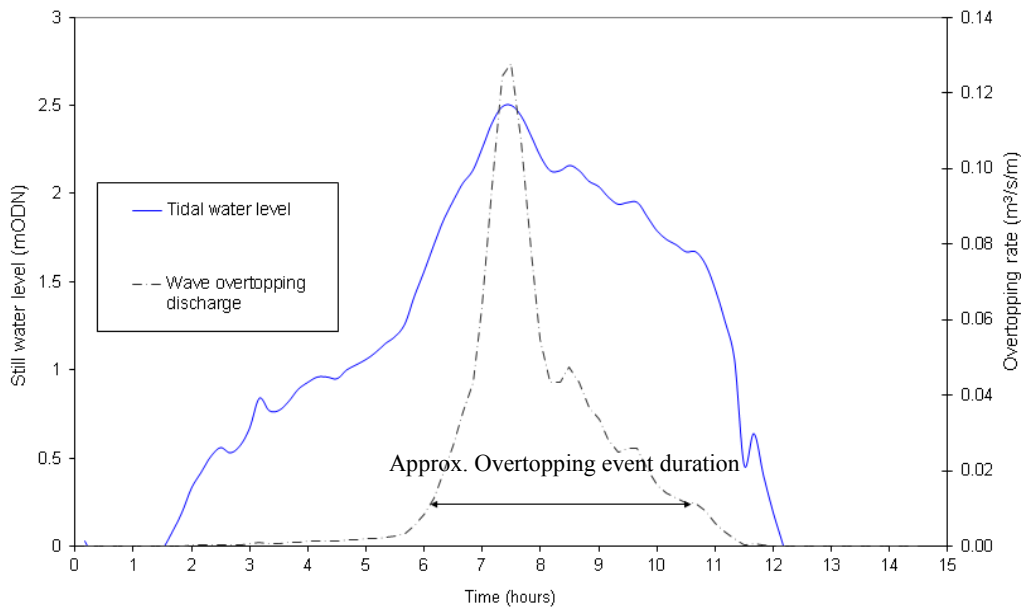


Figure 4.15 A tidal curve segment (Lymington, 10th March 2008), plotted with the corresponding wave overtopping rate (calculated with a fixed $H_s = 2 \text{ m}$, $T_m = 4 \text{ s}$) and likely time-intervals of defence failures

For the **10 m resolution model** a different H_{inflow} value is required because the DEM has defence crest heights inserted onto it and the water level time-series inflows points are located in grid cells *seaward* of defences (rather than landward method of the 50 m model). This is because approximating an overtopped free surface elevation in the boundary cell *landward* of defences in the smaller 10 m by 10 m area generates unrealistically high water levels, whilst the rationale behind the 10 m resolution model is to use higher resolution datasets relating to defence and floodplain configuration. Hence, for any event scenario the V_{event} value (eq. 22) is instead used to vertically adjust the model boundary storm-tidal water level time-series above the defence crest (i.e. greater levels applied for greater event

overtopping volumes). A weir equation (eq. 2) generated a dataset of inflow volumes that would theoretically result from a range of still water overflow scenarios, through a single tidal cycle (according to the location-relevant storm-tide curves). For any given flood simulation the total wave overtopped volume (V_{event}) was calculated (in the same way as the 50 m resolution simulations although taking into consideration the shorter 10 m length of the defence sections). This volume is then related to the volumes generated by the weir formula to generate an overflow head which allows the correct volume of water to be discharged into the floodplain during the overtopping simulation. Shown in Figure 4.16 are the event-overtopped volumes for any 10 m defence section, and the associated peak overflow head required to generate this inflow during one tidal cycle at the two detailed case study sites. For example, a storm event at Lymington may overtop 120 m^3 of water over a 10 m section; resultantly, the storm-tide water level time-series is shifted upwards so that its peak it lies 0.15 m above the crest of the defence.

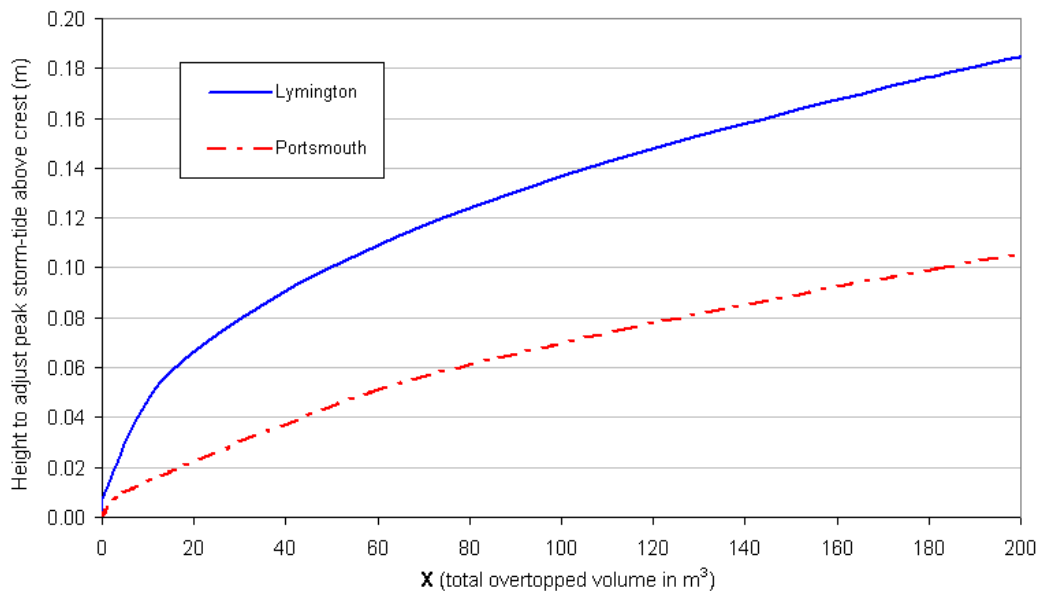


Figure 4.16 Peak values for modified water level time-series (for 10 m resolution wave overtopping inflows)

4.3.2. Breach Modelling

Breach failure of coastal flood defences in England and Wales has been rare since 1953; but is associated with significantly greater flood impacts than other failure mechanisms (Muir Wood and Bateman, 2005). This type of failure was considered in two ways:

Simple ‘full breach’ modelling scenarios:

To enable comparison with overtopping failure simulations, a ‘full breach’ scenario was simulated at each 0.1 m still water level increment. This was combined with the maximum wave scenario, and all defence sections which are man-made/raised structures (defence types 3 to 5 – Table 4.2) were considered as ‘breached and water routed through (for a single tidal cycle). In these simulations,

defences were broken down to floodplain level so that if still water level was at any time above this fixed breach ‘sill’, sea water could flow through. There are also examples provided in Chapter 5 and 7 where more specific breach widths are considered.

Conditional probability of failure using reliability analysis (refer to Section 2.2.1)

As mentioned in Section 2.2.1, the likelihood of a breach in defences can be indicated by developing fragility curves, whilst the underlying concepts of structural reliability are more thoroughly explained by Melchers (1999). For the loading events used in all model runs in the case-study, an output was generated to indicate the probability of breach given the wave and SWL loadings, for all of the inflow locations in the Solent with defence types 3-5 (refer to Table 4.3). Fragility curves were created for the following breach mechanisms:

- Damage due to overflow and/or overtopping;
- Piping (water eroding the inside of defence structures), and
- Rapid erosion of shingle beaches

This analysis used defence parameters (crest height, foreshore and land height, and condition) as inputs to the RELIABLE software which is a Microsoft Excel add-on developed under the FLOODsite (Task 7) EU research project. This tool is coded in Fortran and contains a library of limit state equations from the inventory of flood defence failure modes compiled by Allsop et al (2007). Details of this software are available via Gouldby et al (2008a), and the failure mechanisms assessed in the case study are described further in Appendix C of this thesis. Where breach probabilities are shown (Figure 6.18 and Figure 6.22), these are associated with the peak load of the event and are the maximum probability generated by analysis of the three aforementioned failure mechanisms, applied at each shoreline inflow point.

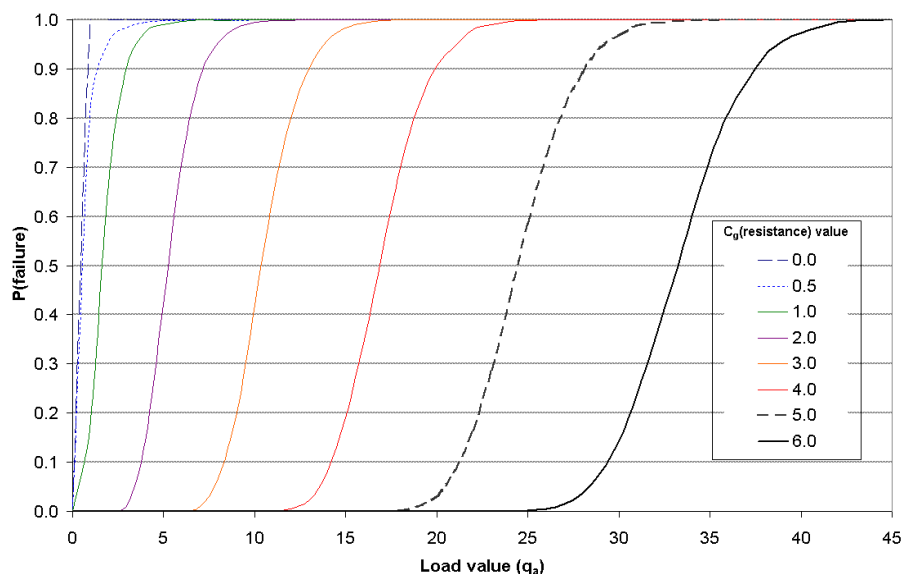


Figure 4.17 Fragility curves for overflow-overtopping induced damage for various defences resistance values

The reliability analysis methods that were used are explained further in Appendix C, and a selection of fragility curves are shown in Figure 4.17. These show along the x-axis an event load (for water passing over the crest in this case), and on the y-axis the probability of failure. The different curves are for defences of different resistance as indicated by the EA structural inspection scores and descriptors of the defences from the defence data sets. These fragility curves are constructed with data of insufficient structural detail to generate scenarios of breach which are commensurate with the flood simulation methodology in the case-study; although for any flood simulation they provide an indicator of defence sections that may be relatively vulnerable to breaching.

Resistance of the Solent's defences was approximated by relating site-specific data (condition, descriptive defence characteristics etc. including the asset data provided by local authorities, and photos) to mean values which can be incorporated by the limit-state equations in the RELIABLE software. These resistance values have been derived for, and used within a national level flood risk assessment in England and Wales (DEFRA and EA, 2005a). Shown in Table 4.3 are the values used to assign the relative strength of defences across the region for the assessment of resistance to overflow and/or overtopping. For example, many of Portsmouth's large concrete and masonry open coast structures defences obtained scores of 4.5 to 6.0, whereas ancient and earth embankments in the harbours and rural areas were often less than 1.5, and hence would be far more likely to breach if they overtopped during a storm event

Table 4.3 Values used to assign resistance to breach by overflow/overtopping mechanisms, for different defences in the Solent – based upon those used in the national level RASP methodology by DEFRA and EA (2005a)

Erosion strength (cg) rating according to front face and surface protection					
Condition Grade	Embankment		Vertical wall		
	Grass (permeable)	Grass (impermeable)	Gabions	Masonry	Sheet piles
Condition 1	1.00	1.50	1.50	3.00	2.50
Condition 2	0.85	1.28	1.28	2.55	2.13
Condition 3	0.60	0.90	0.90	1.80	1.50
Condition 4	0.42	0.62	0.62	1.25	1.04
Condition 5	0.33	0.50	0.50	0.99	0.83
Erosion strength cg: Front face and crest surface protection					
Condition Grade	Embankment		Vertical wall		
	Grass (permeable)	Grass (impermeable)	Gabions	Masonry	Sheet piles
Condition 1	1.50	2.25	2.25	4.50	3.75
Condition 2	1.28	1.91	1.91	3.83	3.19
Condition 3	0.90	1.35	1.35	2.70	2.25
Condition 4	0.62	0.93	0.93	1.87	1.56
Condition 5	0.50	0.74	0.74	1.49	1.24
Erosion strength cg: Front face, crest and rear protection					
Condition Grade	Embankment		Vertical wall		
	Grass (permeable)	Grass (impermeable)	Gabions	Masonry	Sheet piles
Condition 1	2.00	3.00	3.00	6.00	5.00
Condition 2	1.70	2.55	2.55	5.10	4.25
Condition 3	1.20	1.80	1.80	3.60	3.00
Condition 4	0.83	1.25	1.25	2.49	2.08
Condition 5	0.66	0.99	0.99	1.98	1.65

4.4. Numerical simulations of floodplain flow

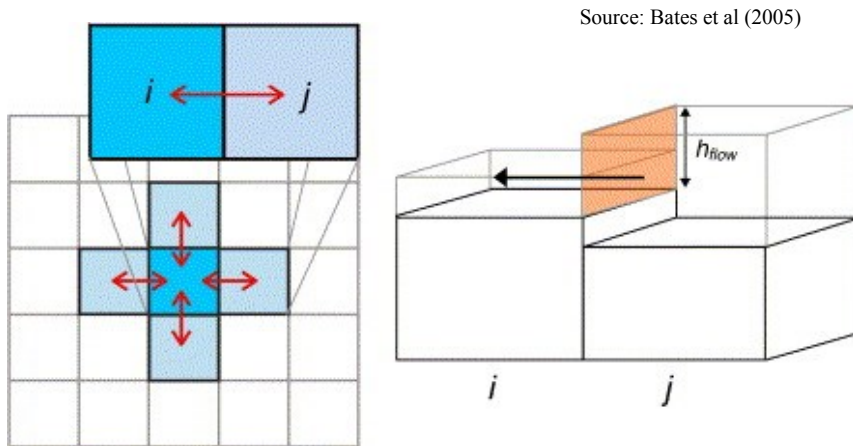
The model which was used to calculate the spread of water on the floodplain during simulated flood events in this case study was LISFLOOD-FP. As depicted in Figure 4.18, floodplain flows are treated using a ‘storage cell’ approach and implemented for a raster grid to allow an approximation to a 2D movement of the flood wave. A continuity equation is solved relating flow into a cell and its change in volume, and a momentum equation for each direction where flow between cells is calculated. With good quality topographic data (e.g. LiDAR) storage cell models can produce similar results to full 2D formulations of the shallow water equations (for sub-critical gradually varied flows only) (e.g. Néelz et al., 2009). The variant of LISFLOOD-FP used for the flood simulations described in this thesis, is an inertial formulation of the shallow water equations (refer to Bates et al, 2010 for a detailed description). Using LISFLOOD-FP, inundation from defence failures was simulated by spreading flow at the boundary of the model to adjacent cells, and then between neighbouring floodplain cells as follows:

$$q^{t+\Delta t} = \frac{q^t - gh_{flow}^t \Delta t \frac{\Delta(h^t + z)}{\Delta x}}{(1 + gh_{flow}^t \Delta t n^2 |q^t| / (h_{flow}^t)^{10/3})} \quad (24)$$

where q is the flow per unit width, h_{flow} is the depth of water available to flow, Δt is the model time step, Δx is the model grid resolution, z is the bed elevation, h is the water depth, and n is the Manning’s friction coefficient. Water depths are updated using Equation (25):

$$h_{i,j}^{t+\Delta t} = h_{ij}^t + \Delta t \frac{Q_{xi-1j}^t - Q_{xij}^t + Q_{yij-1}^t - Q_{yij}^t}{\Delta x^2} \quad (25)$$

where Q is the discharge, h_{ij} is the depth of water in the cell (i,j) .



Source: Bates et al (2005)

Figure 4.18 Representation of flow between raster cells in LISFLOOD-FP. The flow depth (h_{flow}) represents the depth through which water can flow between two cells, and is defined as the difference between the highest water free surface in the two cells and the highest bed elevation.

The stability criterion for this numerical model is given by the Courant–Freidrichs–Levy condition for shallow water flows such that the stable model time step, Δt , is a function of the grid resolution, Δx , and the maximum water depth, h , within the domain:

$$\Delta t_{\max} = \alpha \frac{\Delta x}{\sqrt{gh_t}} \quad (26)$$

where α varies between 0.2 and 0.7.

4.5. Surface features and receptors

For the coarser resolution 50 m resolution Solent-wide model, scope for calibration by varying surface friction values was limited by a lack of accurate flood event observations and the coarse resolution cells being unsuitable for delineating spatially variable surface features and friction values (*c.f.* Fewtrell et al., 2008b). A uniform representative composite value of $n = 0.035$ was used, based on the average range of surface roughness values found across the region. In previous examples of flood modelling with LISFLOOD-FP, n -values of between 0.03 and 0.06 have been applied (Bates et al., 2008).

Alternatively, for the 10 m resolution modelling, spatially variable surface friction values were incorporated. High n -values were used for buildings and lower values for roads, hard surfaces etc. (with the exception of a simulation which compares uniform with variable surface friction parameterisation, described in Section 6.2.1). For the 10 m resolution models at Portsmouth and Pennington variable friction values are appropriate because surface types and transitions (e.g. buildings, roads, and fields) are more obviously delineated. At Selsey for a series of flood event validation simulations, the effects of variable n -values are briefly discussed (Figure 5.5).

Table 4.4 Typical friction values applied to flood modelling.

Model	Class description	Friction values (Manning's n)
50 m resolution model: a spatially uniform value applied	Composite value for Solent floodplains	0.035
10 m resolution model: spatially heterogeneous values (according to surface features identified in the OS land-use maps)	Asphalt and concrete	0.012
	Grass (gardens, recreational areas, parks etc.)	0.035
	Thick grass / marshland vegetation	0.040
	Water bodies	0.010
	Buildings	1.000

The main quantitative indicators of the consequences of the simulated coastal flood events in the case-study, is by intersecting property locations with the inundation results (using the peak water depths of a single tidal cycle event simulation in each cell), and calculating the land area inundated. This is in some

examples accompanied by a more qualitative commentary of the field of flood depths and land-use in the floodplain generated by the simulations.

For the city of Southampton and areas eastwards (including Gosport, Fareham, Havant and Chichester), properties were represented in a database which provides a National Grid co-ordinate for each postal delivery address in Great Britain (OS, 2012a). A property database was created for the New Forest and the Isle of Wight, by digitising buildings using recent (2005-2008) geo-rectified aerial photos, alongside 1 in 10,000 scale OS maps (which showed boundaries for gardens and rectangles for properties) and a database of polygons surrounding postal addresses (OS, 2012b) (e.g. Figure 4.19). The aerial photos, OS maps and Google's Street View were used to verify locations in the property database for the Southampton and the east Solent, and to verify area locations and properties flooded in the validation case studies (described in Chapter 5).

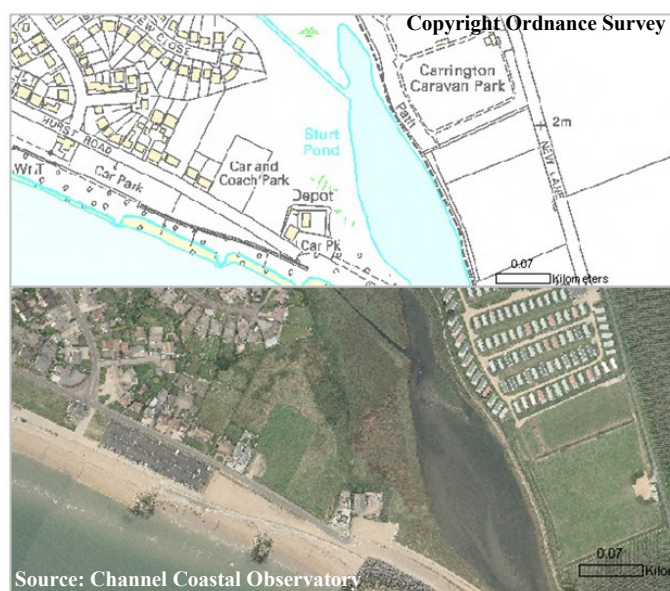


Figure 4.19 Land-use and building polygons and aerial photography

4.6. Scenarios for coastal flood simulations

4.6.1. Solent-wide flooding

A set of regional flood simulations were generated utilising the aforementioned data and boundary conditions. Regionally uniform events were simulated at 0.1 m SWL increments (based upon the spatially variable return periods illustrated in Figure 4.3). Each of these SWL scenarios was accompanied by a specified and regionally uniform level of wave extremity. Three classes of wave condition were selected: no-waves, annual return period waves, and the largest waves possible. This method provides a regional view of hypothetical flood events, demonstrating incremental increases in flood extent in response to loadings. All simulations allow wave and SWL inflows of a single full tidal cycle, and allowed sufficient time for water to spread to its maximum extent on the floodplain beyond

the end of the tidal inflow. These loads approximately cover a range which includes normal tidal levels (combined with no waves) to water levels which accommodated mid-range estimates of 21st century sea-level rise according to recent guidance (Lowe et al., 2009) and the theoretically largest wave extremes. For each SWL increment simulation, peak water depths were extracted to the properties in the dataset to provide a depth at each property.

To indicate a ‘worst case’ flood for each SWL increment, a planar water level result is provided and also a ‘full breaching’ hydraulic coastal flood simulation. The former provides an overview without consideration of event duration, hydraulic connectivity or other flood dynamics; the latter routes the SWL time series and maximum wave inflows onto the floodplain with no defences in place. This allows overtopping onto topography above the SWL and increased wave inflows through the ‘removed’ defence sections; providing a more hydraulically realistic (albeit extreme) version of the worst case coastal flood outline associated with a given set of loads. Furthermore, for the maximum wave and full breach simulations, effects of wave shoaling were removed so that the full effects of waves are accounted for. This allows comparison between maximum non-breach and breach flood events of the equivalent SWL.

As already noted, coastal and flood defences are allocated to the model according to the regional-scale data and analysis of the main shoreline features (Section 4.2.3). The following sub-section introduces more site-specific detail and analysis of flood events at the city of Portsmouth, which has a more complex flood defence system and urban floodplain configuration.

4.6.2. Portsmouth detailed simulations

Portsmouth is one of the two sites in the case-study where 50 m Solent-wide flood simulations are supplemented by more detailed analysis and higher (10 m) resolution simulations (Section 6.2).

Portsmouth is surrounded by a perimeter of seawalls and embankments; most of which are established as flood defences (and hence included in the defence datasets). Additional time was taken to ensure flow routes across the floodplain surface are represented by the DEM, which was manually edited to accurately to schematise important barriers on the edges and within the floodplain since in a number of places gaps resulted from the LiDAR sampling and DTM processing. This was achieved via inspection of aerial and ground-based photos and the 1 m resolution LIDAR DSM, site visits, discussion with local authority engineers, and the validation case studies (Chapter 5). However, as described below, there are several defences which are contentious in terms of their response to loadings and representation in numerical flood event simulations. In living memory at Portsmouth there have not been flood events of the severity to provide observations that indicate patterns of flow within the larger floodplains.

It is apparent that several features which are likely to substantially divert flow during flood events. The coarser 50 m resolution model in particular overly can simplify two features in particular, because of

the interpretation of their response (and subsequent influence) to more extreme loadings than previously observed. These uncertainties are listed below, with (1) and (2) affecting defences and flooding either side of Port Creek (the narrow tidal waterway between Portsea Island and the mainland – refer to Figure 4.21):

1. Tunnels/subways through the A27 road embankment on the southernmost edge of the Portsmouth mainland: Surveys indicate that the A27 mainland defences (Figure 4.20a) are in good condition with minimal wave-exposure, and with crest levels above present day extreme SWLs; hence significant overtopping or breach failure is unlikely. These defences are also foreseen to remain well maintained by the Highways Agency (EA, 2009c). However, the DEM suggests that sections of the path which is seaward of the A27 embankment are flooded to a depth of approx. 0.2 m during a 1 in 200 return period SWL event which could allow sea water to flow through the concrete-lined underpasses (Locations 1 – 3, Figure 4.21). The westerly underpasses connect the seawater in Port Creek and residential land behind; the easterly underpass (Location 4, Figure 4.21) can only flood if the Farlington sea wall fails and the marshes are inundated. The LiDAR DSM suggests that the height of defences at the train tunnel and underpass is equivalent to a current 1 in 50 year SWL. Flooding in the future could also occur under the M27/A27 at the Eastern Road Roundabout (adjacent to Location 3, Figure 4.21). Ground levels in this area are around 3.5 mODN (approximately equivalent to a present-day 1 in 200 year level plus 0.3 m SLR).
2. Historic inland walls – the ‘Hilsea Lines’: these earthworks are classified as historic monuments and nature reserve, rather than flood defences. They are further inland than the lower-lying sea defence embankments on the south shores of Port Creek (also known as ‘Portsbridge Creek’). The Hilsea Lines provide a continuous second-line of raised land and walls (over 9 m high in places) across approx. 3 km of north Portsea, and when high tides have previously overtopped the Port Creek defences (e.g. 13 December 1981 – Table 3.2), the moat and walls have so far prevented seawater from reaching the industrial units and residential areas behind (PCC, 2011). However, the Hilsea Lines are comprised of earth and chalk, and throughways exist (e.g. the passage shown in Figure 4.20b) hence their water retaining capability and structural integrity is uncertain for longer-term coastal flood protection.
3. Buildings: Portsmouth is densely urbanised, and as noted in Section 4.5, the 10 m model is able to incorporate buildings as cells with higher friction values. There are numerous approaches to deal with buildings within inundation models (*c.f.* Syme, 2008) and in view of the larger uncertainties (e.g. overtopping volumes) the method used here is sufficient to provide an approximate comparison with the simulations that exclude this parameter.

For the Solent-wide 50 m resolution simulations (Section 6.1), Locations 1, 2, 3, 4 and 5 (Figure 4.21) are represented as individual cells through which water can propagate if the outer defences are

overtopped. However, the width of these cells in the 50m model, and the likelihood that they could be intentionally and temporarily blocked (e.g. if advised by flood warnings) suggests that the representation of these flow routes is excessive. In the simulations shown in Section 6.2.1, these apertures are represented equivalently for both the 10 m and 50 m models (i.e. as 50 m wide) so that the effects of floodplain resolution and inclusion of friction can be directly compared. In sections 6.2.2 and 6.2.3 the 10 m simulations are adjusted to provide a more realistic and probable representation of the flood system across loadings, by assuming that the Hilsea Lines remain sealed/impervious, whilst the A27 underpasses are represented as only 10 m wide holes.



Figure 4.20. (a) The A27 embankment, and (b) Hilsea Lines (Location 5, Fig. 4.21)

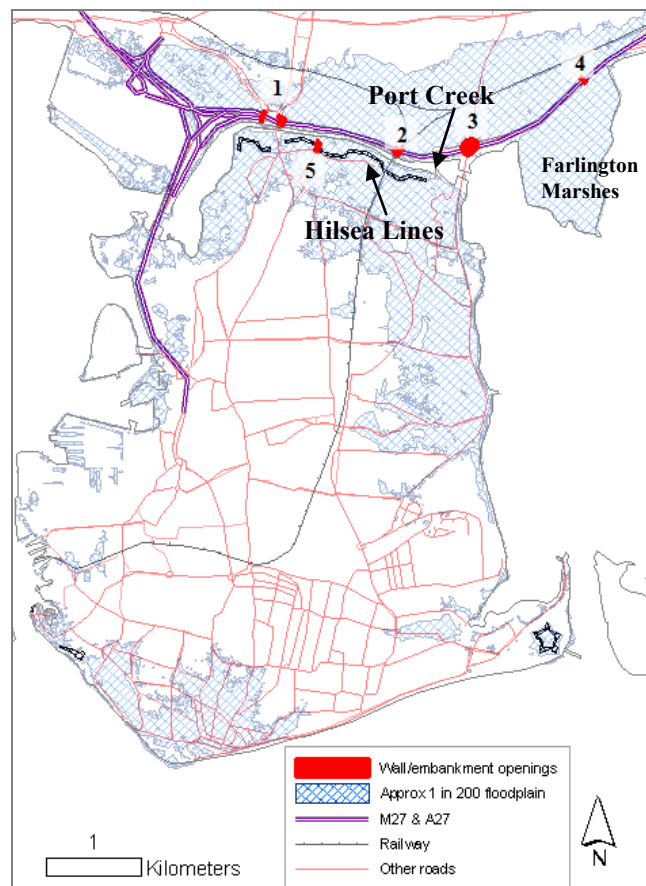


Figure 4.21 Locations of potentially compromised section of flood defences in north Portsmouth

4.6.3. Additional Pennington breach scenario

For the detailed Pennington case-study an additional breach scenario (to the full breaching scenario) is included. Breach events are difficult to predict and therefore complex to prescribe to specific event simulations: the aim of this additional scenario is to demonstrate inundation simulations from specific breach failures (Figure 4.22a) in a flood compartment where there has previously been breaches and significant coastal flooding (Figure 4.22b). Six ‘sub-compartments’ were identified on the basis of intra-floodplain break-lines (which would reduce flow within the floodplain). Up to 4 breaches were selected in each of sub-compartment, and a set of 15 potential breach locations were identified by potential weak points in the defences. Each was schematised as 10 m wide by 1 m deep. Weak points were identified by a combination of fragility curves, transitions between hard and soft defences, and two flood gates at Keyhaven which would normally be closed on extreme tides (these are in sub-compartments 1 and 2, and are not strictly breaches).

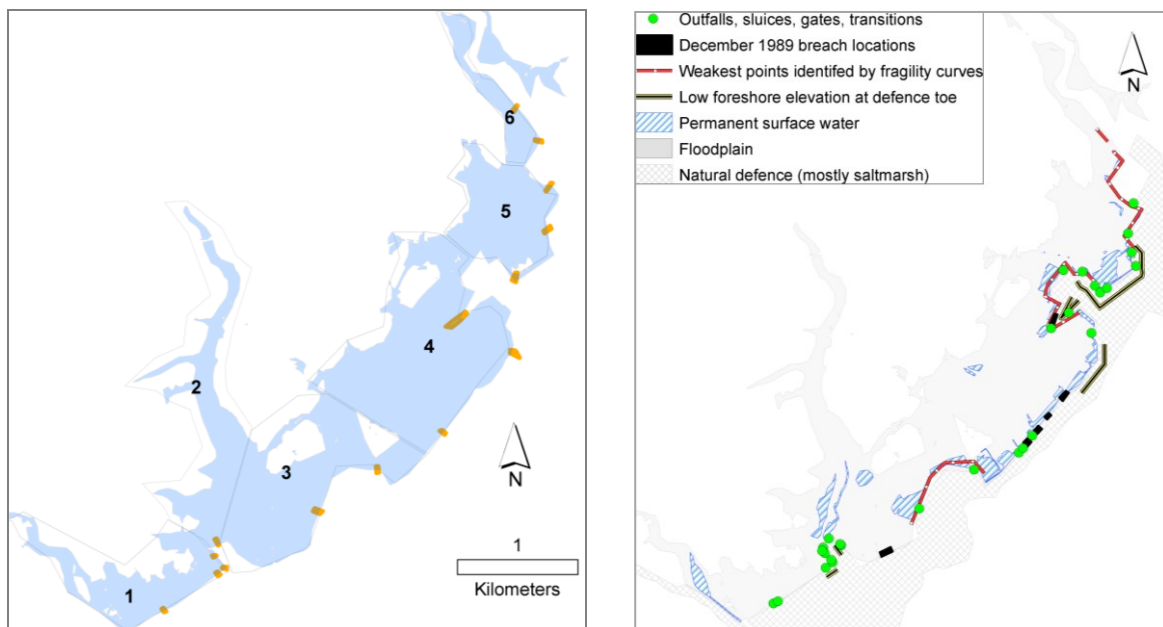


Figure 4.22 (a) Breach locations selected for the additional scenario at Pennington, and sub-compartments which contain topographic break-lines which may restrict hydraulic connectivity; **(b)** defence weak spots and approximate locations of 17th December 1989 breaches

4.7. Summary

This chapter describes a methodology to simulate and analyse coastal flood events for the Solent case-study area. Coastal flood defence data, including crest heights and parameters for overtopping calculations (slope, foreshore height, roughness, berms, gaps etc.) have been assembled and combined with a digital elevation model (DEM) of the floodplain in digital terrain model (DTM) format, derived from high resolution LiDAR data sets. For feasibility of simulating multiple scenarios across the large and varied case-study, this has been resampled to 50 m and 10 m resolution cells using a bilinear

technique, as endorsed by other flood modelling studies (Fewtrell et al., 2008b; Landform, 2011). These data sets are coupled to the inundation model LISFLOOD-FP (although in principle other 2D models could be applied). This requires parameters set by the user, primarily: inflows (locations and volume or water-level time-series), time-step (in this case utilising an adaptive time-step mode), and surface friction.

Notable from this chapter and the literature, is that there are many methods and models available for simulating coastal floods. However, there is no definitive guidance for coupling overtopping and/or breach analysis to numerical simulations of inundation. The development of this methodology required detailed site-specific considerations for the Solent case study floodplains, as well as various assumptions and decisions which highlight generic issues within methods for overtopping, breach and inundation modelling. These are discussed in more detail in Chapter 7. This method can be compared to other coastal flood modelling studies:

- Purvis et al (2008) simulated extreme events (using similar defence and floodplain data sets, and inundation model to this research), for a site in Somerset in the Bristol Channel, UK. Differences to this Solent case study are exclusion of wave inputs and use of a more simplified (triangular) storm-tide water level time-series. However, a larger range of SLR scenarios are evaluated.
- At North Sea coast sites, EA and Mott MacDonald (2010) couple empirical overtopping and full 2D inundation modelling to simulate hypothetical events and generate flood warning maps / hazard maps. The Wash floodplain in Lincolnshire exemplifies some of the key geographic differences between these floodplains and those of the Solent. The Wash floodplain covers more than 2,200 km² and extends 25 km inland. In comparison, the approximately equivalent Solent floodplain (e.g. the 1 in 200 year planar water level floodplain) totals less than 70 km² across approximately 100 hydraulically disconnected units of land. Table 4.5 highlights the relatively compact nature of the case study's floodplains.

Table 4.5 Selection of floodplain volumes (relative to approx. 1 in 50 - 1 in 200 year sea level events)

<i>Location</i>	<i>Volume (km³)</i>	<i>Source</i>
Canvey Island, England (UK)	0.10	Brown et al. (2007)
Towyn, Wales (UK)	0.01	Dawson et al (2011a)
Portsmouth, Solent (UK)	0.02	Wadey et al. (2012)
The Wash (Sleaford & Peterborough)	0.20	MottMacDonald and EA (2010)
New Orleans	0.85	Van Heerden (2007)
London	0.69	Fewtrell et al. (2008a)

- A greater emphasis upon numerical wave and overtopping modelling has been used in other studies to assess extreme floods and SLR scenarios. Chini and Stansby (2012) generate numerical simulations of wave propagation and overtopping processes. These high frequency time-series can

be inputs for inundation modelling (*c.f.* Stansby et al, 2011), and may reduce uncertainties described in empirical calculations of overtopping-inundation. However data and computational costs presently allow this to only be viable at relatively small sites, whilst uncertainties remain (e.g. morphological changes).

To evaluate the data sets and modelling for the simulation of hypothetical events, the following chapter describes an assessment of the methodology against an observed coastal flood event in the case study region. This exercise also underpins the methodological position of this thesis, and informs an understanding of coastal flood events (and their impacts) in the case study region.

Amongst the more contentious overtopping method decisions is generating estimates of overtopping onto floodplains above SWL (e.g. Eastoke, Hayling Island). In these situations, inundation is described as ‘hydrostatic’ rather than ‘hydrodynamic’ (Tsubaki and Kawahara, 2012) with less momentum and pressure gradient than floodplains below the peak SWL. In the absence of detailed numerical simulations of wave overtopping processes, some form of depth limit is necessary to simulate the inflow and subsequent flooding (refer to Section 4.3.1); whilst for all defence and floodplain interfaces the issue of ‘critical’ discharges (which were used here to temporally delimit the duration that waves can discharge water over the crest) can also be viewed as almost subjective in view of the large uncertainty associated with empirical overtopping volumes. However, until further research becomes available, the validation and practicality aspect supports the methods shown in this case study; whilst even more strongly promoting the concepts underpinning the methodology shown here: (1) collecting flood event data, and (2) presenting results across a wide range of failure and load scenarios.

5. Model Validation & Understanding Coastal Flood Events

This chapter describes the collation of data relating to coastal inundation, and to assess the capability of the method to replicate observed floods. Boundary conditions from actual storm events were extracted from available tide gauge and wave records as inputs to the model and to simulate flooding. Results were compared to observed flood extents and impacts (including locations and descriptions of properties and roads that were reported to have flooded). Also described is an overview of coastal flood events and water level history in the Solent case-study. The main source of flooding in the case-study events was extreme still water levels caused by storm surges, high tides and waves. The following events were assessed to evaluate the method and the analysis of the hypothetical coastal flood simulations (Chapter 6):

- *Regional flood event, 10th March 2008*: photos and descriptions of the widespread flood incidents across the region, mostly due to overflow and overtopping;
- *Flood event at Pennington, 14th and 17th December 1989*: although defences have since been upgraded, assessment of these events provides some indication of the DEM accuracy and of how well the model simulates larger defence failures – several breaches occurred on the 17 December 1989 (Figure 4.22). This study focuses upon a single flood compartment, although this event was caused by a prolonged period of storms in the English Channel (Wells et al., 2001) that resulted in widespread flooding across the Solent (Ruocco et al., 2011).

The main stages for validation of the modelling methods are summarised in Figure 5.1 – which is most applicable to the 10 March 2008 event due to the availability of data.

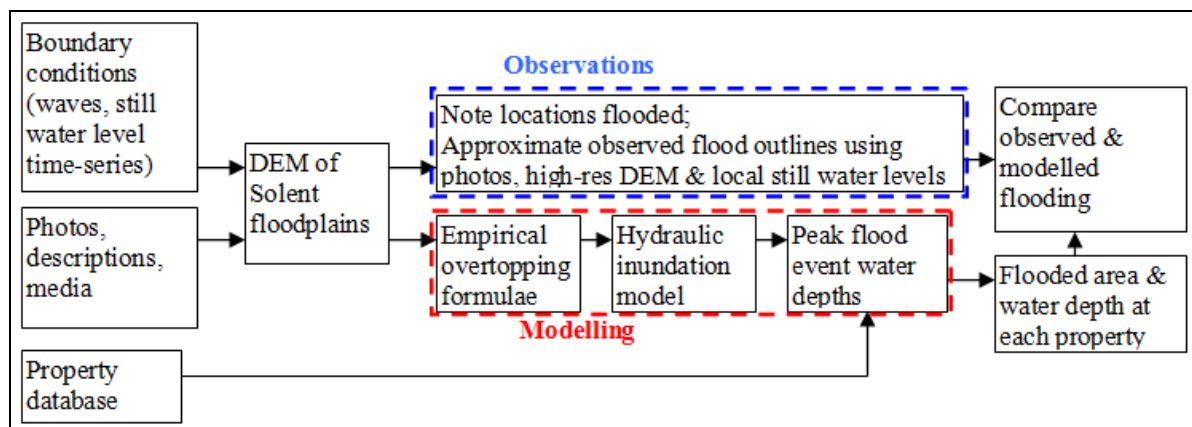


Figure 5.1 Methodology outline: floods were modelled and compared to observations

The observed floods were compared to model results by the following methods:

- Simple binary comparison, i.e. note whether or not the model generates flooding within the same flood compartment(s) that flooding had been reported;

- In some locations, photos or descriptions allowed an approximation of the flood outline to be digitised, aided by the manual inspection of the high resolution DEM (generated by the original LiDAR data), OS maps (containing roads and houses) and the presence of nearby still water level recordings. This allowed modelled and observed coastal flood extents to be compared using a fit measure (F_A) referred to in previous coastal flood modelling studies (Bates et al., 2005; Gallien et al., 2011). This comprises the intersection and union of predicted (E_p) and observed (E_0) flooded pixels. A value of zero corresponds to no agreement, a value of 1 to perfect agreement:

$$F_A = \frac{E_p \cap E_0}{E_p \cup E_0} \quad (27)$$

- Where the model generated flooding, the peak water depth from the simulation was noted; to determine if the model outputs comprised unrealistic depths that would have warranted significant mention (e.g. in the media).

The use of simplified boundary inputs and the large pixel size (50 m) meant that over-prediction or under-prediction by the model was considered negligible unless more than one full flooded cell lay outside of the observed extent. The F_A method and large pixel size also means that in cases of good model fit (e.g. $F_A > 0.75$) not all values qualify as over or under-predictions.

In the assessment of the 10 March 2008 event, the area considered as the ‘observed’ flood extent (E_0 in eq. 27, used for comparison with the simulated flood extent) was represented by polygons. Amongst the data sources used for digitisation of these polygons were photos, which provided spatial-visual reference points for comparison with aerial and ground level data (e.g. OS maps, aerial photography Google Street View). Due to the varying obliquity of the view, the entire flood extent is not fully captured by images taken during the event; hence a spatially extended interpretation of these photos was undertaken via analysis of surrounding topography (LiDAR DEM), defences, and local sea levels.

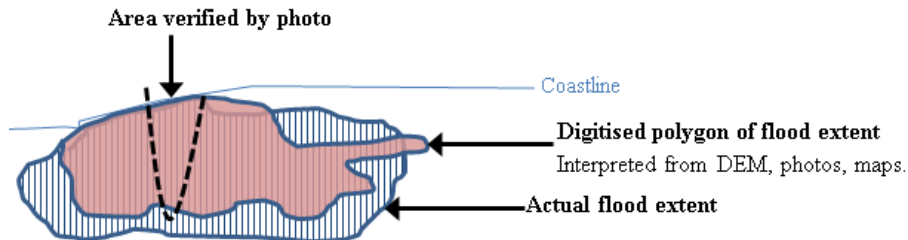


Figure 5.2 Application of flood event photos to verify inundation area and characteristics

In some instances, the timing and view captured by photos allows verification of a large portion of the likely actual flood extent. Often a discrepancy remains, because the method incorporates a varying degree of subjectivity, judgement and local knowledge to delineate boundaries of areas covered by

floodwater. In most cases the flood polygon boundaries are more certain because of the information verified by photos captured throughout the event, and in some instances such as Location 27 (Bosham) accompanied by a description of the spatial extent and characteristics of the floods (West, 2008). A quantification of the summary of the regional availability of photos to generate the observed flood extent polygons is provided in Appendix D.

5.1. The 10 March 2008 Storm Surge

This section focuses on the storm surge event which occurred on the 10 March 2008. This event has been described by Haigh et al (2011). On the 9 March 2008 a strong jet stream across the north Atlantic created a deep low depression off southeast Greenland. As this moved southeast over the northern Atlantic, the central pressure dropped rapidly from 975 mb at 0600h (9 March) to 946 mb 18 hours later. The central pressure remained very low as the system moved over Ireland, across the Midlands and into the North Sea. The path of the storm is shown in Figure 5.3 and was typical of storms that tend to generate large surges in the English Channel (Henderson and Webber, 1977). A high spring tide was predicted for the 10 March and the time of high tide coincided with the passage of the storm. As the event passed over Ireland and England, the low pressure and strong south-west to westerly winds generated a surge of around 1 m in the central regions of the English Channel. The skew surge (Figure 2.5) exceeded 0.7 m at six stations: Weymouth, Southampton, Portsmouth, Jersey, Cherbourg and Le Havre. Further east in the English Channel, the surge was much smaller.

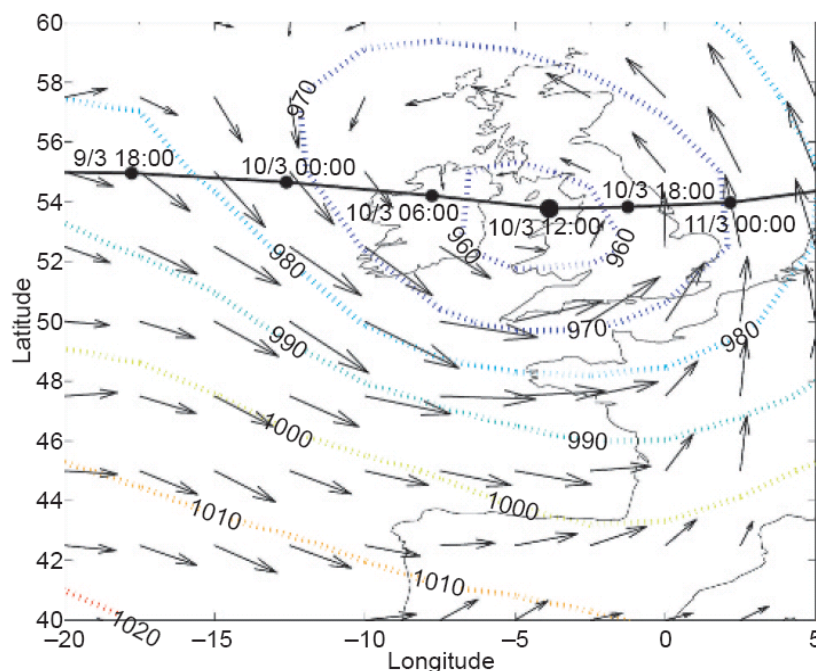


Figure 5.3 Atmospheric pressure at 1200 h on the 10 March 2008 over the British Isles and the approximate storm track (the arrows indicate wind direction and the dotted contours atmospheric pressure). This plot was generated by Haigh et al (2011) using the US National Centre for Environmental Prediction global reanalysis data)

Localised flooding occurred in the western and central Channel including Teignmouth (Devon), Flushing (Cornwall), and in several small towns along the Brittany coastline; whilst in the Cornish town of Perranporth fire-fighters had to pump seawater from a pub and several businesses (BBC, 2008c). Flooding was extensive in the Channel Islands. In Jersey, the damage to sea defences was estimated at about half a million pounds (Le Blancq and Searson, 2008). Flooding also affected Poole in Dorset; forcing road closures and threatening valuable property (BPUA, 2011).

In the Solent, the storm surge peak and tidal high water coincided across most of the region. The time of high water was approximately 12:00 at Lymington, 12:30 at Southampton, 13:00 at Portsmouth, and 13:30 at Selsey Bill (refer to Figure 5.4). Flood warnings were delivered in most of the affected areas (EA, 2010c) and the daytime occurrence of this event allowed the public to respond by moving possessions and building temporary defences. Most flooding was relatively minor, although there were numerous road closures and more than 30 properties reported flooded (12 requiring evacuation) (EA, 2010c). A holiday park in the flood plain at Selsey was evacuated (BBC, 2008a) in what was the most dramatic incident during the event. This was caused by waves flattening an 800 m section of the shingle barrier beach (Cope, 2012). New defences at Portsmouth and Lymington prevented serious flooding in areas which had previously flooded during similar events, and no sea walls or embankment structures in the region were reported to have breached (where breach is defined by formation of an aperture or a reduction in the crest height of a defence). The onset of the flooding from overflow, overtopping and outflanking of defences was however quite rapid, and reports by local resident associations suggest that the event initiated concern about the impacts of climate change and the needs to improve flood event management procedures (e.g. West, 2008; YCDWG, 2010). The event came close to causing more significant impacts in the Solent's cities: sea water was within centimetres of flowing onto Southampton's Docks (Figure 5.10); and in Portsmouth reportedly leaving Southsea's Rock Gardens 'under up to nine inches [0.23 m] of seawater for the first time in the past 60 years' (TN, 2008a).

The official flood event report (EA, 2010c) suggests that 30 properties were affected. Whilst this source provides essential background information, the omission of various flooded locations discounts its role as a comprehensive quantification of the number of properties flooded, and is likely to be an underestimate. For example, it was reported in Bosham (Location 27 in Figure 5.6; see also Figure D7) that the EA were unable to incorporate third-party reporting of flooded properties. In this chapter, an extended understanding of the number of properties close to or in contact with flood water is attained, using a compilation of flood event outlines listed in Table 5.2.

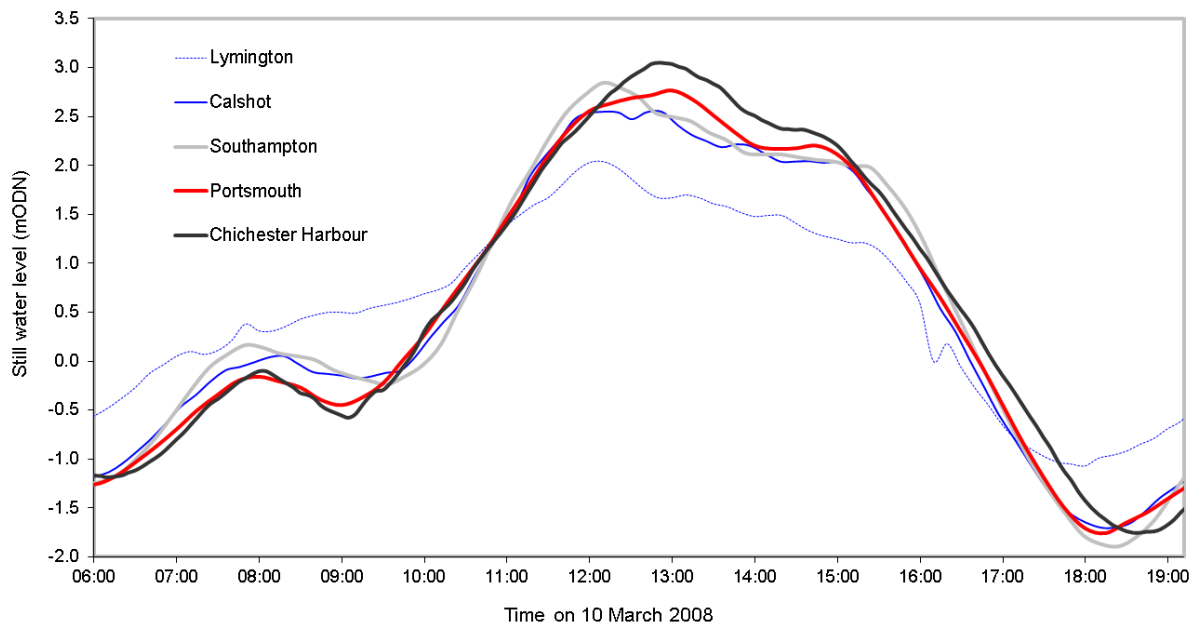


Figure 5.4 Still water level time series across the Solent on 10 March 2008

Measured water levels and waves are available for the tide gauge locations listed in Table 5.1 (time-series also shown in Figure 5.4, locations in Figure 5.7). Distances between these measurements were relatively large, hence spatial interpolation was applied based upon the EA's UK coastal boundary condition guidance described in McMillan et al. (2011), which comprises 2 km alongshore spaced points for different return period water levels (gained from observations, hydrodynamic modelling and extreme value analysis). The gaps between the 10 March 2008 measurements were interpolated and extrapolated using the same proportional spatial water level differences that this guidance suggests, giving a higher resolution boundary water level dataset. Recorded wave heights and periods were interpolated and scaled spatially in proportion to calculations of fetch-limited conditions within the harbours and rivers. Flood event data was compiled from the ad-hoc series of reports and photographs. Most flood extents were in the range $0.01 - 0.03 \text{ km}^2$, and floodplain water depths under 1 m. An exception was more severe flooding at the Selsey caravan park in the East Solent.

The flood extents were too small for a formal calibration and a full analysis of uncertainty (*c.f.* Aronica et al., 2002). However, the observation data suggested a simple addition that could be used to account for the effects of the significant amount of rainfall upon the upper reaches of the tidal rivers, via trial and error. The best results were produced by adding 0.1 m to the boundary water levels at the upper tidal reaches of the region's rivers, and this is included in the results shown in Table 5.3. Locations 2 and 29 (where flood depths were reportedly shallow) could not be flooded by the model without this addition.

Table 5.1 Measured peak water levels and waves on 10 March 2008

Location ref. in Figure 5.7	Tide gauge/measurement location	Peak still water levels		Peak wave conditions (CCO)		
		Recorded water level (mODN) & source of data	Approx. return level	H _s (m)	T _p (s)	Range of annual max. H _s (m) recorded 2003-2008
A	Milford-upon-Sea			3.42	11.0	2.92 – 4.09
B	Lymington	2.04 (CCO); 2.17 (EA)	1 in 10	3.42	11.0	0.81 – 1.44
C	Cowes	2.63 (EA); 2.61 (CHM)	1 in 10			
D	Calshot	2.55 (ABP)	1 in 5			
E	Southampton	2.88 (EA); 2.84 (ABP)	1 in 20			
F	Portsmouth	2.77 (BODC)	1 in 10			
G	Hayling Island			3.79	8.3	2.68 – 3.79
H	Chichester Harbour	3.1 (CHIMET)	1 in 20			
I	Bosham (Chichester Harbour)	3.3 (West, 2008)	1 in 50			
J	Sandown Bay			3.63	8.3	2.79 – 3.79
K	Sandown Pier	2.52 (CCO)	1 in 5	1.62	10.6	1.82 – 2.01

The data in this table was provided by: Channel Coastal Observatory (CCO), Environment Agency (EA), Cowes Harbour Master (CHM), Associated British Ports (ABP), chimet.co.uk (CHIMET); and a land-based measurement in Bosham (West, 2008). The return periods are for the year 2008, approximated according to analysis by McMillan et al (2011). H_s is the significant wave height, T_p is the peak period (as recorded during the same tidal cycle of the highest water levels).

The extent of the largest flood on the day at Selsey (Figure 5.5) is uncertain because: (1) a large area was affected (much of which is out of view of the photo – refer to Table D7), (2) a significant variation in simulated flood extent is generated by varying the friction parameter in the inundation model, (3) the complex temporal and spatial dynamics of breach and overtopping, (4) the management/repair of the breach (and potential for continued inflow on the next high tide). The maximum (likely) theoretical flood extent is gained from laying the nearest known SWL (3.3 mODN) as a planar surface across the DEM, which generates a flood extent of almost 8.8km². Alternatively, using the numerical inundation model to route the nearest recorded SWL time-series through the approximated breach area generates flooded land areas of between 4.7–5.8 km², from the application of friction coefficients (n) of n=0.06 and n=0.035 respectively. The inclusion of wave overtopping volumes generates flood extents of 6.5–8.6 km² for the same range of surface friction values. These results are based upon simplifications such as breach size assumed as fixed for the duration of the tidal cycle. However, each of the numerical simulations generates plausible water depth at the locations where flooding observations were available (Figure 5.5), and there was no conclusive evidence against using the default and homogenous n=0.035 value for the Solent-wide simulations of Chapter 6. However, it is recommended in Section 7.3.2 that future work could focus upon delineating large flood extents more accurately (e.g. via aerial images) to further assess both the flood-spreading and defence failure components of the model.

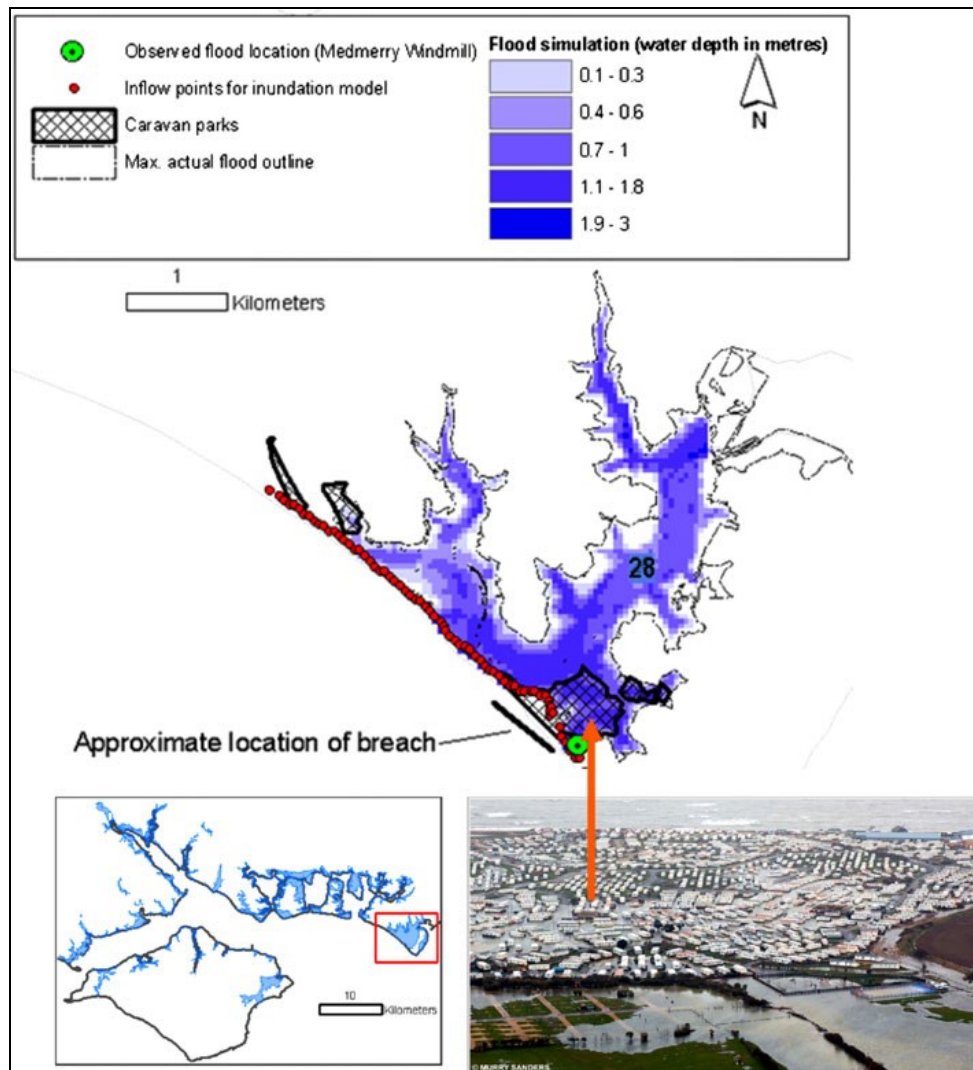


Figure 5.5 Flooding at Selsey, where waves flattened and overtopped the shingle barrier, flooding a caravan park on the 10 March 2008 (Mail, 2008). Shown is an observed flood location where flood waters reached the base of an historic windmill (West, 2010) which lies on the vertices of two cells from the flood simulation, with modelled peak flood depths of 0.15m and 0.70 m.

Whilst Table 5.2 catalogues flood incidences of 10 March 2008; Table 5.3 provides a summary of: (1) flooded land area, (2) the model's performance and (3) the number of properties indicated to be close to flood water. The photos taken during the event cover 30 of the 37 reported flood locations. These indicate that at least 150 properties were in contact with water, for example Figure 5.6 suggests that a minimum of six properties are in contact with flood water. The 'view' of flood extents provided in these photos was extended by digitising flood outlines (facilitated by GIS software) along the path of the likely flooded area (roads, etc., aided by descriptions and the DEM). These polygons indicate that 342 properties were in contact with the flood waters (although as noted in Table 5.3, this estimate increases substantially if the polygon is slightly extended).



Figure 5.6 Example of utilisation of photos to approximate observed inundation extent; (a) this photo looks east along Queen Street, Emsworth (Location 26) allowing two clear reference lines along the side of the street, whereas (b) and (c) allow a closer view enabling locations to be spatially referenced to more distant landmarks, such as the intersection between the two main roads, and the wall surrounding Mill Pond. A useful tool for reference was Google Maps and Street View, as shown by (d) and (e). Figure 5.6 (f) depicts the area captured by these images in proportion to the overall flood extent – the visual interpretation (shown by the red dashed lines in the above photos) is converted to a polygon and the area is then measured in GIS. Photo sources for (a), (b) and (c): Emsworth Residents Association; source for (d) and (e) copy right Google (2013).

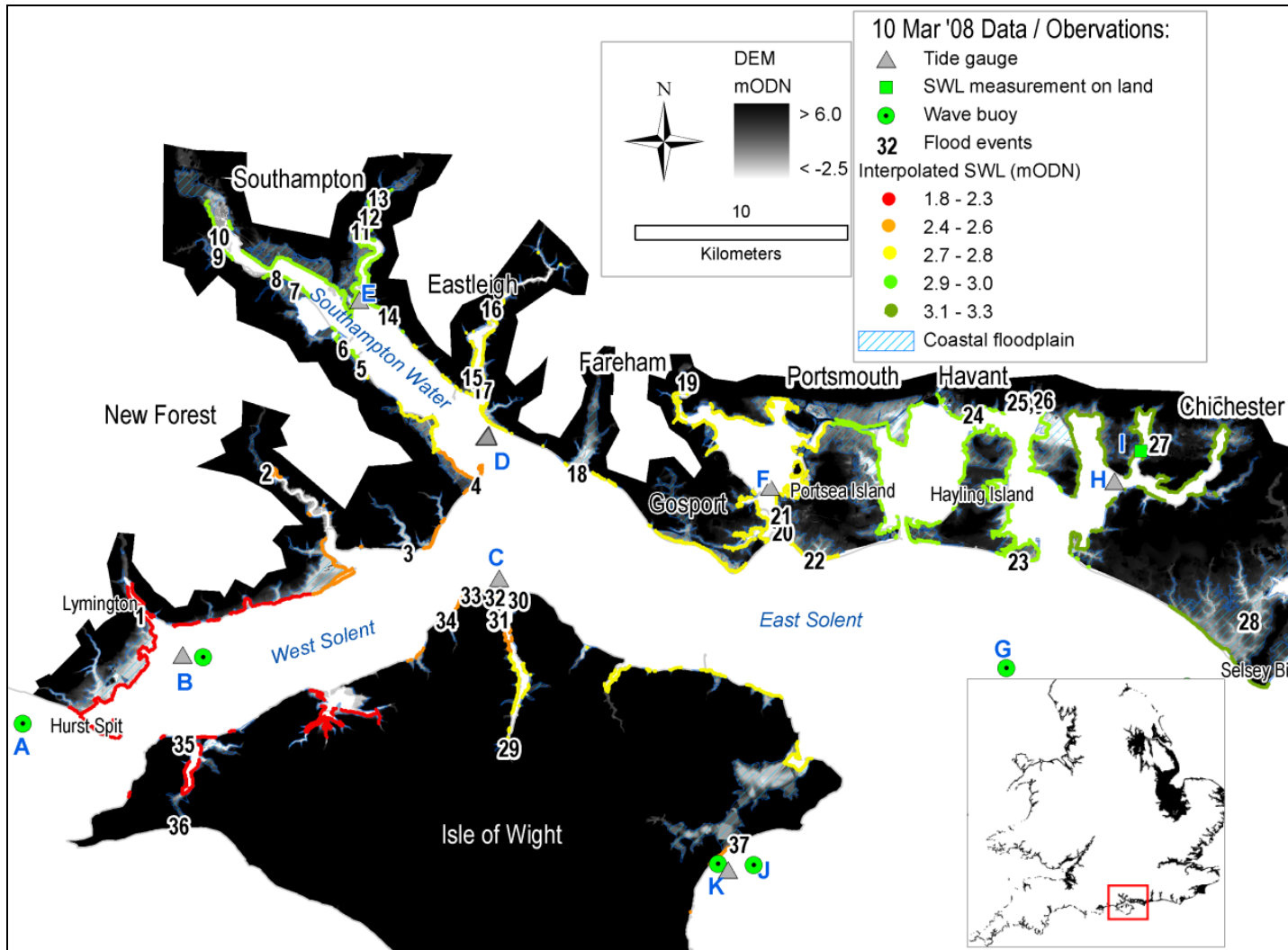


Figure 5.7 The Solent case study and locations of wave, water level and flooding observations during the 10 March 2008 storm surge event. The locations labelled are observations of coastal boundary conditions (Table 5.1), flood events determined by eye-witness accounts and photos (Table 5.2), and SWLs interpolated from the measurements

Table 5.2 Summary of flood locations and mechanisms (OF=overflow/outflanking, OT=overtopping, BR=breach, NC=non-coastal) and observations on 10 March 2008. The model performance is indicated by the goodness of fit score between observed and modelled flood extents (eq.27).

Location no.	Sub-region	Flood compartment / area	Site recorded as flooded	Likely flood extent (km ²)	Mechanism	Model performance (FA) & whether under/over predicted	Main source of observations
1	New Forest	Lymington	Quay Street	0.002	OF	0.90	EA (2010c)
2		Beaulieu	Palace Lane	0.032		0.90 OP	
3		Lepe	Lepe Road	0.025	OT	0.75 UP	
4		Calshot	Calshot Road	0.042	OF	0.60 OP	
5		Hythe	Shore Road & Sailing Club	0.069		0.78	
6			The Promenade & Prospect Place	0.022		0.56	
7			Marchwood: Cracknore Hard	0.017		0.42 UP	
8			Marchwood: Magazine Lane	0.014		0.29 OP	
9		Totton	Eling: Down's Park Crescent & Down's Park Road	0.068		0.97	
10			Commercial Road	0.007		0.88	
11	City of Southampton	Southampton East	River Itchen: Saltmead	0.004	OF	0.92	SCC (2010); EA (2010c)
12			River Itchen/St Denys: Priory Road	0.004		0.57 OP	
13			River Itchen: Woodmill Lane; Oliver Road	0.028		0.38 UP	
14		Weston to Woolston	Weston Shore: Weston Parade	0.025	OT	0.55	SDE (2008)
17	Fareham	Warsash & east River Hamble	Passage Lane & Shore Road	0.017	OF	0.80 UP	EA (2010c)
18		Hill Head	Unknown – “driver had to be rescued by fire-fighters from his car when it was swamped by water”.	N/A	OF, OT	Model indicates 2 pixels of flooding of ~0.3 m depth on road	TN (2008b)
19	Eastleigh	Wallington	Wallington Shore Road & Delme Drive	0.022	OF, NC	0.2 UP	FBC (2011); WVCA (2011)
15		Hamble	Rope Walk, Well Lane & Green Lane	0.005		0 UP	EA (2010c)
16			Bursledon: Blundell Lane	0.026		0.65 UP	
20	City of Portsmouth	Old Portsmouth	East Street &, Broad Street; flooding at ferry terminal & buildings at Camber Quay	0.016	OF, OT	0.50 OP	BBC (2008b); EA (2010c)
21		West Portsea	The Hard (“car engulfed near slipway opposite the Ship Ansom pub”).	N/A		Model indicates a single flooded pixel of ~0.7 m water depth	TN (2008b)
22		Southsea	Clarence Esplanade (including the ‘Rock Gardens’)	N/A	OT	Model indicates shallow (~0.1 m) patches of water in the rock gardens and on Southsea Common	TN (2008a); PCC (2009)
23	Havant	Eastoke, Hayling Island	Southwood Road, Creek Road, Nutbourne Road & Bosmere Road	0.022	OF	0.15 OP	EA (2010c)
24		Langstone / Havant Mainland	High Street; the car park of ‘The Ship’ pub sea water “trapped customers & staff vehicles”.	0.048		0.50 UP	TN (2008b); EA (2010c)
25		Emsworth	Bridge Road Footpath, Bath Road & Mill Pond	0.067		0.86 UP	ERA (2008); EA (2010c)
26			A259, Queen Street & Lumley Road	0.009		0.76 UP	
27	Chichester	Bosham	Shore Road, Bosham Lane, Stumps Lane, The Drive, High Street & Harbour Road	0.077	OT, BR	0.95	West (2008); CO (2008a)
28		Selsey	West Sands Caravan Park (30 people evacuated, 100 caravans damaged)	N/A		4.7 – 8.6 km ² indicated inundated by range of modelling methods	BBC (2008a); CO (2008b); Cope (2012)
29	Isle of Wight	Newport Town Centre	Medina Way, Sea Street & The Quay	0.027	OF, NC	0.33 UP	EA (2010c); IRF (2011); Hodgson (2012); Weymouth (2012)
30		East Cowes	Esplanade	0.012	OF, OT	0.91	
31		West Cowes	Brunswick Street, Medina Road, Bridge Road, Fountain & Town Quays, High Street, Red Funnel Ferry Terminal	0.060		0.62 UP	
32			Egypt & Princes Esplanade	0.026		NK	IOWCP (2008); EA (2010c)
33			Marine Parade	0.004			
34		Gurnard	Marsh Road & Rew Street	0.016			
35		Yarmouth	Bridge Road, Quay Street, The Quay & River Road	0.093	OF	0.85 UP	EA (2010c); YCDWG (2010)
37		Eastern Yar	Yaverland Road (sea water flooded car park at ‘Dinosaur Island’)	N/A (but >0.005)	OT	Model indicates shallow flows (<0.1 m) behind seawall, similar to photos, although full extent unknown.	Price (2013)
36			Freshwater Bay	N/A (~0.001)		Model indicates a flooded pixel of ~0.2 m water depth	IOWCP (2008)

The flood outline generated by the simulation contains more than 1,000 properties (Table 5.3), although because the altitude of the flood-water entry thresholds for each property is not known it is unsurprising that this is an overestimate, especially given other uncertainties (e.g. vertical error in the original LiDAR data and boundary inputs). Therefore, using the model to provide a realistic estimate of properties that could be considered actually or nearly flooded; the simulation’s inundated pixels can be filtered by depth (rather than counting all of the properties within the raw flood outline). Table 5.5

summarises the ‘depth filtering’ that is required for the number of properties within the simulated flood outline to match the number of properties in the observed flood polygon. This only considers the locations where photographic evidence is available. It is noted in flood impact guidelines assessment guidelines (e.g. Penning-Rowsell et al., 2005) that approximately 0.2 – 0.3 m is a typical threshold depth for water to enter property – an approximation which is valid in some of the Solent locations for the 10 March 2008 event, although larger depth cut-offs are required in some locations.

The simulation’s greatest overestimation of the total number of flooded properties is on the densely urbanised Eastoke Peninsula on Hayling Island, Havant, where available reports and photos (Figure D6) suggest that wave overtopping caused shallow flooding on several streets, but no apparent property impacts. Flood predictions here are sensitive to the inaccuracies in the empirical overtopping calculations, a lack of parameterisation of sub-surface drainage and over-spreading of flood water on the coarsened DEM (which did not incorporate buildings). These factors contribute to a poor model fit score (F_A , eq. 27) with more than 350 properties in the overall simulated flood outline. However, the flooded property count here reduces substantially if considering only water depth pixels greater than 0.25 m, and to zero above 0.5 m.

The F_A score indicates good overall agreement in the flooding predictions, in relation to the flood event observations. Instances of poorer comparison occur on narrow strips of floodplain, which could simply be improved by using a less interpolated version of the DEM. A more accurate representation of topography and water depth distribution would be especially beneficial for depicting flow on narrow floodplains, individually flooded roads and over more complex urban topography. This confirms the relevance of applying higher-resolution case-studies (to assess hypothetical events) described in Sections 6.2 and 6.3, where a 10 m (rather than 50 m) grid is deployed. However aforementioned uncertainties in the observation data and the defence failure inputs suggest that a finer DEM may not be a priority for significantly improving inundation simulations in all areas. The under-prediction of flood extent (and properties) was most apparent at locations 15, 19, 26 and 29 (Table 5.2), whilst defence failure inflows and surface friction parameterisation generate uncertainty for flood extent predictions on the open coasts of Selsey and Eastoke (Hayling Island). For future flood modelling, particularly at Eastoke and the tidal river locations, spatial resolution of modelling and boundary water levels should be reviewed (e.g. for the latter of these surge propagation and non-coastal flood sources may be significant to the occurrence and impacts of coastal flooding).

Across the region, the hydraulic modelling and the analysis of the observations indicate that flood waters threatened more locations than was reported. Enlarging the (manually digitised) polygons of observed flood extents generated by the photos and descriptions) by applying a 10 m buffer provides a fuller coverage of areas threatened by flooding (e.g. gardens, driveways) and suggests that in excess of 750 properties were near or in contact with flood water (Table 5.3). Walls, fences, raised floor levels and flood prevention measures (e.g. sandbags) would have reduced the number of incidents where

floodwater entered and damaged the interiors of buildings, and flooding of outbuildings and gardens may not have been reported. The simulation further indicates that aside from the incidents mentioned in Table 5.2, that there may have been as many as 20 additional flooded locations across the Solent during the 10 March 2008, comprising more than 100 properties in flooded pixels of greater than 0.25 m water depth (although this count reduces substantially using depth filtering).

Table 5.3 Summary of the observational data and modelling used to reconstruct the 10 March 2008 coastal flood event in the Solent; including estimates of flooded land area and property. The right-hand columns show the number of properties counted as flooded by the numerical simulation as a function of water depth. Refer to Figure 1.2 for the location of these sub-regions.

Sub-region	No. of flooded locations	Observed land area flooded (km ²)	No of photos available	Properties in contact with floodwater according to source:						
				Photos	Digitised polygon (with 10m buffer)	Numerical simulation: water depth filter (m)				
						total	0.25	0.50	1.00	1.50
New Forest	10	0.30	88	18	28 (59)	136	82	32	6	0
Southampton	4	0.06	22	12	21 (51)	139	21	6	4	1
Eastleigh, Fareham & Gosport	5	0.08	7	16	16 (70)	36	27	18	7	3
Portsmouth	3	0.06	1	2	5 (21)	62	2	2	0	0
Havant	4	0.15	81	61	65 (258)	411	71	24	1	0
Chichester	2	6.65	23	20	179 (260)	155	121	100	78	49
Isle of Wight	9	0.25	98	27	28 (73)	154	115	88	33	10
TOTAL	37	7.65	286	156	342 (792)	1093	439	270	129	63

Notes: the vast majority of caravans at Selsey are excluded from the analysis; although several fixed abode caravans are registered as addresses (and hence counted) – most properties counted here are non-caravan properties. At Selsey, the flood extent quoted is the middle estimate from the simulations.

5.2. The 14 and 17 December 1989 West Solent floods

5.2.1. Event description and available data

To evaluate the model's ability to simulate larger flood events associated with significant overtopping and defence breaching, an analysis was undertaken of the floods which occurred on the 14 and 17 December 1989 along the coast between Keyhaven and Lymington (known as the Pennington flood compartment). Overtopping and overflow flooding occurred on 14 December, and overtopping failures were accompanied by breaching on 17 December. The 17 December 1989 event was characterised by rapid onset and widespread flooding which resulted in environmental damage and severe inundation of 10 properties in the rural area of the floodplain; with overtopping also affecting 50 properties in Lymington (NRA, 1990). Datasets used to replicate this flood were:

- The Environment Agency (Southern Region) provided observed flood outlines (which can also be used to infer which properties are likely to be affected);
- The floodplain DEM of the recent (2007-2008) LiDAR surveys;

- Defence crest heights for December 1989 are available (NRA, 1990) although at lower spatial resolution than for the present-day dataset. For this analysis, the entire defence line of December 1989 was divided into six main alongshore sections of defences with crest heights that were approximately 0.4 m lower than the present-day crest heights;
- Only peak tide level recordings are available at Lymington, with SWLs of 1.92 mODN (14 December 1989) and 2.1 mODN (17 December 1989) (NRA, 1990). Storm-tide time-series data is available for Southampton, Portsmouth and Bembridge but not at Lymington. A tide gauge at Yarmouth (approx. 5 km away) failed to record the peak water level. Hence the time-series used are hourly values recorded at Lymington from the 10 March 2008 surge event which are shifted to the respective SWLs of the December 1989 event.
- The post-flood event report (NRA, 1990) suggests that the weather system on both the 14 and 17 December 1989 comprised exceptionally high winds from the southwest quadrant. At the height of the storm on the 17 December 1989 a mean wind speed of 44 knots, gusting 56 knots was recorded at Lee-on-the-Solent (which provides an indication of likely wind conditions near Lymington). A continuous wind speed of 44 knots can generate wave heights of 1.2 – 1.3 m (approximated in the NRA, 1990 report; and the fetch analysis referred to in Appendix A). As an approximation, wave inputs for the 14 and 17 December 1989 flood simulations were based upon heights and period of the 1 in 10 year and the 1 in 50 year wave conditions respectively.
- Flow through specific breach locations was simulated for the 17 December 1989 flood. The sill height of the breach was approximated by reducing the crest heights by one metre, based upon damage descriptions in the NRA (1990) report. Breaches were applied at six locations (shown in Figure 4.22b) and widths set at 10 m (estimated according to a simplified rule shown, eq. 9). The still water level was routed through these breaches at the boundaries of, and overflow and overtopping applied elsewhere along the coast as relevant.
- Each event was simulated as fifteen hours of real-time flooding. Boundary water levels of 1.92 and 2.1 mODN were applied across the entire site (NRA, 1990) – although as shown in Figure 4.3 there is a decrease in tidal range (and hence extreme water levels) from east to west. However this is a relevant approximation in the absence of more data, and because the breach of Hurst Spit that day (Stripling et al., 2008) would be likely to have altered local hydrodynamics (Nicholls, 1985; Nicholls and Webber, 1987). Present-day event hypothetical flood simulations assume Hurst Spit stays in place, and that tidal range / extreme water levels increase eastwards across the site. Over-washed material from the storm may also have blocked the intertidal area shown (at Milford on Sea) complicating comparison between the observed and modelled floods. Displacement of more than 100,000 tonnes of shingle overnight allowed water to flow through at all states of the tide and resulting in rapid erosion of the salt marsh

behind (Stripling et al., 2008). This barrier has since been reinforced, and is recognised to offer significant protection to much of the Solent (Bradbury and Kidd, 1998).

5.2.2. Summary of validation results

Simulations of the 17 December 1989 flood using a surface friction value of $n = 0.35$ produced F_A values of approximately 0.75 – 0.8, with similar results generated using both the 10 m and 50 m resolution models. The flood simulations were close to but did not exceed the planar water level flood outlines. Roads in Lymington flooded by the model simulation (Bath Road and Waterloo Road) and water depths correspond with those described as flooded (NRA, 1990).

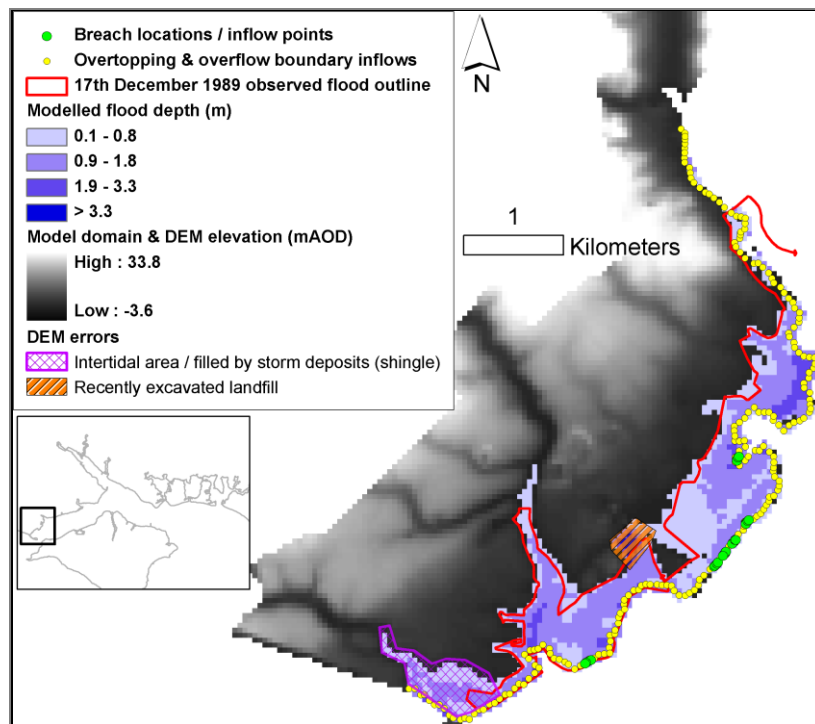


Figure 5.8 The 17 December 1989 flood simulation and observed flood outline.

It should be noted that closeness of the simulations to the actual flood extent is uncertain because the observed flood outlines provided are quite approximate, and simulations did not take into account the two notable discrepancies between the present day DEM and the reported flooding of December 1989 (Figure 5.8). Firstly, the landfill area is dynamic and flooding cannot be assessed, while in the vicinity of Milford-on-Sea, the breaching of Hurst Spit may have sealed a channel, protecting Milford-on-Sea from flooding. It is possible that other areas of the floodplain surface may also have altered between the time of the event and collection of the recent LiDAR data; although the old defence data (which is less detailed than the present-day dataset), nature of breaching, and wave data provides greater uncertainty to the model inputs for this validation exercise. A limitation of the fixed and regularly spaced grid cells

of LISFLOOD-FP is for specifying narrower breach widths than the resolution of the DEM. The 50 m resolution model may have overestimated the real breach inflows.

For the 14 and 17 December 1989 flood simulations, Tables 5.4a and 5.4b respectively show the number of properties in the Pennington compartment which lie within grid cells of depths of up to 1.5 m water depth. Similar to the 10 March 2008 event case-study, the number of properties counted as ‘flooded’ by the simulations converges more closely to the observed/reported flooding only when considering a depth-filtering approach. For example, only counting properties within cells of water depths ≥ 0.5 m indicates that 104 properties are inundated. Counting only properties affected by depths of greater than 1 m indicates that 47 properties are flooded. Notable are differences in the depth-filtering effects which relate to the spatial resolution of the models: the 10 m model predicts more properties to be flooded than the 50 m model for the 14 December, and less for 17 December. The latter of these anomalies is likely to be due to the requirement to specify larger breach sizes in the 50 m model (due to the fixed cell width); whereas the variations in the 14 December 1989 simulations is due to a combination of grid resolution factors and the differences in the overtopping methods

Table 5.4 (a) Properties counted as flooded on 14 December 1989 by the hydraulic model simulations

Dec 14th (SWL & wave inputs only)	Number of properties flooded by the model simulation							
	Total		Depth >0.5 m		Depth > 1.0 m		Depth > 1.5 m	
	10 m	50 m	10 m	50 m	10 m	50 m	10 m	50 m
Lymington	69	56	10	0	17	0	0	0
Keyhaven	22	9	0	0	0	0	0	0
Marshes	30	26	20	1	1	0	0	0
Milford	0	6	0	0	0	0	0	0
TOTAL modelled	121	97	30	17	17	0	0	0
Comparison with observations	The actual total number of flooded properties is unknown, although several properties did flood on this day (NRA, 1990)							

Table 5.4 (b) Properties counted as flooded on 17 December 1989 by the hydraulic model simulations

Dec 17th (SWL, waves, and 6 breaches)	Number of properties flooded by the model simulation							
	Total		Depth > 0.5 m		Depth > 1 m		Depth > 1.5 m	
	10 m	50 m	10 m	50 m	10 m	50 m	10 m	50 m
Lymington	98	105	61	43	33	30	7	0
Keyhaven	57	49	7	23	0	7	0	0
Marshes	58	69	21	35	2	10	0	0
Milford	0	9	0	3	0	0	0	0
TOTAL(observed total: 60)	213	232	89	104	35	47	7	0
Comparison with observations	Filtering results for properties in cells of between 0.5 and 1.0 m depth provides the best comparison with the 60 properties actually reported as flooded.							

The fragility curve methodology (Section 4.3.2 and Appendix C) was also partly verified. Data that indicates the condition and height of the Pennington Embankment sea wall in December 1989 is contained in the post-event report (NRA, 1990) which describes the structural condition of the sea wall, including cracks and subsidence, and indicates that crest levels were approximately 0.4 m lower than the rebuilt wall (that is in place today). Using these descriptors, Condition Grades of 3 to 5 were

allocated to this sea wall which was composed of a protected (concrete) front face, no crest protection and with a permeable rear slope (refer to Table 4.3). The present day sea wall is rated as Condition Grade 2, has some crest protection (geotextile underlay), although the back slope is unprotected.

The NRA (1990) report suggests that the most likely breach failure mechanism during 17 December 1989 was damage to the crest and back slope by water overflowing and overtopping the crest. The SWL of 17 December 1989 (2.10 mODN) is a more certain parameter than the wave inputs, because of the availability of hard data. However, inputting the likely range of significant wave heights (of 1-2 m) to the overtopping formulae, there is minimal difference to the resultant load-conditional failure probability; because the main contributor of water passing over the defence is the SWL and overtopping is substantial (even with small waves) at the given freeboards. Analysis of this event for the old sea wall produces breach failure probabilities ranging between 0.8 – 1.00 when subjected to these 17 December 1989 loadings (i.e. the reliability analysis indicated definitive exceedance of the limit state for several sections of the sea wall). The same loadings applied to the present-day sea wall data indicates minor inundation from overtopping, although no definitive defence section failures with breach probabilities of 0.6 to 0.9. This site was not reported to have flooded on the 10 March 2008, despite that the water levels were similar to those of the 17 December 1989 (between 2.04 – 2.17 mODN; Table 5.1).

5.3. Historic water levels & flood events in the Solent

Good quality SWL datasets date to 1935 at Southampton and to 1961 at Portsmouth (Haigh, 2009). Annual extremes and return periods are shown in Figures 5.9a and 5.9b.

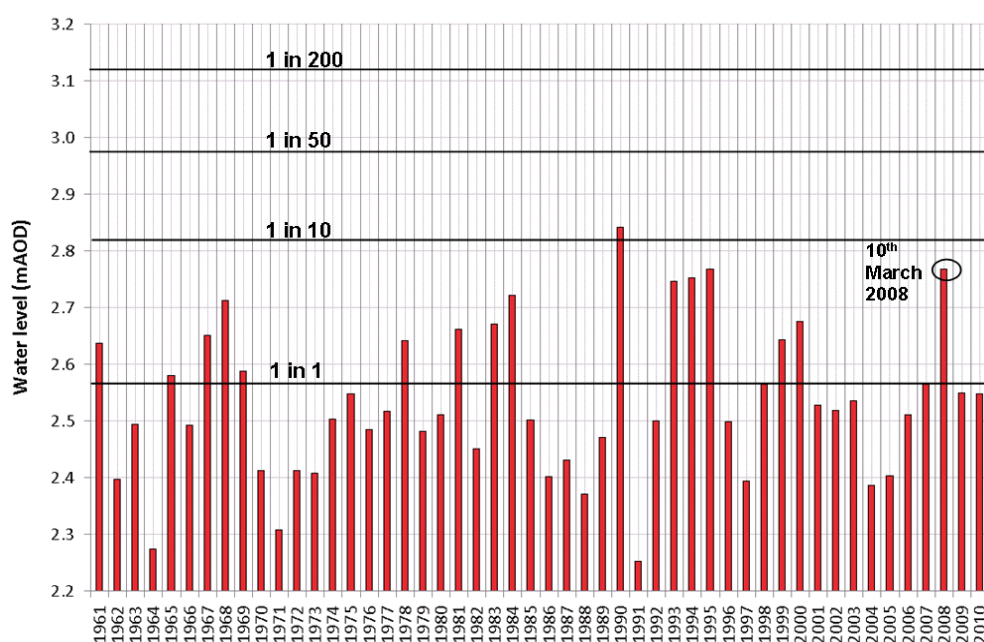


Figure 5.9 (a) Plot of the highest annual still water levels recorded since 1961 at Portsmouth (using data from Haigh et al., 2009). These are shown in relation to the 2008 return period water level elevations for Portsmouth (from EA, 2011) and referenced to Ordnance Survey Datum (which is approximately mean sea level).

Extreme water levels worthy of mention outside of the data shown in Figure 5.9a include an equivalent SWL to 10 March 2008 of 2.86 mODN at Southampton on 27 November 1924 which is noted in tide tables produced by Associated British Ports (ABP, 2010). A SWL of 3.2 mODN at Portsmouth is mentioned to have occurred in 1840 within a coastal engineering report produced by Portsmouth City Council (Easterling, 1991). The exact date or accuracy of the 1840 Portsmouth recording (which exceeds the present-day 1 in 200 year event return period) is unknown although a significant flood event is documented in the city that year (Sherwood and Backhouse, 2012). The highest SWL at Portsmouth (in the record since 1961) is that of 27 February 1990 (2.84 mODN) but flooding is not known to be associated with this event, whereas a few months earlier the complex and prolonged surge event on 13-17 December 1989 (documented in Section 5.2 for Pennington) caused a series of incidents across the region which amount to be the worst storm surge flood event in the Solent in the last 50 years, despite that the Portsmouth tide-gauge suggests the SWL did not exceed 2.48 mODN which is less than an annual event at present-day MSL (Wells et al., 2001; Ruocco et al., 2011). This suggests multiple and interacting flood-causing mechanisms related duration of surge events, local wind and wave conditions, tide-surge interactions, and interactions with other flood sources and pathways (drainage, pluvial and fluvial).

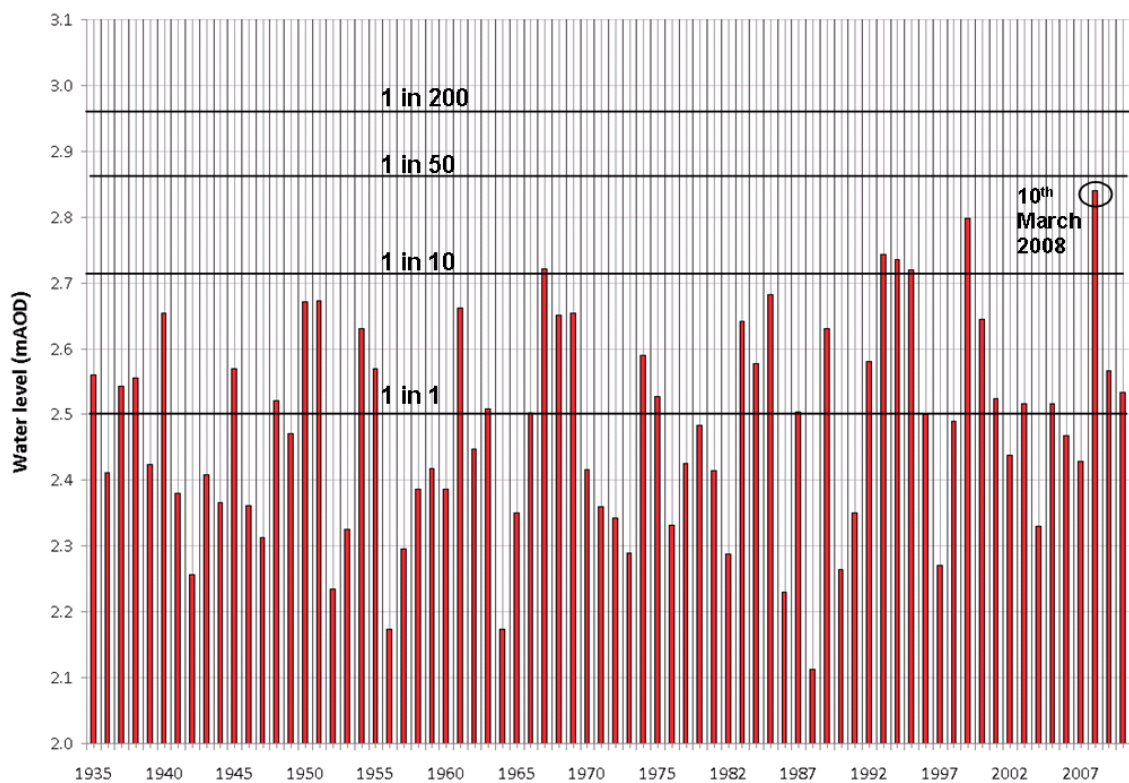


Figure 5.9 (b) The highest annual still water levels recorded since 1935 at Southampton (data from Haigh et al., 2009)

Some of these water level events and associated flood incidences may indicate whether the flood simulation results (generated by analysis of extrapolated water levels, larger than previously seen) are

likely to cause flooding. The 10 March 2008 SWLs peaked at 2.77 mODN at Portsmouth and 2.84 mODN at Southampton. Hence, with reference to Figures 5.9a and 5.9b the 10 March 2008 storm surge and tide generated the second highest SWL event recorded at Portsmouth since 1961 and the highest at Southampton since 1935, approximating at the time as 1 in 50 and a 1 in 20 year events at these sites respectively (Haigh et al., 2011), although revised return periods (McMillan et al., 2011) suggest a 1 in 10 year event at Portsmouth (Table 5.1a). However, wave action was also significant (Table 5.1) and caused overtopping of beaches in the East Solent. Far worse flooding occurred on Hayling Island on the 3 November 2005 when a lesser still water level (approximately 0.3 m less than the 10 March 2008 event at Portsmouth) combined with long period (>18 seconds) swell wave conditions to rapidly erode and overtop the managed shingle beaches which protect numerous properties at Eastoke (HBC, 2006; Mason et al., 2009; Ruocco et al., 2011), demonstrating the importance of wave period to flood risk at this location (swell is incorporated in the ‘maximum waves’ scenario flood simulations that are described in the following section). The wave conditions of both the 10 March 2008 and 3 November 2005 events are detailed by Palmer (2010).



Figure 5.10 High water at Southampton docks (photo taken at 13:04, 10 March 2008 from the window of the Channel Coastal Observatory, National Oceanography Centre). The nearest peak still water level recording was 2.84 mODN (at Dock Head, ABP). The docks around this location are built to a level of approximately 3.3 to 3.6 mODN. This suggests a minimum freeboard of approximately 0.5 – 0.7 m, although the peaks of the oscillating water surface are seen to be level with the dock surface and sea water was observed to overtop onto the docks (although notable incidents of flooding were not reported here).

5.4. Summary

This chapter reviewed two recent and regionally significant coastal floods in the Solent case study. This demonstrates how data about such events can be collated and used to assess a flood simulation methodology. These events included:

- Coastal floods in the west Solent during December 1989 (floods occurred elsewhere but the best available observational data sets is at the Lymington-Pennington compartment).

- The 10 March 2008 storm surge and coastal floods. This event comprised the largest and third largest SWLs at Southampton and Portsmouth respectively (in the available tide gauge records). Multiple flood incidents occurred, 37 of which are itemised in Table 5.2. This event yielded a greater volume of photos and observations than December 1989, and the recentness of the event allows the present-day defence and floodplain data to be valid for comparison with the data used by the model for the hypothetical simulations (Chapter 6).

Historic water levels and floods are also reviewed, and reinforce the vertical closeness between SWLs of variable return period (Figure 5.9) and an insight to the nature of coastal floods in the case study.

The numerical simulations of inundation provided a good replication of the observed coastal floods outlines, as quantified by measures of overlap between model-inundated and observed-inundated pixels (eq. 27, where 1 = perfect match between observed and modelled flood outline; 0 = no overlap).

- For the 10 March 2008 floods, an averaged fit score of 0.67 is observed across the Solent sub-regions, using the same model configuration (defence heights, friction, DEM) as used for the hypothetical flood simulations (Chapter 6).
- Another dimension to the analysis is gained by considering flood depths at the properties in the modelled and observed flood outlines. Analysis of the December 1989 and March 2010 events suggests that assuming that all properties within the flood simulation outlines are ‘inundated’ provides a substantial overestimate of the number of properties that are actually flooded. This has implications to the flooding consequences indicated by simulations of hypothetical events. For the December 1989 floods at Pennington, counting properties in cells with flood depths of 0.5 m to 1 m provides a closer match with the number of properties actually flooded (equivalent to 25 per cent of the properties in the total raw flood simulation output actually experiencing damage). The 10 March 2008 case study suggests that counting only the properties in flood simulation output cells of greater than 0.5 m depth provided a truer indication of actual flood impacts, although this criterion varies with location (Table 5.3 and Table 5.5).
- Visual evidence verifies approximately 40 per cent of the flooded polygons, if excluding the large and uncertain flood extent at Location 28 (Selsey) (Table D1). More widespread photographic evidence could allow some of the defined observations to be revised. For example at several of the 12 locations where simulations under predict flood extent (refer to Table 5.2 and Table 5.5) the polygons lack photographic coverage in areas where more complex fluvial and wave overtopping inputs were prevalent. However, the photos confirm many of the flood event boundaries; verifying much of the DEM, inflow routes, and assumptions about local sea levels. The photos also verify the presence of significant loads (water levels, waves), defence failure mechanisms and flow routes within the floodplain.

The coarsening of topography introduced by the 50 m resolution model provides some uncertainty to the approximation of topographic elevation and replication of flow routes, particularly for urban floodplains – hence higher resolution simulations are also provided for the city of Portsmouth in Chapter 6. However, uncertainties within the December 1989 example (e.g. hydrodynamic impacts of the Hurst Spit breach, breach of the Pennington seawall, defence crest heights, changes to floodplain topography) highlight the importance of collecting and archiving detailed data near the time of the flood (when attempting to use observed floods to validate modelling).

The fit score (generated by eq. 27) for the Solent by the 10 March 2008 analysis is worsened by poorer prediction of inundation from wave overtopping onto the urban floodplain at Eastoke (Hayling Island, Havant) – where inundation simulation is sensitive to the inflow volume (e.g. from overtopping inputs and drainage) and schematisation of the floodplain (e.g. buildings). In these circumstances flow tends to be more ‘hydrostatic’, whereas flow into lower-lying floodplains has a greater velocity head (and water is accelerated) (e.g. Tsubaki and Kawahara, 2012). Widespread flows at Selsey are seen to add greater uncertainty for the overall inundation extent, although flood depths within the observed flooded area are plausible. In all cases, approximation of thresholds for which water is likely to enter properties has much potential to more realistically quantify the amount of flooded property (even in areas of over-predicted flood extent). This has implications for risk analysis and future research (Sections 7.3 and 8.2.1).

For many of the areas that have been most severely affected by flooding over the span of the water level datasets in the Solent case-study, defences have been significantly upgraded (particularly during the 1980s and 1990s – Ruocco et al, 2011). However, the water level history and the consequences of the 10 March 2008 flood event suggest that undefended areas are still vulnerable to extreme water levels. Some areas were within centimetres of seawater overflowing or overtopping onto floodplains (Figure 5.10) and entering a greater number of properties (Figure 5.6). The observations and modelling of the 10 March 2008 event suggests flood waters threatened many more properties than reported – a slightly larger storm surge or tide level may have caused substantially greater flooding.

Importantly, these case study event examples indicated that the main components of the model (DEM, defence data etc.) provide a good basis upon which to model hypothetical coastal flood events, although with caution applicable to interpreting the outputs. The observational data from these flood events supports a better understanding of the outputs from synthetic flood simulations including potential benefits to the plausibility and interpretation of the synthetic flood event simulations, which are described in the following chapter.

Table 5.5 The ‘depth criteria’ required to evaluate the model’s predictions of flood depth at properties, and a summary of the number of cases of under-prediction (UP) and over-prediction (OP) of flood extent (FE) by the simulation. This is based on locations in table 2 where photographs depicting the event are available.

Sub-region	Average depth criteria (m) for optimal observed vs. actual comparison of flooded property	Average F_A value	UP	OP	Comments upon model performance
New Forest	0.40	0.94	2	3	Flood outlines recreated well, therefore 0.4 m perhaps a reasonable approximation to flood water being able to surround property
Southampton	0.25	0.61	1	1	Mostly shallow flows, some of which could be captured better with finer DEM
Eastleigh, Fareham & Gosport	0.65	0.50	3	0	Worst known flooding was in Wallington (northwest Portsmouth Harbour), and where the simulation under-predicted this flood – most likely due to the given sea level boundary conditions.
Portsmouth	0.11	0.50	0	1	Too many flooded pixels at Old Portsmouth predicted by the model (overtopping), although most indicate <0.2m depth
Havant	0.17	0.64	3	1	Greater depth-filtering required at Eastoke, and less at Emsworth. The poor fit is due to under-prediction of FE at Langstone High St & over-prediction at Eastoke comprises (both improved using a higher resolution DEM); part of Emsworth flood was under-predicted due to possible influence of non-coastal flood source.
Chichester	0.72	0.95	0	0	For the two locations (Bosham & Selsey) there is a good match between observed & predicted flood (using mid-approximation of the large flood at Selsey), although quite a substantial depth filter required to avoid over-prediction of flooded property.
Isle of Wight	0.75	0.68	3	0	Finer resolution appropriate for delineation of flood extents on roads in Cowes.
SOLENT	0.49	0.67	12	6	

6. Coastal Flood Simulations: Hypothetical Events in the Solent

This chapter presents idealised, hypothetical coastal flood event simulations across the Solent. These are each characterised by a regional still water level (SWL) event (with spatial variations according to Figures 4.3 and 4.4) combined with three wave scenarios: no waves, annual extreme waves, and largest possible waves. These scenarios assume that present-day coastal flood defences are in place. An additional ‘full breach’ scenario (in which all shoreline defences are removed) is simulated in combination with extreme waves.

Section 6.1 shows results generated using the 50 m resolution version of the hydraulic flood model for the entire Solent. Sections 6.2 and 6.3 focus upon the two detailed case-studies (Portsmouth and Pennington), where the 50 m results are supplemented by a detailed approach and a 10 m resolution version of the model. These two sites are also of coastal flooding significance within the Solent due to past flood events and known risk of breaching. The simulations and analysis in Sections 6.2 and 6.3 also aim to determine whether the more simplified overview of flood events provided by the Solent-wide flood simulations can benefit from greater detail, for example, modelling of urban inundation is known to benefit significantly from finer discretisation of space (Fewtrell et al., 2008b; Hunter et al., 2008) and coarser grids tend to overestimate flood extent and underestimate depth compared to finer resolution and less interpolated versions (Fewtrell et al., 2008b). This is significant because it has been suggested that the city of Portsmouth accounts for approximately half of the Solent’s properties at risk of coastal flooding. The structure of each section will be as follows:

- Analysis of an extreme (1 in 200 SWL) synthetic coastal flood event, with reference to the main sub-areas in each model. From the Solent-wide perspective these sub-areas are city-sized or larger, as shown in Figure 1.2. From the detailed results perspective, the sub-areas described are separate flood compartments;
- Coastal flood modelling results across a range of regional water levels, including comparison of the effects of the different main defence failure mechanisms, and indicating increased impacts of coastal flooding with sea-level rise.

The results for properties exposed to flooding as defined by the planar water level method are included alongside the hydraulic modelling results, although a fuller description of this exposure to coastal flooding in the Solent is contained in Appendix B.

6.1. Solent-wide coastal flood simulations

6.1.1. A present day extreme water level event

To introduce the present-day distribution of coastal flood threatened land and property in the Solent; this section describes flood simulations which comprise a 1 in 200 year SWL in combination with wave and breach scenarios. This water level return period is approximately the indicative standard of protection for most urban areas in England and Wales, and is also the criteria to define coastal flood outlines in Environment Agency Flood Zone 3 maps. Included in the results are the counts of properties within the maximum flood outlines from the numerical simulations. Also, as a consequence of the validation case studies in Chapter 5 (which indicated uncertainty for the threshold at which water is likely to enter properties), the counts of properties flooded to ≥ 1 m are also included. Table 6.1 also compares these new inundation modelling results with those from an existing hypothetical extreme flood outline dataset: the Environment Agency's Flood Zone (FZ) 3 maps, which depict the extent of the natural floodplain (with no flood defences) for a 1 in 200 year coastal flood scenario.

Table 6.1 Properties and land area in the Solent affected by a 1 in 200 year SWL coastal flood simulation, including planar water level flood analysis (refer to Figure 1.2 for locations; Section 4.2.1 for SWLs). Numbers in brackets include land area and properties inundated to ≥ 1 m depth. Also shown for comparison is the 2008 Environment Agency FZ3 outline (most comparable with the planar water level and full-breach results).

REGION (Fig. 1.2)	Location	EA FZ3		Exposure (non-hydraulic flood outlines)		Properties flooded by hydraulic simulations (brackets show count of properties inundated to ≥ 1 m depth)			
		Area (km ²)	Properties	Area (km ²)	Properties	Breach of all defences & max. waves	Max. waves	1 in 1 yr. waves	No waves
1	New Forest	12.2	687	14.1 (6.6)	736 (134)	639 (147)	591 (112)	430 (55)	329 (34)
2	City of Southampton	2.8	2250	2.0 (0.1)	2148 (249)	978 (21)	973 (21)	919 (21)	715 (10)
3	Eastleigh, Fareham & Gosport	8.5	2485	7.2 (2.4)	1789 (106)	1395 (109)	1321 (93)	1163 (91)	564 (52)
4	City of Portsmouth	12.5	15075	13.8 (4.9)	14055 (3483)	11042 (2734)	6557 (459)	4769 (110)	1900 (8)
5	Havant & Chichester	37.5	4213	29.8 (13.2)	3781 (1657)	3168 (613)	2995 (448)	2602 (329)	1033 (90)
6	Isle of Wight (all)	9.4	503	11.4 (5.6)	617 (155)	505 (114)	377 (67)	354 (67)	255 (25)
Total	Solent	82.9	25213	78.3 (32.8)	23126 (5784)	17727 (3728)	12814 (1200)	10237 (673)	4793 (219)

It should be noted that the available version of the EA FZ3 maps use the superseded return period analysis of Dixon and Tawn (1997), which for the Solent is equivalent to input SWLs of approximately 0.1 m more (equivalent to 3.2 mODN at Portsmouth) than those used here which are derived from the newer analysis of McMillan et al (2011). EA flood maps are generated by a variety of methods and numerical models (EA, 2010a) which adds additional complication to a comparison with the results

shown here. However, shown in Figure 6.1, the addition of 0.1 m to the regional SWL for this research's exposure/planar water level method (i.e. to generate an equivalent SWL input to that used for the 2008 EA FZ3) allows an almost identical estimate (approx. 25300) of the number of properties flooded in the Solent, and for the estimates of inundated land area. The North Solent Shoreline Management Plan (NFDC, 2009) also generated estimates of property exposed to coastal flooding via the planar water level method (an assessment which excludes the Isle of Wight) – this approximated that 24,138 properties are exposed to a 1 in 200 year SWL (also using the older return period SWLs).

In the city of Portsmouth, a substantial amount of the region's property is threatened by flooding under all loading scenarios. However it is apparent from the hydraulic flood simulations that the city's flood defences greatly reduce the number of properties exposed to more than 1 m flood depth; and in comparisons with the lesser wave loadings, the extreme wave and breaching scenarios are required to significantly increase the count of buildings likely to be flooded to greater than 1 m. In the city of Southampton only 21 properties are inundated to greater than 1 m depth, although the added effect of waves with SWL expands the total number of properties (and the flooded area) significantly, despite the fetch-limited shoreline; demonstrating the importance of incorporating even small wave inflows to these flood simulations. At present-day sea levels Southampton is likely to be subject to disruptive impacts from coastal flooding (rather than the more significant impacts which the results suggest for Portsmouth).

Across the case-study, this SWL allows 531 properties to be flooded to greater than 2 m depth for a maximum breaching (hydraulic simulation) scenario, and approximately 130 for the maximum and annual wave scenarios. The majority of these are in Portsmouth under the breach scenario; whilst most are in Chichester and Havant (102 properties) when applying the non-breach maximum waves scenario. There are also large areas where flood depths are between 1 m and 2 m, a dangerous situation when floodwaters are fast moving (e.g. Jonkman and Penning-Rowsell, 2008). The extraction of this information from the model indicates pockets of particularly high damage potential and risk to life, which is discussed in Section 7.5. Inclusion of widespread breaching is shown to increase regional flooding impacts substantially, although only a relatively small length of coastline actually appears at high risk of this kind of failure (Figure 6.12).

6.1.2. Coastal flood simulations across a range of loadings

Flood simulation results across a range of SWLs are shown in Figures 6.1a, 6.2a and 6.3a (all flood simulations assumed the present defences). Also shown for each measure of inundation, is the proportion of flooding caused by non-breach defence failures in comparison to inundation simulations where all defences were removed (Figures 6.1b, 6.2b and 6.3b).

These results indicate that substantial land area and property are threatened with coastal flooding from frequently occurring SWLs, and defences play a crucial role in preventing and controlling the magnitude of flooding consequences. The number of properties in the modelled flood outlines increase steadily with increasing SWLs. The difference in the total number of flooded properties and land area when comparing the hydraulically simulated floods and the planar water level (exposure) flood extents indicates that much of the wider floodplain may not be hydraulically well-connected over a single tidal cycle. At the same time, the effects of overtopping can be significant and these results show that at the highest SWLs that were simulated and for counts of properties flooded to ≥ 1 m depth; overtopping floods can almost match the planar water level estimates (Figure 6.2a). For some individual flood compartments the number of properties inundated by the non-breach defence failure mechanisms increases most distinctly within the approximately 0.1 m band of SWLs either side of the 1 in 200 year extreme, because the protective capacity of many coastal defences is exceeded in this range of loadings. The 1 m depth criteria indicates that for the Solent as a whole there a particularly large increase in the count of flooded properties beyond the approximate present day 1 in 200 year SWL.

Figures 6.1b and 6.3b show, in response to increasing SWLs, an increase in the percentage of inundation that arises from overflow/overtopping failures in relation to breach. This is expected as defences become increasingly overwhelmed beyond their protective capacity due to rising SWL boundary conditions allowing larger and prolonged discharges into floodplains during flood events. However, reading (from left to right) across the chart that shows the relative effects of breach and non-breach impacts for the 1 m flood depth criteria (Figure 6.2b) there is an interesting sequence of a peak, trough and then a rise again (in the flooded property counts). This is because this chart highlights the potential for breach failures to exert greater flood damages at smaller SWLs (at which overflow or overtopping are reduced because defences are in place). As defences fail, non-breach failures become relatively more significant, especially beyond present-day SWL extremes, and the gap between breaching and overtopping flood impacts diminishes.

It should be noted that the ‘peaks’ seen in Figures 6.1b and 6.2b (i.e. both rise and fall in the non-breach flood simulation lines of the graph when reading from left to right) are because these results account for the floodplain extent associated with the given SWL (a ‘theoretical maximum’ floodplain as indicated by the maximum breach inflow simulation) and also the flooding generated by non-breach failures (and how these can contribute towards this theoretical maximum). For example, Figure 6.1b shows that for a 3.2 mODN SWL combined with an annual wave event scenario, a slightly larger percentage of the theoretical maximum floodplain is filled than at the equivalent wave load estimate for the SWL increments either side (3.1 mODN and 3.3 mODN). This is because in comparison to the lesser modelled SWL increment (3.1 mODN) the relative increase in breach floodplain size (the theoretical maximum floodplain for this SWL) is less than the change in overtopping extent generated by the simulations. Another important feature of these results charts is seen at the top right of Figure 6.2a,

where the number of properties counted as flooded by the maximum-wave and breach simulations crossover with the results for the planar water level method. This represents the filling of many floodplains across the Solent by these loadings (across a single tidal cycle) as well as the projection of water onto additional floodplains from the model's ability to capture high overtopping inflows onto floodplains above the SWL.

UKCP09 (Lowe et al., 2009) global mean sea level projections derived from the IPCC Fourth Assessment Report (IPCC, 2007) give an estimated range (5th to 95th percentile) for sea level increase of 18–59 cm between present day (assuming a 1980–1999 baseline) and 2090–2099. For simplicity the effects of a medium UKC09 scenario (of approximately 0.5 m SLR) upon a 1 in 200 year SWL flood event are shown. This simplified 21st century SLR scenario substantially increases the amount of property affected by at an extreme coastal flood event in the Solent. For example, in the case of a 1 in 200 year SWL flood combined with an annual wave extreme, the total number of buildings in the regionally modelled flood outline increases from 10,128 to almost 24,000 (approximately 140 per cent change), although there is a more dramatic 600 per cent increase if considering ≥ 1 m depth flooding, and probably provides a better indication of actual impacts assuming no adaptation (Figure 6.2a). Even without the effects of waves, a 1 in 200 year flood event in addition to 0.5 m SLR (and no defence improvements) allows nearly 4400 properties to be inundated to greater than 1 m depth.

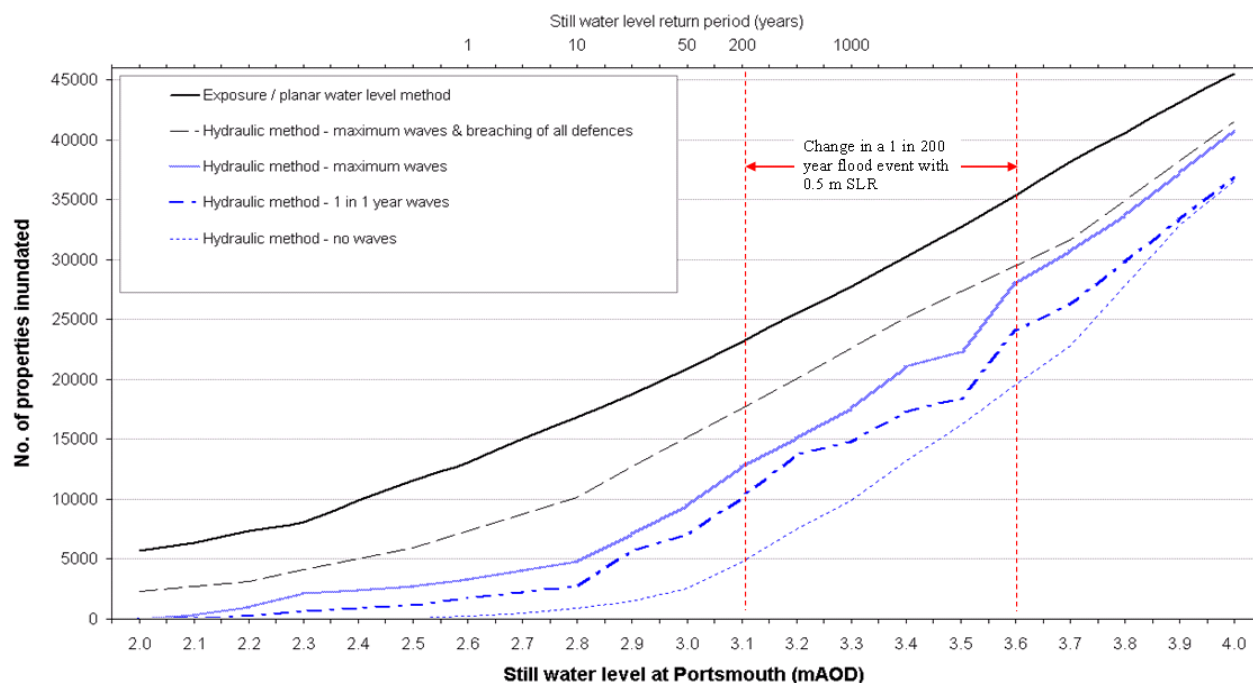


Figure 6.1 (a) Inundation modelling results: the total number of properties within modelled coastal flood outlines across the Solent (water level return period refers to annual probability of that water level for 2008)

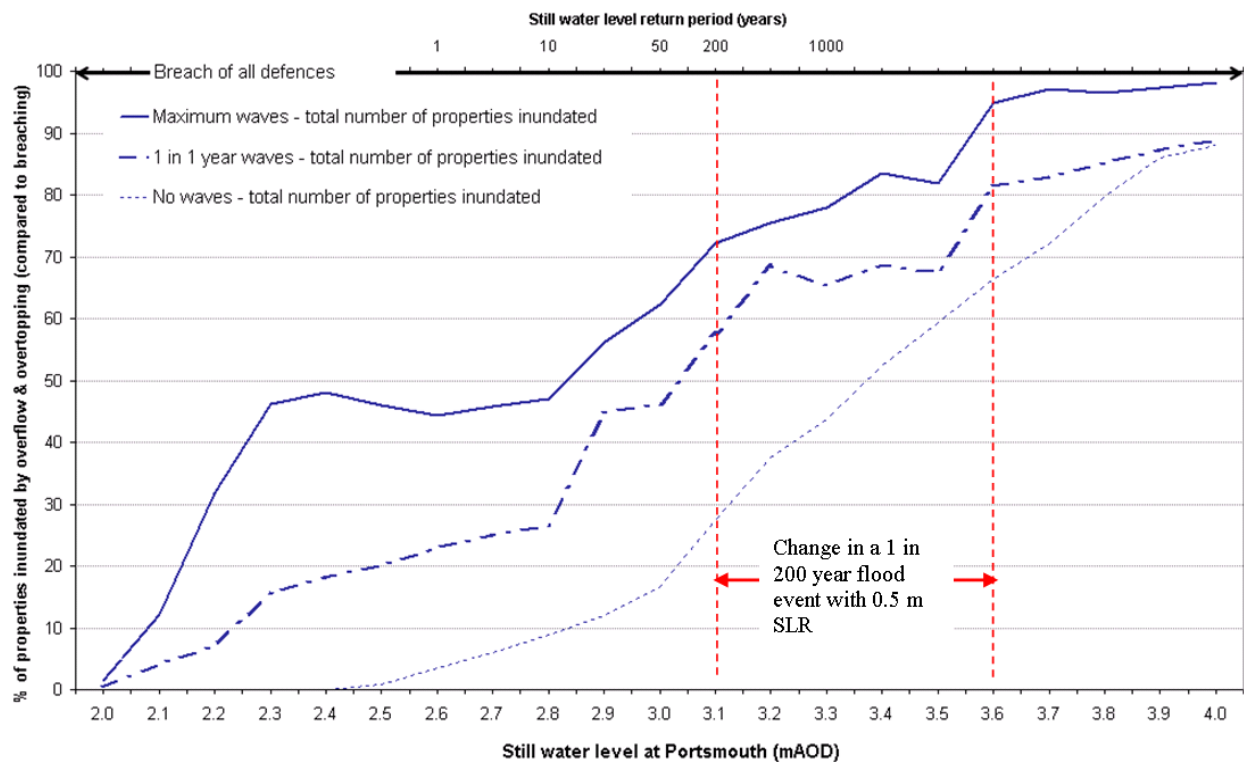


Figure 6.1 (b) Percentage of properties inundated by overflow and overtopping defence failures (compared to breach of all defences)

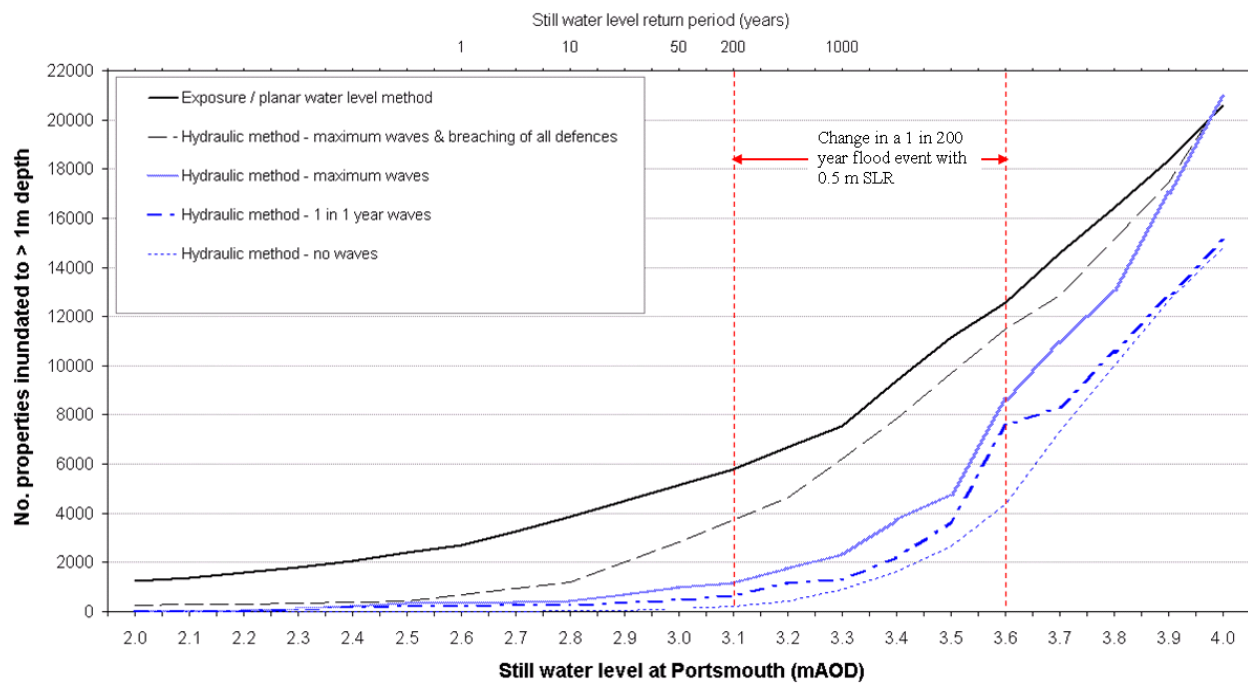


Figure 6.2 (a) The number of properties in the Solent inundated to a water depth of greater than 1 m

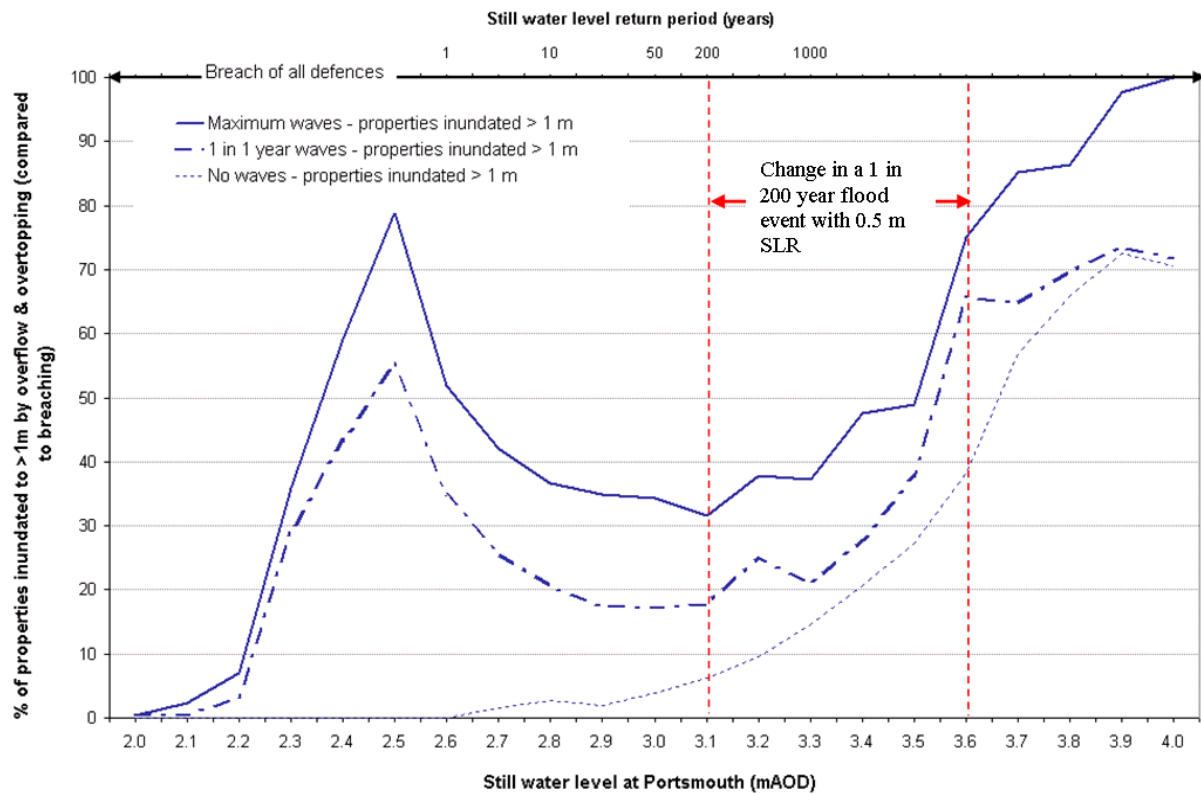


Figure 6.2 (b) Percentage of properties inundated to greater than 1 m water depth by overflow and overtopping defence failures (compared to breach of all defences)

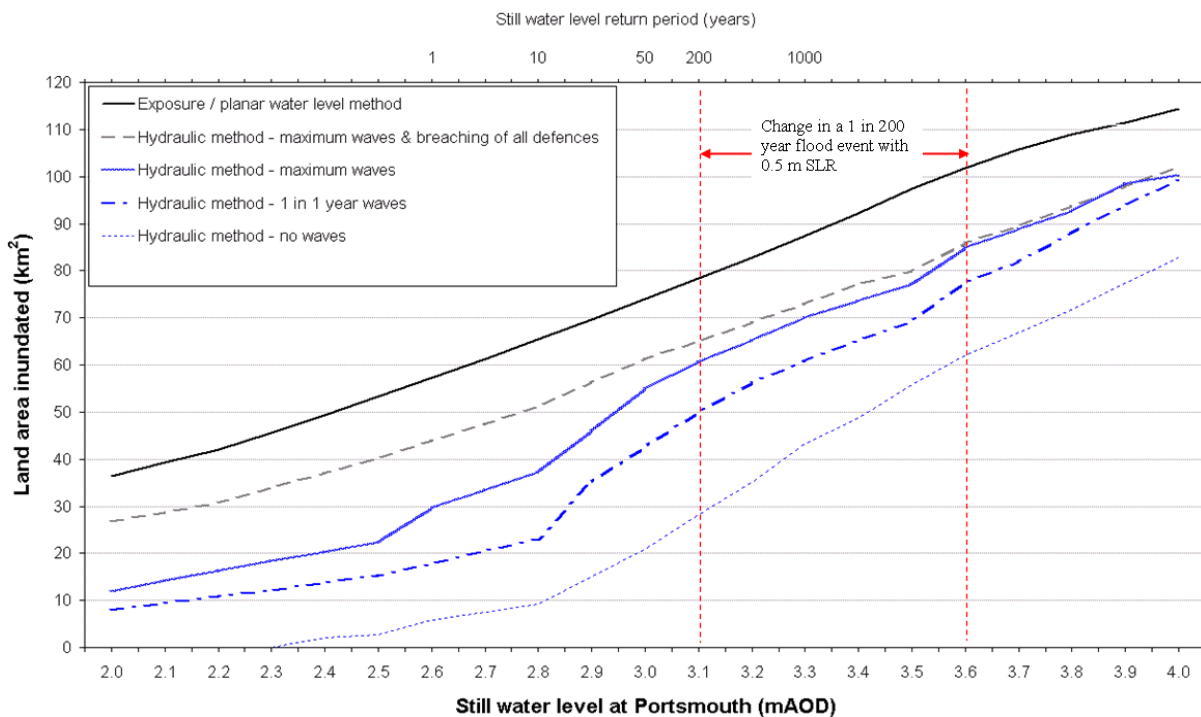


Figure 6.3 (a) Land area inundated by the Solent-wide coastal flood simulations

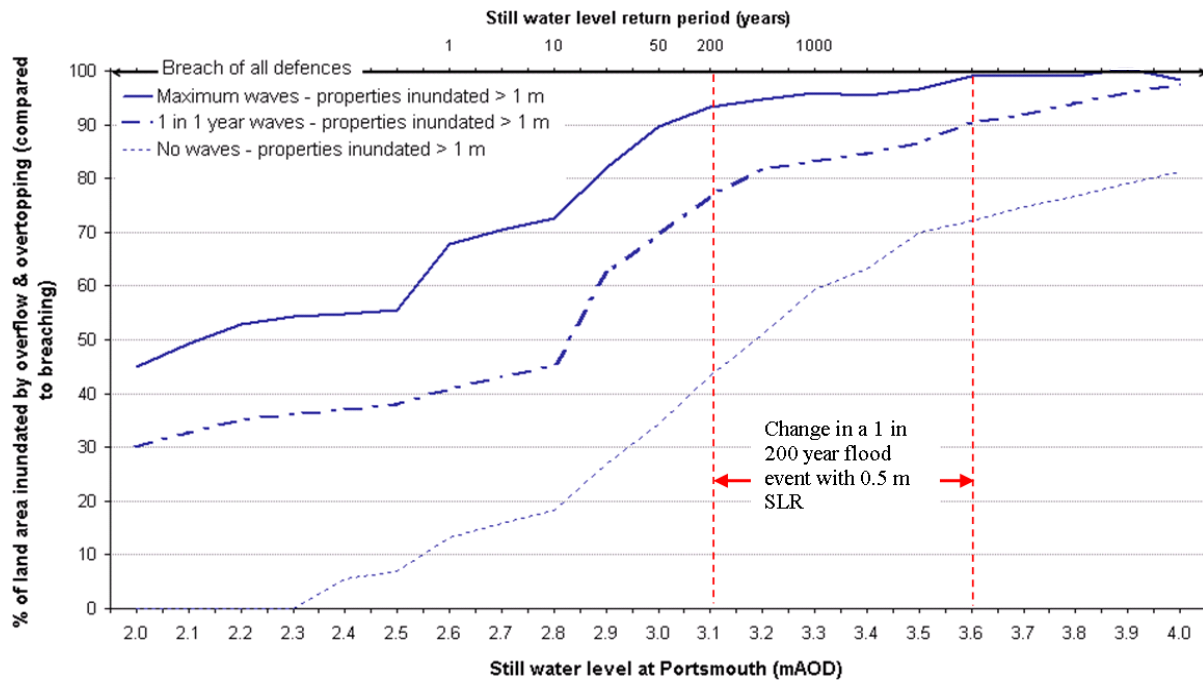


Figure 6.3 (b) Percentage of land area in the Solent that would be inundated by overflow and overtopping defence failures (compared to breach of all defences).

These results displayed in Table 6.1 reaffirm the regional significance of coastal flooding in Portsmouth, which contains the largest amount of property at threat of flooding for any urban area in the Solent case-study. Therefore, as discussed, Portsmouth is the first detailed case-study.

6.2. Detailed case study 1: Portsmouth

In Section 6.2.1 the effects of spatial resolution of the 10 m and 50 m models are directly compared, by allowing inflows to Portsmouth's floodplains with the shoreline defences removed. Section 6.2.2 compares the 10 m and 50 m models with the inclusion of a wider range of load and defence failure scenarios.

6.2.1. Direct comparison of grid resolution for an extreme breach scenario

The 50 m and 10 m resolution versions of the model are compared in this section, using a 1 in 200 year SWL alongside a simple, idealised breach inflow scenario (refer to Section 4.6.2). SWL inflows alone and no waves were included in these simulations, for simplicity and to prioritise analysis of effects caused by varying the grid resolution and surface friction. This scenario, like the regional modelling of 'full breach' scenarios in the previous section assumes all shoreline defences to be breached. Identical tidal time-series inputs and simulation time (60,000 seconds) are applied.

SWL time series were applied at the model boundary for an entire single tidal cycle, and water was allowed to spread until the maximum flood extent had been reached. An additional 10 m resolution model simulation was undertaken to test the significance of variable surface friction values, for comparison with the simulations which used spatially heterogeneous surface Manning values (of $n=0.035$). The results of the 10 m and 50 resolution simulations (of which both used $n=0.035$) are shown in Figure 6.4; and the number of properties inundated for all simulations in each Portsmouth flood compartment are summarised in Table 6.2.

Table 6.2 Summary of properties inundated by the 1 in 200 year SWL plus full breaching simulation. Results are segregated by Portsmouth's flood compartments as shown in Figure 6.4

FC no.	FC name	50m model, $n=0.035$			10m model, $n=0.035$			10m model, $n=variable$		
		Number of properties inundated (total, and to ≥ 1 m & 2 m depth)								
		Total	1 m	2 m	Total	1 m	2 m	Total	1 m	2 m
1	Mainland	3370	443	0	3437	905	22	3211	562	0
2	Portsea North	3086	562	75	3143	737	92	2893	685	77
3	Eastney	26	1	0	30	17	16	28	17	16
4	Southsea	4135	1088	242	4948	2082	703	4933	2067	701
5	Old Portsmouth	316	4	1	310	71	68	308	71	68
6	Tipner	9	1	0	9	1	1	9	1	1
7	Stamshaw	21	0	0	35	0	0	35	0	0
8	Horsea Island	5	0	0	5	2	1	4	2	1
9	Port Solent	501	43	0	359	58	58	359	58	58
Totals		11469	2142	318	12276	3873	961	11780	3463	922

The 50 m and 10 m models generated flood extents of 9.58 km² and 9.55 km² respectively. More significant variations are observed for the total numbers of flooded properties. The 10 m model results suggested approximately 800 more properties to be within the flood outline than the equivalent output from the 50 m resolution model. A much larger difference is seen for the number of properties flooded to depths of greater than 1 m and 2 m using the 10 m model, which predicted greater water depths across the floodplain (than the 50 m version). The 10 m resolution simulation allowed greater flooding at the northern fringes of the Mainland floodplain, compared to the 50 m resolution model. Increased detail and associated representation of topographic effects are also noted to allow increased representation of flood extent and depth predictions for Southsea. The 10 m model more accurately represents the channels of the ancient waterways of the 'Morass', which are now urbanised topographic relicts of this former marsh area.

Surface friction (refer to Section 4.5) also had a notable influence upon differences between the 10 m resolution flood simulations. Inclusion of friction values (derived from surface features) caused a 4 per cent reduction in the total number of properties inundated for all of Portsmouth; and a 10 per cent reduction for the number of properties inundated to greater than 1 m depth (compared to the $n=0.035$ uniform friction setting). When comparing the 10 m resolution simulations, the largest variation is seen within the Mainland floodplain, where the inclusion of high friction values for buildings on this shallow

gradient floodplain reduces propagation of the flood wave, and causes a 40 per cent decrease in the number of properties inundated to greater than 1 m depth. However the 10 m resolution model almost doubles the number of properties inundated to greater than 1 m if comparing the effects of grid resolution only.

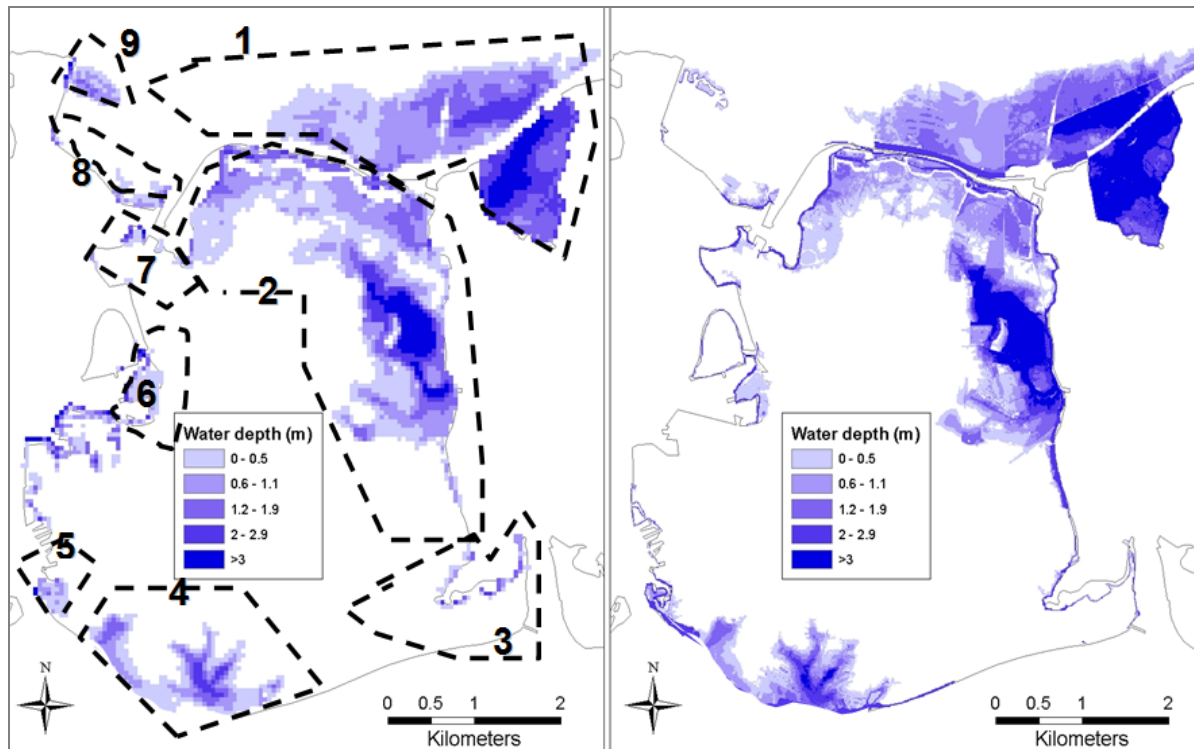


Figure 6.4 (a) peak flood depths from the breach simulation for the 50 m resolution model, and (b) the 10 m resolution model

6.2.2. Simulations of a present day extreme event

This section summarises simulations of a 1 in 200 year SWL, although describing more simulations and scenarios than the previous section. The full-breaching simulations are included (although these vary slightly to those of the previous section). The 50 m flood simulations are identical to the Solent-wide flood simulations (Section 6.1), whilst the 10 m simulations consider a different schematisation of the A27 and Hilsea Lines inland flood walls, and spatially variable friction values (refer to Section 4.6.2).

For the city as a whole, Table 6.3 highlights that in non-breach situations at the 1 in 200 year SWL, the 50 m resolution model predicts more coastal flooding (when this is quantified by total land area and total number of properties inundated). However as noted in the previous subsection (6.2.1), largely due to DEM interpolation effects, the 10 m model continues to predict a greater number of properties flooded to depths of ≥ 1 m. However, these differences between the coarser and finer (and application of more modelling detail for the 10 m resolution version) are more complex when comparing between defence-failure types in different floodplains, which is now explained.

Table 6.3 Coastal flood simulations with 1 in 200 year (2008) still water level for Portsmouth

FC no.	FC name	Number of properties inundated (brackets is number flooded to ≥ 1 m depth)							
		No waves		1 in 1 waves		Max waves		Breach & max waves	
		50m	10m	50m	10m	50m	10m	50m	10m
1	Mainland	790 (6)	6 (0)	1963 (94)	11 (0)	2122 (103)	14 (0)	3609 (1083)	3392 (901)
2	Portsea North	885 (0)	491 (1)	1096 (0)	527 (1)	1428 (68)	938 (3)	2968 (603)	2720 (640)
3	Eastney	2 (0)	6 (1)	16 (0)	216 (3)	20 (0)	366 (6)	20 (0)	367 (17)
4	Southsea	0 (0)	0 (0)	971 (0)	5 (0)	2534 (294)	2433 (810)	3878 (1041)	4770 (2035)
5	Old Portsmouth	212 (2)	154 (5)	429 (7)	855 (103)	466 (3)	1112 (105)	466 (7)	1112 (107)
6	Tipner	1 (0)	4 (0)	1 (0)	4 (0)	1 (0)	6 (0)	1 (0)	7 (1)
7	Stamshaw	10 (0)	24 (0)	22 (0)	24 (0)	22 (0)	24 (0)	22 (0)	25 (0)
8	Horsea Island	0 (0)	0 (0)	0 (0)	4 (2)	0 (0)	6 (2)	0 (0)	6 (2)
9	Port Solent	0 (0)	0 (0)	112 (0)	36 (1)	123 (0)	78 (1)	123 (0)	295 (58)
Total		1900 (8)	685 (7)	4769 (110)	1682 (110)	6557 (459)	4977 (927)	11087 (2734)	12694 (3761)

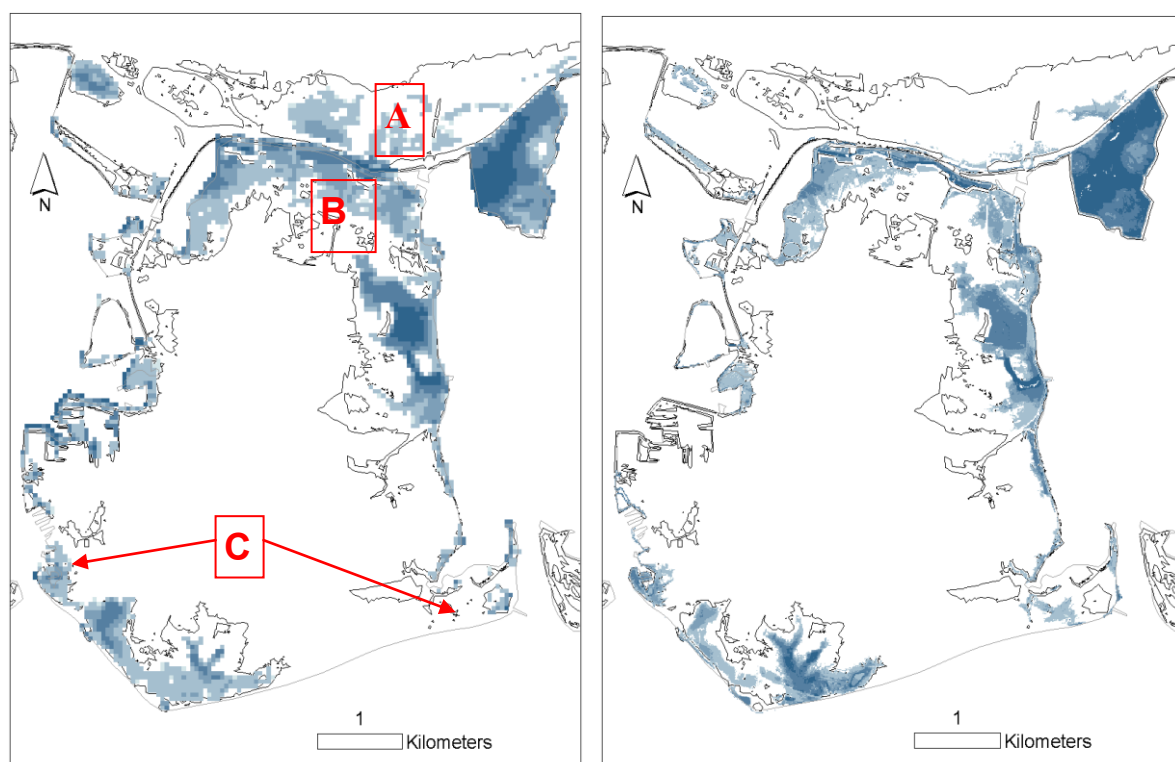


Figure 6.5 (a) The 50 m, and (b) the 10 m resolution models; both showing peak flood depths for simulations of a 1 in 200 year SWL combined with maximum waves. Darker blue indicates greater water depth. The planar water level flood outline for the same still water level is also shown.

From the simulation results for numbers of properties inundated (Table 6.3) it is apparent that larger wave loadings have a prominent effect upon the impacts of coastal flooding in the city, particularly due to the increase in the propagation of the flood wave and larger water depths at Southsea. However, other

significant differences are identified when comparing the simulation outputs from the 10 m and 50 m resolution methods. The three main areas of difference are shown in Figure 6.5. These significantly influence the predicted consequences from the Portsmouth coastal flood event simulations:

- The narrower representation of the underpasses beneath the M27 embankment in the 10 m resolution model substantially reduces the predicted effects of coastal flood events on the Mainland (difference 'A', Figure 6.5). Portsmouth's flood history indicates no previous significant coastal flooding to the mainland, although the DEM and photos indicate that it is possible that water could flow under the A27 during a 1 in 200 year SWL event. However, this flow is likely to be limited during a single tidal cycle, and the 10 m wide cells (providing a reasonable approximation to the actual width of the conduits) utilised by the higher resolution DEM provide a more realistic indication of the flood event. Gaps of this size may also be manageable (e.g. with sandbags, temporary barriers) in the event of an extreme SWL warning. This is most likely to reflect an improvement in accuracy as a result of using the 10 m model.
- The inclusion of the Hilsea Lines walls (Difference 'B') which are inserted onto the DEM in the 10 m resolution model reduces (by approximately 800) the number of properties (mostly industrial buildings) predicted as flooded in north Portsea. Difference B is uncertain in the event of a structural failure, because the Hilsea Lines are an archaeological feature rather than dedicated flood defences (i.e. their performance under loading is not known). At present-day sea levels, these features are likely to provide substantial protection by blocking and/or dampening the flood wave if defences along Port Creek fail.
- More properties are predicted as flooded by wave overtopping at certain locations due to the lower land heights captured by the 10 m resolution model (difference 'C', Figure 6.5). This includes approximately 0.2 m deep floods at a caravan park near Fort Cumberland at Eastney, and a similar depth of flooding north of Old Portsmouth. Difference C is a probable improvement gained from the 10 m model, particularly on the Eastney coast where this output from the modelling concurs with overtopping and breach that was observed on 16 December 1989 when up to 0.2 m flooding occurred across the peninsula (Table 3.2 and Figure 6.8). The potential for high overtopping rates at Eastney are also noted by run-up calculations (e.g. Eq. 8). Under extreme wave conditions, wave run-up on the gravel beach is likely to project sea water to approx. 2 m above SWL, due to the 180 km fetch in the 150° south-easterly direction (which theoretically allows significant wave heights to exceed 2 m and peak period to exceed 7 seconds). Interpolation of the original LiDAR survey data to generate 50 m resolution cells appears to smear out a lower-lying band of topography across this peninsula, although the topographic representation is well preserved at 10 m resolution. This effect is also seen north of Old Portsmouth where overtopping from the fetch-limited harbour waves onto the quayside causes shallow flooding. Vertical wall empirical overtopping discharges are available at this part of Old Portsmouth which may in reality be more wind dependent (historical information

does not indicate significant overtopping here in the past). However, overtopping calculations and inundation simulations suggest high discharges even for 1-2 m H_s harbour waves combined with the 1 in 200 year SWL. In combination with the deeper flows represented elsewhere in Old Portsmouth flood compartment, the 10 m model substantially increases flooded property predictions (compared to the 50 m resolution wave inflow simulations).

6.2.3. Flood simulations across a range of loadings

The comparison between the 10 m and 50 m models is continued across a range of loadings. The no-waves and maximum-waves results provide an envelope of the likely range of flood outlines possible as a result of non-breach defence failures, and the ‘full breach’ and planar water level results are also shown. A key observation from these comparisons is that for predictions of inundation due to non-breach (overtopping and overflow) failures, the difference between the results generated by the two different resolution models diverges with increasing SWLs. This effect is accentuated at 3.5 mODN and 3.7 mODN SWLs for maximum wave and no-wave loads respectively, and is more pronounced when using the 1 m depth inundation criterion. A large part of this effect is due to the inclusion of the Hilsea Lines walls (in north Portsea) and the more accurately represented sub-A27 flow routes in the 10 m model. The effect of wider flow routes and inflow volumes generated within the 50 m resolution model become magnified as SWL loads increase. Also notable is that the ‘full breaching’ combined with maximum wave scenario overtakes the planar water level estimates beyond approximately 3.8 mODN because the larger floodplains fill up whilst in some areas waves also overtop a significant volume of water onto floodplains which are above these SWLs.

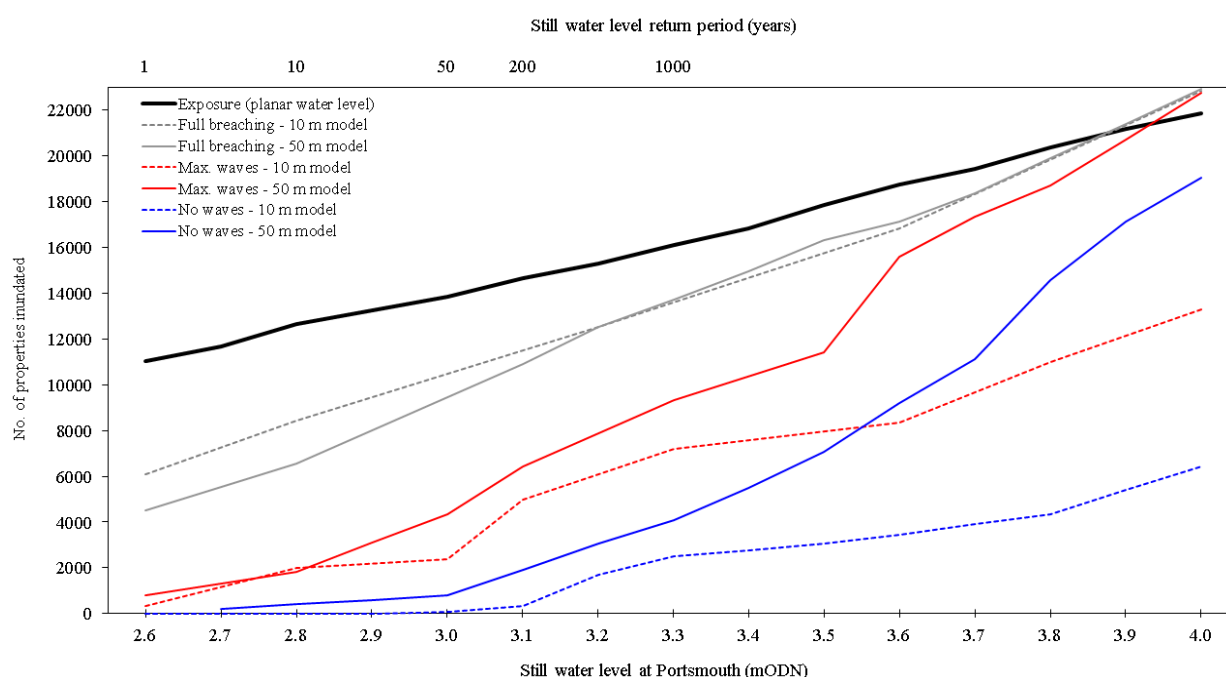


Figure 6.6 (a) Properties flooded in Portsmouth (10 m and 50 m resolution simulations)

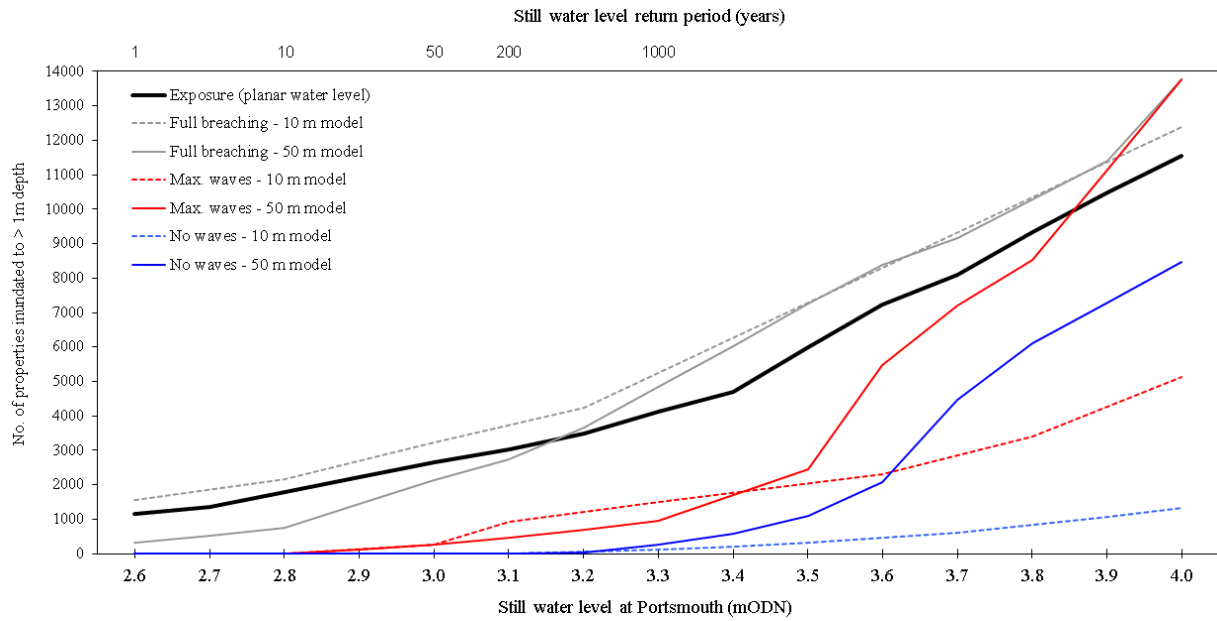


Figure 6.6 (b) Number of properties flooded in to ≥ 1 m depth (10 m and 50 m resolution simulations)

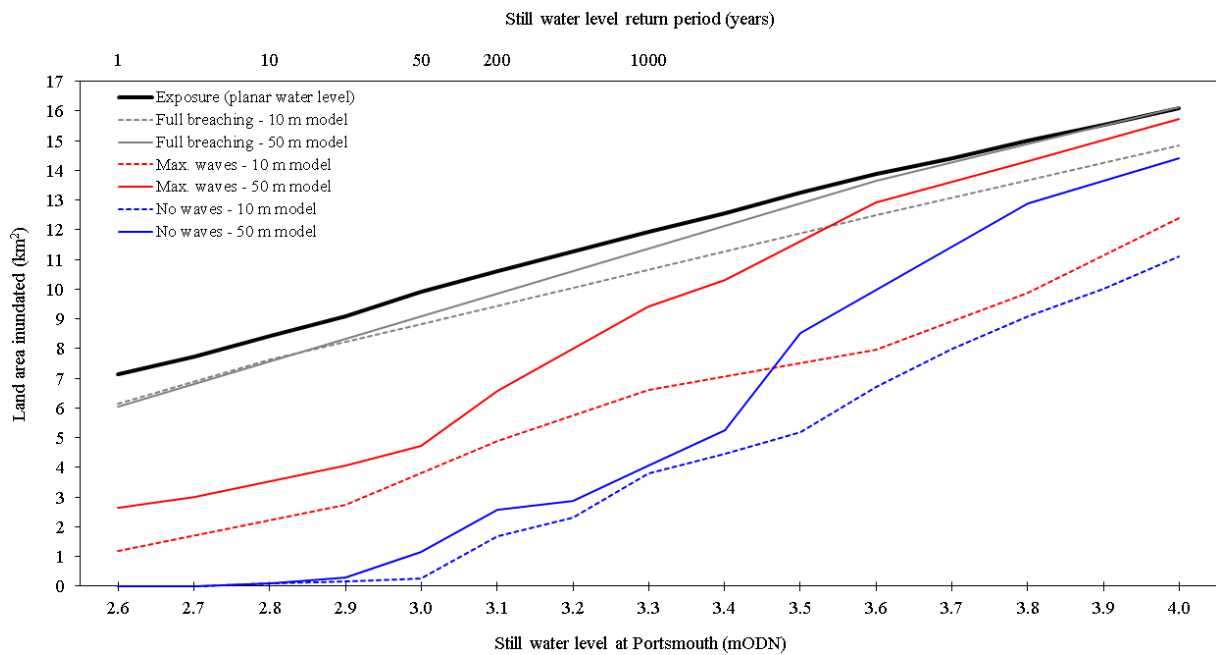


Figure 6.6 (c) Land area flooded in Portsmouth (10 m and 50 m resolution simulations)

6.2.4. Review of extreme coastal flood events Portsmouth

This section reviews past events, return period analysis, and the hypothetical coastal flood simulations, to comment upon the likelihood and characteristics of coastal flooding in Portsmouth. This section comments upon property and land-use impacts in the city (incorporating data from OS maps and aerial photos). Changes to inundation patterns as a result of SLR are also discussed (Figure 6.7).

South Portsmouth (Compartments 3 – 5): Southsea is the lowest-lying and most densely populated flood compartment in the case-study region – almost 5000 properties lie beneath a 1 in 200 year SWL, of which 2000 could be flooded to in excess of 1 m depth (Table 6.3) and almost 1000 properties can be inundated to depths of more than 2 m. Overtopping and flood incidences have occurred during storm events (e.g. 10 March 2008 – Table 5.2), characterised by high tides and storm surges allowing waves to overtop onto the coastal fringes (which include promenade/esplanade which separate the sea from the main urban areas). The Pyramids entertainment complex was flooded on 7 December 1994 due to wave overtopping, and the wave return wall was subsequently extended 20 m eastwards (PCC, 2008). However there is a lack of evidence to confirm whether enough sea water has ever overtopped the substantial masonry open coast defences to inundate the populated areas inland. Several sources (including photos) concur that a significant coastal flood event occurred in December 1912 which inundated Southsea Common (and Old Portsmouth) (Gonella, 2011; Pomeroy, 2012; Sherwood and Backhouse, 2012). These past overtopping events and the empirical analysis support the plausibility that at more extreme load scenario in the region of a 1 in 200 year SWL. For example a simple relationship described by FEMA (2007) approximates that the when the ratio of the freeboard to significant wave height progresses to <0.75 (Appendix E) that splash overtopping can progress to more serious waveform overtopping. As indicated by crest heights at Southsea (Figure 3.2) and storm wave conditions, this could occur with approximately 0.3 m addition to the 10 March 2008 SWL (which would constitute an approx. 1 in 200 year event). Coupling the empirical relationships with the inflow and inundation methods, indicate that (using 10 m resolution flood simulations) that without breaching, the maximum possible waves combined with the 1 in 200 year (present-day) SWL would could cause widespread flooding, with seawater reaching more than 1 km inland (predominantly due to wave run-up and overtopping along a 1 km length of coast at the eastern section of the Southsea floodplain). In this event, floodwaters surround more than 2000 properties, approximately 800 of these to a water depth of greater than 1 m, and more than 60 to more than 2 m. Most of these are residential properties, although two schools are within cells exceeding 1.5 m depth and more than 20 roads are made impassable by waters exceeding 1 m depth.

Simulations indicate that Old Portsmouth is impacted severely by an extreme wave scenarios and a 1 in 200 year SWL. Broad Street (which runs through the centre of Old Portsmouth) is flooded to over 1.5 m, similar to the floods in December 1989 (Figure 3.4). However, magnitudes of flood events in this compartment at the 1 in 200 year SWL are sensitive to the magnitude of the wave loadings. A significant threshold is crossed between the 1 in 1 year wave and the maximum (similar to approximately 1 in 50 year probability) wave loading inputs, which may also reflect uncertainties about structural input parameters to the empirical overtopping formulae. The difference between the predicted impacts between these two magnitudes of wave loading is much greater for the 10 m resolution model (which does not trigger such widespread and rapid onset flooding at the annual return period waves; whereas substantial inundation is triggered at this load by the 50 m resolution model).

The scenario event of a 1 in 200 SWL and maximum waves allows more than half a metre of water to surround Portsmouth Cathedral, and 0.3 m to surround parts of the Gunwharf Quays shopping complex. A section of the nearby train station and an almost 200 m section of track are also inundated to more than 0.5 m. At Eastney, the maximum extreme wave conditions also cause enough overtopping to allow flood depths of less than 0.2 m across much of this compartment. On the southeast Eastney open coast, Fort Cumberland is likely to be surrounded by flood water, although the secondary defences of this military base provide further protection. The overtopping and inundation calculations suggest that water may flow over the peninsula, connecting the harbour and open coast whilst flooding two caravan parks to depths of over 0.6 m across a 300 metre wide zone.

North Portsea (Compartment 2): The 1 in 200 SWL simulations with maximum waves suggest that at the residential and industrial areas Anchorage Park, flood depths could exceed 0.8 m. At annual probability wave loadings, a smaller flood extent and a reduction of approximately 0.3 m water depth occurs across much of the affected area. Wave overtopping also deposits water onto Saltern's Golf Course and Eastern Road, with segments of Eastern Road flooded to more than 0.3 m, which threatens to block this important transport route. Hilsea Lines is a source of some uncertainty for potential flood impacts in the north (whether it blocks or allows water through). SWL in excess of the 1 in 200 year extreme (approximately 3.2 mODN along Ports Creek) are likely to cause sea water to be in contact with the entire length of these walls (having overflowed the outer moat and defences). Whether or not the Hilsea Lines (refer to Section 4.6.2) can block an inflowing storm-tide during a single (or multiple) high water events has implications for approximately 800-1000 predominantly industrial properties. Increased SWLs and wave loadings beyond the 1 in 200 probability extreme begin to outflank these defences; and a 0.4 m SWL increase upon a 1 in 200 year still water level suggest that overflow failures from the Portsmouth and Langstone Harbour shorelines could almost completely outflank the Hilsea Lines (Figure 6.7).

West Portsea (Compartments 6-8): Simulations and the assets in these compartments, suggest that flood events are mostly characterised by potential for disruption and environmental damage due to inundation of the coastal landfills. The empirical calculations indicate that waves can overtop defences on the south of the Whale Island military base during a 1 in 200 year SWL (and maximum waves) simulation, although land levels are too high to inundate buildings. Simulations also suggest that the vehicular area of the Continental Ferry Port is inundated to 0.2 - 0.3 m. On the west coast, Alexandra Park and Sports Ground are also flooded to an average of 0.3 m. Inundation at nearby houses is less than 0.3 m, although flooding on some of the nearby roads and allotments exceeds 0.5 m depth. Playing fields next to the coast near northwest Hilsea dampen flows to depths of less than 0.3 m depth by the time they reach the fringes of built-up areas (which lie 150 m inland). Water intersects roads for all exit routes from the western part of the city to depths of greater than 0.2 m.

Mainland, Horsea Island and Port Solent (Compartments 1, 8 and 9): This area of the city has the greater discrepancy between the results generated by the two different modelling approaches (of resolution 10 m and 50 m), and similarly there is a large difference between the extent of flooding indicated by breaching scenarios and non-breach scenarios. The Hilsea Lines are a flow diverting feature with a significant effect on the predicted flood event outcome, whilst incorporate uncertainty with regard to their future response to loads and management. The ultimate outcome of events is however increasingly certain with SWLs beyond those plausible at present-day mean sea level and if defences remain unchanged. The most likely defence failure to significantly affect the Mainland is inundation to (and via) Farlington. There are however fewer implications for property (at present sea levels) at Farlington relative to failure of other defences in Portsmouth. Waves on top of the 1 in 200 year SWL severely overtop the Farlington defences, causing an obvious risk of breach (although the volume of inflow is already substantial even without breach failure). Figure 6.7 depicts the depth distribution for a non-breach 1 in 200 year SWL scenario (present day and also with 0.5 m SLR).

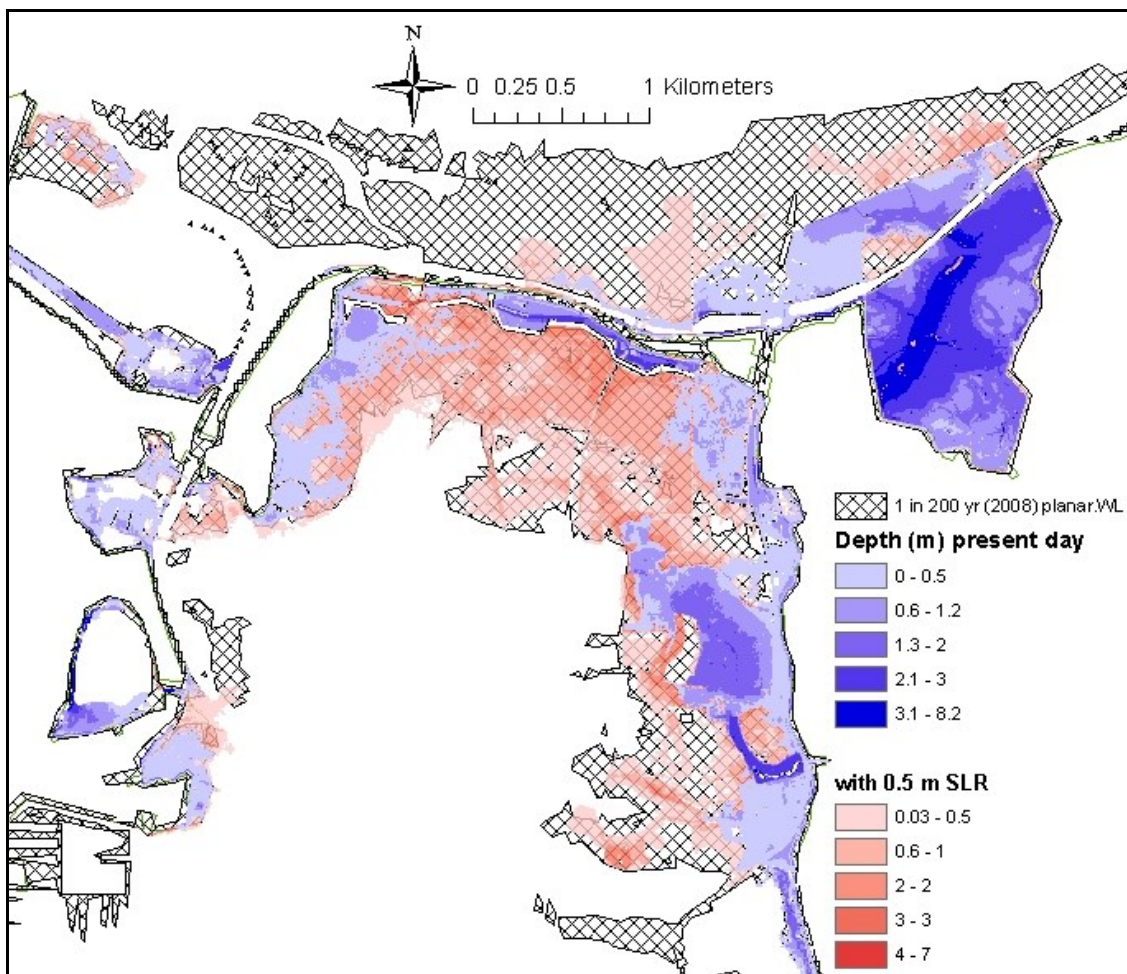


Figure 6.7 Water depth distribution for a 1 in 200 year SWL flood (and maximum waves) in northern Portsmouth, at present-day and with 0.5 m SLR

Simulations show water to flow underneath the A27 main road and onto the fields behind via severe overtopping at Farlington: consequently a hotel and industrial estate northwest of Farlington would be threatened by flood depths of between 0.2 - 0.3 m. The Farlington sea wall is a known weak spot in the Portsmouth defence, and sections of defence are undergoing recent improvement (EA, 2012). Water enters the tunnels in the central mainland embankment and Hilsea Lines but the model indicates negligible flooding. However, beyond the 1 in 200 year SWL the inflow significantly increases as the Hilsea lines are outflanked. With 0.5 m SLR, Figure 6.7 also indicates that enough water flows through the central Mainland A27 defences to inundate the mainland behind; due to the larger hydraulic head and prolonged high water. Figure 6.8 shows an outline of a hydraulic 1 in 200 year SWL coastal flood simulation, overlying the planar water level flood outline, and with a series of captions outlining key locations and aforementioned flooding issues. Also shown is the probability of failure related to these loadings, from the fragility curves. As already noted, due to a lack of specific structural data, the fragility curves developed did not form an integral part of the flood analysis but demonstrate the spatially variable likelihood of breach as indicated by crest height, structural condition, and the combined exposure of the shoreline to wave-water level loads.

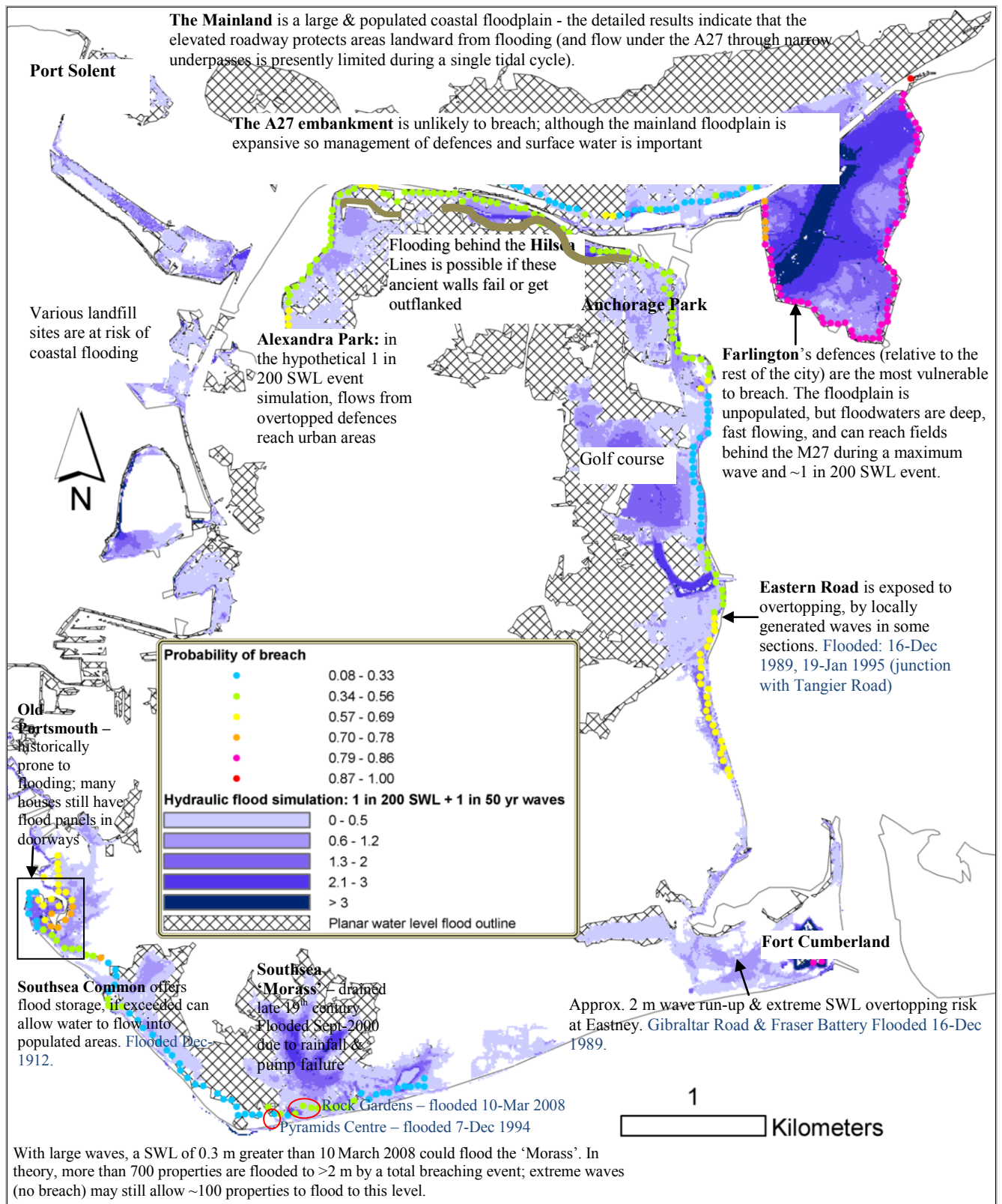


Figure 6.8 Flood event map of Portsmouth, showing: (year 2008) 1 in 200 year planar water level floodplain overlain with, (1) 1 in 200 year SWL and maximum waves simulation output, and (2) conditional probabilities of breach (indicated by the fragility curves) in response to these loadings.

6.3. Detailed case study 2: the Pennington flood compartment

This section assesses coastal flood in the second detailed case study, the flood compartment named here as Pennington. This section firstly focuses upon an extreme sea level event example, using results from the 10 m model (Section 6.3.1). The differences between the 10 m and the 50 m resolution model are less pronounced than for the Portsmouth case study, as shown in Section 6.3.2 which provides comparison between the 10 m and 50 m resolution simulations across loadings.

6.3.1. A present day extreme sea level event

Table 6.5 summarises results for a simulation of a 1 in 200 year SWL event, divided according to the main ‘sub-areas’ of this flood compartment (shown in Figures 3.4 and 6.9). The peak flood depths generated by this SWL scenario, combined with annual waves are shown in Figure 6.9. As indicated in Table 6.4 breaching substantially increases the number of properties flooded. The rationale for the additional ‘selected’ breach scenario is explained in Section 4.6.3; and in these results is seen to exert a high impact upon the Marshes and Keyhaven areas. This indicates the specific importance of defences in these areas, for example the closure of the gated defences at Keyhaven and prevention of structural failure at the described potential weak spots. Application of breach simulations per sub-compartment (rather than all breaches occurring simultaneously as was undertaken here) suggests that at present sea levels, flooding due only to specific breaches in any one compartment may be exert affects that are quite discrete laterally across the site. However, with defences in their current state, large waves (more than annual probability) and extreme SWLs allow heavy wave overtopping across the site which has the potential to connect flows between adjacent areas.

Table 6.4 Number of properties inundated at the Pennington flood compartment by a 1 in 200 year still water level in combination with wave and breach scenarios (using the 10 m resolution model)

FC	Area	Number of properties inundated (brackets, those inundated to > 1 m depth)				
		No waves	1 in 1 waves	Maximum waves	Breach of all defences	Selected breach scenario (Section 4.6.3) & no waves
1	Lymington Town	2 (0)	91 (32)	106 (40)	160 (107)	106 (55)
2	Keyhaven	28 (1)	44 (1)	71 (2)	101 (60)	88 (33)
3	Milford	6 (0)	11 (0)	11 (0)	11 (1)	11 (1)
4	The Marshes	10 (0)	41 (0)	62 (5)	138 (103)	109 (55)
	TOTAL	46 (1)	187 (33)	250 (47)	410 (271)	314 (144)

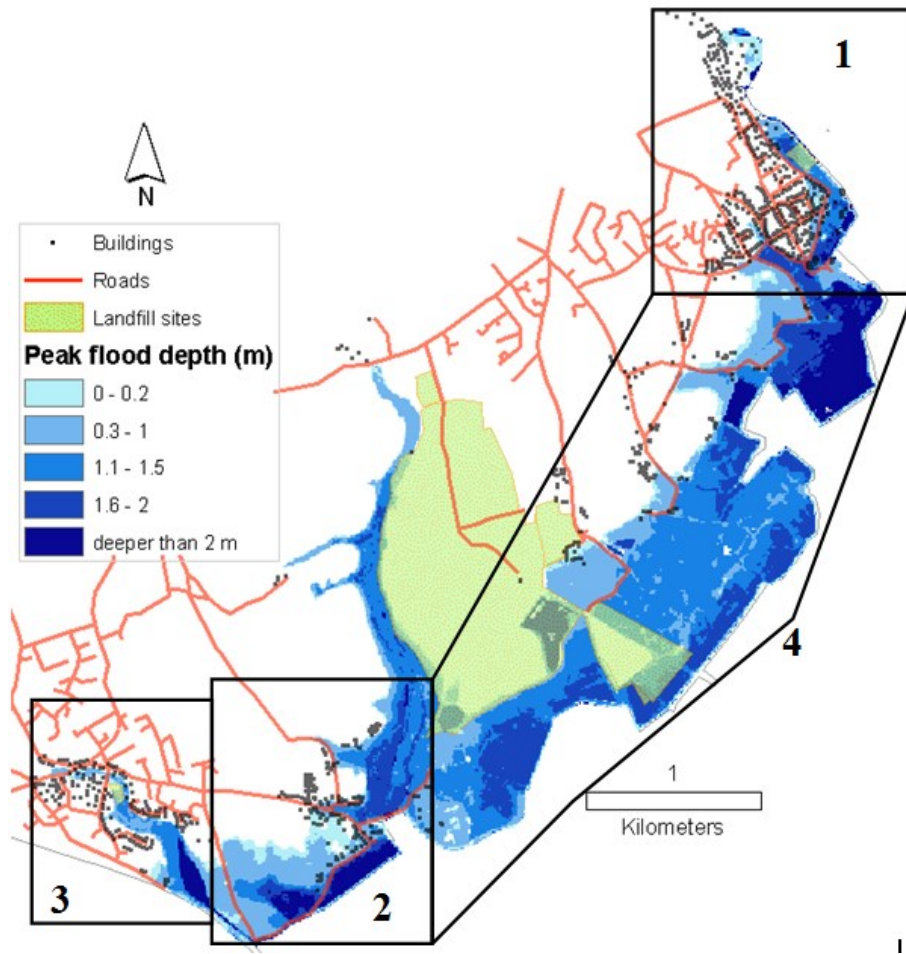


Figure 6.9 Flood simulation output at Pennington (1 in 200 year water level and annual wave loads) and the main sub-areas summarised in Table 6.5

The simulations show that Lymington is the location in this compartment with the most incidences of property that could flood to ≥ 1 m. Increasing the wave inputs beyond the annual extremes substantially worsens this effect. Of the settlements in this compartment, Milford contains the least properties affected by flooding. However, if Hurst Spit was to breach, the effects of waves breaking within the floodplain would cause additional severe flood impacts that are not captured in this approach, although are implied by the full breach flood extent. All of the 1 in 200 year SWL simulations indicate rapid onset flooding within the marshes, which would be hazardous to people and livestock in these rural areas.

Under the full-breach scenario, approximately 10 properties in Lymington are flooded to between 1.75 - 2 m depth. Floodwaters also surround the historic landfill site, and touch the edge of the active landfill. The NRA (1990) post-event report states that sea water from the December 1989 floods did not drain from the area for three weeks after the event. This is cause for concern for the properties and landfill encroached by sea water, which could be exacerbated if breaches were left unclosed due to the potential for repeated inflows.

Shown in Figures 6.10a, 6.10b and 6.10c are comparisons between the 10 m and 50 m model simulations for a range of still water level and wave loadings.

The amount of land and property flooded expands considerably with increasing boundary still water levels. The 50 m resolution simulations indicate higher estimates of inundation – for total counts and for properties in cells exceeding 1 m water depth. There is not as large a discrepancy between the different resolution simulations applied to Portsmouth, although there is some divergence between the two models for the ‘no wave’ simulations due to some of the transitions in the sea wall crest heights at Lymington and Keyhaven. The 50 m resolution model utilises evenly spaced points alongshore and oversimplifies several lower crest height sections near Keyhaven, allowing larger volumes of overflow.

The effects of sea level rise upon the existing defences can also be viewed. The 0.5 m SLR scenario (that is mentioned in previous sections) causes an extreme coastal flood event to impact approximately 150 properties to at least 1 m depth (Figure 6.10b) regardless of any wave loading. Also in this SLR scenario, the 1 in 200 year event of the present day also threatens to become approximately an annual event.

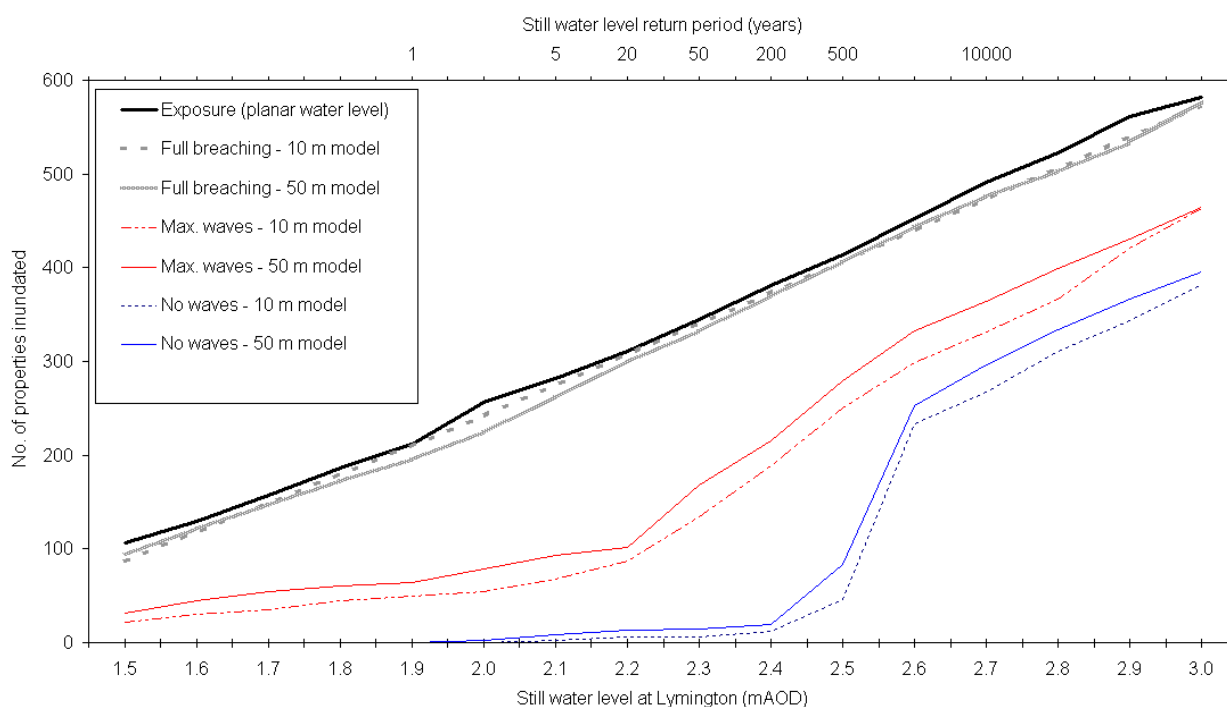


Figure 6.10 (a) Flood modelling results for Pennington by the total number of properties flooded (return periods are for 2008 from McMillan et al, 2011)

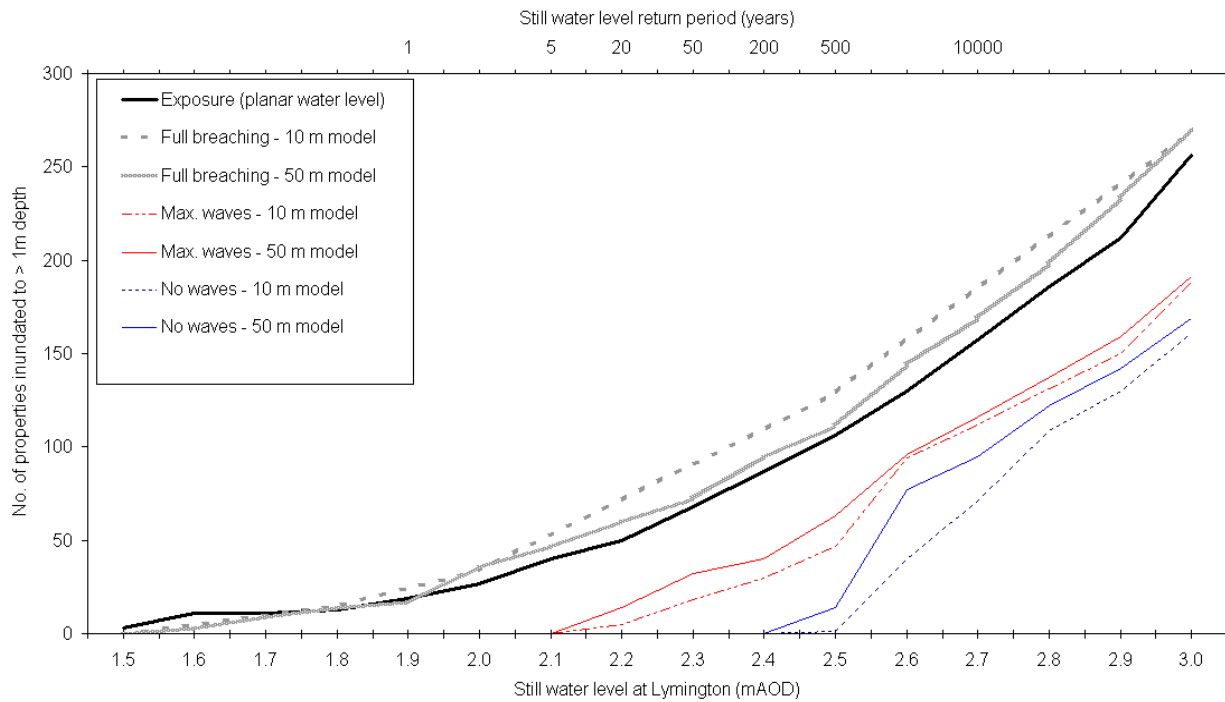


Figure 6.10 (b) Results for the 10 m and 50 m flood simulations at Pennington by the number of properties inundated to > 1m depth

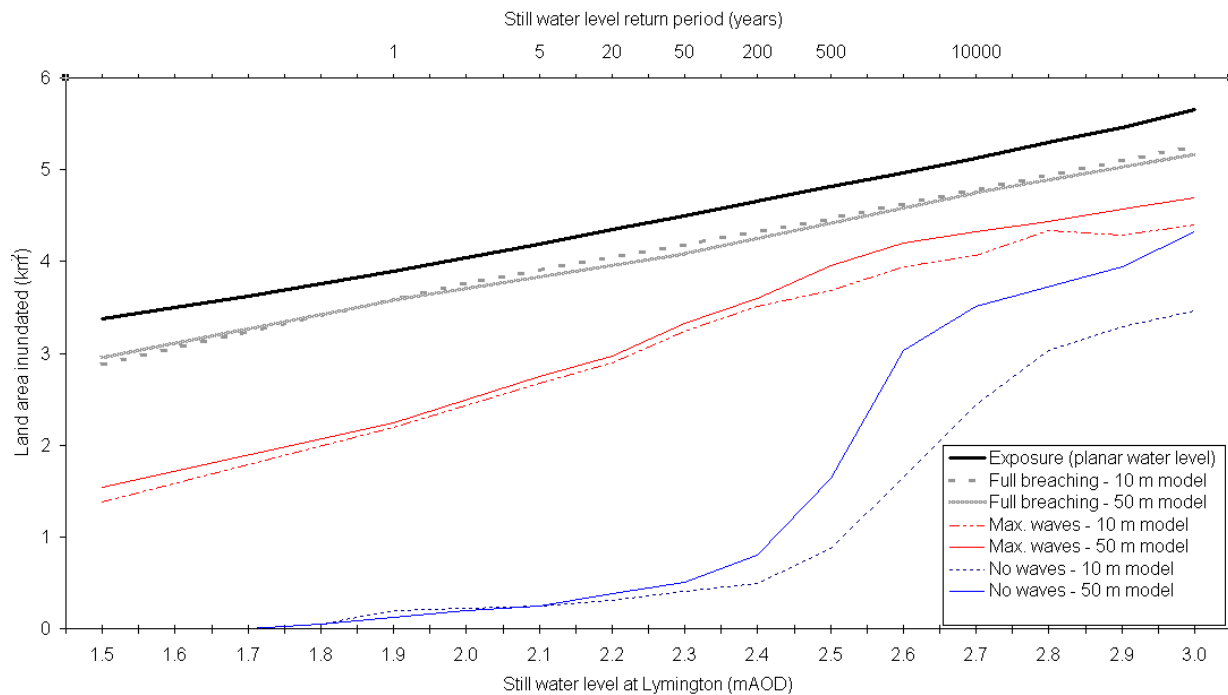


Figure 6.10 (c) Results for the 10 m and 50 m flood simulations at Pennington by land area

At the flood compartment of Pennington the 10 m and 50 m models provide quite similar results, with the greatest discrepancy for the no wave scenario where there is apparent sensitivity of the model to the accurate assignment of crest heights at larger negative freeboards. Overflow flooding near Keyhaven may have been over-estimated by the coarser resolution model due to spatial variation in crest heights

alongshore. Flood simulation results indicate that future flood management of the rural and urban areas of this site will include important decisions related to management of the environmental risks (to the waste sites) and improving the height and strength of the sea wall to reduce overtopping (which will worsen with SLR and the retreating saltmarshes). With present-day defences and a 0.5 m sea-level rise scenario, the number of properties flooded to greater than 1 m depth at least doubles (with non-wave and large waves both exerting significant effects), and SLR beyond this allowing regular inflows on spring high tides. Flooding in the rural Pennington area has the potential to be hazardous, hence maintaining structural integrity and the presence of Hurst Spit are important; unless this becomes unviable and the coast is allowed to retreat, with flood defence construction focusing upon rebuilding defences around the more densely populated areas such as Lymington.

6.4. Summary

6.4.1. Method

The modelling methodology described in Chapter 4 and validated in Chapter 5, has been used to generate coastal flood simulations for hypothetical events in the case-study. The method couples still water levels, waves, defence failures, and a 2D inundation model. The peak flood depths and extent were extracted from these simulations, and used to indicate the amount of property and land area that would be inundated by this range of hydraulic loads and defence failures. The model captures incremental increases in coastal flooding resulting this range of inflows, including flow onto undefended floodplains, and overtopping by small waves (in fetch-limited areas), swell waves, and flow through breaches. Results also compare flood consequences caused by breach and non-breach mechanisms. This section summarises these results and implications to the case study. More generic concepts and a discussion of the implications for future coastal flood management are provided in Chapter 7.

The regional hydraulic flood simulations for the Solent case-study incorporate 4910 defence inflow point locations along 246 km of intertidal shoreline. 116 km of these comprise (to a varying degree) some risk of breaching, whereas 108 km defences are affected by overtopping only. The remaining 22 km have no clear defence system. Approximately 45 km of this defence length appears to be at relatively high risk of breaching, (although a more thorough analysis would be needed to verify this). As shown in Table 6.1, the planar water level method can be compared to previous estimates of coastal flood exposure, by the Environment Agency Flood Maps and the most recent Shoreline Management Plan (NFDC, 2009) – this contributes to verification of the DEM component of this model. The additional planar water level and hydraulic simulations then demonstrate the advantages of the method approach, including (1) flood outlines associated with different loading scenarios, (2) the effect of defences, and (3) spatially variable peak flood depths.

6.4.2. Coastal flood events in the Solent: regional to flood compartment perspectives

This sub-section evaluates the coastal flood simulation results from a flood-compartment perspective. As shown, the hypothetical flood simulations indicate onset of more significant flood impacts beyond the previously observed largest SWLs, notably an on-setting of significantly greater floods with an increase of 0.2 – 0.3 m upon the SWLs observed on 10 March 2008. The 1 in 200 year SWL scenario provides an example overview of an extreme present-day coastal flood, and Table 6.5a lists the top ten flood Solent compartments according to property flooded by a present-day 1 in 200 year SWL and full breach event (numerical simulation), and in the adjacent column shows the proportion that *non*-breach events can contribute towards this number. For example, Southsea (on the Portsmouth open coast) contains the greatest number of properties (in the Solent) that could theoretically be flooded in the event of significant breaching, yet no properties are affected in no-wave scenarios because of high crest levels. Table 6.5b considers the 1 m depth criteria, which demonstrates some more dramatic shifts in the ranks of flood compartment most at threat, for example the city of Southampton moves out of the top ten. Locations of the flood compartments are shown in Figure 6.11.

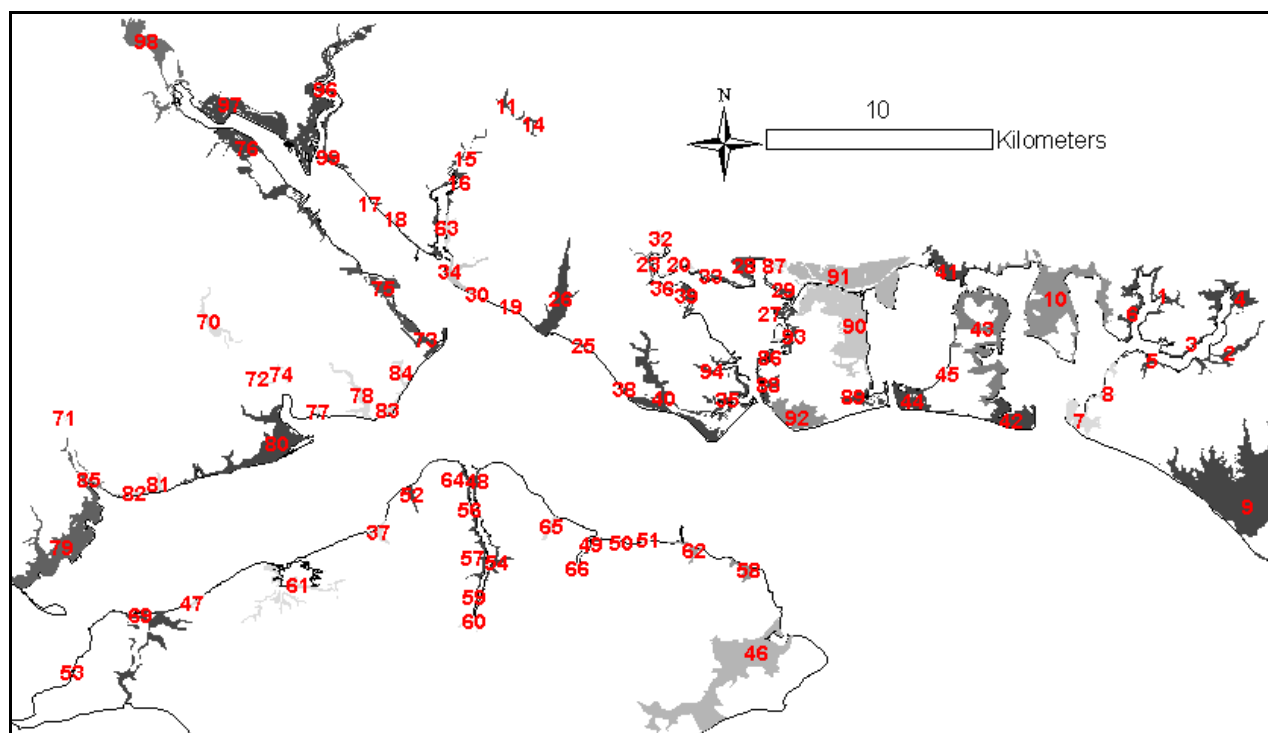


Figure 6.11 Flood compartments in the Solent (for use alongside Tables 6.5 and 6.6).

With four flood compartments in the top 10 (Table 6.5a) it is clear that Portsmouth is the regional focal point for the threat of coastal flooding, although is at present relatively well defended. The Mainland contains a large amount of property in low-lying areas, and is currently well defended from overflow and not exposed to large waves, but dependent upon strong defences to minimise the risk of breach.

Significant wave overtopping flooding in the Southsea ‘Morass’ is plausible at a 1 in 200 year SWL, and viewing results across loadings also suggests the possibility of severe flooding at 0.1 m less (approx. 1 in 50 year) than the 1 in 200 year SWL. The 10 m resolution simulations and detailed approach emphasise Southsea is the flood compartment with the highest potential for coastal flooding even without breach. Elsewhere in southern Portsmouth, as well as the finer resolution DEM allowing deeper propagation of flood water into Southsea, the finer DEM provides a better plan-shape representation of Broad Street – the main receptor and conduit for deeper inundation in this smaller but highly urbanised compartment of Old Portsmouth. The wave-exposed shorelines of Eastoke (Hayling, Havant) and Selsey (Chichester), and the more sheltered locations of Southampton and East Portchester (Fareham) contain a substantial amount of property threatened by coastal flooding. Southampton’s present-day coastal flood threat is characterised by a lack of defences but mostly shallow flood depths. At the large floodplain at Selsey, flood simulations identify significant flooding in populated areas outside of the building dataset, notably at the Solent’s largest holiday park (which can accommodate up to 12,500 people). Areas of this site were inundated to depths between 1 - 2 m during the 10 March 2008 event. However significant defence improvements are currently underway (Pearce et al., 2011).

Table 6.5a The top 10 Solent coastal flood compartments according to the total number of properties potentially within a full breach and overtopping flood outline (of a 1in 200 year still water level event)

FC ID	FC area (km ²)	No. of properties flooded (full breach)		Solent Rank	FC Name	Impact of flood event loadings towards full breach /max flood outcome		
		50 m model	10 m model			No waves	Annual waves	Max waves
92	1.9	3878	4770	1	Southsea	0.00	0.25	0.51
91	5.2	3609	3392	2	Mainland Portsmouth	0.00	0.00	(0.00)
90	5.7	2968	2720	3	Portsea North	0.18	0.19	0.34
42	1.6	1609	N/A	4	Eastoke, Havant	0.26	0.95	1.00
9	14.4	818		5	Selsey, Chichester	0.00	0.49	1.00
97	6.1	801		6	Southampton	0.68	0.93	1.00
28	0.7	486		7	East Portchester, Fareham	0.76	0.94	0.94
88	0.4	466 (1112)		8	Old Portsmouth	0.14	0.77	1.00
79	5.5	431		9	Pennington- Lymington	0.39	0.58	0.90
10	6.8	410		10	Thorney Island, Havant	0.39	0.57	0.65

Table 6.5b The top 10 Solent coastal flood compartments according to the number of properties flooded to >1 m depth (within a full breach and overtopping flood outline of a 1 in 200 year still water level event)

FC ID	FC area (km ²)	No. of properties flooded to >1m (full breach)		Solent Rank (& rank in Table 6a)	FC Name	Impact of flood event loadings towards full breach outcome		
		50 m model	10 m model			Overflow	Annual waves	Max waves
91	5.2	1083	901	1 (2)	Mainland Portsmouth	0.00	0.00	0.00
92	1.9	1041	2035	2 (1)	Southsea	0.00	0.00	0.40
90	5.7	603	640	3 (3)	Portsea North	0.00	0.00	0 - 0.11
9	14.4	315	N/A	4 (5)	Selsey, Chichester	0.00	0.54	1.00
42	1.6	213		5 (4)	Eastoke, Havant	0.02	0.37	1.00
79	5.5	127		6 (9)	Pennington-Lymington	0.17	0.30	0.74
35	1.0	62		7 (11)	Alverstoke, Gosport	0.60	1.00	1.00
10	6.8	58		8 (10)	Thorney Island, Havant	0.35	0.36	0.38
43	4.8	49		9 (13)	Hayling North, Havant	0.06	0.10	0.12
46	8.6	45		10 (12)	Bembridge-Sandown, Isle of Wight	0.07	0.21	0.22

The fragility curves and defence reliability assessment which were based on descriptive information of coastal defences and EA condition scores (refer to Section 4.3.2) did not incorporate sufficiently detailed structural data to be integrated with the Solent-wide scenario simulations, although do indicate relatively the location of weaker/stronger defences (Figure 6.12). Based upon the 1 in 200 year SWL and maximum wave loading, these indicate a higher relative probability of breach in rural areas and on tidal rivers and harbours. For a present-day 1 in 200 SWL and maximum wave load event, the failure probability exceeds 90 per cent along approximately 35 km of defence line. Simulating breaches water through these defences generates slightly greater floodplain water depths than the extreme wave overtopping scenario, although defences are likely to have already significantly overtopped and caused floods prior to breaching. Impacts would be dependent upon factors such the timing of breach initiation and growth, and repair measures. In Portsmouth breach probability is relatively low (compared to the rest of the Solent) with the exception of Farlington.

6.4.3. Changes to mean sea-level and/or extreme events

The outputs also allow changes to flood impacts due to SLR to be considered. Small vertical increases in SWL exert a greater increase to impacts at some loading ranges; and the use of the 1 m depth filter captures a notably steeper increase in flood impacts along with increasing loading (e.g. Figure 6.2a). Table 6.6 considers 0.5 m SLR added to a 1 in 200 year SWL flood event (for comparison with Tables 6.5a and 6.5b), using the 1 m depth filter. These results reflect both changes to the natural potential for flooding (due to the larger floodplain defined by the larger SWL and potential breach inflow) and regionally changing patterns of coastal flood threats as natural land barriers and defences are submerged or lose effectiveness. With the 0.5 m SLR Southampton moves from 23rd to 4th in the Solent ranking of

coastal flood-threatened compartments. In such instances, the changing ranks invoked by this SWL increase imply regional shifts in flood management requirements for places currently without a formal flood defence system. For example, Figure 6.13 shows a deepening of potential flood water and enlargement of the floodplains, with the generation of new areas of floodplain in the densely urbanised and industrialised Southampton Water. Section 7.5 further discusses coastal flood events in the Solent case study (including changes associated with SLR); although Chapter 7 predominantly discusses generic insights gained by the modelling methodology and case study approach.

Table 6.6 The top 10 Solent coastal flood compartments according to the number of properties flooded to >1 m depth (with an additional of 0.5 m SLR compared to a present day 1 in 200 year still water level event)

FC. ID	No. of properties flooded to >1m (full breach)	Per cent (%) increase due to 0.5 m SLR		Rank (pre-SLR)	FC Name	Impact of flood event loadings towards full breach outcome		
		50 m model	10 m model			Overflow	Annual waves	Maximum waves
92	3281 (3332)	215	48	1 (2)	Southsea	0.00 (0.00)	0.07 (0.04)	0.18 (0.37)
91	3028 (2937)	180	226	2 (1)	Mainland Portsmouth	0.18 (0.00)	0.51 (0.01)	0.51 (0.01)
90	1829 (1822)	203	185	3 (3)	Portsea North	0.82	0.84	0.84
97	548	7729	N/A	4 (23)	Southampton	1.00	1.00	1.00
42	493	131		5 (5)	Eastoke, Havant	0.62	0.62	0.62
9	402	28		6 (4)	Selsey, Chichester	0.00	0.62	0.62
28	341	2523		7 (14)	East Portchester, Fareham	1.00	1.00	1.00
79	296	133		8 (6)	Pennington-Lymington	0.91	0.97	0.97
35	250	302		9 (7)	Alverstoke, Gosport	0.72	1.00	1.00
10	159	173		10 (8)	Thorney Island, Havant	0.40	0.50	0.59

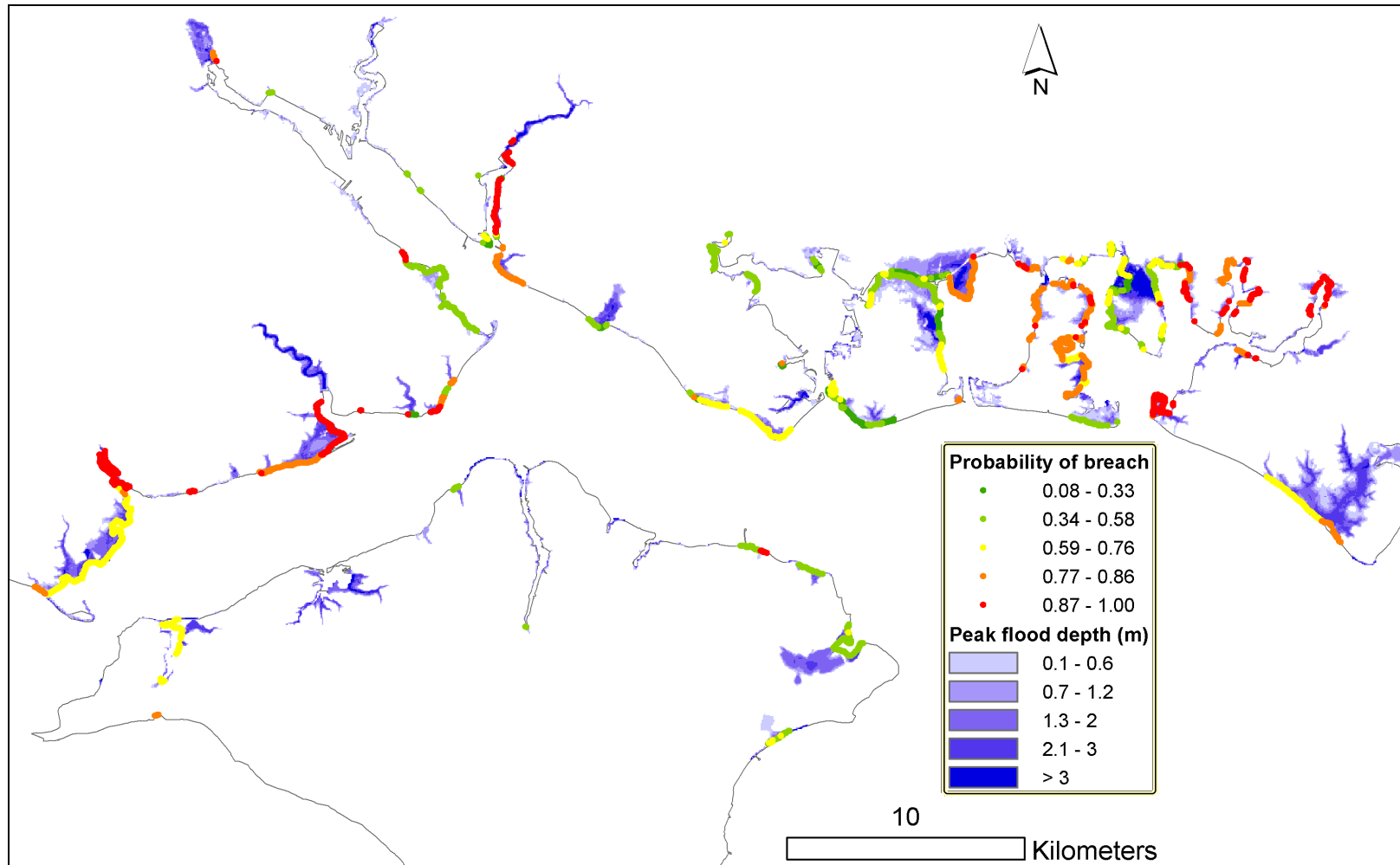


Figure 6.12 Example model output showing: grid of (peak) floodplain water depths for a 1 in 200 year SWL and full breach simulation, and probability of breach for each defence section

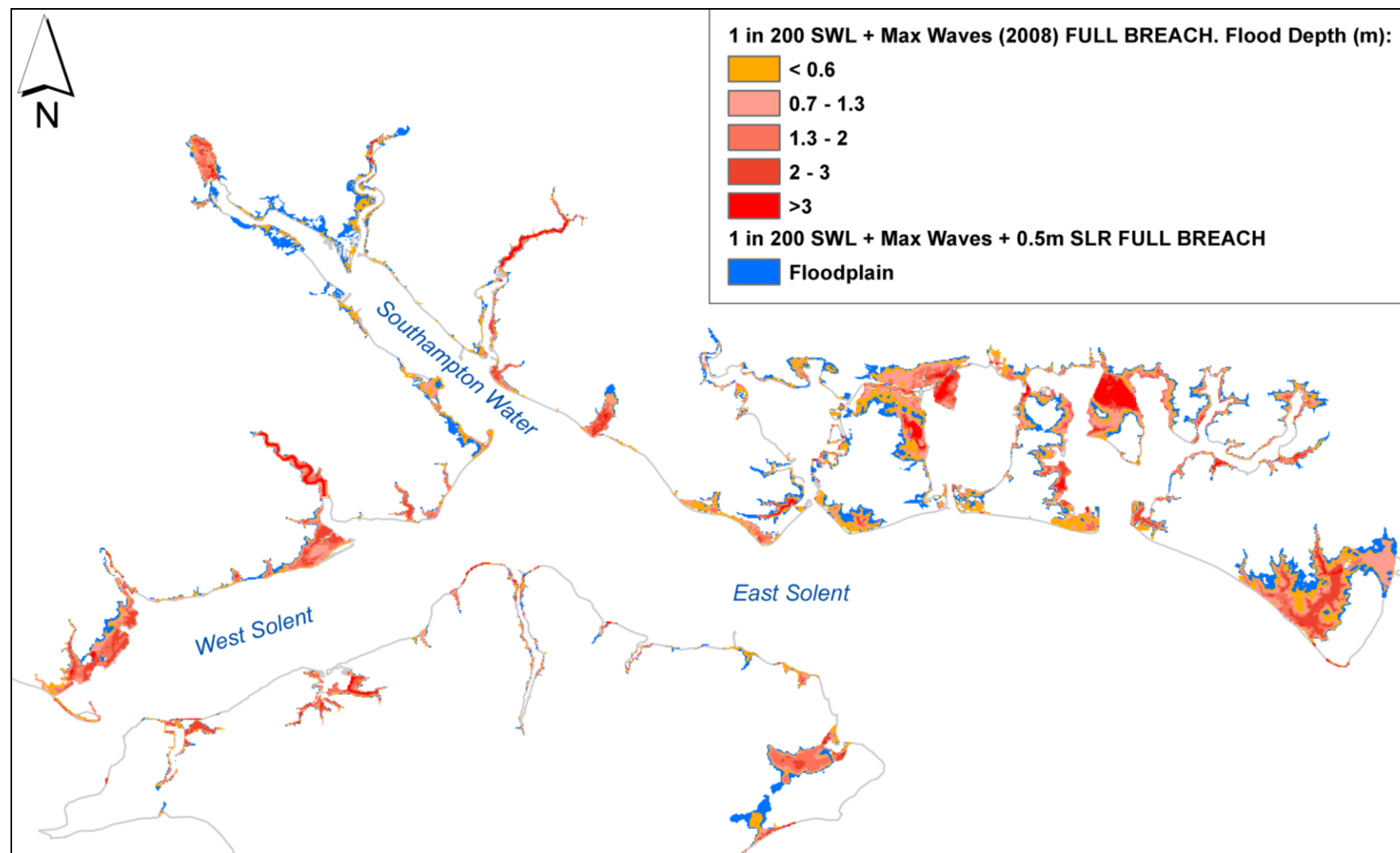


Figure 6.13 Present day flood outline and depth distribution for a 1 in 200 year SWL and full breach event, and in blue the additional floodplain that this scenario generates with 0.5 m SLR

7. Discussion

The aim of this research was to develop a methodology to improve the understanding of coastal flood events, by applying a case study approach. This chapter discusses this aim and the objectives to achieve this; which included the development of an integrated, validated coastal flood simulation method, and coastal flood events which were simulated with a coupled emphasis upon defence responses to loading, and resultant inundation. Both generic and specific insights to the case study are discussed. In this chapter, Section 7.1 provides an overview of the methods and context of them in relation to other coastal flood modelling, and potential applications. Method items are discussed more specifically in 7.2. Section 7.3 discusses the validation, and makes recommendations that could be incorporated into further work. Section 7.4 outlines the outcomes of the detailed/higher resolution case-studies; Section 7.5 discusses insights to present-day and future coastal flood events in the case study region.

7.1. Overview of the methodological position

7.1.1. Novelty and context in coastal flood modelling research

The context of this coastal flooding focused research can initially be reviewed against the main categories of flood modelling which are considered as tools for shoreline management planning, as described by Dawson et al. (2003). These categories include ‘risk-based’, ‘scenario-based’ and ‘model-based’ approaches. The type of modelling described in this thesis and applied to the Solent case study, shares some of the methods of the risk-based approaches. Unlike traditional risk based analysis, the case study flood simulations did not explicitly depict defence failure probabilities, although have used probabilistic load information (e.g. water level return periods) to discuss the consequences of different failures events. This case study research shares concepts with ‘scenario-based’ modelling, due the flood simulation results having potential to challenge pre-existing assumptions and encouraging imaginative thinking about sustainable coastal management, as further described in this chapter. Meanwhile, a ‘model-based’ concept/approach is encompassed via the promotion of standard coastal dynamics (e.g. incorporating information about nearshore bathymetry, waves, and tides) to enable quantified analysis of flood events which could be used to assess coastal management options. Listed below are the primary data components and method used for the integrated flood modelling in this research:

1. Spatial and temporal load distributions;
2. Compilation of a defence database (which included ad-hoc and natural defences, and hard structures);
3. Methods for quantifying wave overtopping (empirical formulae);
4. Assembling and processing topographic data to represent the floodplain surface;
5. Linkage of the above to a numerical inundation model;

6. Simulations of regionally uniform hypothetical coastal flood events, inclusive of spatially variable extreme sea level characteristics and water level time-series (associated with tides, and waves);
7. Simulations of coastal flood events from overtopping, overflow and outflanking along a long and varied shoreline;
8. A comparison of overtopping and breach defence failures (incrementally) across loadings for individual coastal flood events, covering loading scenarios relevant to a range of extreme present day coastal floods, and with implications of SLR included;
9. Combining this analysis with historic flood event and water level data to validate the model – including compiling these data sets where necessary;
10. Deploying higher detail (including spatial resolution) at selected sites to supplement the regional analysis.

These methods and integrated modelling concepts are not new, whilst there are various available data and model options. For example Bates et al. (2005), Dawson et al (2005b), Brown et al (2007); Gallien et al. (2011) and Smith et al. (2012b) and many unpublished consultancy assignments already demonstrate a variety of 2D coastal inundation modelling methods. However from the above list; items 7, 8, 9 and 10 are at present rarely seen in coastal modelling practice or research, whilst the combination of all items is not noted elsewhere. Detailed and accurate 2D schematisation of the defence system and floodplain are demonstrated by Purvis et al (2008) and Gallien et al (2011) although without applying the same loading ranges (e.g. wave overtopping), whilst many method components (and their uncertainties) are not widely discussed, e.g. the overtopping link to inundation models, or simple comparison of the planar water level method with hydraulic simulations at different sea level increments. The assessment of actual events is rare, and Smith et al (2012b) apply a comparable ‘forensic’ style analysis and validation of a coastal flood event and modelling. Despite many flood modelling studies and risk assessment tools being available, detailed case-studies across large and varied coastal regions are few.

7.1.2. Overview of applications

In many region regions around the world, exposure of people or property to coastal flooding, (if assessed at all) is often determined by coarse resolution studies and/or analysis of a small number of potential events. In the Solent case study, prior to this research there was no published work covering the entire area, which considered flood dynamics and defence failures across a wide range of coastal flood events. Detailed study of loads, defence systems and inundation is shown to provide much more specific estimates of land area and property potentially affected by coastal flood events, than previously available. Older and less-specific estimates of inundation (e.g. via the planar water level method) become even more ambiguous if reviewing the basic components used for exposure assessment, e.g.

vertical accuracy of the DEM and the subjectivity of definitions of inundation (e.g. whether a flooded garden is counted as a flooded property). For example, ± 0.15 m vertical DEM uncertainty (considered typical of LiDAR data) and assignment of a 20 m buffer (to approximate the spatial footprint of properties) allows property exposure estimates across the Solent to vary upwards by approximately 30 per cent, and downwards by 10 per cent (Appendix B). Modelling across loads via the hydraulic simulations focuses the demarcation of areas likely to be impacted by coastal flooding, which is further improved by more detailed modelling and validation assessments (as explained in Sections 7.3 and 7.4). The detail and validation are also seen to highlight areas of higher uncertainty whilst facilitating identification of priority areas for data improvements. Incrementally modelling floods across loads also allows greater flexibility in the application of the model outputs. This is important to view some of the sensitivities and uncertainties which are present across events; particularly because the boundary conditions of interest (e.g. SWL return periods) are non-stationary as new methods and knowledge become available. For example, studies often present a set of results derived from a selection of return period scenarios (e.g. Mott MacDonald and EA, 2010; URS, 2012). In the Solent case study this was shown to be limiting, due to the high sensitivity of flood event outcomes counts to small variations in regional SWL, whilst there have been significant revisions between older SWL return period calculations (Dixon and Tawn, 1994; Dixon and Tawn, 1997; EA, 2007b) and newer analysis (Haigh, 2009; Haigh et al., 2010a; Haigh et al., 2010b; McMillan et al., 2011). These older/newer return period analyses comprise a vertical variation of 0.1 m for a 1 in 200 year event (which at present is equivalent to a SWL of 3.1 mODN at the Portsmouth tide gauge, previously 3.2 mODN); ± 0.1 m uncertainty in the present-day 1 in 200 SWL (i.e. considering a range of 3.0 - 3.2 mODN) varies the count of flooded properties in non-breach simulations by approximately 5000 (this difference reduces to approximately 500 properties if only counting those inundated to ≥ 1 m depth, and to 50 for ≥ 2 m). Expanding this error to ± 0.2 m (i.e. 2.9 - 3.3 mODN) almost doubles these variations.

Generating results across a range of SWLs allows a rapid revision of flood impacts associated with any specific return period of interest; and it should also be noted that SWL return periods within any region may also be of variable quality (e.g., in the Solent the observed record at Lymington is much shorter than at Portsmouth, hence more dependent upon interpolation and/or modelling from surrounding sites). Hence it is apparent that presenting simulation results in the manner shown in Chapter 6 is important for understanding flood risk and identifying locations particular in need of good forecasting, warning and potential flood incident management. In the absence of calibration the sensitivity of the modelling is at least better understood by this approach. For example the Pennington case study (Section 6.3) like many locations in the UK has an uncertain future wave climate due to climate change and wave attenuation exerted by the progressively declining saltmarsh/mudflat systems. Varying the flood simulation wave inputs (e.g. from the annual extremes to theoretical maximum) significantly increase the number of properties predicted as flooded, indicating the potential importance of the intertidal area and future crest levels improvements.

In view of the above, potential applications of the model include:

- Comparing breach and non-breach (overflow, overtopping, outflanking etc.) defence failure and inundation: this is valuable to shoreline management planning and coastal strategy studies. Breach evolution is complex to predict and model (Section 2.2.1) although for regions such as the Solent case study, even hydraulic simulations and analysis of simple ‘full breaching’ scenarios indicate the relative importance of defences and flood event management for different parts of the region and across a range of loadings. It is also simple to assign specific breach location scenarios to the model, as shown in the assessment of the 17 December 1989 Pennington flood event. Upgrade to defences can also be easily incorporated and simulations rapidly re-run (over a relatively large area these can be run quickly even when using a standard PC – Table 7.1). This model therefore has uses as a scenario development and analysis tool for coastal managers.
- The configuration of inflows to a full storm-tide water level time-series at the model boundaries coupled to an inundation model allows for an approximation of the spatial and temporal evolution of flood events. With the fast run-time and the capability to predict the peak floodplain depth distribution from loading events this has potential applications for flood mapping and flood warning. Defence failure and inundation mapping have much potential to be further integrated into real-time flood forecasting, warning, and management (Section 2.4.2) (DEFRA and EA, 2004; Twigger-Ross et al., 2009; Ray et al., 2011; Wadey et al., 2011), and the recent launch of the Environment Agency’s online ‘Live Flood Warning Map’ covering England and Wales implies future effort/investment towards systems which provide clearer information for the public. This may eventually include real-time updating flood maps of defence failure and inundation forecasts. Accurate and specific predictions of coastal flood consequences would benefit strategic flood warning dissemination and provide better opportunities for the public, emergency services, and flood managers to respond. Integration of coastal inundation mapping within real-time operational systems could also improve the quantitative appraisal of the performance of warning systems (Hawkes and Whitlow, 2005).
- Jude et al. (2013) remark upon the importance of effectively communicating the potential risks of coastal change and options for adaptation. The validation demonstrated in Chapter 5 supports the plausibility of subsequent hypothetical model outputs, which themselves can be used to visualise and explain changes to coastal flood events due to SLR scenarios which may help decision-makers to engage the public.
- The flood event analysis has more specific potential applications for validating models and assessing coastal flood risks, as discussed in Sections 7.3 and 8.1.

7.2. Review of flood simulation methods

This section discusses the methods used to couple SWLs and wave conditions to inundation simulations. A selection of other coastal inundation analyses which undertake similar modelling to this thesis (detailed defence and floodplain simulation) are also reviewed in Section 4.7 which explains some of the unique aspects and site-specific requirements for the Solent case study. The various decisions and uncertainties which were incorporated are reviewed in Table 7.3. Aspects that can be improved upon in future work are discussed in Section 8.2.

7.2.1. Modelling overtopping failures

- Most of the east Solent's open coast is subject to large waves, including a significant swell component. Meanwhile many areas of land and defence within estuary areas and harbours have small freeboards relative to SWL during significant storm events (e.g. Figure 5.10), and it has been observed that even small waves can make a significant contribution to flooding. Hence inclusion of overtopping inflows from large and small waves was important to approximate flood consequences beyond SWLs (Figures 6.1, 6.2 and 6.3 show markedly increased impacts beyond 'no wave' scenarios).
- Critical to the modelling method for the case study was the manual editing of the DEM and spatial assignment of boundary inflow points. Defence failure inflow calculations utilised accurate ground-surveyed defence heights, important because the results (Chapter 6) are sensitive to small SWL variations, hence the availability of ± 0.03 m accuracy for most of the defence crest height data is an obvious advantage.
- Overtopping and overflow inflows were expressed as water level time-series (rather than volumes). Direct application of volume time-series (from weir equations for overflow and empirical formulae for overtopping) generated unrealistically large flood extents. The water level time-series input method is suitable for the case study, because whilst able to capture incremental changes to flooding due to wave and SWL combinations, the peak of these time-series can be logically limited at each boundary point according to the defence and floodplain configuration, for example overtopping could not exceed breach inflows (with the exception of floodplains above SWLs). As explained in Section 4.7, caution with overtopping inflows is relevant due to the inherent uncertainties in the empirical formulae, the small size of the Solent floodplains (Table 4.5) and the prolonged high waters in the Solent, e.g. the 'double high tide in Southampton Water can magnify overtopping flux calculation inaccuracies across the duration of inundation simulations. For example Smith et al. (2012b) review empirical overtopping inputs for inundation simulations via analysis of the 13 December 1981 Bristol Channel storm surge and flood event; whilst Bates et al (2005) also demonstrate inundation modelling from overtopping. These studies focus upon the

replication of inundation for specific overtopping flood events (rather than a range of synthetic/hypothetical events) using well-known input parameters and observed flood outlines. However a shortage of literature relating to this topic highlights that overtopping methods and linkages to inundation simulations incorporate large uncertainty. For application to regional inundation case studies, this is strongly identified as an important area of future research.

7.2.2. Inundation modelling

The LISFOOD-FP inundation model was used to generate flood outlines from the inflows in this case study; although in theory various numerical inundation models could be applied. ‘Full’ 2D models (Section 2.2.2) provide additional benefits (e.g. shock-capturing, and to simulate more advanced temporal flood dynamics such as recession of the flood) (e.g. Néelz et al., 2009). LISFLOOD-FP originated as a relatively simple storage cell model solving an analytical approximation of the 2D shallow water equations (Bates and De Roo, 2000; Hunter et al., 2005). A significant development included an adaptive time-step (ATS) mode so that the model can configure itself to resolves flow between floodplain cells optimally in relation to grid size (Hunter et al., 2005) allowing more temporally realistic simulation of the flood wave travel time and realistic response to friction parameterisation (Hunter et al., 2007; Hunter et al., 2008). At higher grid resolutions this older ‘diffusive’ flow approximation required very small time-steps for stable simulations (Hunter et al., 2005; Hunter et al., 2007), prompting development of an ‘inertial’ formulation of the 2D shallow water equation (Bates et al., 2010). Inclusion of the inertial terms allows larger time-steps for equivalent performance, hence much smaller run-times (at least ten times computationally faster) and physically more realistic simulations of water movement (Bates et al., 2010; Fewtrell et al., 2011). This is via inclusion of an acceleration term in the flow equations which allows the water being modelled to have some mass, and therefore is less likely to generate the rapid flow reversals (and undesirable oscillations) (Bates et al., 2010). The newer inertial LISFLOOD-FP directly benefited this case study, which contains relatively low gradient floodplains and a requirement to simulate large areas of shallow flows where inertial processes are important. A set of model runs with ‘diffusive’ LISFLOOD-FP (Wadey et al., 2011) generated smaller (approximately 10 per cent) estimates of inundation than results shown in Chapter 6. Also, the fast computational run-time of the model (Table 7.1) supports the concept that such models should be able to rapidly re-integrate new data and generate updated results (e.g. due to defence upgrade). The 10 m resolution model simulations in the diffusive version were computationally prohibitive, thus the inertial LISFLOOD-FP code also provided a more viable means to run a large number of simulations at this resolution.

Parameterisation of surface friction is an uncertainty (e.g. 10 March 2008 Selsey flood, Section 5.1), although results in Section 6.2.1 and 6.2.2 (Portsmouth simulations) suggest that for the case study defence failures, model resolution, and inflow dynamics are more significant. The version and

parameterisation of inertial LISFLOOD-FP is also considered to provide a realistic response to the prescribed surface friction values, and friction values from land-use maps and aerial photos were incorporated into the 10 m simulations. In the DEM, uncertainties remain beyond the quoted vertical accuracy of the LiDAR surveys. The ‘data cleaning’ that produces the ‘DTM’ product is widely acknowledged to have methodological issues and limitations. Separating LiDAR survey points into ground and non-ground returns (carried out by the EA prior to this research) is the most critical and difficult step for DEM generation (Liu, 2008).

Table 7.1 Summary of the model scale and run-time (for a standard 2.5 GHz desktop PC); although note that newer LISFLOOD-FP developments may be able to utilise multiple processors for accelerated simulations or massively parallel graphics processing unit (GPU) cards (Neal et al., 2009).

Model	Domain size		DEM resolution (m) and file size (MB)		Number of inflow points	Time-step (seconds)	Run-time to simulate 18 hours of flooding (minutes)
	Km ²	columns, rows					
Solent	105.7	1227, 846	50	3.94	4909	4.2–6.3	15
City of Portsmouth	15.2	150, 168		0.01	595	5.4–8	<1
		1125, 902	10	3.87	3310	0.6 – 0.8	58

7.3. Historic floods, data sets and validation

The observational data and validation studies were integral to the understanding of coastal flood events in the case study region, and indicated that approximate replication of real events with numerical inundation modelling is achievable, and that systematic monitoring of flood events is important to the assessment of coastal flooding for case studies such as this.

7.3.1 Overview and implications

Other work has recognised a need for more coastal flood model validation an (e.g. Bates et al, 2005; Brown et al, 2007; Smith et al, 2012). A key component of this thesis was the analysis of the 10 March 2008 storm surge and flood event, whilst less detailed analysis/verification was attained by reviewing other historic water levels and floods. Simulations to replicate these events are shown to compare favourably with observed flood extents, although uncertainty in overall flooded area grew with larger overtopping events and for floodplains where a lack of hard data was available for a complete validation (e.g. Selsey, Section 5.1). Importantly, such assessments of real events provide verification of the main modelling data sets (DEM, defence crests) for further coastal flood simulations, as well as validation of the methods for inflow (e.g. interpolation of boundary points, overtopping and flood spreading). Further generic outcomes of the case study analysis also highlight the following:

1. Simplified depth-damage and hazard assessments can provide limited guidance for coastal flood event case studies: within the available observed and simulated flood outlines of 10 March 2008 and 17 December 1989; between 1-5% of the properties in these outlines experienced flooded

interiors. This led to the inclusion of a depth criterion/filter to present the hypothetical event simulation results. From a more generic perspective this analysis highlights the importance of the interpretation of flood simulation outputs beyond simply the raw results (i.e. via a review of floodplain water depths and entry thresholds into properties), and that further scrutiny of the DEM (see previous section) should be considered. Implications of this for regional-scale economic impact or risk analysis can also be demonstrated by intersecting flood simulation data with depth-damage curves (e.g. Penning-Rowsell et al, 2003; Penning-Rowsell et al, 2005). If intersecting each property in the outline of the 10 March 2008 simulation with the mid-value depth-damage curves for UK residential properties (Figure 2.13) this suggests approximately £900 million worth of damage which is not consistent with the amount of media exposure. The analysis flood of observed (Chapter 5) infers how water will not penetrate into the interiors of all of the properties in this outline, and re-applying depth-damage rules only to properties in cells of water depth ≥ 1 m reduces the damage estimate to less than £10 million. From a loss of life estimation perspective, Jonkman and Vrijling (2008) and Jonkman et al (2008) suggest that, as indicated by empirical data, the rate of mortality in large scale coastal floods is approximately one per cent (Figure 2.11). During the 10 March 2008 at least 300 people (and probably many more) are likely to have been exposed to flood water (and similar numbers in previous events such as December 1989) which suggests uncertainty in definitions of exposure, and how such relationships should be reviewed for hazard assessments in regions such as the case study.

2. Analysis of actual flood events in crucial to emphasise site-specific uncertainties and requirements for further data and/or modelling: this includes flood sources or pathways which may be possible to resolve in the scope of any given assessment, but provides an improved and specific ‘starting point’ understanding of the flood system (e.g. in the 10 March 2008 case study, potentially important interactions with drainage and non-coastal sources were identified).
3. Verification and critical evaluation of the characteristics of coastal flooding in a case study. For example in the Solent this justified the simplified hypothetical simulation scenario approach that considered simultaneously occurring spatially (spatially homogenous) return period events across the region, whilst also highlighting the potential for anomalistic waves and water levels in some locations (e.g. extremely long period swell waves at Eastoke).

7.3.2 Recommendations for future flood event data collection and analysis

The collation of the flood data shown in Chapter 5 provided a basic coastal flood model calibration via records of flooded area and property. This also provided a record of flood defence and human responses which are now archived for future use. Subsequently, recommendations include:

- Utilising digital images and technology to observe and recreate the spatial extent of floods, and collate data relating to individual events (refer also to Appendix D). For example, in recent years there is a growing abundance of photography associated with time and location, and can serve as freely available online data sets to yield flood outline observations. Photos, descriptive reports and manual analysis of high-resolution DEMs, and analysis is complimented by verifying and comparing these with the nearest boundary water levels (e.g. storm-tide time-series), aerial photos and OS maps. Applications such as Google's Street View can used to manually follow the path of the flood, and relate the photos taken during the event with referenced locations. Geo-tagged and time-stamped photos can be integrated with GIS, and associated with the corresponding rising water levels gained from nearby tide-gauges.
- As demonstrated in Chapter 5, fundamental data sets that can be obtained from the above (photos, reports etc.) and allow improved modelling / coastal flood event analysis include:
 - Maximum flood extent
 - Flood depths
 - The locations of buildings and roads flooded
 - Descriptions/pictures of defence failure modes
 - Observed boundary conditions from tide gauges and waves buoys
 - Extending boundary condition resolution via numerical modelling or interpolation.
- An improvement to the methods shown in Chapter 5 would include:
 - Recording flood depths within each building. This would comprise evidence of floodwater entry thresholds to property, and a record of impacts. Future research would benefit from an improved version of the observed-simulated flood extent comparison score (eq. 27) that compares actually inundated and predicted inundated properties, if possible integrating flood depth.
 - Collection of data associated with the dynamics and propagation of the flood wave. This is vital for calibrating models which explicitly depict flood hazards (e.g. flow velocities). This could be collected via a network of sensors which until recently has been considered expensive and impractical in public areas;
 - Remotely-sensed data. An upgrade to the methods shown would be to constrain flood extent by the use of remotely sensed data captured during the event (Mason et al., 2012; Schumann et al., 2011), which is increasingly available from both aircraft and satellite platforms. This is particularly recommended to improve the predictions of flood extent where flood water has spread a considerable distance inland, such as at Selsey (which was

by far the largest flood during the 10 March 2008 Solent event). In such cases, large floodplains may conceal the scale of inaccurate inflow volumes which in many situations are simply accepted as uncertain due to complexities such as morphological dynamics and the nature of wave overtopping. The above-mentioned efforts to procure aerial flood images, and integrate these with ground-based images, DEM and inundation analysis and storm hydrodynamics, should be prioritised in such cases to advance this field of coastal engineering research.

Other recommendations which relate to the above and future flood event research include:

- Prioritisation/urgency of data collection. Flood event data capture is dependent upon the collation of datasets as soon as possible following any given event (e.g. much information was lost following the December 1989 English Channel Storm surges and floods). Whilst many contemporary data sets may remain stored digitally this must not be assumed, whilst people's memories/accounts of events may become less accurate or lost over time. Furthermore, defence data sets (which indicate crest heights, condition at any given time) are also not always stored digitally, or may be overwritten as defences are upgraded. The U.S Federal Emergency Management Agency (FEMA) have a rapid response capacity to document the effects of coastal and inland flood events, whilst collection of detailed data during coastal floods analysis only happens sporadically in the UK in response to coastal flood events. For example on 3 November 2005 when waves flooded Eastoke (Havant, UK), local authority engineers logged the flood outline, depths, and properties affected. This was however only for a small area and is not routinely carried out. As already noted, in the absence of hard data, other information may prove beneficial and is a potential area of significant future development. For example the increasing proliferation of social media can yield a large volume of temporally and spatially referenced photos and observations, as already noted during floods elsewhere (Merchant et al., 2011, Charlwood et al., 2012, Bird et al., 2012).
- Observations of wave overtopping. A system has already been proposed by the Channel Coastal Observatory (www.channelcoast.org) to upload photos of overtopping taken during storms, which can then be assessed against other real-time data sets (e.g. wave and tide time-series) and sea defence surveys. The flood simulation and analysis approach in this research strongly suggests that this initiative would be a valuable data set for future coastal flood analysis.

7.4. Detailed analysis and higher resolution studies: findings and applications

The model was applied at 50 m resolution for the Solent-wide coastal flood simulations, and at 10 m resolution for two sites (Portsmouth and Pennington). This increase in resolution was applied due to the perceived benefits from reduced coarsening and spatial interpolation of the original data: the 10 m resolution model of Portsmouth increases the number of inflow points from 595 to 3310 as a result of the additional cells, whilst providing 25 times greater sampling of spatial topographic variability. The analysis partially confirmed findings from previous studies (e.g. Fewtrell et al, 2008b), such as high resolution DEMs generating greater floodplain water depths (due to less spatial interpolation of the original LiDAR data) and the benefits of being able to prescribe more accurate (e.g. narrow) inflows at defences and in the floodplain. However, the detailed approach also underlined areas of uncertainty and decision-making for optimising any model set-up, as described:

1. The first effect seen was the coarser (50 m) resolution DEM tended to spread water over a wider area than the finer (10 m) resolution grid, although this issue is complex and site specific because it involves both the interaction of boundary waves and SWLs with interpolated cells at the land-sea interface, and subsequent flows inside the floodplain. In particular the higher-resolution simulations indicated significantly greater flooding of property from overtopping and breach inflow in Southsea (Portsmouth) due to connecting flows via larger flow depths within the ancient and now urbanised channel-like features of the natural floodplain.
2. The use of higher resolution models can capture important and higher resolution alongshore crest height variations. This was significant at certain SWL thresholds for predicted overflow and overtopping impacts at the Pennington and Portsmouth case studies. For storage cell models which have a spatially uniform / fixed grid cell size (e.g. LISFLOOD-FP) allowing for higher resolution is particularly important in selected areas, and inundation models which deploy flexible grids may provide a more computationally efficient solution over very large areas.
3. Due to the better sampling of defence and floodplain data, higher resolution models are more accurate for flood simulations of SWL (e.g. ‘no wave’ scenarios and deterministic simulations of breach inflow); whereas for wave overtopping failure the magnitude of the volumetric inflow uncertainty (due to the available methods and knowledge) is not certain enough to conclude whether higher model resolution offered significant benefits. However, the greater vertical accuracy and representation of the floodplain surface in the finer resolution grids, better identifies potential flood onset thresholds – as seen for two areas of Portsmouth where the 10 m DEM identified high overtopping volumes and flooding at Eastney (e.g. 0.2 m depth floods on the Eastney open coast) and Old Portsmouth (Figures 6.5 and 6.8).
4. The largest discrepancy between the different model results across load ranges (i.e. on the city-scale case-study of Portsmouth) was from modelling decisions relating to the schematisation of

potentially compromised or weak defences, which may form flow routes into the floodplain. To more realistically simulate event outcomes at some defences the following require a detailed prior understanding: of (1) the structural layout of potential defence weak spots and narrow conduits, (2) structural integrity, and (3) viable flood management (during the event). This is particular relates to the Hilsea Lines defences which can be described as a non-formal ‘second line’ defence, which are not subject to standard safety inspections, although may be increasingly relied upon in the future. This is discussed further in Section 7.5.

5. Compared to the initial Solent-wide modelling results the Portsmouth case high-resolution study provides a potentially significant adjustment to a quantification of properties impacted regionally. Assuming the prescribed defence responses, this alternative set of inundation simulations gives a reduction of the total number of properties flooded accompanied by a large increase in the likely damages to property (i.e. the 10 m DEM increases the estimate of those inundated to water depths ≥ 1 m).
6. The application of different surface friction values had variable effects according to the different floodplain types, and types of flood. Chapter 5 illustrates a large uncertainty effect upon flood spreading at the large rural floodplain at Selsey, for the 10 March 2008 event. However, the net effect for the 1 in 200 year hypothetical flood scenario demonstrated at Portsmouth was a variation of 5% (comparing homogenous and spatially variable friction values) where friction exerted a more significant effect for the prediction of impacts on the fringes of larger flatter floodplains. The deployment of spatially heterogeneous values is a more relevant undertaking for higher resolution work because of the ability to recognise and integrate spatially the main delineations and transitions between different types of surface feature.

7.5. Coastal flood events in the Solent

7.5.1 UK context of the case study

Implications of the flood simulation results for the case study are summarised at the end of Chapter 6, and are discussed further here. During the past century, coastal floods in the Solent are a frequently occurring phenomenon, although with less severe impacts than events seen on the UK east and west coasts. Many coastal settlements in the Solent have rapidly developed over the last century, a period in which sea levels rise has been quite gradual, but significant enough to increase the probability of coastal flood events (Haigh et al., 2011). For the Solent, the application of this method to simulate a series of synthetic coastal flood events across a range of defence failures and loadings provides a renewed dataset indicative of coastal flood extents and impacts. Uncertainties are acknowledged although modelling across many scenarios provides the capacity to easily read results across a range of loadings and hence indicate the magnitude of some of these uncertainties. Anecdotal evidence suggests that more

severe events have occurred prior to the 20th century, due to less developed defence systems (than the present day), and also the occurrence of rare extreme weather events (*c.f.* West, 2010). Whilst significant to the areas affected, the 10 March 2008 event was a small event compared to other post-1953 coastal floods in the UK (e.g. as shown in Table 7.2). However, the observations and simulations results across loads suggest that this event came close to causing much greater impacts.

The 10 March 2008 Solent event case study mostly comprised small floods, associated with between 1 in 5 and 1 in 20 annual event probabilities (according to the most recent return period analysis). However the vertical differences in SWL between events of much lower probability return period events is relatively small. The 1 in 200 year SWL scenario described throughout Chapter 6 provides an insight into a more extreme Solent coastal flood event; comprising SWLs which peaks at only 0.07 - 0.14 m more than the present-day 1 in 50 - 1 in 100 year SWL respectively, although the flood simulations indicate significantly greater than impacts that have ever been seen in living memory. The approximately 0.3 m increase in regional still water levels associated with the 1 in 200 year event (compared to 10 March 2008) exposes more widespread defence failures and floodplains hydraulic connections. As shown in Table 7.2, the scale of the flood and number of properties impacted (approximated by those inundated to > 1 m depth) imply that such an event in the Solent would flood a similar land area to the 13 December 1981 Somerset/Bristol Channel event. That event caused £6 million worth of damages (Proctor and Flather, 1989), allowed water to “pour into over 1000 homes” and incurred huge livestock losses, whilst “miraculously there was no loss of human life” (EA, 2011b). The Towyn and Fleetwood floods were also severe events (Section 2.3.2), and despite that no people drowned there remains significant impacts to the communities affected (EA and DEFRA, 2009).

For the Solent 1 in 200 year event, approximately 100 properties may be inundated to depths of greater than 2 m (the finer resolution Portsmouth analysis suggests that there may be even more properties exposed to this depth), hence the timing of the flood and dissemination/effectiveness of warnings is crucial to manage future extreme events. Applying the depth-damage relationships of Figure 2.13 to all 10,237 properties in a 1 in 200 year annual wave (no breach) Solent event indicates regional damages exceeding £1.03 billion, whereas counting damage only to properties inundated to ≥ 1 m reduces the estimate to £23 million. This suggests significant (but also uncertain) potential estimates of coastal flood damages across the Solent; and highlights (1) the value of this case-study approach and past event analysis for generating more plausible damage estimates, and (2) suggests more research is needed to improve assessments of property damage for accuracy within future flood risk assessments (Wadey et al., 2013). The occurrence of a major storm surge and flood event severe event in the Solent would have profound economic, environmental and social implications for the region itself, whilst depending upon the state of economies, politics and sequences of other events could also have wider-reaching implications to the UK and European economies and insurance markets (e.g. Dawson et al., 2011b).

Table 7.2 A selection of flood events in the UK and coastal floods in the Solent (the 2007 river floods are included to highlight the high mortality aspect of large coastal events).

Event		Defence failure mechanisms	Properties flooded	People exposed	Land area flooded (km ²)	Fatalities
Coastal floods	East UK coast, 1953	Breach, overtopping	24,000	32,000	600	307
	Fleetwood, 1977	Overtopping	1,800	3,600	5	0
	Bristol Channel, 1981	Breach, overtopping	1,000	2,000	50	0
	Towyn, 1990		2,800	5,600	10	0
River floods	UK, 2007		47,000	100,000	420	13
Coastal flood	Solent, 2008	Overtopping	156 to 342 (photos & observed polygon)	351 to 770	5	0
			129 to 270 (to 1m & 0.5m depth in flood simulation)	290 to 608		
Hypothetical coastal floods in the Solent	1 in 200 event present day	Annual wave event, no breaching	7,150 total 673 to >1m, ~100 to >2m	16,088 1531 to >1m 227 to >2m	49	?
	1 in 200 event + 0.5 m SLR		20,000 total 5500 to > 1m 850 to >2m	45,500 total 12,500 to > 1m 1900 to >2m	75	

*Exposure of people generally includes those in contact with floodwater or within the total flood outline. The population stated as 'exposed' to the coastal floods for Solent simulations is approximated from 2001 Census data (refer to Table 3.1); which suggests that average household sizes are ~ 2.24 - 2.45 people, occupancy rate of ~ 0.97 people. The hypothetical event provided is for annual wave inputs and 1 in 200 year still water level, and includes the detailed Portsmouth results

7.5.2 Future coastal flooding

The 1953 North Sea floods account for the worst post-war disaster in the UK. These floods are still remembered by east coast communities and, particularly in the case of the Thames Estuary, form the region which is most starkly associated with the UK's coastal flood risk. A perpetual reminder of the threat to low lying North Sea communities is the extensive sea defences and occurrence of large surge events (e.g. Horsburgh et al., 2008). The perception that coastal floods in the Solent constitute hazard to life is relatively low (e.g. compared to the east and west UK coasts) and in some locations there is even considered to be complacency about the need for incident management strategies (Shackleton et al., 2007). The Chapter 6 results and analysis imply loading ranges at which this situation may change, and suggest the various shifts in regional coastal management that may have to be considered if a severe flood were to occur, due to either an extreme present day event and due to SLR scenarios. Any loss of life or substantial property damage would be likely to prompt more sweeping reforms to reduce risk to life and property (as seen for example post 1953). The increasing popularity of flood resilience measures for homes is one adaptation option (Dawson et al., 2011b) which has already been adopted in flood-prone parts of the Solent such as Wallington (FBC, 2011). This approach appears more suited to

specific parts of the region such as the city of Southampton and other locations where inundation poses more of a threat to property than to human life, and where there are long shorelines currently without defences. Cost estimates for such schemes vary, e.g. protection against shallow floods is typically less than £10,000 per property, whilst can exceed £30,000 for more severe or prolonged floods (Bowker, 2007). With a 0.5 m SLR scenario and a 1 in 200 year SWL event, Southampton's lack of a defence system exposes more than 500 properties to significant inundation (> 1 m depth) and with an additional 1000 properties potentially surrounded by sea water. Hence flood-proofing all properties may prove expensive and time-consuming, and the more costly option of building sea walls around the coast may have to be considered in the future. Depending upon the insurance situation, and without infrastructure in place to rapidly adapt; an extreme flood event occurring unexpectedly or without significant warning, can be disastrous enough to prompt communities to retreat or abandon property (e.g. as observed at some locations affected by the 2010 Xynthia event).

Portsmouth is presently the regional focal point for coastal flooding, with long defence lengths and complex, densely populated urban floodplains. The inundation simulations (particularly the attempts to include greater detail and realistic defence responses to extreme loading events) raise significant questions over defence and management responses, which could be highly influential to the outcome of future extreme sea level events. Beyond an approximately 1 in 100 year present-day SWL it is plausible that coastal floods would increasingly exert detrimental impacts upon the city. Continued defence upgrade is an obvious option to mitigate the risks to these properties and contamination from coastal landfills. Two stretches of defence were identified as an area of contention in the flood simulation results: the A27 Mainland flood walls and Hilsea Lines (north Portsea) which both significantly lessen the impacts of flood events although may allow sea water through. At north Portsea, heightening of the outer defences or reinforcement and/or monitoring of the inner Hilsea Line defences is required to reduce the risk of inundation to an additional 1000 properties during extreme present day events (in the example of an approximately 1 in 200 year SWL). With an additional 0.4 m of SWL (i.e. approximately a 1 in 10,000 year annual probability at present day MSL, or a 1 in 200 year event with 0.2 – 0.3 m SLR) these defences are compromised as a result of failures elsewhere in the flood compartment. If considering the costs involved (e.g. £2000 per metre length for increasing defence crest levels by 1 m – Allsop et al, 2005) heightening the 10 km of sea walls in the north Portsea flood compartment could easily exceed £20 million whilst only accommodating a relatively small amount of SLR, and may further be complicated by the need for more robust drainage infrastructure (e.g. pumps). Also, higher maintenance standards are likely to be required to increase safety in view of the worsened potential flood hazard/greater water depths. Therefore, depending upon the magnitude of SLR and cost appraisals, more radical future defence option could be considered. For example, the benefits of a barrage across the harbour inlets are discussed by RIBA and ICE (2009) which could allow time to manage the waste sites and allow greater confidence in future development schemes, whilst avoiding the need to construct large dikes in the northern areas of the city – preserving the historic character and

saving valuable land space in this densely populated area. Discussion of potential adaptation scenarios become far more complicated when discussing much lower probability and more extreme SLR scenarios, which are shown by the planar water level flood map in Appendix B (Figure B3). The UKCP09 H++ scenario (1.9 m SLR) substantially expands the East Solent floodplains, whilst Portsea, Hayling and much of the eastern region are connected as one large floodplain with 5 m SLR.

7.5.3 Significance of non-coastal sources

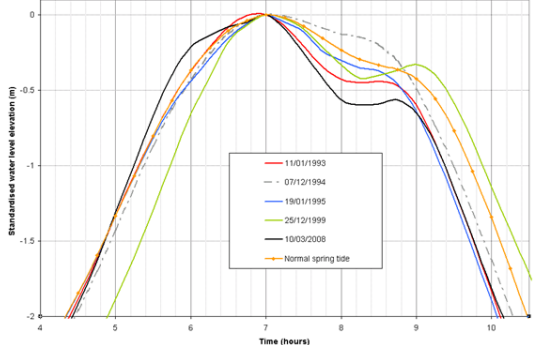
In the Solent case study area, it was noted that other non-coastal flood sources and pathways can be significant, and hence may exacerbate a coastal flood event. These include freshwater from the Solent's rivers, which is a source of flood risk in Southampton Water and various other tidal locations (refer to Figure 3.2). However, relative to the tidal (and potential storm surge) input, the contribution of freshwater input is mostly quite small. For example if comparing flow from the three rivers flow into Southampton Water (Test, Itchen and Hamble), to the volume of water exchanged during each tide (i.e. the tidal prism defined as the difference in water volume between low water and high water), the total river flow rate based on average winter conditions is $23.7\text{m}^3/\text{s}$. Over a 9-hour flood phase this provides a volume of less than 0.1 million m^3 of freshwater input. The equivalent tidal prism for neap tides is 54 million m^3 and 109 million m^3 on spring tides (Townend, 2008).


Portsmouth's most significant flood event in the last half century was caused by heavy rainfall combined with failure of pumps at Eastney on 15 September 2000, which flooded more than 20 roads in central Southsea. However, substantial recent investment now provides protection against similar rainfall events, including higher capacity pumps and more robust systems. The old pumps have a capacity of approximately $18\text{m}^3/\text{s}$ (18,000 l/s) which is now backed up by another station, providing a further $9\text{m}^3/\text{s}$. The main subsurface drainage system at Southsea holds a further 40,000 m^3 . The inflow volumes from the extreme coastal flood event flood simulations (Chapter 6) can be compared. The 1 in 200 year SWL and maximum wave (and non-breach) scenario event discharges a total of 4.5 million m^3 of water into Portsmouth, of which more than 1 million m^3 pours into Southsea (along more than 1 km of overtopped defences). Different wave parameter scenarios suggest this could occur across a time interval of approximately 4 to 6 hours. Assuming a constant, uninterrupted pumping rate of $27\text{m}^3/\text{s}$; between 388,000 m^3 and 583,200 m^3 of sea water could theoretically be removed by the pumping system during such an event, although the rate of inflow in such overtopping events is much greater near high tide and for a period the pumps would be overwhelmed and flooding inevitable. Furthermore, as observed in previous events at some stage the storm is likely to be accompanied by rain.

Whilst it is apparent that tide and surge still water levels dominate the amount of water that could fill the Solent's floodplains, the 10 March 2008 event suggested several locations where tide-locking in the higher reaches of several rivers may have exacerbated floodplain levels and this is discussed further in

Section 8.2. Meanwhile, the magnitude of a large overtopping or breach failure coastal event would appear to dominate the coastal flood threat that exists at Portsmouth; although if reliable the pumps are likely to significantly mitigate lesser overtopping events – and it is noted in Section 8.2 that the incorporation of such scenarios should be considered in future work.

Table 7.3 Summary of method decisions and uncertainties in the case study flood simulations

Type	Parameter/data source & purpose	Decisions / assumptions	Reason / Explanation	Likely uncertainty & impact upon flood event simulations
Source (boundary)	Load return periods (to define load ranges & support flood event analysis)	<ul style="list-style-type: none"> EA return periods for SWL Various data for wave loads including fetch-analysis, observations & return period analysis. 	<ul style="list-style-type: none"> The latest SWL return periods deploy the best available methods & data (skew surge JPM). The observed wave record is shorter & more intermittent than the SWLs; based upon a mixture of modelling and observations by the Channel Coastal Observatory & HR Wallingford. 	Relative to many regions, the available observed data sets in the case study are good quality. However, event probabilities are non-stationary (due to SLR, data & other factors).
	Spatial distribution of the load inputs	<ul style="list-style-type: none"> Assumed that each regional hypothetical event would exert a uniform return period Interpolation between observed water levels & use of 'tide zone' concept Linear interpolation of waves along the coast & use of fetch analysis 	<ul style="list-style-type: none"> The methods used, account for spatial variability in waves & water levels in the absence of a numerical model. Review of previous events and the validation suggested that these assumptions were acceptable. For different real events the following will vary: (1) the relative contribution of tide & surge, (2) the timing of these SWL components, (3) the astronomical tide conditions. 	<ul style="list-style-type: none"> This provides an idealised/simplified representation of event which focuses upon the main load variations that can be expected. The hourly time-series is an appropriate simplification for the simulation of synthetic events; although this, and the selection of a single time-series shape incorporates assumptions about tide-surge. This can significantly influence the shape of the SWL time-series, including the duration of high water – an illustration of storm-tide variability for events with similar (within 0.3 m total SWL) sea levels at Portsmouth is shown in Figure 7.1.
	Wave incidence; shoaling & transformation	<ul style="list-style-type: none"> Assumed waves approached coast directly Approximated the slope between point of observation & structure using bathymetry/ beach surveys – applied this to EurOtop curves to generate changes to H_s used a fixed breaker coefficient of 0.78 	<ul style="list-style-type: none"> The justification of the given approaches relied upon prior knowledge & review of coastal flood history & water levels in the case-study. Individual meteorological events – although has been observed for smaller events (and is possible for future events) that loads may be non-uniform across the region (e.g. swell waves). 	<ul style="list-style-type: none"> Higher temporal resolution loading inputs (e.g. 15 minutely sampled storm-tide curves) were used to simulate inflow for real/observed events. More specific empirical and numerical modelling could be used to inform a larger range of scenarios in the future.
	Temporal distribution of loadings Geomorphic & structural responses during flood events	<ul style="list-style-type: none"> Hourly storm-tide hydrograph input for SWL Overtopping discharges calculated at hourly stages of the tidal cycle; Eq. 6 used to account for intermittency of wave overtopping. Defences remained static during simulations. 	 <p>Figure 7.1 Range of storm-tide time series for SL events (standardised to same level to show potential variability in duration of inflow).</p>	<ul style="list-style-type: none"> A significant influence upon inundation is variation between the wave scenarios (i.e. no waves, annual waves, maximum waves) using wave load inputs (H_s, T_p); although in fetch-limited locations there is less difference between a 1 in 1 year wave and the maximum possible wave, hence incorporating local wind conditions, angle of approach & transformation would be significant (i.e. a coefficient of 0.6 to reduce for wave incidence is as significant as changing the return period scenario). Sensitivity of the flood simulation outputs to different temporal resolution inputs (wave & SWL) is a recommended area of future coastal flood research.
Pathway (inflow)	Overflow failure (when the SWL > defence crest height, water flows over)	<ul style="list-style-type: none"> Crest heights were appended to the DEM 	<ul style="list-style-type: none"> The built-in cell-to-cell flow formula of the chosen inundation model (LISFLOOD-FP) was used to 	<ul style="list-style-type: none"> The method performed well for simulating the observed floods (Table 5.2) & does not

		<ul style="list-style-type: none"> The fluctuating boundary SWL is simply routed over lower cells according to the numerical inundation model 	<p>calculate the flow from the boundary SWL exceeding the defence crest height (eq. 24). This has been observed to generate more realistic flood outlines than coupling the model to different weir formulae (Marshman, 2009) & is a practical method of routing water over the variety of defended & undefended shoreline configurations.</p> <ul style="list-style-type: none"> This is a well-accepted method (e.g. Bates et al, 2005; Purvis et al, 2008); and accurate given the quality of the crest height & storm-tide data. 	<p>incorporate a high degree of uncertainty for a given SWL scenario.</p> <ul style="list-style-type: none"> For much larger overflow heads (presently less relevant to the case study) a fuller representation of the hydraulics of flow over different structure would be relevant – which could be facilitated by full 2D models, and/or testing of different weir formulae. Not explicitly simulated by the model was that overflow & overtopping duration (& volume) may perturb the floodwater's surface on the landward side of a defence & would hence be expected to allow water to propagate further inland. Wind/swell/seiche effects are not included. Seepage through defences, and water flowing over structures (e.g. like a weir) are also not simulated, and would add to inflows to the floodplain. These omissions are quite a common feature of the simplified nearshore & 2D inundation models; although future studies should investigate (1) the optimum spatial placement of inflow cells to minimise mass balance errors, (2) utilise weir formulae where possible to accurately simulate overflow. Empirically-generated OT volumes are notoriously uncertain to a high order of magnitude (due to incongruity between 'test' structure for which formulae developed & the configurations of case study structure). Importantly, the method chosen incrementally increased the height of the peak inflow in the boundary cell (of the inundation model). Numerical models (e.g. simulating wave-by-wave overtopping) could facilitate a better description of wave overtopping processes (Section 2.2.1) although still require calibration & are computationally demanding across the scale of the case-study region. The scale of OT uncertainty is great enough so that it is not possible to definitively state whether there was under of over-prediction. Crest height: along an extensive shoreline there is potential for vertical error, gaps, spatial distribution/sampling within data, although the regional 10 March 2008 validation simulations did not detect significant errors from this.
	Overtopping (OT) models	Empirical formulae were applied according to the EurOtop Manual (Pullen et al, 2007). Sloping structures, beaches & vertical structures were differentiated.	<ul style="list-style-type: none"> Various rates of overtopping are interpreted as significant to the onset of coastal flooding, e.g. 50 l/s/m for a coarse-resolution flood risk study (HRW, 2003, HRW, 2004b); whilst 10 l/s/m has been shown to discharge enough water over a defence to damage the crest or back-slope of un-reinforced structures (Pullen et al., 2007). A rate of 20 l/s/m has been considered by coastal engineers as a failure threshold at defences in the West Solent (NFDC, 2004). A threshold of 10 l/s/m for critical overtopping was selected to ensure a fuller range of possibilities was captured; and because the model could capture the effects of small incremental changes in overtopping volume. The OT method does simulate flows both ways across the land-sea boundary. As pictured here, in reality water drains seaward if the SWL is below the land height. 	
	Case-study specific wave overtopping calculation methods for linkage to 2D inundation simulations	<ul style="list-style-type: none"> For inflow, a rate of 10 l/s/m was selected as the threshold to determine the start & end (and hence duration) of overtopping failures. Under all wave scenarios, inflow was facilitated (1) for the 50m resolution Solent-wide modelling by wave inflows filling the area in the lee of defences (2) for the 10m resolution simulations by generating a water-level time-series to discharge a specific amount of water over the crest (representative of OT). 		
	Crest heights (to calculate spatial distributions of inflow – e.g. overtopping, overflow, outflanking) and probabilities of breach.	<ul style="list-style-type: none"> The data provided is good quality & resolution (mainly ground-based surveys which seek to capture key transitions / distinguishing defence features). Aerial photography & higher-resolution LiDAR data supplemented the defence data in an attempt to find potential gaps. 	 <p>Source: 'The News' (Portsmouth)</p> <p>Figure 7.2 Overtopping at Southsea seafront, Portsmouth. Date unknown.</p>	
Pathway (floodplain) & additional	LiDAR data as supplied (raw data 'DSM' and cleaned 'DTM'). Primarily used to generate floodplain grids for inundation	LiDAR was checked manually & resampled via bilinear interpolation (using ESRI's ArcGIS).	For the Solent case study, the RMSE for different LiDAR tiles is quoted as follows (in metres):	<ul style="list-style-type: none"> Accurate inclusion of houses & fences etc. would slightly decrease the final simulated

sources	simulation.	50 m-resolution cells were considered commensurate with run-time & region-wide data availability; 10 m is the upper range of grid cells considered good for accurate urban inundation modelling.	<ul style="list-style-type: none"> • Lymington-Hurst: 0.055 • Portsmouth & surrounding harbour shores: 0.045 • Hamble: 0.07 • Southampton Water: <0.03 • Chichester & Langstone: 0.05 	<p>flood outline (Brown et al, 2007); although considering the larger effects of defence failure uncertainties this is not feasible for the entire case-study.</p> <ul style="list-style-type: none"> • Larger uncertainties are considered to exist within the DTM (which is cleaned by the EA for the case-study) although manual checks & the validation do not indicate any prominent issues in the case study. • The detailed case study at Portsmouth suggested that the 50 m resolution model under-predicted overtopping on some sections of coastline, due to coarsening of lower lying topography by the interpolation method. Hence it is possible that the 50 m regional simulations under-predicted inundation in some areas.
	LiDAR coarsening / interpolation	50 m & 10 m grids generated	This is impressive in terms of vertical accuracy and likely to remain so at the coarser resolution, using the recommended bilinear resampling.	
	Floodplain friction	A composite value of 0.035 used for the Solent-wide modelling.	However, the ‘cleaned’ DTM contains an un-known level of error due to the lack of knowledge available about the algorithms and manual procedures used to generate this product.	
	Floodplain artefacts (buildings, fences, walls)	Excluded from the flood modelling as surface features, although buildings included as high friction values in the 10 m resolution model.		
	Floodplain numerical modelling (e.g. vertical errors introduced by the numerical model; representation of flow processes)	The model used in this study was inertial LISFLOOD-FP which deploys an analytical approximation to flow derived from the Shallow Water Equations (refer to Bates et al, 2010).	The model used provides a good approximation of flow dynamics up to the peak SWL; and in view of the many other uncertainties with the volumes and dynamics of coastal inflow during flood events, there is little justification for requiring a more physically-advanced 2D model if only seeking to determine peak flood extents, depths and impacts. In a previous LISFLOOD-FP study Hunter et al (2008) made allowance for errors in the DEM and model physics (e.g. oscillation effects observed when the model attempts to predict flow from very shallow flow) by excluding analysis for flooded in cells where water depths < 0.05 m. This is less a problem for the inertial version of LISFLOOD-FP (Bates et al., 2010) (used in this research); although the model developers highlight caution when applying surface friction values of less than $n=0.01$, where cells inundated to less 0.05 m depth may be subject to error. For simulation of deeper, faster flowing water (e.g. from breaching) there are benefits with full 2D models (which deploy full depth-integrated solutions of the Shallow Water Equations), especially if requiring flow velocities and to simulate the receding flood waters. There are also advantages to deploying models with a flexible grid (LISFLOOD-FP uses a regular array of cells) for simulating floods over larger regions with variable data availability and accuracy requirements (e.g. retain high resolution for urban areas or places with complex topography, lower resolution for large rural floodplains).	
	Other sources (fluvial)	Fluvial & drainage (e.g. in the form of subsurface features & pumps) excluded from the modelling methodology. In the 10 March 2008 case-study, the addition of 0.1 m to storm-tide water levels in the upper reaches of the Hamble (via trial & error approach) provided an approximation in the absence of formal backwater calculations, although was not carried forward to the hypothetical simulations.	Tide-locking is poorly resolved in flood impact modelling, with methods lacking for integration of this process with coastal inundation. Examples of this integration are rare (<i>c.f.</i> Smith et al, 2012). However, as explained in Section 7.5.3, both fluvial and drainage sources of flooding contribute a much smaller potential inflow volume to the Solent case study in comparison to tide-surge extremes (particularly within the floodplains where most of the region’s population resides – the cities of Southampton and Portsmouth). It is likely that additional (although mainly minor) flood impacts would be predicted if this was incorporated into the hypothetical flood simulation scenarios; although should be considered in future case-studies based upon modelling and at least collation of observational data where available. Whilst relatively small in volume, it needs to be assessed whether fluvial and drainage inputs could be accountable for significantly exacerbating coastal flood scenarios & results in particular SPRC thresholds being exceeded.	

8. Conclusions

The aim of this research was to develop and apply a methodology to simulate and improve the understanding of coastal flood events via a case-study approach. This was in recognition of an increasing need to assess the likelihood and consequences of coastal floods, particularly in regions such as the Solent where detailed analysis of coastal flooding does not already exist. Coastal flood sources in this case-study (sea levels and waves) are well studied (Haigh et al., 2004; Haigh, 2009; Haigh et al., 2009; Haigh et al., 2010a; Palmer, 2010; Quinn et al., 2012) whereas pathways (e.g. defence failures and hydraulic connections) are less understood. Coastal flood event simulations were generated across a range of sea levels, waves and defence failures. These provided estimates of property and land area impacted. Analysis of real events (notably the 10 March 2008 Solent floods) validated the model and improved inferences about coastal flood event consequences from the more extreme hypothetical event simulations. The novelty of this research (also refer to Section 7.1) is primarily due to the combination of:

1. Using an integrated modelling approach (defence failures and inundation) to simulate coastal flood events across the widest possible range of loading and defence failure scenarios, accommodating 0.5 – 1 m sea level rise (compared to the present day);
2. The development and use of validation data through the ‘forensic’ analysis of historic inundation events;
3. A more detailed approach / higher resolution modelling in selected areas;
4. The modelling generated a review of present and future coastal flood event consequences, and also highlighted uncertainties and recommendations for future coastal flood event modelling.

This chapter summarises the attainment of the aims and objectives (Section 8.1), followed by an overview of the findings and recommendations for future research (Section 8.2).

8.1. Achievement of aims and objectives

The parallel development of validation data and higher-resolution studies, alongside the regional-scale analysis illustrates the potential impacts of individual coastal flood events in the large and varied case-study area. These simulations also indicate the consequences of extreme coastal flood events, inclusive of changes due to SLR. The main outcome is achievement of the aim, and an improved understanding of coastal flood events in the Solent case-study. The integrated modelling approach (loadings, defence failures, floodplain flows) enables flood outlines to be generated rapidly and associated with specific loads and defence configurations. The objectives were achieved by validating the model, and using this to simulate of coastal flood events in the case study region. Conclusions in relation to each of the key objectives (Section 1.3) are summarised:

Objective 1: Develop an integrated method (inclusive of loadings, defence failures, floodplain flows and validation) to simulate coastal flood events.

- This method incorporates wave overtopping and inflows along a large and varied shoreline, including the main natural and structural defences;
- Sea-level and media records were compiled and assessed which indicated the previous scale of coastal floods in the region;
- Chapter 5 demonstrated a rare collation of a data set upon coastal flooding for a storm surge and flood event in the Solent on 10 March 2008 (Wadey et al., 2013). The detailed analysis of this event utilised more than 30 sources (official reports, media, web, eye witness accounts etc.) and over 280 photos to identify and describe flood incidents at 37 locations covering more than 7km² of land. This allowed a validation of the model and highlighted the need to consider outputs relating to hypothetical flood simulations. The validation indicated that the model performed relatively well, with an average fit score (indicative of the overlap between observed and modelled flood outlines) of 0.67 and ranging from 0.15 to 0.95 (1 is perfect, 0 indicates no corresponding pixels). There were more cases of under-prediction than over-prediction of flood extent. By far the largest flood in the region (at Selsey) was of uncertain extent, although the modelled depths of flooding at the areas of observation matched well. The model's performance is good due to high resolution and accurate floodplain (LiDAR) and defence crest (RTK GPS survey) data suggest; although consideration of water depth is relevant when interpreting the simulated flood outlines (i.e. cells inundated to 0.5 – 1 m allowed counts of inundated property from the observed and modelled floods to converge, due to thresholds of entry to property and other uncertainties).
- The on-going systematic monitoring of waves, water levels, and flood events has additional value (i.e. not only for model validation). Aviation, healthcare, and other high-risk industries have shown extensive progress when they have deployed a robust systematic methodology of incident analysis and critical incident reporting (Mahajan, 2010) and this is a relevant concept to be explored further in view of highly populated coastal regions and changing flood risks. Monitoring flood events via the type of dataset described – whether large or small events – is important for flood management and safety, to understand key mechanisms, characteristics, and decrease errors in flood management activities (e.g. verifying hazard hotspots and justifying defences). For example in Bosham, Chichester on 10 March 2008, West (2008) itemises practical problems highlighted by the flood event (e.g. worn/leaking tide-flap seals, blocked drainage routes), whilst the Chichester Observer (2008a) highlight hazards such as bursting manhole covers and failing electrics (causing short-circuiting and arcing explosions) as the rising tide crept along the high street. Elsewhere in the Solent there were at least three incidences of people rescued from cars; whilst greater flood consequences would also have occurred if a flood gate at Old Portsmouth (which initially jammed and would not close – refer to Table 5.2) had not eventually been closed. For regions such as the

case-study where the threat of coastal flood events threatens to gradually escalate given SLR, there is potential for a time-lag between realising changes to sea levels (and other hydrodynamics) and defence degradation, and then establishing significant changes to flood sources, pathways, receptors and consequences.

Objective 2: Apply the method regionally for a series of synthetic coastal flood events across a range of defence failures and loadings; **Objective 3,** repeat this in greater detail for site-specific studies within the case-study region.

- Coastal flood events were simulated across the full range of loadings and defence failures, for the whole Solent, and more detail was applied for simulations at two sites (the city of Portsmouth, and the single flood compartment of Pennington). The benefits of validation, detailed studies and generating results across a range of loadings and defence failures are recommended for any regional-scale assessment of coastal flood events, as explained in the following;
- Multiple simulations and attempting validation are important to confronting flood event uncertainty. For example, the vertical accuracy of the LiDAR floodplain data set contains both known and concealed uncertainties, and boundary conditions of interest (e.g. return periods SWLs) may change. Viewing results across loads in the Solent case-study suggests that uncertainties of the order of 10s of cm (in both boundary water levels and floodplain depths) are significant to predicting the onset and/or consequences of flood events.
- Grid resolution was observed to have a significant effect upon the predicted distribution of floodplain water depths – and hence flood consequences. This effect is more pronounced for the more complex urban Portsmouth floodplain.
- Modelling decisions and secondary defences are important: the largest discrepancy between different models in the detailed case studies was due to conscious decision-making by the modeller – the schematisation or choosing ‘to fail’ potentially weak / less conventional flood defences (e.g. openings in embankments that could be managed, flood gates, features with an unknown structural integrity etc.).
- The ‘hotspot’ analysis provided a closer view of flood simulations at Portsmouth and Pennington which is more useful for flood mapping/visualisation at city to flood compartment scale, because of the practical modelling advantages of finer representation of flow process (from the less interpolated DEM and delineation of spatially variable surface friction effects).
- Detailed results provide a potential correction to ‘region-wide’ results, even if a full region-wide analysis at the finer resolution is not feasible. By selecting the most densely populated areas to assess in detail; the case study’s results were significantly adjusted (the detailed case study of Portsmouth indicated that for a 1 in 200 year SWL and annual wave event, the total number of

properties flooded could be reduced by approximately 3000 in comparison to the 50 m Solent-wide modelling).

- A dual and opposing effect to note from the detailed / higher resolution simulations was that despite the down-scaling of estimates of the total number of properties within the predicted flood outline, there was a significant increase in the number of properties that could be affected by deeper flood water. For example, for the 1 in 200 year maximum wave simulations, suggested a decrease from 6557 to 4977 in the total properties flooded by the 50 m and 10 m resolution models respectively, but an increase from 459 to 927 properties inundation to ≥ 1 m depth.

Objective 4: This method will allow the impacts of extreme present day events and sea-level rise to be considered, as discussed in later chapters.

- Records suggest that pre-20th century flood events were more extreme in the case-study than those seen since (which although frequent have mostly been minor, albeit affected by fluctuations in storminess and gradual defence improvements). Hence in contrast to many communities on the east and west coasts of the UK, more of the coastal population living in the Solent (similar to many other communities on the south coast) have not experienced severe flooding in their lifetime or are aware of a significant threat. However, the population threatened by coastal flood events in the Solent case study region is substantial and will grow significantly with 21st century SLR. Assuming population remains similar to the present day, the analysis shown here indicates that without changes to defences there is a large increase in the amount of property regionally threatened by flooding, and the increasing impacts of overflow and overtopping failures with SLR (Figures 6.1b, 6.2b and 6.3b). Future changes in adaptation and management are necessary to prevent a significant increase in flood consequences is.
- Reports of flooding during the 10 March 2008 Solent event reveal that despite the relatively small floods, flood incidents and near-misses took communities by surprise and initiated discussion about climate change (YCDWG, 2010). Presently, UK coastal flood forecasting and warning resources are prioritised towards managing the storm surge threat on the east coast (ABI, 2006; Hu and Wotherspoon, 2007). However, increase to the coastal flood threat in the Solent over forthcoming decades may be inevitable without a strategy for adaptation (Section 7.5). The flood simulations and SWL return periods suggest that the Solent contains approximately 10,000 properties threatened by an extreme present day coastal event (without including the effects of breaches), as beaches and sea walls are overtopped and ‘ad-hoc’ defence systems are outflanked. Defence systems are likely to fail significantly by overflow and/or overtopping. Any contention over return periods is partly diverted by the model results suggesting that a 1 in 50 and 1 in 200 year SWL (there is a 0.14 m vertical difference in these SWLs) would exert similar impacts when considering variable wave loadings. Approximately 1500 people could be affected by flood waters ≥ 1 m depth during a 1 in 200 year event (based upon people occupying properties in the Solent), a serious event

from a national perspective in today's society, perhaps with comparable impacts to the Towyn 1990 and Bristol Channel 1981 floods (UK west coast). Breaching could generate significantly greater impacts although the probability of structural breaches under present day loading extremes is uncertain. Across the range of SWLs expected in relation to 21st century SLR, the effects of overflow and overtopping become markedly more severe with almost a tenfold increase possible in the number of people exposed to depths of 1 m or more (using the simple 0.5 m SLR scenario). Assuming no defence improvements, these impacts become similar to the effects of broad-scale breaching (Figure 6.2b).

- Sea levels are currently increasing around the UK. Projections provided by the UK Climate Impacts Programme (UKCP09) (Lowe et al., 2009) suggest that middle probability estimates for the year 2050 of approximately 0.18 – 0.26 m SLR in the south of England (the range for low-to high-emission scenarios) would enable the 10 March 2008 still water levels to become an event with an approximately 1 in 1 year return period probability in most areas of the Solent. Alternatively, a similar probability event in 2050 would exert a fourfold increase in properties inundated to greater than 1 m depth (assuming defences are maintained but not upgraded).
- Investment into flood management in the Solent is likely to centre upon the most populated areas, the two cities of Portsmouth and Southampton. For the former, risk is already high and investments in defences already exist with the need for upgrade recognised. Southampton is at present mostly undefended, therefore adaptation will represent a bigger change from current practice. The mean estimates of sea-level rise have remained steady over the past decade, although larger rises due to melting of large ice-sheets in Greenland and West Antarctica are considered a small, but real possibility by 2080 (Section 2.5).

The flood event simulation outputs and the rapid run-time have multiple potential uses including (1) flood warning and management, (2) defence prioritisation, and (3) floodplain mapping and land-use planning. Furthermore outputs are simple and flexible enough to communicate flood impacts to non-scientific audiences, with the uncertainty in events being easily viewable across loadings. These applications are significant because although flood warning systems and management practices exist in many regions around the world, the case of Storm Xynthia in France during 2010 illustrated how coastal flooding can be a surprise phenomenon even in wealthy countries which contain advanced meteorological forecasting systems. Furthermore, globally it is possible that for many coasts such as the Solent where surges are not large and flooding is currently not a major issue; SLR will significantly exacerbate existing risks. The hydraulic flood simulations are seen to provide a more specific view of coastal flood event consequences in response to waves and still water levels, than existing published information in the case study region; and these results can easily and quickly be updated to incorporate or be combined with new information (e.g. defence heights, receptor databases).

As shown in this example, case-studies can provide site-specific and generic insights to coastal flooding, and this thesis presents a methodology to approach such case-studies. The significance of this case study relates to numerical flood modelling, coastal science, data collection and many elements of flood event research. The generation of results and the compilation of datasets such as those described, can significantly improve the understanding of coastal flood events. Similar case studies should be undertaken more frequently and in a systematic manner elsewhere.

8.2. Recommendations for further research

This section summarises directions for further research that have emerged as a result of the literature reviewed, method-development and analysis in this thesis – of generic relevance to coastal flood event modelling/analysis, and with specific relevance to the case-study region.

8.2.1. Generic to coastal flood event analysis

1. ***Defence failures:*** for regions with defence structures in place to protect against wave overtopping, the use of higher-resolution (temporally and spatially) and advanced numerical simulations of overtopping and inundation would reduce some of the assumptions and simplifications within the method applied in this thesis. For example, the overtopping method did not incorporate the effects of drainage back to the sea for floodplains above SWL (Figure 7.2), whilst consequences of perturbation to water in the floodplain by waves (and wind) are also not simulated. However, full physically descriptive overtopping and inundation models would not necessarily improve inundation predictions unless uncertainties within defence failure predictions are resolved further. There is currently limited guidance for (1) coupling wave overtopping and coastal inundation for modelling floods on the scale as described in this case study, (2) uncertainties associated with different overtopping methods (e.g. empirical and numerical) and (3) with the cross and alongshore spatial-temporal patterns of overtopping during storms (which are further complicated by morphological change). Fundamentally, guidance that could serve as a reference or starting point for regional-scale studies, to optimise linkage between overtopping methods (empirical or numerical) to inundation models is not discussed elsewhere, and which different methods are suited to different types of floodplain and defence configuration. This issue interfaces with the need for greater flood event monitoring. The collation of numerous actual overtopping events in a database (whether or not part of a formal experiment) by including photos and details of any local observed hydrodynamic and wind parameters, would support the development of appropriate modelling methods.
2. ***Flood event datasets:*** as highlighted in Wadey et al. (2013), post- and during-flood event data collection is recommended. This should be developed further in other regions, starting with the principles described in Chapter 5 and Section 7.3; although key limiting factors include human

resource and safety. On-going improvements in the understanding of the links between hydrodynamic models and actual storm events could be made possible with increased calibration (e.g. more water level and wave sensor deployments), overtopping measurements, and flood event information records. This issue is also related to items (1), (5) and (6) in this sub-section.

3. ***Multiple/interacting sources and pathways***: highlighted by the 10 March 2008 analyses, the effects of rainfall on some floodplains, and tide-locking in the upper reaches of several rivers were significant. Combining hydrological models with tidal effects has been shown to be important to flood forecasting and warning on the River Dee (North Wales) by Smith et al (2012a). However, studies which evaluate the impacts of tide-locking caused by extreme coastal water level scenarios are uncommon.
4. ***More complex events and coastal boundary conditions***: this research has evaluated individual loading event and coastal inundation scenarios (i.e. a single tidal cycle per simulation), and compared these to return period loadings (sea level and waves) generated by the Skew Surge Joint Probability Method. It is recognised that the Solent case study flood simulations are idealised representations of extreme regional events, and the statistical-spatial load information (used to both prescribe boundary conditions and analyse model outputs) although the best data available was used, it has been proposed that traditional return period calculations could be extended to incorporate more parameters (e.g. surge duration and intensity, wind direction, wave set-up) into multivariate analysis of hydrodynamic boundary conditions that can be used for risk analyses (Wahl et al., 2012). For example, it has been observed that successive hazard events can exert more severe losses than single events, with probable maximum loss calculations (e.g. for insurance) highly sensitive to temporal event clustering (Mailier et al., 2006). Broad-scale weather patterns/mechanisms (e.g. NAO, ENSO) have been associated with repeated storms and floods (e.g. Villarini et al., 2012), including a statistical link to extreme sea level clusters (Scotto et al., 2009). If floods strike in a sequence that does not allow defences and communities sufficient recovery time, a series of smaller events may be as damaging as larger single events. Evidence for this is mostly anecdotal – although for the Solent case-study it is well-documented that the successive high water levels during December 1989 caused amongst the worst flooding seen across the Solent in the last half century (Ruocco et al., 2011), despite that the peak water levels were smaller than a 1 in 1 year return period (and have repeatedly been exceeded since). The influence of successive loads upon structures and cumulative effects of wave overtopping (e.g. upon floodplain storage and drainage) are not widely published or integrated within coastal flood modelling, and would offer another dimension to the understanding of coastal flood events and their consequences. Linkage of the defence failure and inundation simulation method to hydrodynamic models could be used to apply boundary conditions that are representative of the characteristics of a wider range of different coastal floods in the Solent (e.g. Quinn et al., 2012). More complex event analysis could also

constitute a greater variety of boundary condition load parameters within return period sea level definitions (Wahl et al, 2012). Scenarios for breach closure and the effects of repeated overtopping over successive tidal cycles would also be insightful, although would be required to deploy a more physically realistic representation of floodplain hydraulics than applied in this thesis.

5. ***Uncertainty analysis***: the inclusion of some form of uncertainty analysis is widely considered essential to the integrity of numerical modelling studies (Pappenberger and Beven, 2006) and could be more formally integrated for a more comprehensive analysis of present and future flood impacts (e.g. Purvis et al., 2008). This uncertainty relates to defences, loadings and inundation; whilst even when floods are simulated accurately flood loss estimation can also be substantially affected by inaccuracies in the data used for estimating economic losses (Apel et al., 2009).
6. ***Regional monitoring programmes, research and data sharing***: in principle this modelling approach is transferable to other coastal regions. Despite recognition of the many uncertainties across the model and data sets; the LiDAR survey grids provided the Solent case study with amongst the most high-resolution and accurate floodplain data set currently available, whilst flood model outputs are also sensitive to small variations in crest height and boundary water level (both of which are based upon high quality observations in the case-study region). Such high resolution and recent datasets are not available everywhere, and the survey (defence crest, LiDAR and aerial photography) and wave data sets were made available through a coastal monitoring programme in the case study region (Bradbury et al., 2002). Other aspects such as the availability of a freely available and well-developed inundation model (LISFLOOD-FP) and return period analysis data set were also valuable (see Acknowledgements).

8.2.2. The Solent and surrounding regions

1. ***Sources***: a fuller understanding of waves and water levels within rivers and harbours from hydrodynamic modelling and/or metocean deployments (e.g. wave buoys in the harbours). Indicated by discussion of the data in Table 7.6 is that a combination of minimising water level forecasting errors, increasing spatial resolution and generating wave forecasts closer to the coast, may substantially increase the accuracy of inundation model outputs for coastal flood warnings. This is likely to be an increasingly important aspect of flood management in the Solent, as shown by the flood simulations which indicate that the consequences of extreme present-day and future coastal inundation events are likely to be higher than previously seen.
2. ***Pathways – structural defence data***: the probability of breaching remains a large uncertainty that was not easily incorporated into the methodology (although is currently less of an issue than overtopping in the Solent). Impacts of climate change and sea-level rise could be the focus of future studies, using future sea-level scenarios beyond the range shown in this research. Recent LiDAR

surveys could be used to cross check the quality of the existing DEM, and to improve the DEM quality on some of the outer floodplain and tidal rivers (if of sufficient coverage).

3. **Receptor data sets:** The impacts of coastal flooding in the Solent indicated by the simulations described in Chapter 6 could be supplemented by more detailed spatial distributions of population, vulnerability, and key infrastructure.
4. **Climate change and SLR:** the 0.5 m SLR scenario provides limited scope for analysis of changes to coastal flood events (e.g. due to the range of sea level, coastal population and management) expected over the coming century. An insight beyond 0.5 m is provided in Figure B3 via the planar water level method. This is basic although indicates very large changes to the floodplain with low probability (e.g. UKCP09 H++) SLR scenarios. Simulations of future flood event scenarios could also take into account changes to tide and surge dynamics (e.g. Pickering et al., 2012), which would affect the duration of loads, defence failures and inflows to the floodplain.
5. **Spatial extent of the model:** it is noted that other locations on the English south which flank the Solent coast are threatened by or already have experienced significant coastal flood events. To the east, this includes Pevensey and Dungeness (Sussex); whilst to the west communities in the lee of Chesil Beach, Dorset have historically experienced fatal incidences of coastal flooding. Poole, Dorset is a large town which is vulnerable to a large increase in coastal flood risk with SLR (EA, 2011a). It is recommended that this methodology be extended geographically to these areas, potentially utilising overlapping datasets (e.g. hydrodynamic simulations, validation) and where relevant applying the higher resolution and detailed approach according to the guidance in this thesis. Priorities also include improving the spatial understanding of wave and sea-level conditions in the harbours and the upper reaches of tidal rivers, where data recorders and return periods are currently unavailable. Primarily, for the reasons already described, the integration of a larger number of case studies generates models and data sets useful for coastal management and planning of site-specific interest, whilst providing an opportunity to extract generic information about coastal and flood modelling science.

7. References

- A Plüß, A., Rudolph, E. & Schrödter, D. 2001. Characteristics of storm surges in German estuaries. *Climate Research*, 18, 71-76.
- ABI 2006. Coastal Flood Risk – Thinking for Tomorrow, Acting Today.: Research report commissioned by the Association of British Insurers, carried out by Entec in collaboration with Risk Management Solutions and Risk & Policy Analysts. ISBN 1-903193-31-1.
- ABP 2010. Associated British Ports Southampton - Tide Tables 2010. ISSN 1748-0043.
- Ali, A. 1999. Climate change impacts and adaptation assessment in Bangladesh. *Climate Research*, 12, 109-116.
- Allsop, W., Bruce, T., Pearson, J. & Besley, P. 2005. Wave overtopping at vertical and steep seawalls. *Proceedings of the ICE - Water Maritime and Energy*, 158, 103-114.
- Allsop, W., Kortenhaus, A. & Morris, M. 2007. Failure mechanisms for flood defence structures. Floodsite report number: T04-06-01. © FLOODsite Consortium: Task leader: HR Wallingford Ltd.
- Anthoff, D., Nicholls, R. J., Tol, R. S. J. & Vafeidis, A. T. 2006. Global and regional exposure to large rises in sea-level: a sensitivity analysis, Tyndall Centre for Climate Change Research Working Paper 96.
- Apel, H., Aronica, G., Kreibich, H. & Thielen, A. 2009. Flood risk analyses—how detailed do we need to be? *Natural Hazards*, 49, 79-98.
- Aronica, G., Bates, P. D. & Horritt, M. S. 2002. Assessing the uncertainty in distributed model predictions using observed binary pattern information within GLUE. *Hydrological Processes*, 16, 2001-2016.
- Atkins 2007. Strategic Flood Risk Assessment for the Partnership for Urban South Hampshire, document number: 5049258/72/DG/048. Atkins limited, UK, available at: http://www.environment-agency.gov.uk/static/documents/Research/PUSH_SFRA.pdf [Accessed 24th April 2012].
- Bates, P., Fewtrell, T., Trigg, M. & Neal, J. 2008. LISFLOOD-FP: user manual and technical note. Code release 4.3.6. Document version 1.2.
- Bates, P. D., Dawson, R. J., Hall, J. W., Horritt, M. S., Nicholls, R. J., Wicks, J. & Mohamed Ahmed Ali Mohamed, H. 2005. Simplified two-dimensional numerical modelling of coastal flooding and example applications. *Coastal Engineering*, 52, 793-810.
- Bates, P. D. & De Roo, A. P. J. 2000. A simple raster-based model for flood inundation simulation. *Journal of Hydrology*, 236, 54-77.
- Bates, P. D., Horritt, M. S. & Fewtrell, T. J. 2010. A simple inertial formulation of the shallow water equations for efficient two-dimensional flood inundation modelling. *Journal of Hydrology*, 387, 33-45.
- Battjes, J. & Gerritsen, H. 2002. Coastal modelling for flood defence. *Philosophical Transactions of the Royal Society of London. Series A: Mathematical, Physical and Engineering Sciences*, 360, 1461-1475.
- Battjes, J. A. & Groenendijk, H. W. 2000. Wave height distributions on shallow foreshores. *Coastal Engineering*, 40, 161-182.
- Baxter, P. J. 2005. The east coast Big Flood, 31 January–1 February 1953: a summary of the human disaster. *Philosophical Transactions of the Royal Society A: Mathematical, Physical and Engineering Sciences*, 363, 1293-1312.
- BBC. 2008a. *Evacuations as waves flood park. News report on Monday, 10 March 2008, 16:25 GMT* [Online]. <http://news.bbc.co.uk/1/hi/england/sussex/7287880.stm>. [Accessed: 25th January 2012].

- BBC. 2008b. "Pompey locals show Dunkirk spirit" - article by Dan Bell, *BBC News*, Monday, 10 March 2008, 18:25 GMT [Online]. Available: <http://news.bbc.co.uk/1/hi/uk/7288399.stm> [Accessed 7th January 2013].
- BBC. 2008c. "UK storm causes 14 flood warnings" - *BBC News Channel* Monday, 10 March 2008, 23:29 GMT [Online]. Available: <http://news.bbc.co.uk/1/hi/7287662.stm> [Accessed 15th June 2011].
- Bernitt, L. & Lynett, P. Breaching of sea dikes. ICCE No 32 (2010): Proceedings of 32nd Conference on Coastal Engineering, Shanghai, China, 2010, 2010.
- Beven, K. & Freer, J. 2001. Equifinality, data assimilation, and uncertainty estimation in mechanistic modelling of complex environmental systems using the GLUE methodology. *Journal of Hydrology*, 249, 11-29.
- Blake, E. A. & Landsea, C. W. 2011. The deadliest, costliest, and most intense United States tropical cyclones from 1851 to 2010 (and other frequently requested hurricane facts) - NOAA Technical Memorandum NWS NHC-6, August 2011.
- Bode, I. & Hardy, T. A. 1997. Progress and recent developments in storm surge modelling. *J. Hydraul. Eng.*, 123, 315-331.
- Booij, N., Ris, R. C. & Holthuijsen, L. H. 1999. A third-generation wave model for coastal regions 1. Model description and validation. *Journal of Geophysical Research*, 104, 7649-7666.
- Bowker, P. 2007. Flood resistance and resilience solutions: an R&D scoping study. *R&D Technical Report*. DEFRA.
- BPUA 2011. Borough of Poole Unitary Authority - Preliminary Flood Risk Assessment - Final Report v3 - June 2011. Poole Borough Council & the Environment Agency: Available at: <http://publications.environment-agency.gov.uk/PDF/FLHO1211BVTI-E-E.pdf> [Accessed 28/04/2012].
- Bradbury, A. & Kidd, R. 1998. Hurst spit stabilisation scheme. Design and construction of beach recharge. *33rd MAFF conference of river and coastal engineers 1-3 July 1998*. Keele University, UK.
- Bradbury, A. P., McFarland, S., Horne, J. & Eastick, C. Development of a strategic coastal monitoring programme for southeast England. International Coastal Engineering Conference 2002 Cardiff.
- Bradley, S. L., Milne, G. A., Teferle, F. N., Bingley, R. M. & Orliac, E. J. 2009. Glacial isostatic adjustment of the British Isles: new constraints from GPS measurements of crustal motion. *Geophysical Journal International*, 178, 14-22.
- Brown, J. D. & Damery, S. L. 2002. Managing flood risk in the UK: towards an integration of social and technical perspectives. *Transactions of the Institute of British Geographers*, 27, 412-426.
- Brown, J. D., Spencer, T. & Moeller, I. 2007. Modeling storm surge flooding of an urban area with particular reference to modeling uncertainties: A case study of Canvey Island, United Kingdom. *Water Resour. Res.*, 43, W06402.
- Burgess, K. & Townend, I. The impact of climate change upon coastal defence structures. 39th Defra flood and coastal management conference, 2004. 14.
- Bütow, H. 1963. Die große Flut in Hamburg. Eine Chronik der Katastrophe vom Februar 1962. Freie und Hansestadt Hamburg, Schulbehörde.
- Casciati, F. & Faravelli, L. 1991. *Fragility analysis of complex structural systems*. Taunton, UK: Research Studies Press.
- CCO 2012. Channel Coastal Observatory - Strategic Regional Coastal Monitoring Programmes. Data available at: www.channelcoast.org.
- CERC 1984. Coastal Engineering Research Center 1984: Shore protection manual. 4 ed.: Department of the Army, Waterways Experiment Station, Corps of Engineers, Coastal Engineering Research Center, Vicksburg, United States Government Printing Office.

- Cerovečki, I., Orlić, M. & Hendershott, M. C. 1997. Adriatic seiche decay and energy loss to the Mediterranean. *Deep Sea Research Part I: Oceanographic Research Papers*, 44, 2007-2029.
- Chadwick, A., Morfett, J. & Borthwick, M. 2009. *Hydraulics in Civil and Environmental Engineering*, SPON Press, London.
- Cheung, K. F., Phadke, A. C., Wei, Y., Rojas, R., Douyere, Y. J. M., Martino, C. D., Houston, S. H., Liu, P. L. F., Lynett, P. J., Dodd, N., Liao, S. & Nakazaki, E. 2003. Modeling of storm-induced coastal flooding for emergency management. *Ocean Engineering*, 30, 1353-1386.
- Chini, N. & Stansby, P. 2012. Extreme values of coastal wave overtopping accounting for climate change and sea level rise. *Coastal Engineering*, 65, 27-37.
- Church, J. A., Hunter, J. R., McInnes, K. I. & White, N. J. 2006. Sea-level rise around the Australian coastline and the changing frequency of extreme sea-level events. *Aust. Met. Mag.*, 55, 253-260.
- CO. 2008a. Camaraderie helps traders through an awful day - Tuesday 11 March 2008. *Chichester Observer*.
- CO. 2008b. *VIDEO: Selsey flood devastation update and more pictures - Published on Monday 10 March 2008 19:47* [Online]. Chichester Observer. Available: <http://www.chichester.co.uk/news/local/video-selsey-flood-devastation-update-and-more-pictures-1-1504144> [Accessed 6th January 2013].
- Coles, S., Heffernan, J. & Tawn, J. 1999. Dependence Measures for Extreme Value Analyses. *Extremes*, 2, 339-365.
- Cope, S. 2004. *Breaching of U.K coarse-clastic barrier beach systems methods developed for predicting breach occurrence, stability and flooded hinterland evolution*. Ph.D, University of Portsmouth.
- Cope, S. 13th March 2012 2012. *RE: Details of the breach of the Medmerry/Selsey shingle barrier during the storm of 10th March 2008; personal communication: Dr Samantha Cope (New Forest District Council/Channel Coastal Observatory, Southampton) received 13th March 2012 (based upon information collected by Chichester Borough Council)*.
- Coulet, C., Evaux, L. & Rebai, A. Floods study through coupled numerical modeling of 2D and sewerage network flows. In: *Flood risk management and practice*, S. e. a. e., ed., 2008. Taylor & Francis Group, London.
- Cugier, P. & Le Hir, P. 2002. Development of a 3D Hydrodynamic Model for Coastal Ecosystem Modelling. Application to the Plume of the Seine River (France). *Estuarine, Coastal and Shelf Science*, 55, 673-695.
- D'Eliso, C. 2007. *Breaching of sea dikes initiated by wave overtopping - a tiered and modular modelling approach*. Ph.D, University of Braunschweig - Institute of Technology & the University of Florence.
- Davidson, A. C. & Smith, R. I. 1990. Models for exceedance over high thresholds. *Journal of the Royal Statistical Society*, B52, 393-442.
- Davison, M., Currie, I. & Ogley, B. 1993. *The Hampshire and Isle of Wight Weather Book*, Froglets Publications Ltd.
- Dawson, R., Dickson, M., Nicholls, R., Hall, J., Walkden, M., Stansby, P., Mokrech, M., Richards, J., Zhou, J., Milligan, J., Jordan, A., Pearson, S., Rees, J., Bates, P., Koukoulas, S. & Watkinson, A. 2009. Integrated analysis of risks of coastal flooding and cliff erosion under scenarios of long term change. *Climatic Change*, 95, 249-288.
- Dawson, R. & Hall, J. 2002. Probabilistic condition characterisation of coastal structures using imprecise information. In: J. McKee-Smith (ed.) *28th Int. Conf. Coastal Engineering* Cardiff, UK: World Scientific, Hackensack, NJ.

- Dawson, R. & Hall, J. 2006. Adaptive importance sampling for risk analysis of complex infrastructure systems. *Proceedings of the Royal Society A: Mathematical, Physical and Engineering Science*, 462, 3343-3362.
- Dawson, R., Hall, J., Sayers, P. & Bates, P. 2003. Flood risk assessment for shoreline management planning. *Coastal Management*, 83-97.
- Dawson, R., Hall, J., Sayers, P., Bates, P. & Rosu, C. 2005a. Sampling-based flood risk analysis for fluvial dike systems. *Stochastic Environmental Research and Risk Assessment*, 19, 388-402.
- Dawson, R., Peppe, R. & Wang, M. 2011a. An agent-based model for risk-based flood incident management. *Natural Hazards*, 59, 167-189.
- Dawson, R., Speight, L., Hall, J. W., Djordavic, S., Savic, D. & Leandro, J. 2008. Attribution of flood risk in urban areas. *Journal of Hydroinformatics*, 10, 275-288.
- Dawson, R. J., Ball, T., Werritty, J., Werritty, A., Hall, J. W. & Roche, N. 2011b. Assessing the effectiveness of non-structural flood management measures in the Thames Estuary under conditions of socio-economic and environmental change. *Global Environmental Change*, 21, 628-646.
- Dawson, R. J., Hall, J. W., Bates, P. D. & Nicholls, R. J. 2005b. Quantified Analysis of the Probability of Flooding in the Thames Estuary under Imaginable Worst-case Sea Level Rise Scenarios. *International Journal of Water Resources Development*, 21, 577-591.
- De Kraker, A. M. J. 2006. Flood events in the southwestern Netherlands and coastal Belgium, 1400–1953. *Hydrological Sciences Journal*, 51, 913-929.
- de la Vega-Leinert, A. C. & Nicholls, R. J. 2008. Potential implications of sea-level rise for Great Britain. *Journal of Coastal Research*, 24, 342-357.
- de Moel, H., van Alphen, J. & Aerts, J. C. J. H. 2009. Flood maps in Europe – methods, availability and use. *Nat. Hazards Earth Syst. Sci.*, 9, 289-301.
- Debsarma, S. K. 2009. Simulations of Storm Surges in the Bay of Bengal. *Marine Geodesy*, 32, 178-198.
- Defra 2006. Shoreline management plan guidance Volume 1: Aims and requirements, March 2006. Published by: DEFRA, available online: <http://www.defra.gov.uk/publications/files/pb11726-smpg-vol1-060308.pdf> [Accessed on: 25th January 2012].
- DEFRA 2008. *Assessing and valuing the risk to life from flooding for use in appraisal of risk management measures. Defra flood and coastal defence appraisal guidance - social appraisal. Supplementary note to operating authorities, May 2008. Available at: <http://archive.defra.gov.uk/environment/flooding/documents/policy/guidance/fcdpag/risktopeople.pdf>*, DEFRA, London.
- DEFRA 2012. UK Climate Change Risk Assessment (CCRA). Series of detailed reports available online at: <http://www.defra.gov.uk/environment/climate/government/risk-assessment/> [last accessed: 24th October, 2012].
- DEFRA & EA 2003. *Flood risks to people phase 1: R&D Technical Report FD2317*, DEFRA, London.
- DEFRA & EA 2004. *Best Practice in Coastal Flood Forecasting: R&D Technical Report FD2206/TR1; HR Wallingford Report TR 132*, DEFRA, London.
- DEFRA & EA 2005a. Performance and Reliability of Flood and Coastal Defences: R&D Technical Report FD2318/TR 2, Authors: F. Buijjs, J. Simm, M. Wallis, P. Sayers. DEFRA, London.
- DEFRA & EA 2005b. Use of Joint Probability Methods in Flood Management: A Guide to Best Practice. R&D Technical Report FD2308/TR2. Author: PJ Hawkes.
- DEFRA & EA 2006. *Flood risks to people: guidance document, phase 2 FD2321 & 2*, DEFRA, London.

- DEFRA & EA 2007. Performance and Reliability of Flood and Coastal Defences: R&D Technical Report FD2318/TR 1, Authors: F. Buijjs, J. Simm, M. Wallis, P. Sayers. DEFRA, London.
- DeMers, M. N. 2009. *Fundamentals of geographic information systems*, John Wiley & Sons Inc., USA.
- DETR & EA 2000. Department of Environment, Transport and Regions & Environment Agency - Guidelines for environmental risk assessment and management—revised departmental guidance. The Stationery Office, London (2000).
- Di Mauro, M. & Lumbroso, D. Hydrodynamic and loss of life modelling for the 1953 Canvey Island flood. *In: Flood risk management and practice*, S. e. a. e., ed., 2008. Taylor & Francis Group, London.
- Dixon, M. J. & Tawn, J. A. 1994. Extreme sea-levels at the UK A-class sites: site-by-site analysis. POL Internal Document Number 65. . (<http://www.pol.ac.uk/ntslf/pdf/id65.pdf>).
- Dixon, M. J. & Tawn, J. A. 1995. Extreme sea-levels at the UK A-class sites: optimal site-bysite analysis and spatial analyses for the East Coast.: Proudman Oceanographic Laboratory, Internal Document, No 72, 298pp.
- Dixon, M. J. & Tawn, J. A. 1997. Estimates of extreme sea conditions — final report, spatial analysis for the UK coast.: Proudman Oceanographic Laboratory, Internal Document, No 112, 217pp.
- Dube, S., Jain, I., Rao, A. & Murty, T. 2009. Storm surge modelling for the Bay of Bengal and Arabian Sea. *Natural Hazards*, 51, 3-27.
- EA 2007a. Coastal flood forecasting: model development and evaluation, Authors: J. Flowerdew, P. Hawkes, K. Mylne, T. Pullen, A. Saulter, N. Tozer. Collaborators: Meteorological Office, Proudman Oceanographic Laboratory. Science project: SC050069/SR1.
- EA 2007b. Extreme Water Levels: Bournemouth to Littlehampton.: Environment Agency, UK; prepared by the Flood Risk Mapping and Data Management Team (T. Burch and S. Laeger) 1st June.
- EA 2009a. Flooding in England: A National Assessment of Flood Risk. Published by the Environment Agency, available at: <http://publications.environment-agency.gov.uk/PDF/GEHO0609BQDS-E-E.pdf>.
- EA 2009b. Flooding in Wales: A National Assessment of Flood Risk. Published by the Environment Agency Wales, available at: [http://www.environment-agency.gov.uk/static/documents/Research/ENV0005_Flooding_in_Wales_ENGLISH_AW_LR\(1\).pdf](http://www.environment-agency.gov.uk/static/documents/Research/ENV0005_Flooding_in_Wales_ENGLISH_AW_LR(1).pdf).
- EA 2009c. Portchester Castle to Emsworth draft coastal flood and erosion risk management strategy - summary document. Environment Agency in partnership with Fareham Borough, Portsmouth City, Havant Borough and Chichester District Councils.
- EA. 2010a. *RE: Meeting with Environment Agency (Southern Region) Flood Management/Forecasting Team, Colden Common, Hampshire, on 22nd June 2010*.
- EA 2010b. Scoping study for coastal asset management, Authors: M. Wallis, J. McConkey, B. Hamer, P. Sayers, J. Simm. Collaborators: Halcrow Group Ltd. Project: SC070061/R1; Product Code: SCHO0110BRTA-E-P. Published by the Environment Agency; available at: <http://publications.environment-agency.gov.uk/PDF/SCHO0110BRTA-E-E.pdf> [accessed: 9th June 2012].
- EA 2010c. Solent & South Downs Area Report 10 March tidal flooding event, Hampshire & Isle of Wight. A report of events, consequences and conclusions. Version 2 Jan 2010. Environment Agency.
- EA 2011a. Poole Bay, Poole Harbour and Wareham - SMP2 policy and some public comments. Environment Agency. Report available at: <http://www.environment->

- agency.gov.uk/static/documents/Leisure/Poole_wareham_exhib_boards.pdf [accessed: October 2012].
- EA. 2011b. *Somerset Floods - 30 Years On! 13-Dec-2011* [Online]. Environment Agency. Available: <http://www.environment-agency.gov.uk/news/135721.aspx>.
- EA. 2012. *Work set to get underway to shore up Farlington sea wall* [Online]. Environment Agency. Available: <http://www.environment-agency.gov.uk/news/143505.aspx> [Accessed 12th December 2012].
- EA & DEFRA 2009. Communication and dissemination of probabilistic flood warnings, Environment Agency science project SC070060/SR4, Authors: Kashefi, E; Lumbroso, D; Orr, P; Twigger-Ross, C; Walker, G; Watson, N. Environment Agency.
- Easterling, J. C. 1991. Portsmouth's Sea Defences: Towards 2050. The City Engineer's Report on the Sea Defences of Portsmouth.: Portsmouth City Council.
- Entec 2007. Isle of Wight Strategic Flood Risk Assessment for Isle of Wight Council by Entec UK Limited, Doc Reg No. c011.
- ERA. 2008. *Flooding in Emsworth, Borough of Havant, during a storm surge in March 2008* [Online]. Emsworth Residents Association. Available: <http://www.floods.emsworthhants.org.uk/>.
- EuroSION 2004. Living with coastal erosion in Europe: sediment and space for sustainability. major findings and policy recommendations of the EUROSION project. *European Commission, Directorate General Environment, Service contract B4-3301/2001/329175/MAR/B3*.
- Evans, E., Office of, S. & Technology 2004. *Foresight : scientific summary. Volume II, Managing future risks*, London, Office of Science and Technology.
- Faber. 2007. *Introduction to reliability analysis - structural reliability analysis, presentation Lecture 11* [Online]. ETH Zurich. Available: http://www.ibk.ethz.ch/emeritus/fa/education/Seminare/Seminar0607/Lecture_11_Faber.pdf.
- FBC 2011. Review of the Completed Wallington Household Flood Mitigation Scheme - Report to the Strategic Planning and Environment Policy Development and Review Panel (ref: spe-110628-r02-mma). Fareham Borough Council. Available at: <https://www.fareham.gov.uk/crs/planandtranspa/110628/reports-public/spe-110628-r02-mma.pdf> [last accessed: 7th January, 2013].
- FEMA 2005. Guidelines and specifications for Flood Hazard Mapping. Federal Emergency Management Agency, available online at: www.fema.gov/library/file?type=publishedFile&file=frm..
- FEMA 2007. D2.8 Wave runup and overtopping. Guidelines and specifications for Flood Hazard Mapping. Federal Emergency Management Agency, available online at: www.fema.gov/library/file?type=publishedFile&file=frm..
- FEMA 2011. *Coastal Construction Manual: Principles and Practices of Planning, Siting, Designing, Constructing, and Maintaining Residential Buildings in Coastal Areas (4th ed.)*, FEMA. <http://www.fema.gov/library/viewRecord.do?id=1671> [accessed: 10th February 2012].
- Fewtrell, T. J., Bates, P. D., de Wit, A., Asselman, N. & Sayers, P. Comparison of varying complexity numerical models for the prediction of flood inundation in Greenwich, UK. *In: Flood risk management and practice*, S. e. a. e., ed., 2008a. Taylor & Francis Group, London.
- Fewtrell, T. J., Bates, P. D., Horritt, M. & Hunter, N. M. 2008b. Evaluating the effect of scale in flood inundation modelling in urban environments. *Hydrological Processes*, 22, 5107-5118.

- Fewtrell, T. J., Duncan, A., Sampson, C. C., Neal, J. C. & Bates, P. D. 2011. Benchmarking urban flood models of varying complexity and scale using high resolution terrestrial LiDAR data. *Physics and Chemistry of the Earth, Parts A/B/C*, 36, 281-291.
- Flather, R. A. 2000. Existing operational oceanography. *Coastal Engineering*, 41, 13-40.
- Flikweert, J. & Simm, J. 2008. Improving performance targets for flood defence assets. *Journal of Flood Risk Management*, 1, 201-212.
- Fritz, H. M., Blount, C., Sokoloski, R., Singleton, J., Fuggle, A., McAdoo, B. G., Moore, A., Grass, C. & Tate, B. 2007. Hurricane Katrina storm surge distribution and field observations on the Mississippi Barrier Islands. *Estuarine, Coastal and Shelf Science*, 74, 12-20.
- Gallien, T. W., Schubert, J. E. & Sanders, B. F. 2011. Predicting tidal flooding of urbanized embayments: A modeling framework and data requirements. *Coastal Engineering*, 58, 567-577.
- Gardiner, S., Hanson, S., Nicholls, R. J., Zhang, Z., Jude, S., Jones, A., Richards, J., Williams, A., Spencer, T., Cope, S., Gorczynska, M., Brabdry, A., McInnes, R., Ingleby, A. & Dalton, H. 2007. The Habitats Directive, Coastal Habitats and Climate Change – Case Studies from the South Coast of the UK. Southampton, Tyndall Centre for Climate Change Research: pp17. Available at: <http://www3.hants.gov.uk/shiow/habitats.pdf>.
- Gerritsen, H. 2005. What happened in 1953? The Big Flood in the Netherlands in retrospect. *Philosophical Transactions of the Royal Society A: Mathematical, Physical and Engineering Sciences*, 363, 1271-1291.
- Gill, A. E. 1982. *Atmosphere-Ocean Dynamics*, Academic Press.
- Golding, B. W. 2009a. Long lead time flood warnings: reality or fantasy? *Meteorological Applications*, 16, 3-12.
- Golding, B. W. 2009b. Uncertainty propagation in a London flood simulation. *Journal of Flood Risk Management*, 2, 2-15.
- Gonella, P. 2011. *Southsea Common Flood 1912* [Online]. Published in "Vintage & Historical Portsmouth" on Strong Island Media Website: Available online: <http://www.strong-island.co.uk/2011/03/07/southsea-common-flood-1912/> [accessed: 15 July 2013].
- Gönnert, G., S.K., D., Murty, T. & Siefert, W. 2001. *Global storm surges: Theory observation and application - issue 63*.
- Gouldby, B., Kingston, G., Wills, M., Van Gelder, P., Buijjs, F. & Kortenhaus, A. 2008a. Flood defence reliability calculator: RELIABLE User Manual, Floodsite Report Number: T07-10-08. © FLOODsite Consortium.
- Gouldby, B., Krzhizhanovskaya, V. & Simm, J. 2010. Multiscale modelling in real-time flood forecasting systems: From sand grain to dike failure and inundation. *Procedia Computer Science*, 1, 809.
- Gouldby, B., Sayers, P., Mulet-Marti, J., Hassan, M. & Benwell, D. 2008b. A methodology for regional-scale flood risk assessment. *Water Management*, 161, 169-182.
- Gumbel, E. J. 1958. *Statistics of extremes.*, New York, Columbia University Press.
- Guza, R. T. & Thornton, E. B. 1985. Observation of surf beat. *Journal of Geophysical Research*, 90, 3161-3172.
- Haigh, I. 2009. *Extreme Sea Levels in the English Channel*. Ph.D, University of Southampton.
- Haigh, I. 2011. *RE: Quantification of sea-level rise at the Southampton and Portsmouth tide gauges. Personal communication with Ivan Haigh on 25th January 2012.*
- Haigh, I., Butcher, P., Harris, J. M., Cooper, N. J. & Trip, I. 2004. Developing an improved understanding of storm surges in the Solent. *39th DEFRA flood and coastal management conference, June 29 - July 1 2004*. York, UK.
- Haigh, I., Nicholls, R. & Wells, N. 2009. Mean sea level trends around the English Channel over the 20th century and their wider context. *Continental Shelf Research*, 29, 2083-2098.

- Haigh, I., Nicholls, R. & Wells, N. 2010a. Assessing changes in extreme sea levels: Application to the English Channel, 1900–2006. *Continental Shelf Research*, 30, 1042-1055.
- Haigh, I. D., Nicholls, R. & Wells, N. 2010b. A comparison of the main methods for estimating probabilities of extreme still water levels. *Coastal Engineering*, 57, 838-849.
- Haigh, I. D., Nicholls, R. J. & Wells, N. C. 2011. Rising sea levels in the English Channel 1900 to 2100. *Proceedings of the Inst Civ Eng - Maritime Engineering*, 164, 81-92.
- Halcrow 1998. Shoreline Management Plan: Western Solent and Southampton Water. 2 Volumes Report to Western Solent and Southampton Water Coastal Group (Lead Authority: New Forest District Council), analysis by Halcrow and Partners Ltd.
- Hall, J. 2010. Journal of Flood Risk Management. *Journal of Flood Risk Management*, 3, 1-2.
- Hall, J., Dawson, R. J., Sayers, P. B., Rosu, C., Chatterton, J. B. & Deakin, R. A. 2003. A methodology for national-scale flood risk assessment. *Water and Maritime Engineering, ICE*, 156, 235-247.
- Hall, J., Tarantola, S., Bates, P. & Horritt, M. 2005. Distributed sensitivity analysis of flood inundation model calibration. *Journal of Hydraulic Engineering*, 131, 117-126.
- Hanson, S., Nicholls, R., Ranger, N., Hallegatte, S., Corfee-Morlot, J., Herweijer, C. & Chateau, J. 2011. A global ranking of port cities with high exposure to climate extremes. *Climatic Change*, 104, 89-111.
- Harlow, F. 2012. *Incidences and causes of flooding in Portsmouth*. MSc Engineering, University of Southampton.
- Hawkes, P. J., Gouldby, B. P., Tawn, J. A. & Owen, M. W. 2002. The joint probability of waves and water levels in coastal engineering design. *Journal of Hydraulic Research*, 40, 241-251.
- Hawkes, P. J. & Whitlow, C. 2005. Performance Measures for Flood Forecasting; Review and recommendations - R&D Technical Report W5C-021/2b/TR. Defra/Environment Agency - Flood and Coastal Erosion Risk Management R&D Programme.
- HBC 2006. Flood incident 3rd November 2005 - internal report. Havant Borough Council, Havant.
- Hedges, T. S. & Reis, M. T. 1998. Random wave overtopping of simple sea walls : a new regression model. *Water, Maritime and Energy Journal*, 130, 1-10.
- Henderson, G. & Webber, N. B. 1977. Storm surges in the UK south coast. *Dock and Harbour Authority*, 57, 21-22.
- Hodgson, R. 2012. *RE: Rod Hodgson, Deputy Harbour Master, Cowes Harbour Commission, personal communication and unpublished photographs*.
- Holman, R. A. & Bowen, A. J. 1982. Bars, Bumps, and Holes: Models for the Generation of Complex Beach Topography. *J. Geophys. Res.*, 87, 457-468.
- Horrillo-Caraballo, J. M. & Reeve, D. E. 2008. An investigation of the link between beach morphology and wave climate at Duck, NC, USA. *Journal of Flood Risk Management*, 1, 110-122.
- Horsburgh, K. & Horritt, M. 2006. The Bristol Channel floods of 1607 –reconstruction and analysis. *Weather*, 61, 272-277.
- Horsburgh, K., Maskell, J. & Williams, J. 2011. Numerical modelling of storm surges in the Irish Sea and the Isle of Man, and analysis of those factors determining extreme sea levels of the region in a future climate. *National Oceanography Centre Research & Consultancy Report No. 12*.
- Horsburgh, K. J. & Flowerdew, J. 2009. Real time coastal flood forecasting. In: Beven, K. & Hall, J. (eds.) *World Scientific Press*. World Scientific Press.
- Horsburgh, K. J., Williams, J. A., Flowerdew, J. & Mylne, K. 2008. Aspects of operational forecast model skill during an extreme storm surge event. *Journal of Flood Risk Management*, 1, 213-221.

- Horsburgh, K. J. & Wilson, C. 2007. Tide-surge interaction and its role in the distribution of surge residuals in the North Sea. *Journal of Geophysical Research*, 112, 1-13.
- HRW 1995. Pagham Harbour to River Hamble (Coastal) Strategy Study, Volume 1: Pagham Harbour to Portsmouth Harbour, Report EX 3121, Report to Pagham to Hamble Coast Strategy Group (Lead Authority: Chichester District Council), 134pp, 145 tables and figures.
- HRW 2003. Risk Assessment for Flood and Coastal Defence for Strategic Planning: High Level Method - Technical Report. Environment Agency Report Number W5B-030/TR1, HR Wallingford Report SR603.
- HRW 2004a. HR Wallingford - Investigation of extreme flood processes & uncertainty. (IMPACT) EC Research Project no. EVG1-CT2001-00037. See www.impact-project.net.
- HRW 2004b. National Flood Risk Assessment 2004: Supported by the RASP HLM plus: Methodology. HR Wallingford Report SR659.
- HRW 2007. National Flood Risk Assessment for Northern Ireland: Flood Mapping Strategy (Interim) Executive Summary. Report EX5299, Release 5.0, July 2007. . HR Wallingford, authors: P. Sayers and M. Calvert.
<http://www.dardni.gov.uk/riversagency/flood-mapping-strategy-executive-summary-4.pdf>.
- HRW & HPR 1997. East Solent Shoreline Management Plan, Report 3441EX, by HR Wallingford and High-Point Rendel, available online at:
<http://www.havant.gov.uk/Council/Coastal/MainContents.htm>.
- Hu, K. & Wotherspoon, C. 2007. Numerical Modelling in Coastal Flood Forecasting and Warning in England and Wales. *In*: Begum, S., Stive, M. J. F. & Hall, J. W. (eds.). Springer Netherlands.
- Hunter, N. M., Bates, P. D., Horritt, M. S. & Wilson, M. D. 2007. Simple spatially-distributed models for predicting flood inundation: A review. *Geomorphology*, 90, 208-225.
- Hunter, N. M., Bates, P. D., Neelz, S., Pender, G., Villanueva, I., Wright, N. G., Liang, D., Falconer, R. A., Lin, B., Waller, S., Crossley, A. J. & Mason, D. C. 2008. Benchmarking 2D hydraulic models for urban flooding. *Proceedings of the Institution of Civil Engineers Water Management*, 161, 13-30.
- Hunter, N. M., Horritt, M. S., Bates, P. D., Wilson, M. D. & Werner, M. G. F. 2005. An adaptive time step solution for raster-based storage cell modelling of floodplain inundation. *Advances in Water Resources*, 28, 975-991.
- IOWCP. 2008. "Islanders go on Flood Alert" - by Emily Pearce, Monday, March 10, 2008 [Online]. Available: <http://www.iwcp.co.uk/news/islanders-go-on-flood-alert-19593.aspx> [Accessed 7th January, 2013].
- IPCC 2007. Ipcc, Climate Change 2007: Synthesis Report. Contribution of Working Groups I, II and III to the Fourth Assessment Report of the Intergovernmental Panel on Climate Change R. K. Pachauri, A. Reisinger, Eds. (IPCC, 2007; http://www.ipcc.ch/publications_and_data/ar4/syr/en/contents.html), p. 104.
- IRF. 2011. *Multi-Agency Flood Response Plan - v1.1, March 2011* [Online]. Isle of Wight Resilience Forum - report prepared by Isle of Wight Local Authority Emergency Management. Available:
http://www.iwight.com/home/emergency/emergency_planning/images/iwightIRFFloodPlan-v1.1March2011Annex4.pdf [Accessed 11th January 2013].
- Ivica, V. 2006. The role of the fundamental seiche in the Adriatic coastal floods. *Continental Shelf Research*, 26, 206-216.
- Jeslesnianski, C. P., Chen, J. & Shaffer, W. A. 1992. SLOSH: Sea, lake, and overland surges from hurricanes - NOAA Tech. Rep.NWS 48, Silver Spring, MD, 71 pp. [Available

- from Techniques Development Lab-NWS, 1325 East-West Highway, Silver Spring, MD 20910.].
- Jonkman, S., Vrijling, J. & Vrouwenvelder, A. 2008. Methods for the estimation of loss of life due to floods: a literature review and a proposal for a new method. *Natural Hazards*, 46, 353-389.
- Jonkman, S. N., Maaskant, B., Boyd, E. & Levitan, M. L. 2009. Loss of Life Caused by the Flooding of New Orleans After Hurricane Katrina: Analysis of the Relationship Between Flood Characteristics and Mortality. *Risk Analysis*, 29, 676-698.
- Jonkman, S. N. & Penning-Rowsell, E. 2008. Human Instability in Flood Flows. *JAWRA Journal of the American Water Resources Association*, 44, 1208-1218.
- Jonkman, S. N. & Vrijling, J. K. 2008. Loss of life due to floods. *Journal of Flood Risk Management*, 1, 43-56.
- Jude, S., Mokrech, M., Walkden, M., Thomas, J. & Koukoulas, S. 2013. Visualising potential coastal change: communicating results using visualisation techniques. In: Nicholls, R. J., Dawson, R. J. & Day, S. A. (eds.) *Broad Scale Coastal Simulation New Techniques to Understand and Manage Shorelines in the Third Millennium*. Springer.
- Kamphuis, J. W. 2000. *Introduction to coastal engineering and management*, World Scientific.
- Kamrath, P., Disse, M., Hammer, M. & Köngeter, J. 2006. Assessment of Discharge through a Dike Breach and Simulation of Flood Wave Propagation. *Natural Hazards*, 38, 63-78.
- Kanning, W., van Baars, S., van Gelder, P. H. A. J. M. & Vrijling, J. K. 2007. Lessons from New Orleans for the design and maintenance of flood defence systems. In Risk, Reliability and Societal Safety – Aven & Vinnem (eds) © 2007 Taylor & Francis Group, London.
- Kebede, A. 2009. *Assessing Potential Risks of Impacts of Climate Change on Coastal Landfill Sites; a Case Study of Pennington Landfill Site – Hampshire, UK*. MS.c, University of Southampton.
- Kolen, B., Slomp, R., van Balen, W., Terpstra, T., Bottema, M. & Nieuwenhuis, S. 2010. Learning from French experiences with storm Xynthia – damages after a flood. © HKV LIJN IN WATER and Rijkswaterstaat, Waterdienst.
- Kortenhaus, A. & Kaiser, G. 2009. Lessons learned from flood risk analyses at the North Sea coast. *Journal of Coastal Research, Special Issue 56*, 822-826.
- Krzhizhanovskaya, V. V., Shirshov, G. S., Melnikova, N. B., Belleman, R. G., Rusadi, F. I., Broekhuijsen, B. J., Gouldby, B. P., Lhomme, J., Balis, B., Bubak, M., Pyayt, A. L., Mokhov, I. I., Ozhigin, A. V., Lang, B. & Meijer, R. J. 2011. Flood early warning system: design, implementation and computational modules. *Procedia Computer Science*, 4, 106-115.
- Lamb, H. 1991. *Historic storms of the North Sea, British Isles and Northwest Europe*, Cambridge, Cambridge University Press.
- Landform. Coastal flood risk – from storm surge and waves to inundation. Report of a workshop organised by the Flood Risk Management Consortium and LANDFORM. Speakers: C. Wilson, N. Chini, M. McCabe, A. Borthwick; Chairman: P. Stansby. Landform event: E11501, 26th May 2011 2011 CIRIA, Classic House, 174-180 Old Street, London.
- Lane, A., Hu, K., Hedges, T. S. & Reis, M. T. 2008. New north east of England tidal flood forecasting system. *FLOODrisk 2008*. Keble College, Oxford, UK.
- Law, C. R. 1975. Storm surges in the English Channel. *Hydrogr J*, 2, 30-34.
- Le Blancq, F. W. & Searson, J. 2008. Effects of the 10 March 2008 storm surge on defences in the Channel Islands - unpublished report. Jersey Meteorological Department.
- Le Pard, G. 1999. The Great Storm of 1824. *Proceedings of Dorset Natural History and Archaeological Society*, 121, 23-36.

- Levasseur, A., Shi, L., Wells, N. C., Purdie, D. A. & Kelly-Gerreyn, B. A. 2007. A three-dimensional hydrodynamic model of estuarine circulation with an application to Southampton Water, UK. *Estuarine, Coastal and Shelf Science*, 73, 753-767.
- Lewis, J. 1979. Vulnerability to a natural hazard: geomorphic, technological and social change at Chiswell, Dorset. Working Paper 37. In: Centre for Development Studies, S. o. H. a. S. S., University of Bath (ed.).
- Lichter, M., Vafeidis, A. T., Nicholls, R. J. & Kaiser, G. 2010. Exploring Data-Related Uncertainties in Analyses of Land Area and Population in the “Low-Elevation Coastal Zone” (LECZ). *Journal of Coastal Research*, 757-768.
- Lionello, P., Sanna, A., Elvini, E. & Mufato, R. 2006. A data assimilation procedure for operational prediction of storm surge in the northern Adriatic Sea. *Continental Shelf Research*, 26, 539-553.
- Liu, X. 2008. Airborne LiDAR for DEM generation: some critical issues. *Progress in Physical Geography*, 32, 31-49.
- Longuet-Higgins, M. S. & Stewart, R. w. 1964. Radiation stresses in water waves; a physical discussion, with applications. *Deep Sea Research and Oceanographic Abstracts*, 11, 529-562.
- Lowe, J. A., Howard, T., Pardaens, A., Tinker, J., Holt, J., Wakelin, S., Glenn, M., Leake, J., Wolf, J., Horsburgh, K., Reeder, T., Jenkins, G., Ridley, J., Dye, S. & Bradley, S. 2009. UK Climate Projections Science Report: Marine and Coastal Projections. Exeter, UK: Met Office Hadley Centre.
- Lumbroso, D. M. & Vinet, F. 2011. A comparison of the causes, effects and aftermaths of the coastal flooding of England in 1953 and France in 2010. *Nat. Hazards Earth Syst. Sci.*, 11, 2321-2333.
- Madrell, R. J., Reeve, D. E. & Heaton, C. R. 1998. Establishing coastal flood risks from single storms and the distribution of the risk of structural failure. *Proc. Coastlines, Structures and Breakwaters*. London, UK: Thomas Telford.
- Mahajan, R. 2010. Critical incident reporting and learning. *British journal of anaesthesia*, 105, 69-75.
- Mail. 2008. *Britain braced for new storm front as forecasters warn 'the worst is yet to come'* [Online]. The Daily Mail. Available: <http://www.dailymail.co.uk/news/article-528769/Britain-braced-new-storm-forecasters-warn-worst-come.html> [Accessed 26th January 2012].
- Mailier, P. J., Stephenson, D. B., Ferro, C. A. T. & Hodges, K. I. 2006. Serial clustering of extratropical cyclones. *Monthly weather review*, 134, 2224-2240.
- Marks, K. & Bates, P. 2000. Integration of high-resolution topographic data with floodplain flow models. *Hydrological Processes*, 14, 2109-2122.
- Marshman, S. 2010. *Sensitivity Testing the Effect of Breach Representation on Two Contrasting Coastal Floodplain*. MS.c, University of Southampton.
- Martin, D. J. 1994. The Impact of Conservation Issues on a Sea-Defence Scheme at Pennington. *Water and Environment Journal*, 8, 567-575.
- Mason, D. C., Davenport, I. J., Neal, J. C., Schumann, G. J. P. & Bates, P. D. 2012. Near Real-Time Flood Detection in Urban and Rural Areas Using High-Resolution Synthetic Aperture Radar Images. *Geoscience and Remote Sensing, IEEE Transactions on*, 50, 3041-3052.
- Mason, T., Bradbury, A., Poate, T. & Newman, R. 2009. Nearshore wave climate of the English Channel—evidence for bi-modal seas. In: World Scientific, S. (ed.) *31st International Conference on Coastal Engineering*. Hamburg: World Scientific, Singapore.
- Masselink, G. & Hughes, M. G. 2003. *Introduction to coastal processes and geomorphology*, Hodder Arnold.

- McCallum, E. & Heming, J. 2006. Hurricane Katrina: an environmental perspective. *Philosophical Transactions of the Royal Society A: Mathematical, Physical and Engineering Sciences*, 364, 2099-2115.
- McGranahan, G., Balk, D. & Anderson, B. 2007. The rising tide: assessing the risks of climate change and human settlements in low elevation coastal zones. *Environment and Urbanization*, 19, 17-37.
- McMillan, A., Batstone, C., Worth, D., Tawn, J. A., Horsburgh, K. & Lawless, M. 2011. Coastal flood boundary conditions for UK mainland and islands. Project: SC060064/TR2: Design sea levels.: Published by: Environment Agency, Bristol, UK.
- McRobie, A., Spencer, T. & Gerritsen, H. 2005. The Big Flood: North Sea storm surge. *Philosophical Transactions of the Royal Society A: Mathematical, Physical and Engineering Sciences*, 363, 1263-1270.
- Melchers, R. E. 1999. *Structural reliability analysis and prediction*, John Wiley & Son Ltd.
- Menéndez, M. & Woodworth, P. L. 2010. Changes in extreme high water levels based on a quasi-global tide-gauge data set. *J. Geophys. Res.*, 115, C10011.
- Merz, B., Thielen, A. H. & Gocht, M. 2007. Flood Risk Mapping At The Local Scale: Concepts and Challenges
Flood Risk Management in Europe. In: Begum, S., Stive, M. J. F. & Hall, J. W. (eds.). Springer Netherlands.
- Messner, F., Penning-Rowsell, E., Green, C., Mayer, V., Tunstall, S. M., van der Veen, A., Tapsell, S., Wilson, T., Krywkow, J., Logtmeijer, C., Fernandez-Bilbao, A., Geurts, P., Haase, D. & Parker, D. 2007. Evaluating flood damages: guidance and recommendations on principles and methods, Floodsite report number: T09-06-01.
- Millin, S. 2010. UKCP09 sea level change estimates, DECEMBER 2010. Available at: <http://www.ukcip.org.uk/resources/ukcp09/>.
- Möller, I. & Spencer, T. 2002. Wave dissipation over macro-tidal saltmarshes: Effects of marsh edge typology and vegetation change. Special issue 36. *Journal of Coastal Research*, 506-521.
- Morris, M., Hanson, G. & Hassan, M. 2008. Improving the accuracy of breach modelling: why are we not progressing faster? *Journal of Flood Risk Management*, 1, 150-161.
- Mott MacDonald & EA 2010. Northern Area Tidal Modelling - Volume 3: Overtopping Flood Mapping. Consultancy Report produced by Mott MacDonald Ltd for the Environment Agency.
- Motyka, J. M. & Brampton, A. H. 1993. Coastal management: mapping of littoral cells, HR Wallingford Report SR328.
- Muir-Wood, R. & Grossi, P. 2006. Hurricane Katrina: Profile of a Super Cat: Lessons and Implications for Catastrophe Risk Management.: Risk Management Solutions (RMS). Available online: http://www.rms.com/publications/katrinareport_lessonsandimplications.pdf [accessed: 18th May 2012].
- Muir Wood, R. & Bateman, W. 2005. Uncertainties and constraints on breaching and their implications for flood loss estimation. *Philosophical Transactions of the Royal Society A: Mathematical, Physical and Engineering Sciences*, 363, 1423-1430.
- Muir Wood, R., Drayton, M., Berger, A., Burgess, P. & Wright, T. 2005. Catastrophe loss modelling of storm-surge flood risk in eastern England. *Philosophical Transactions of the Royal Society A: Mathematical, Physical and Engineering Sciences*, 363, 1407-1422.
- Myatt, L. B., Scrimshaw, M. D. & Lester, J. N. 2003. Public perceptions and attitudes towards a forthcoming managed realignment scheme: Freiston Shore, Lincolnshire, UK. *Ocean & Coastal Management*, 46, 565-582.

- Narayan, S., Hanson, S., Nicholls, R. J., Clarke, D., Willems, P., Ntegaka, V. & Monbaliu, J. 2012. A Holistic Assessment of Coastal Flood Systems Using System Diagrams and the Source – Pathway – Receptor (SPR) Concept *Journal of Natural Hazards and Earth System Sciences* - in press.
- Naulin, M., Kortenhaus, A. & Oumeraci, H. 2011. Reliability Analysis and Breach Modelling of Coastal and Estuarine Flood Defences. ISGSR 2011 - Vogt, Schuppener, Straub & Bräu (eds) - © 2011 Bundesanstalt für Wasserbau ISBN 978-3-939230-01-4.
- Neal, J., Fewtrell, T. & Trigg, M. 2009. Parallelisation of storage cell flood models using OpenMP. *Environmental Modelling & Software*, 24, 872-877.
- Néelz, S., Pender, G., Bates, P., Falconer, R., Lin, B. & Wright, N. G. 2009. Desktop review of 2D hydraulic modelling packages. Science Report: SC080035. Environment Agency, UK.
- NFDC 2004. Western Solent Coastal Defence Strategy Study: Technical Annex - Condition Assessment & Standard of Service Assessment of Coastal Defences. Report prepared by Andrew Colenutt for New Forest District Council.
- NFDC 2009. Cabinet 06/07/09 Report A: North Solent Shoreline Management Plan. New Forest District Council, available online: <http://www.newforest.gov.uk/committeedocs/cab/CDR05054.pdf> [accessed 15 Dec 2011].
- NFDC 2010. North Solent Shoreline Management Plan, Appendix C Baseline Process Understanding, C.1 ASSESSMENT OF SHORELINE DYNAMICS. New Forest District Council, UK. Available at: http://www.newforest.gov.uk/media/adobe/o/s/C1_Coastal_Processes_Literature_Review_%28final_draft%29.pdf [accessed: 30th June 2011].
- Nicholls, R. 1985. *The stability of the shingle beaches in the eastern half of Christchurch Bay*, Ph.D thesis .University of Southampton.
- Nicholls, R. 2010. Impacts of and responses to sea-level rise. In: J.A.Church, P. L. W., T. Aarup, and W.W. Wilson (ed.) *Understanding Sea-Level Rise and Variability*. Wiley-Blackwell.
- Nicholls, R. J. 2011. Planning for the impacts of sea level rise. *Oceanography*, 24, 142-155.
- Nicholls, R. J. & Cazenave, A. 2010. Sea-level rise and its impact on coastal zones. *science*, 328, 1517-1520.
- Nicholls, R. J., Hoozemans, F. M. J. & Marchand, M. 1999. Increasing flood risk and wetland losses due to global sea-level rise: regional and global analyses. *Global Environmental Change*, 9, S69-S87.
- Nicholls, R. J., Mockrech, M., Richards, J., Bates, P. D., Dawson, R., Hall, J., Walkden, M., Dickson, M., Jordan, A. & Milligan, J. 2005. Assessing coastal flood risk at specific sites and regional scales: Regional assessment of coastal flood risk. Technical report No 45. October 2005, from project T2.46.
- Nicholls, R. J. & Webber, N. B. 1987. The past, present and future evolution of Hurst Castle spit, Hampshire. *Progress In Oceanography*, 18, 119-137.
- Nott, J. & Hayne, M. 2000. How high was the storm surge from Tropical Cyclone Mahina? North Queensland, 1899. *Australian Journal of Emergency Management*, 11-13.
- NRA 1990. Lymington/Pennington flood investigation – interim report. Environment Agency report reference number: IMP/SCH/008/5054. Report produced for National Rivers Authority Southern Region by Southern Projects Ltd.
- O'Connell, N. 2000. Final Report of Flood event - 24th December to 26th December 1999. Environment Agency Southern Region, Hants & IoW Area.
- Ohl, C. A. & Tapsell, S. 2000. Flooding and human health. *BMJ*, 321, 1167-1168.
- OS. 2001. *Ordnance Survey Land-Form PROFILE™ User guide. v4.0 – 5/2001* © Crown copyright. www.ordnancesurvey.co.uk [Online]. [Accessed 3rd July 2011].

- OS 2012a. ADDRESS-POINT® Vector Data (locates residential, business and public postal addresses in Great Britain - created by matching information from digital map databases with more than 27 million addresses recorded in the Royal Mail® Postcode Address File (PAF®). *In*: Survey, O. (ed.). Ordnance Survey.
- OS 2012b. Code-Point Polygons - which represent postcode unit boundaries in Great Britain; obtained from the Edina Digimap service (<http://edina.ac.uk/digimap/>). *In*: Survey, O. (ed.). Ordnance Survey / Edina.
- Owen, M. W. 1980. Design of seawalls allowing for wave overtopping. HR Wallingford, Report EX 924.
- Palmer, H. R. 1831. Description of graphical register of tides and winds. *Philosophical Transactions of the Royal Society London*, 121, 209-213.
- Palmer, T. 2010. *Energetic Swell Waves in the English Channel*. Ph.D, University of Southampton.
- Pappenberger, F. & Beven, K. J. 2006. Ignorance is bliss: Or seven reasons not to use uncertainty analysis. *Water Resour. Res.*, 42, W05302.
- PCC 2004. Portsmouth City Local Plan, First Review 2001 – 2011. Supplementary Planning Guidance: Flood protection. Approved by the Executive Member for Planning, Regeneration, Economic Development and Property 6th February 2004. . Portsmouth City Council, UK. Available at: http://www.portsmouth.gov.uk/media/Flood_Protection_SPG.pdf [accessed 26th August 2009].
- PCC 2008. Flooding in Portsmouth; list of flood incidents. Unpublished report provided by Portsmouth City Council.
- PCC 2009. Portsea Island Coastal Strategy Study - Strategy approval report. CPA Project Code: KY09. February 2009.: Portsmouth City Council; report available online: <http://www.portsmouth.gov.uk/media/cab20090703r10app3.pdf> [accessed 28 April 2012].
- PCC & Halcrow 2008. Portsea Island Coastal Strategy Study, Strategic Environmental Assessment, Environmental Report by Halcrow Group Limited for Portsmouth City Council. Final draft - June 2008. Available online at: http://www.havant.gov.uk/PDF/5.1_PICSS-Strategic-Environmental-Assessment-Report_June-2008_FINAL.pdf.
- Pearce, J., Khan, S. & Lewis, P. 2011. Medmerry managed realignment - sustainable coastal management to gain multiple benefits. *ICE Coastal Management. Innovative Coastal Zone Management: Sustainable Engineering for a Dynamic Coast. Belfast, UK*.
- Penning-Rowsell, E., Johnson, C., Tunstall, S., Tapsell, S., Morris, J., Chatterton, J., Coker, A. & Green, C. 2003. The Benefits of flood and coastal defence: techniques and data for 2003. Flood Hazard Research Centre, Middlesex University.
- Penning-Rowsell, E., Johnson, C., Tunstall, S., Tapsell, S., Morris, J., Chatterton, J., Green, C., Wilson, T., Koussela, K. & Fernandez-Bilbao, A. 2005. *The benefits of flood and coastal risk management: a manual of assessment techniques*, Middlesex University Press: London.
- Pickering, M., Wells, N., Horsburgh, K. & Green, J. 2012. The impact of future sea-level rise on the European Shelf tides. *Continental Shelf Research*, 35, 1-15.
- Pielke, R. A., Gratz, J., Landsea, C. W., Collins, D., Saunders, M. A. & Musulin, R. 2008. Normalized Hurricane Damages in the United States: 1900-2005. *Natural Hazards Review*, 9, 29-42.
- Pineau-Guillou, L., Lathuiliere, C., Magne, R., Louazel, S., Corman, D. & Perherin, C. 2012. Sea levels analysis and surge modelling during storm Xynthia. *European Journal of Environmental and Civil Engineering*, 1-10.
- Pitt, M. 2008. *Learning lessons from the 2007 floods*, Pitt Review.

- Pomeroy, S. 2012. *Pomeroy's of Portsmouth (Britain's Island City) - Weather and Natural Phenomena* [Online]. Website on local history by Stephen Pomeroy. Available: <http://homepage.ntlworld.com/stephen.pomeroy/local/weather.pdf> [Accessed 18th January 2013].
- Posner, R. 2004. Wyre Flood and Coastal Defence Strategy Plan, March 2004, report produced by Wyre Borough Council.
- Powell, K. A. 1990. Predicting the short term profile response for shingle beaches, Hydraulics Research report SR219, Wallingford.
- Price, T. 2013. *RE: Photos of wave overtopping taken near Dinosaur Island, Isle of Wight by Trevor Price, 10th March 2008.*
- Proctor, R. & Flather, R. 1989. Storm surge prediction in the Bristol Channel—the floods of 13 December 1981. *Continental Shelf Research*, 9, 889-918.
- Proudman, J. 1953. *Dynamical oceanography*. London: Methuen.
- Pugh, D. T. 1987. *Tides, surges and mean sea-level. A handbook for engineers and scientists*, Wiley, Chichester.
- Pullen, T., Allsop, N. W. H., Bruce, T., Kortenhaus, A., Schüttrumpf, H. & Van der Meer, J. W. 2007. EurOtop, Wave Overtopping of Sea Defences and Related Structures — Assessment Manual. Funded in the UK by the Environmental Agency, in Germany by the German Coastal Engineering Research Council (KFKI), in the Netherlands by Rijkswaterstaat and Netherlands Expertise Network (ENW) on Flood Protection: www.overtopping-manual.com.
- Pullen, T., Allsop, W., Bruce, T. & Pearson, J. 2009. Field and laboratory measurements of mean overtopping discharges and spatial distributions at vertical seawalls. *Coastal Engineering*, 56, 121-140.
- Purvis, M. J., Bates, P. D. & Hayes, C. M. 2008. A probabilistic methodology to estimate future coastal flood risk due to sea level rise. *Coastal Engineering*, 55, 1062-1073.
- Pyayt, A. L., Mokhov, I. I., Kozionov, A., Kusherbaeva, V., Melnikova, N. B., Krzhizhanovskaya, V. V. & Meijer, R. J. Artificial intelligence and finite element modelling for monitoring flood defence structures. Environmental Energy and Structural Monitoring Systems (EESMS), 2011 IEEE Workshop on, 28-28 Sept. 2011 2011. 1-7.
- Quinn, N., Atkinson, P. & Wells, N. C. 2012. Modelling of Tide and Surge Elevations in the Solent and Surrounding Waters: The Importance of Tide-Surge Interactions. *Estuarine, Coastal and Shelf Science*, Accepted journal article: 20th July 2012.
- Ray, J., Coulling, E., Evans, S. Y. & Spink, K. 2011. Developing a Practical Tool for Coastal Flood Forecasting and Warning. *ICE Coastal Management. Innovative Coastal Zone Management: Sustainable Engineering for a Dynamic Coast*. Belfast, UK.
- Reeve, D. E. & Burgess, K. A. 1993. A method for the assesment of coastal flood risk. *IMA Journal of Management Mathematics*, 5, 197-209.
- Reeve, D. E., Li, Y., Larson, M., Hanson, H., Donelly, C., Jimenez, J., Mendoza, E. T., Zech, Y., Soares Frazao, S., Bettess, R., Stripling, S. & Brampton, A. 2009. Predicting morphological changes in rivers, estuaries and coasts: executive summary. Floodsite report no. T05-07-03. Task Leader: University of Plymouth, Co-ordinator: HR Wallingford.
- Reis, M. T., Hu, K., Hedges, T. S. & Mase, H. 2008. A Comparison of Empirical, Semiempirical, and Numerical Wave Overtopping Models. *Journal of Coastal Research*, 250-262.
- Rennie, A. & Hansom, J. 2011. Sea level trend reversal: Land uplift outpaced by sea level rise on Scotland's coast. *Geomorphology*, 125, 193-202.
- RIBA & ICE 2009. Facing up to rising sea-levels: retreat? defend? attack? The future of our coastal and estuarine cities. *Royal Institute for British Architects, London, UK &*

- Institute of Civil Engineers,*
http://www.buildingfutures.org.uk/assets/downloads/Facing_Up_To_Rising_Sea_Level_s.pdf [accessed January, 2010].
- RMS 2003a. 1953 UK floods: 50 year retrospective. Risk Management Solutions.
- RMS 2003b. December 1703 Windstorm, 300-year retrospective, Risk Management Solutions Report.
- RMS 2007. 1607 Bristol Channel Floods: 400-year retrospective. Risk Management Solutions Report. http://rms.com/Publications/1607_Bristol_Flood.pdf.
- Rohling, E. J., Grant, K., Hemleben, C., Siddall, M., Hoogakker, B. A. A., Bolshaw, M. & Kucera, M. 2008. High rates of sea-level rise during the last interglacial period. *Nature Geosci*, 1, 38-42.
- Rouse, H. & Ince, S. 1963. *History of Hydraulics*, Dover Publications, Inc. New York, 138 pp.
- Ruocco, A. 2009. *Reconstructing coastal flood occurrence in the Solent since 1935 using historical data*. MSc Integrated Environmental Studies MSc, University of Southampton.
- Ruocco, A., Nicholls, R.J., Haigh, I.D., & Wadey, M.P. 2011. Reconstructing coastal flood occurrence combining sea level and media sources: a case study of the Solent, UK since 1935. *Natural Hazards*, 59, 1773-1796.
- Sayers, P., Hall, J., Dawson, R., Rosu, C., Chatterton, J. & Deakin, R. 2002. Risk assessment of flood and coastal defences for strategic planning (RASP) – a high level methodology. Paper presented at Conference of Coastal and River Engineers, Dep. for Environ., Food and Rural Affairs, Keele, U. K.
- SCC 2010. Southampton City Council strategic flood risk assessment: volume 2 technical appendices - final version. Report prepared by Capita Symonds. Available online: http://www.southampton.gov.uk/Images/Southampton%20SFRA%20Level%202%20Volume%202%20CSL%20August2010_tcm46-270925.pdf.
- SCC 2011. Southampton Multi Agency Flood Response Plan, Version 4.0, available online: http://www.southampton.gov.uk/Images/Southampton%20Multi-Agency%20Flood%20Response%20Plan_tcm46-303085.pdf.
- Schumann, G. J. P., Neal, J. C., Mason, D. C. & Bates, P. D. 2011. The accuracy of sequential aerial photography and SAR data for observing urban flood dynamics, a case study of the UK summer 2007 floods. *Remote Sensing of Environment*, 115, 2536-2546.
- Schüttrumpf, H. & Oumeraci, H. 2005. Layer thicknesses and velocities of wave overtopping flow at seadikes. *Coastal Engineering*, 52, 473-495.
- SCOPAC. 2004. *SCOPAC (Standing Conference on Problems Associated with the Coastline) Sediment Transport Study, prepared by RACER (River and Coastal Environments Research) in the Department of Geography at the University of Portsmouth, mainly compiled by David Carter and written by Dr Malcolm Bray*. [Online]. Available: <http://stream.port.ac.uk/environment/scopac5/index.htm> [Accessed during 2008-2012].
- Scotto, M. G., Alonso, A. M. & Barbosa, S. M. 2009. Clustering time series of sea levels: Extreme value approach. *Journal of waterway, port, coastal, and ocean engineering*, 136, 215-225.
- SDE. 2008. "More gales on the way" - Newspaper article on 11 March 2008. *The Southern Daily Echo (Southampton)*.
- SEPA 2011. National Flood Risk Assessment. Scottish Environment Protection Agency, available at http://www.sepa.org.uk/flooding/flood_risk_management/national_flood_risk_assessment.aspx.
- Shackleton, E. C., Potts, J., Carter, D. & Ballinger, R. 2007. Residents' perceptions of coastal flood risk and its management through Coastal Defence Strategies at Emsworth, United Kingdom. *La Houille Blanche*, 62, 66.

- Shennan, I. & Horton, B. 2002. Holocene land- and sea-level changes in Great Britain. *Journal of Quaternary Science*, 17, 511-526.
- Sherwood, S. & Backhouse, T. 2012. "Flooding in Broad Street, Old Portsmouth", article adapted from research by Cynthia Sherwood on "History in Portsmouth". Part of the INPORTSMOUTH group of sites; designed and sponsored by Community Internet Services Copyright © 2007 - 2012 - Tim Backhouse. [Online]. Available: <http://www.history.inportsmouth.co.uk/events/broad-street-floods.htm> 2012].
- Smith, P., Beven, K. & Horsburgh, K. 2012a. Data-based mechanistic modelling of tidally affected river reaches for flood warning purposes: an example on the River Dee, UK. *Quarterly Journal of the Royal Meteorological Society*.
- Smith, R. A. E., Bates, P. D. & Hayes, C. 2012b. Evaluation of a coastal flood inundation model using hard and soft data. *Environmental Modelling & Software*, 30, 35-46.
- Stanczak, G. 2008. *Breaching of sea dikes initiated from the seaside by breaking wave impacts*. Ph.D, University of Braunschweig - Institute of Technology & the University of Florence.
- Stansby, P., Wilson, C., Chini, N., McCabe, M. & Borthwick, A. 2011. Coastal flood risk – from storm surge and waves to inundation Report of a workshop organised by the Flood Risk Management Research Consortium and LANDFORM held at CIRIA, Classic House, 174-180 Old Street, London on 26th May 2011. Available at: <http://www.ciria.com/landform/pdf/Final%20Report%20LANDFORM%20Event%206%20May%202011.pdf>.
- Stripling, S., Bradbury, A. P., Cope, S. N. & Brampton, A. H. 2008. Understanding Barrier Beaches. R&D Technical Report FD1925/TR. Published by the Joint Defra/EA Flood and Coastal Erosion Risk Management R&D Programme. Available from: <http://sciencesearch.defra.gov.uk>.
- Syme, W. J. 2008. Flooding in Urban Areas - 2D Modelling Approaches for Buildings and Fences. *Engineers Australia, 9th National Conference on Hydraulics in Water Engineering*. Darwin Convention Centre, Australia.
- Syvitski, J. P. M., Kettner, A. J., Overeem, I., Hutton, E. W. H., Hannon, M. T., Brakenridge, G. R., Day, J., Vörösmarty, C., Saito, Y. & Giosan, L. 2009. Sinking deltas due to human activities. *Nature Geoscience*, 2, 681-686.
- TAW 2002. Technical Report – Wave run-up and wave overtopping at dikes. Technical Advisory Committee for Flood Defence in the Netherlands (TAW). Delft. 2002.
- Tawn, J. A. 1992. Estimating probabilities of extreme sea levels. *Applied statistics*, 41, 77-93.
- Terzaghi, K. & Peck, R. B. 1967. *Soil Mechanics in Engineering Practice*, New York, John Wiley & Sons.
- Thompson, K., Bernier, N. & Chan, P. 2009. Extreme sea levels, coastal flooding and climate change with a focus on Atlantic Canada. *Natural Hazards*, 51, 139-150.
- TN 2008a. "At mercy of the storm" (article in 'The News' - Portsmouth's local Newspaper - about flooding on 10 March 2008). 'The News' (Portsmouth's local Newspaper) Published on Tuesday 11 March 2008 09:12, online: <http://www.portsmouth.co.uk/news/local/at-mercy-of-the-storm-1-1292138> [last accessed: 28th April 2012].
- TN. 2008b. "Storm map: Where the damage was done" - flooding on 10 March 2008 [Online]. The News (Portsmouth's local Newspaper). Available: <http://www.portsmouth.co.uk/news/local/storm-map-where-the-damage-was-done-1-1292067> [Accessed 7th January 2013].
- Tompkins, E. L., Few, R. & Brown, K. 2008. Scenario-based stakeholder engagement: Incorporating stakeholders preferences into coastal planning for climate change. *Journal of Environmental Management*, 88, 1580-1592.

- Townend, I. 2008. A conceptual model of Southampton Water, ABPmer report 21/05/2008, V1.0 produced with EA and DEFRA, available at http://www.estuary-guide.net/pdfs/southampton_water_case_study.pdf.
- Tribbia, J. & Moser, S. C. 2008. More than information: what coastal managers need to plan for climate change. *Environmental Science & Policy*, 11, 315-328.
- Tsubaki, R. & Kawahara, Y. 2012. The Categorisation of Inundation Flow Over Complex Topography. *XIX International Conference on Water Resources, CMWR 2012*. University of Illinois at Urbana-Champaign, June 17-22, 2012.
- Twigger-Ross, C., Fernández-Bilbao, A., Tapsell, S., Walker, G., Watson, N., Rose, C., Dade, P., Deeming, H. & Kashefi, E. 2009. Improving flood warnings: Final report: Improving Institutional and Social Responses to Flooding. Science Report: SC060019 - Work Package 1a, Report produced by Defra and the Environment Agency, ISBN: 978-1-84911-058-7. DEFRA, London.
- UNEP, U. N. E. P. 2002. GEO: Global Environment Outlook 3: Past, Present and Future Perspectives.
- URS 2012. Southampton Coastal Flood and Erosion Risk Management Strategy. Main Document. Prepared for: Southampton City Council, Ref: EC09/01/1673MD.
- Van Heerden, I. L. 2007. The Failure of the New Orleans Levee System Following Hurricane Katrina and the Pathway Forward. *Public Administration Review*, 67, 24-35.
- Vanderkimpfen, P., Peeters, P. & Van der Biest, K. Optimization of 2D flood models by semi-automated incorporation of flood diverting landscape elements. In: Flood risk management and practice, S. e. a. e., ed., 2008. Taylor & Francis Group, London.
- VanKoningsveld, M., Mulder, J. P. M., Stive, M. J. F., VanDerValk, L. & VanDerWeck, A. W. 2008. Living with Sea-Level Rise and Climate Change: A Case Study of the Netherlands. *Journal of Coastal Research*, 367-379.
- Verlaan, M., Zijderfeld, A., de Vries, H. & Kroos, J. 2005. Operational storm surge forecasting in the Netherlands: developments in the last decade. *Philosophical Transactions of the Royal Society A: Mathematical, Physical and Engineering Sciences*, 363, 1441-1453.
- Villarini, G., Smith, J. A., Vitolo, R. & Stephenson, D. B. 2012. On the temporal clustering of US floods and its relationship to climate teleconnection patterns. *International Journal of Climatology*.
- Visser, P. J. 1998. Breach growth in sand defences. Communication on hydraulic and geotechnical engineering, TU Delft Report no. 98-91.
- von Storch, H. & Woth, K. 2006. Storm surges – the case of Hamburg, Germany. ESSP OSC panel session on “GEC, natural disasters, and their implications for human security in coastal urban areas”. Available online: <http://www.safecoast.nl/editor/databank/File/hamburg-storms.pdf> [accessed 26th January 2012].
- von Storch, H. & Woth, K. 2008. Storm surges: perspectives and options. *Sustainability Science*, 3, 33-43.
- Vorogushyn, S., Merz, B. & Apel, H. 2009. Development of dike fragility curves for piping and micro-instability breach mechanisms. *Nat. Hazards Earth Syst. Sci.*, 9, 1383-1401.
- Vrouwenvelder, A. C. W. M., Steenbergen, H. M. G. M. & Slijkhuis, K. A. H. 2001. Theoretical manual of PC-Ring, Part B: statistical models (in Dutch), Nr. 98-CON-R1431, Delft.
- Wadey, M., Nicholls, R. & Hutton, C. 2011. Threat of coastal inundation in the Solent: real-time forecasting. *ICE Coastal Management. Innovative Coastal Zone Management: Sustainable Engineering for a Dynamic Coast*. Belfast, UK.
- Wadey, M. P., Nicholls, R. J. & Haigh, I. 2013. Understanding a coastal flood event: the 10th March 2008 storm surge event in the Solent, UK. *Natural Hazards*, 1-26.

- Wadey, M. P., Nicholls, R. J. & Hutton, C. 2012. Coastal Flooding in the Solent: An Integrated Analysis of Defences and Inundation. *Water*, 4, 430-459.
- Wahl, T. L. 2004. Uncertainty of Predictions of Embankment Dam Breach Parameters. *J. Hydraul. Eng.*, 130, 389-397.
- Wahl, T., Jensen, J., Frank, T. & Haigh, I. 2011. Improved estimates of mean sea level changes in the German Bight over the last 166 years. *Ocean Dynamics*, 61, 701-715.
- Wahl, T., Muddersbach, C. & Jensen, J. 2012. Assessing the hydrodynamic boundary conditions for risk analyses in coastal areas: a multivariate statistical approach based on Copula functions. *Nat. Hazards Earth Syst. Sci.*, 12, 495–510.
- Wearmouth, M. 2012. *Present and future frequency of flooding on the coastal road between Gurnard and Cowes, Isle of Wight*. Unpublished MSc Thesis, University of Southampton.
- Webster, T. L., Forbes, D. L., MacKinnon, E. & Roberts, D. 2006. Flood-risk mapping for storm-surge events and sea-level rise using lidar for southeast New Brunswick. *Can. J. Remote Sensing*, 32, 194-211.
- Wells, N. C., D.J. B., Wang, J. Y. & Collins, M. B. 2001. Modelling of extreme storm surge events in the English Channel for the period 14–18 December 1989. *Glob Atmos Ocean Syst*, 7, 275-294.
- West, D. 2008. Special report on sea surge at bosham 10th march 2008, by David West, Bosham Parish Council Water Bailiff 12th March 2008.
- West, I. M. 2010. *Hurst Spit, Barrier Beach of the West Solent, Hampshire: geology of the Wessex Coast* [Online]. Available: <http://www.soton.ac.uk/~imw/Hurst-Castle-Spit.htm#Hurst-Spit-Erosion-History> [Accessed 27 June 2010].
- Whittingham, H. E. 1958. The Bathurst Bay hurricane and associated storm surge. *Australian Meteorological Magazine*, 23, 14-16.
- Wolf, J. 2009. Coastal flooding: impacts of coupled wave–surge–tide models. *Natural Hazards*, 49, 241-260.
- Wolf, J. & Flather, R. A. 2005. Modelling waves and surges during the 1953 storm. *Philosophical Transactions of the Royal Society A: Mathematical, Physical and Engineering Sciences*, 363, 1359-1375.
- Woodworth, P. L., Rickards, L. J. & Pérez, B. 2009. A survey of European sea level infrastructure. *Nat. Hazards Earth Syst. Sci.*, 9, 927-934.
- WVCA 2011. Flood Emergency Plan. Wallington Village Community Association; report available at: http://www.wvca.co.uk/sites/default/files/Emergency_Flood_Plan_2011.pdf [last accessed: 7th January 2013].
- Xharde, R., Long, B. & Forbes, D. 2006. Accuracy and Limitations of Airborne LiDAR Surveys in Coastal Environment, Print ISBN: 0-7803-9510-7. *Geoscience and Remote Sensing Symposium, 2006. IGARSS 2006. IEEE International Conference*. Denver, CO, USA.
- YCDWG 2010. Adapting to coastal flooding in the Yarmouth area in the 21st century - a report by Yarmouth Coastal Defence Working Group, December 2010.
- Zhang, K., Xiao, C. & Shen, J. 2008. Comparison of the CEST and SLOSH Models for Storm Surge Flooding. *Journal of Coastal Research*, 489-499.
- Zong, Y. & Tooley, M. J. 2003. A historical record of coastal floods in Britain: frequencies and associated storm tracks. *Natural hazards*, 29, 13-36.
- Zou, C. & Reeve, D. E. 2009. Modelling water from clouds to coast. NERC. Available online: <http://planetearth.nerc.ac.uk/features/story.aspx?id=524> [accessed: 7th May, 2012].

Appendices

Appendix A – Additional information of case study datasets

Table A1. Return period data for waves at Portsmouth. The source of this data is from analysis generated for the first shoreline management plan in this region (HRW and HPR, 1997) unless stated otherwise. Where shown, ranges in values reflect shoreline variations in fetch or wave exposure. For example, on the Portsmouth open coast, wave height increases from west to east (a linear spatial interpolation was applied to generate boundary conditions for the coastal flood modelling).

Waves at Portsmouth	Largest measured H_s (m)	Return period and H_s (m)				Approximated fetch-limited conditions	
		1	10	50	100	H_s	T_p
West open coast (Old Portsmouth – Southsea)	N/A	1.2	1.4	1.5	-	1.5 – 1.6	2.7 – 2.9
East open coast (Southsea – Eastney)		1.2 – 2.1	1.4 – 2.4	1.5 – 2.6	-	1.5 – 2.7	10
Langstone Harbour	0.8 m (SCOPAC, 2004)	-	-	1.1 m at Anchorage Park (HRW, 1995) 1.2 m for areas exposed to south & southwest	-	1.3 – 1.75	3.5 – 4.0
Portsmouth Harbour <i>Most extreme conditions</i>	N/A	-	-	1.1 m	1.9 m (HRW, 1995)	1.1 – 1.9	2.8 – 3.0

Table A2. Wave calculations by Kebede (2009) for the Pennington flood open coast compartment

Wind direction	Fetch (km)	Return period (years)					
		5		10		50	
		H_s (m)	T_p (s)	H_s (m)	T_p (s)	H_s (m)	T_p (s)
North-east	10	1.4	4.2	1.7	4.5	2.1	5.0
East	7	1.2	3.9	1.5	4.3	1.8	4.7
South-east	4	0.9	3.4	1.2	3.7	1.4	4.2

Table A3. Wave return periods for the Pennington area from NFDC (2010)

Site	Data range	Return period for significant wave height (m)					10 th March 2008	
		1	10	50	100	200	H_s (m)	T_p (s)
Milford-on-Sea	(1996-2007)	3.90	4.56	4.99	5.17	5.34	3.42	11.0
Lymington (hindcast)	(1991-2002)	1.09	1.20	1.28	1.31	1.34	0.91	3.3

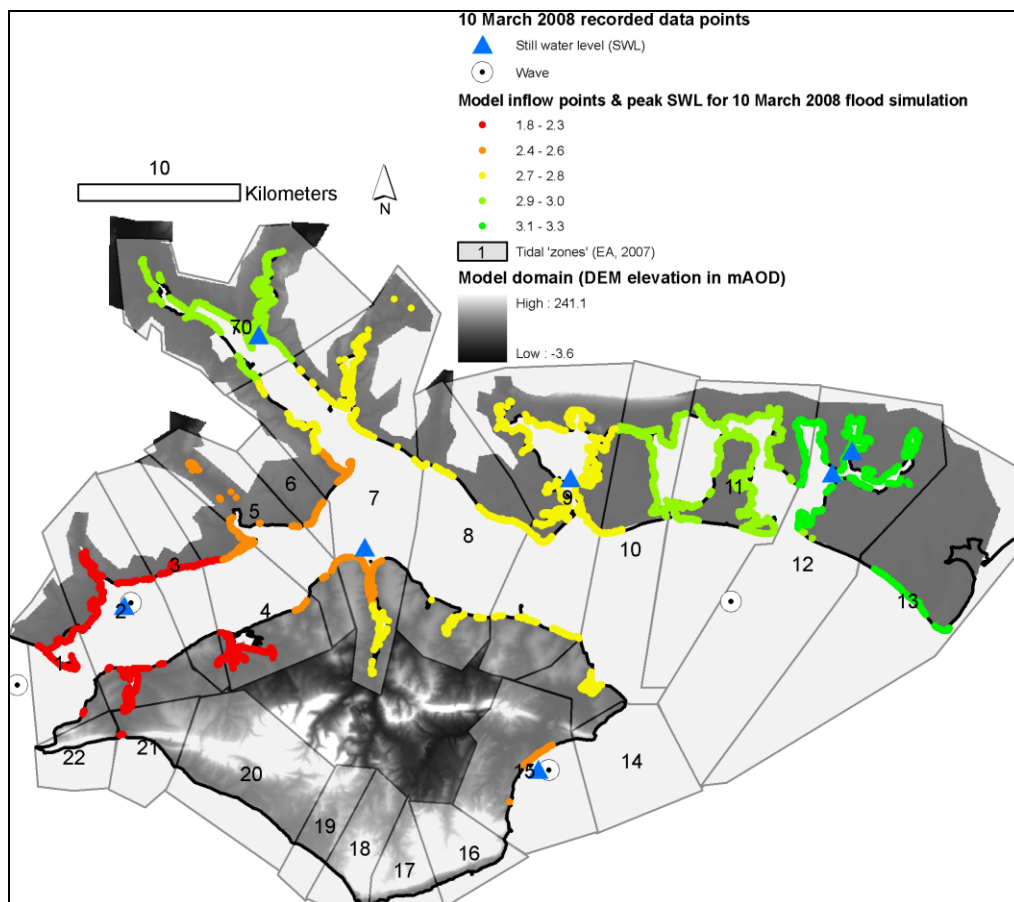
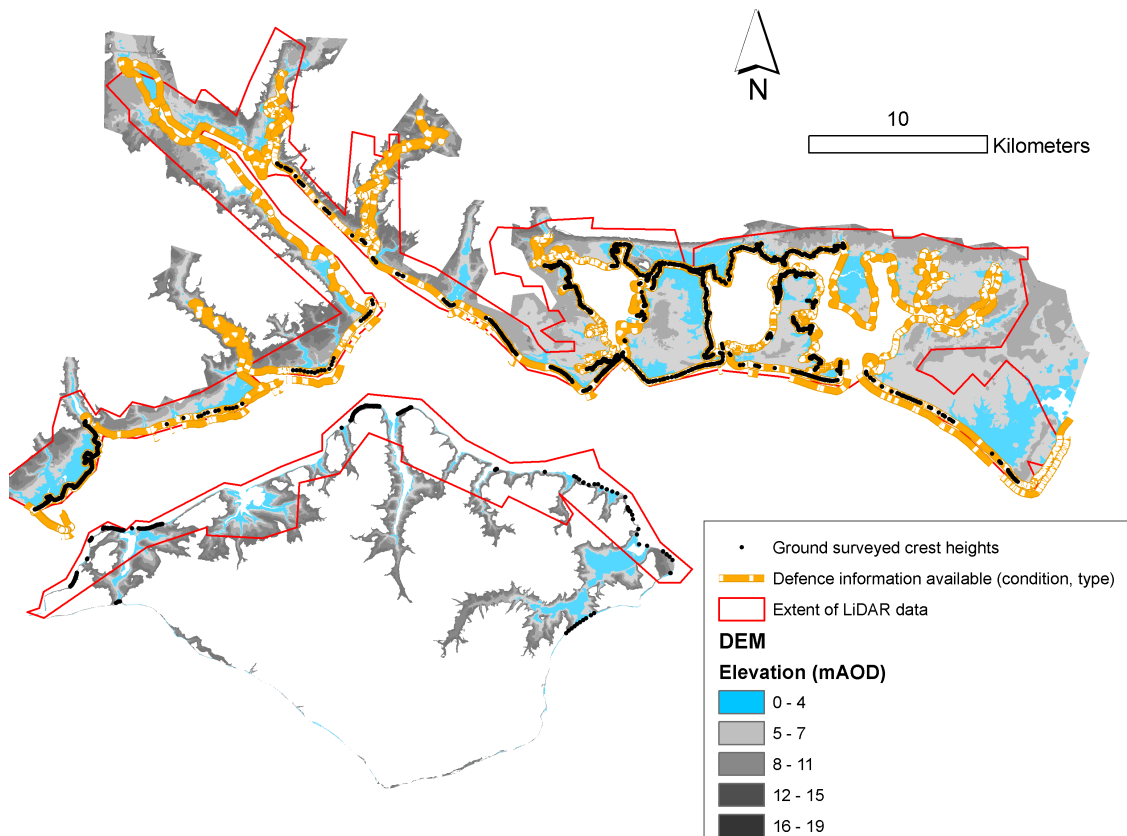


Figure A1. The digital terrain model (DEM) and defence data sets used for the Solent case study; **Figure A2.** Integration of DEM, tide zones, wave & tide recorders, and inflow boundary points for the inundation model

Appendix B - Exposure to coastal flooding in the Solent

These estimates of flooding are based upon land height alone, and do not account for defences or the dynamics of flooding.

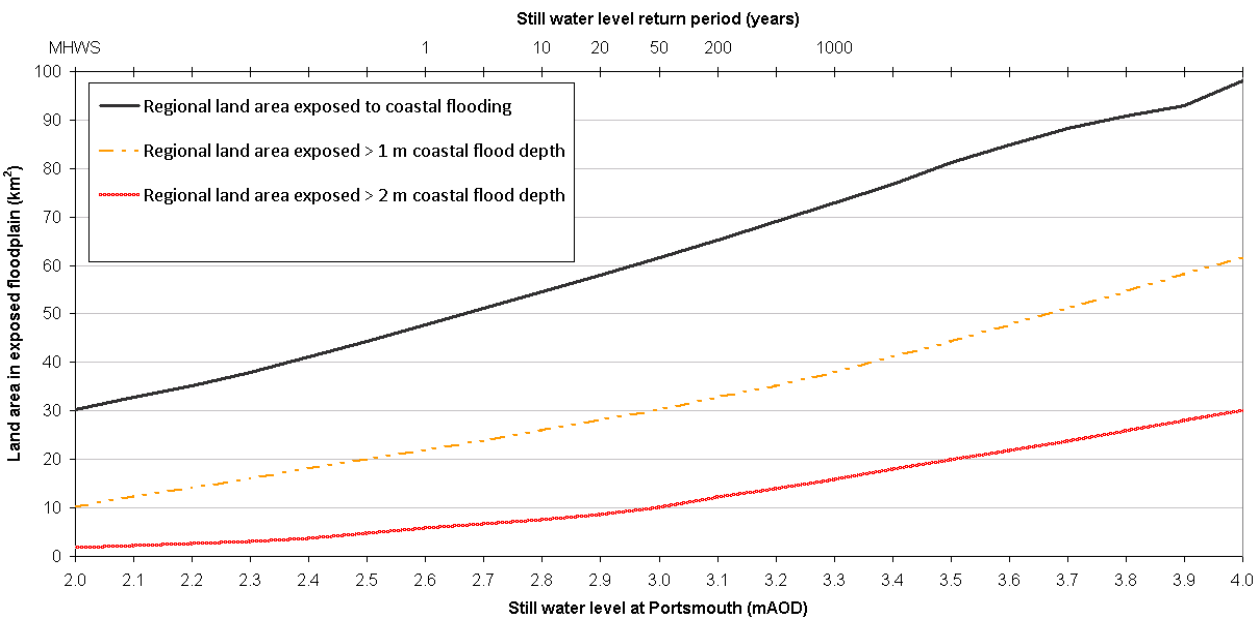


Figure B1 Regional exposure to flooding by land area

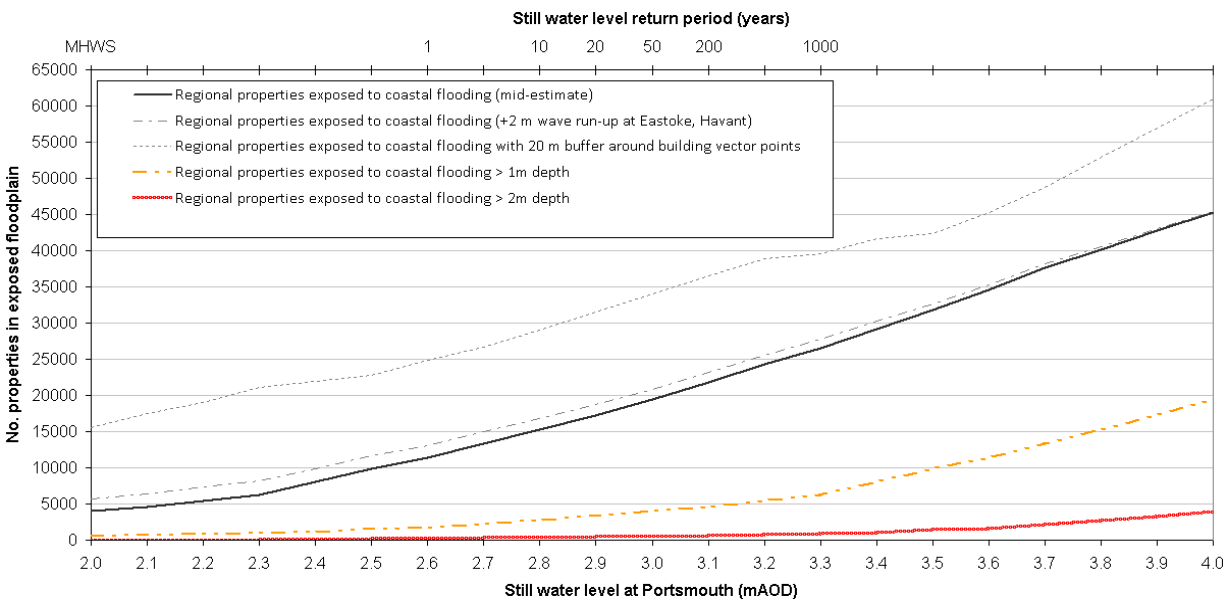


Figure B2 Regional exposure to flooding by properties in flood outlines

The exposure/planar water level method indicated 16,000 - 26,000 properties in the Solent are at risk from flooding at a 1 in 200 year SWL, acknowledged as an overestimate due to real spatial defence responses and other flood dynamics. This range takes into account possible LiDAR DEM error (uncertainty in the vertical elevation of the DEM approximated by reading ± 15 cm either side of the

SWL of interest). The spatial footprint of properties (approximated here as 20 m by 20 m) adds to the upper limit of this estimate. On 3rd November 2005 and 10th March 2008 at Eastoke Peninsula (Hayling Island) wave run-up caused flooding when the SWL was approx. 2m lower than the land. Hence the planar water level here for exposure assessment is raised by 2 m (representing wave run-up), increasing the estimate from 500 to nearly 2200 properties.

The planar water level method was used to delineate 99 hydraulically discrete floodplain compartments at present mean sea level, 12 of which are likely to experience significantly greater flood event impacts in the event of breach failures (in comparison to severe overtopping events), these accounting for 40 per cent of the land area at risk of flooding in the Solent. The planar water level method also provides a likely upper limit to further flood estimates for each compartment at any given set of loading conditions.

Figure B3 indicate areas of the Solent beneath various SWLs. Coastal flood threatened land in the 2-4m AOD range is approximately beneath present day extremes. Beyond this, many of the flood compartments merge and with 5 m SLR (e.g. a scenario associated with collapse of the West Antarctic Ice Sheet large areas) the East Solent is completely submerged.

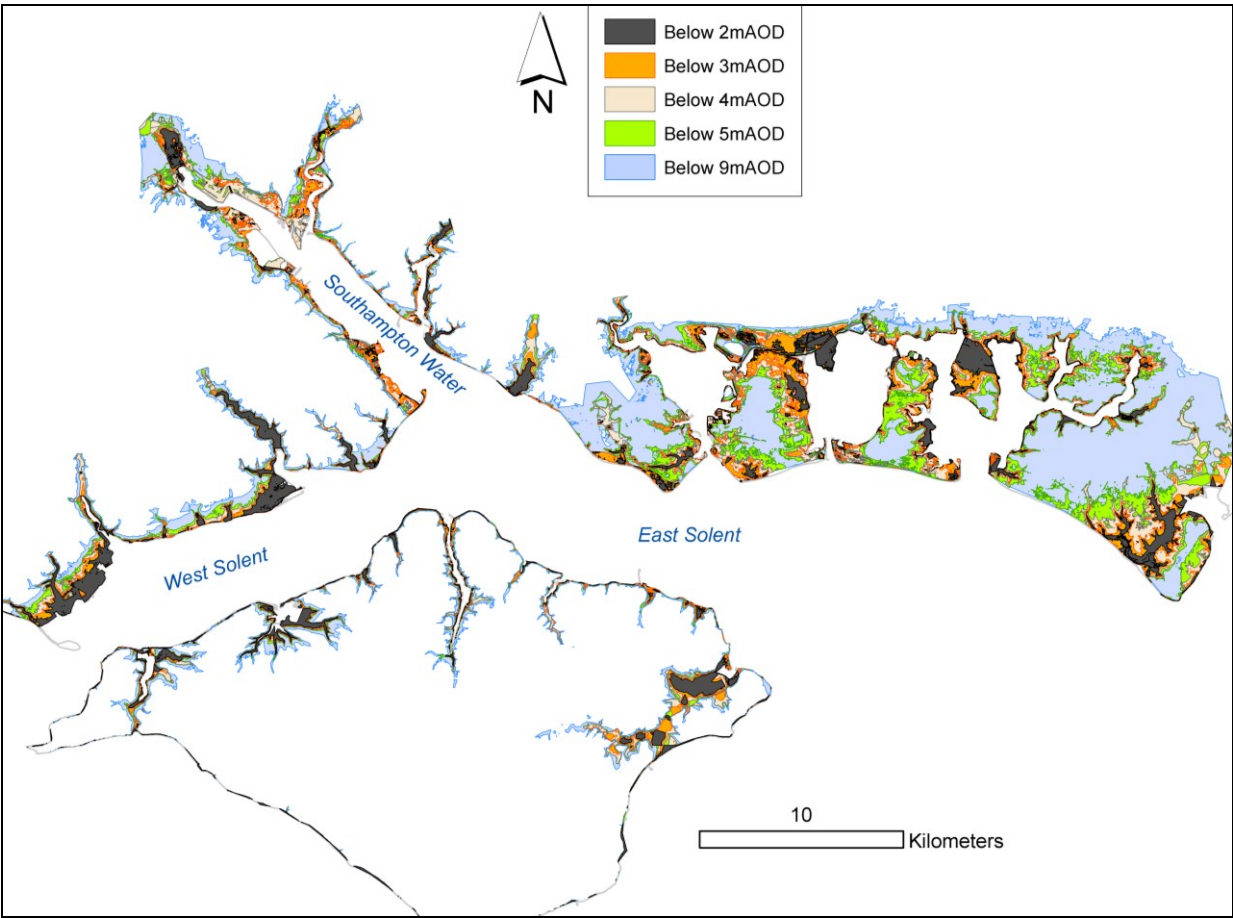


Figure B3 Land beneath hypothetical planar water levels

Appendix C - Breach analysis - Fragility curves

Described in Section 4.3.3, fragility curves for three different breach failure mechanisms were generated so that for a given loading the conditional probability of failure could be approximate across the 5,000 defence sections in the Solent flood modelling case study. This was achieved using the RELIABLE software and guidance from Gouldby et al. (2008a). This analysis did not form an integral part of the methodology for simulating coastal flood events but provided an indication of areas of defences more susceptible to breach. Section C1 provides an introduction to the methods that underpin the reliability analysis, to generate the coastal flood defence fragility curves. This summarises information from Melchers (1999), and Faber (2007).

C1. Overview of reliability concepts and Monte Carlo Analysis

Reliability analysis of systems and their components requires an evaluation of the probability of failure corresponding to a specified reference period. It is appropriate to describe failure events in terms of functional relations, here known as the ‘limit state function’ $g(x)$, which if fulfilled define that the considered event will occur. The limit state is described as follows:

$$F = g(x) \leq 0 \quad \text{eq. (C1)}$$

where the components of the vector x are realisations of the so-called basic random variables X representing all the relevant uncertainties influencing the probability of failure. In Eq.C1 the failure event F is simply defined as the set of realisation of the function $g(x)$, which is zero or negative. Having defined the failure event the probability of failure may be determined by the following integral:

$$P_F = \int_{g(x) \leq 0} f_x(x) dx \quad \text{eq. (C2)}$$

where $f_x(x)$ is the joint probability density function of the random variables X . This integral is non-trivial to solve and numerical approximations are advantageous. Various methods for the solution of the integral in Equation (C2) have been proposed (e.g. including numerical integration techniques) although described here are simulation techniques often referred to as Monte Carlo simulations which involve sampling at random to artificially simulate a large number of experiments. This automatically deals with non-linearity in functions and non-normal random variables. Subsequently, the basis for simulation techniques is well illustrated by rewriting the probability integral in Equation (C2) by means of an indicator function as shown in Equation (C3):

$$P_F = \int_{g(x) \leq 0} f_x(x) dx = \int I[g(x) \leq 0] f_x(x) dx \quad \text{eq. (C3)}$$

where the integration domain is changed from the part of the sample space of the vector $X=(X_1, X_2, \dots, X_n)^T$ for which $g(x) \leq 0$ to the entire sample space of X and where $I[g(x) \leq 0]$ is an indicator function equal to 1 if $g(x) \leq 0$ and otherwise equal to zero. Equation (C3) is in this way seen to yield the expected value of the indicator function $I[g(x) \leq 0]$. Therefore if now N realisations of the vector X , i.e. $x_j, j=1, 2, \dots, N$ are sampled it follows (from sample statistics) that:

$$P_F = \frac{1}{N} \sum_{j=1}^N I[g(x) \leq 0] \quad eq. (C4)$$

is an unbiased estimator of the failure probability P_F . The basis for Monte Carlo simulations rests directly on the application of Equation (C4). A large number of realisations of the basic random variables X , i.e. $\hat{x}_j, j = 1 \dots N$ are simulated and for each of the outcomes \hat{x}_j it is checked whether or not the limit state function taken in \hat{x}_j is positive. All the simulations for which this is not the case are counted (n_f) and after N simulations the failure probability P_F may be estimated through:

$$P_F = \frac{n_f}{N} \quad eq. (C5)$$

which then may be considered a sample expected value of the probability of failure. For $N \rightarrow \infty$ the estimate of the failure probability becomes exact. The simulation of the N outcomes of the joint density function in Equation (C5) in principle comprises two steps (assuming that the n components of the random vector X are independent):

- (1) A “pseudo random” number between 0 and 1 is generated for each of the components in \hat{x}_j i.e. $\hat{x}_{ij}, i=1, \dots, n$. The generation of such numbers may be facilitated by functions built into a programming language or spreadsheet software;
- (2) the outcomes of the “pseudo random” numbers \hat{z}_{ij} are transformed to outcomes of \hat{x}_{ij} by:

$$x_{ji} = F_{xi}^{-1}(z_{ji}) \quad eq. (C6)$$

where $F_x()$ is the probability distribution function for the random variable X_i as illustrated:

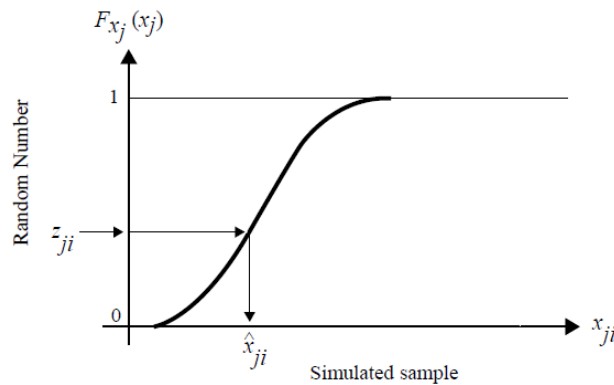


Figure C1. Principle for simulation of a random variable

This process is continued until all components of the vector \hat{x}_j have been generated. However the aforementioned ‘direct sampling’ approach, samples points uniformly. This can waste considerable effort in sampling areas that are not in the failure region. Techniques to overcome this problem increase the density of sampling in the region of interest by ensuring a more efficient selection of random variables and hence increase the overall efficiency of the simulation. This requires selection of an ‘importance-sampling’ density function, $h_v(\underline{v})$ that approximates the failure function over the region of interest. The failure probability is estimated using:

$$P_F = \frac{1}{N} \sum_{j=1}^N I \left(g(v_i) \leq 0 \right) \frac{f(v_i)}{h(v_i)} \quad eq. (C7)$$

where \underline{V} is a vector with a probability density function $h_v(\underline{v})$, and v'_i is a vector of sample values from the importance function $h_v(\cdot)$. Choosing appropriate importance functions can be challenging as it is important not to bias the estimate. Melchers (1999) suggests defining the importance function as $h_v = \phi_n(\underline{v}, \underline{C}_v)$ where \underline{C}_v is a diagonal matrix of σ_i^2 with the mean of \underline{V} placed at \underline{x}' (the maximum likelihood of \underline{x}). This can reduce the number of required sample points significantly, generating sample points that are unbiased with respect to each variable.

C2.Breach assessment in the case study using RELIABLE

Breach mechanism 1: damage initiated by overflow and/or overtopping

National flood risk assessments in the England and Wales (DEFRA and EA, 2007) have used data sets derived from a process-based model of failure by Vrouwenvelder (2001). This provides a limit state equation (LSE) where overflow and/or overtopping discharges are used as loads (these can be amalgamated into one variable for hydraulic loading (q_a) by calculating the volume of water discharged over a defence during a given event). In RELIABLE (refer to Section 4.4.4) the load value is inputted in the form of a water level height and crest height. The LSE and Monte Carlo analysis generate a probability that resistance (q_c) of defence will be exceeded by the actual overtopping-overflow discharge (q_a) is:

$$Z = q_c - q_a \quad eq. (C8)$$

The load values (during a loading or storm event) are: (1) the height of water above the defence, (2) the duration, and (3) percentage that these loads prevailed. Overflow and overtopping were amalgamated into one load number (the ‘WaterL’ value in Figure D1) and a tidally controlled duration of water passing over the crest was calculated. The overflow percentage (‘OverPercen’) was ‘1’ if assuming a continuous discharge for the duration of overflow. For wave overtopping wave run-up ($Ru_{2\%}$ value) above the crest of the defence was used instead of the overflow head (refer to Equation 8) and the

duration was for that which the $Ru_{2\%}$ value exceeded the crest of the defence (also using Equation 6 for overtopping percentage).

Figure C1 RELIABLE user interface (loads highlighted top; resistance parameters in lower box)

Table C1. In the RELIABLE software (Figure C1), although most inputs are fixed and deterministic values, the user is in some instances required to specify statistical distribution function and its associated parameter values for each variable within each LSE. These were approximated using guidance from Allsop et al (2007), Gouldby et al. (2008a), the defence data sets, alongside some estimation/judgement.

Parameter	Failure Mode	Distribution	Parameters assigned to distribution for Monte Carlo simulations
Revetment strength (C_g)	1: damage initiated by overflow and/or overtopping	Normal	Using values from Table 4.3 fragility curves were generated for 0.25 increments of C_g (different defences across the case study fell into the range 0 – 7). The mean used to generate each fragility curve was the associated increment. The SD was the standard deviation of all of the assigned C_g values (which used the information in Table 4.3, surveys etc.) for all defences in the case study (=0.07)
Coefficients for consideration of the crest width & sharp-crested-ness of the weir			Normal
Inner slope angle			
Manning’s friction coefficient			
Storm duration		Lognormal	Mean=3.0 hours; standard deviation =0.65 (based upon approximation from previous observations of how long storms are likely to attack defences during extreme SL events)
Seepage length	2: damage initiated by piping		
Groundwater level			
Wave height	3: foreshore erosion	Weibull	Dependent upon exposure at each site / inflow point location
Wave period		Normal	
D ₅₀ (grain size distribution)			Specific values available at Hayling Island; approximated elsewhere.

Breach mechanism 2: damage initiated by piping

If a positive water head over a structure persists for long enough, a piping process may initiate. The limit state equation used, determined piping failure if the critical head difference between the coastal and hinterland water level (dh_c) is exceeded by the occurring head difference between the coastal and hinterland water level (dh) (Terzaghi and Peck, 1967):

$$Z = dh_c - dh \quad \text{eq. (C9)}$$

The critical head difference (dh_c) is expressed as:

$$dh_c = \frac{t + \frac{1}{3}L}{C_w} \quad \text{eq. (C10)}$$

Where t is the thickness of the impervious layers underneath the embankment, L is the horizontal seepage length (reaching from the point seaward of the defence where the water conductive layer is in contact with water level, to a weak point behind the embankment formed where uplifting of the impervious layer might occur). C_w is the creep ratio, which takes on different values in relation to the soil type. The configuration of most coastal defence structures in the UK suggests that piping is most likely to be caused by water internally eroding underneath (rather than the body) of defences (DEFRA and EA, 2005a), although insufficient data is available to generate accurate values to accurately populate the aforementioned loading and resistance equations. Hence, the likelihood of this type of failure was estimated by using this model, and assuming that $t=0$, and the distance L = the width of the embankment. Hence the likelihood of finding a weak or deteriorated stratum in the defence is based upon creep ratios that relate to condition of the defence from DEFRA and EA (2005a).

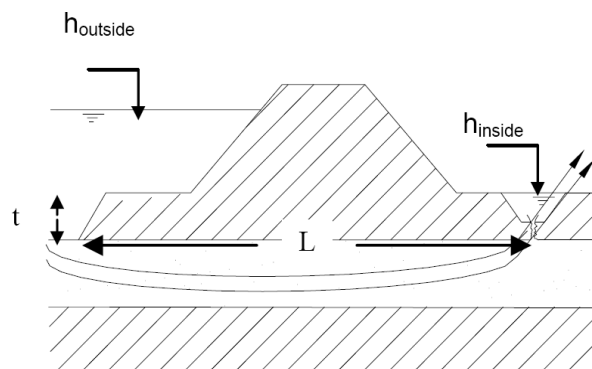


Figure C2. Illustration of piping failure assessment based upon thickness of the impervious later and the horizontal seepage length

Table C2. The values used for resistance (i.e. the creep ratio)

Condition Grade	Seepage Length L (m)
1	60
2	60
3	60
4	10
5	6

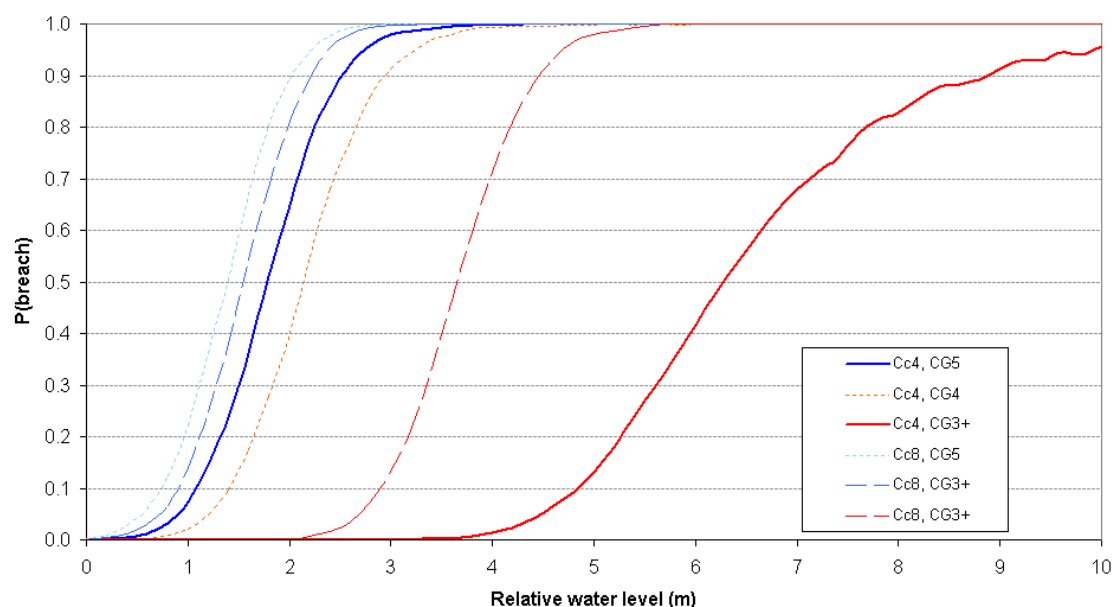


Figure C3. Illustration of piping failure assessment based upon thickness of the impervious later and the horizontal seepage length (Cc=creep coefficient, CG= Condition Grade).

Breach mechanism 3: foreshore erosion

Shingle beaches comprise important defences in many areas across the Solent; in some incidences forming a barrier between the sea and hinterland in their own right, or being essential for the stability of other coastal defences.

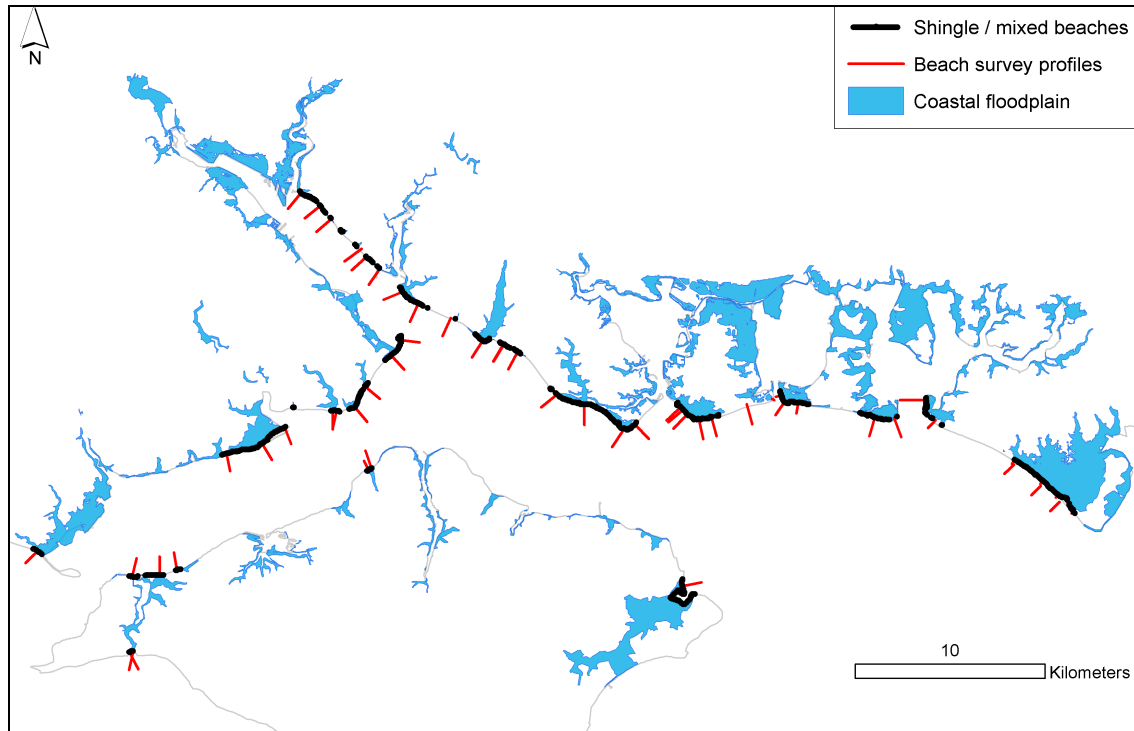


Figure C4. Location of shingle beaches in the Solent and survey profiles used for analysis

The likelihood of critical erosion in response to storm loadings was approximated using a parametric model that was developed by a series of tests conducted in a flume by (Powell, 1990). Topographic beach survey profile surveys (CCO, 2011) were used to populate this model. The location of these profiles and shingle beaches within the Solent are shown in Figure D5. Failure corresponds with the probability that retreat of the crest p_c (given the loading conditions) exceeds the width of the shingle beach w (taken to be the front edge of the beach crest):

$$Z = w - p_c \quad \text{eq. (C11)}$$

Beach thickness was effectively the load for each fragility function, assumed to reduce with increasing water level at a rate dependent on the slope for any given profile. Resistance parameters include material size, for which specific data was not available, but can be approximately in relation to slope using guidance from DEFRA and EA, (2005a), and calculated from inspection of the profiles. At the shingle beach locations shown in Figure D5, not all were within the range of 1:12 and 1:7 slopes. These values were approximated by basic linear regression and extrapolated when required.

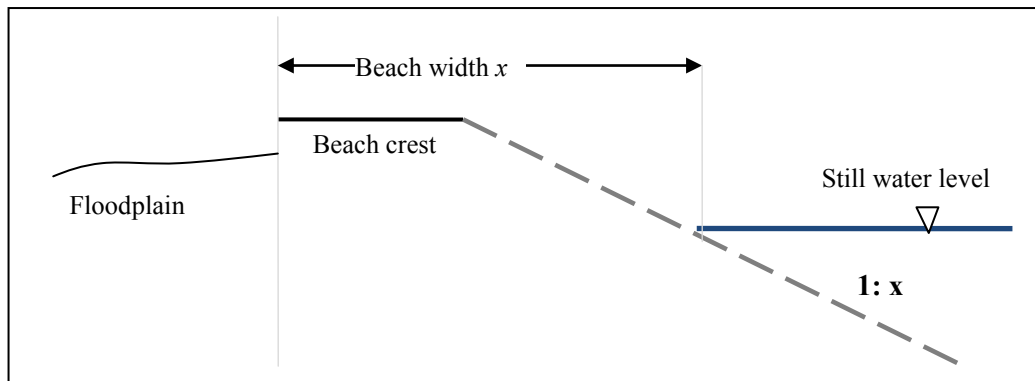


Figure C5. Simplified representation of the Powell (1990) model, relating potentially eroded beach width to beach gradient at a given water level.

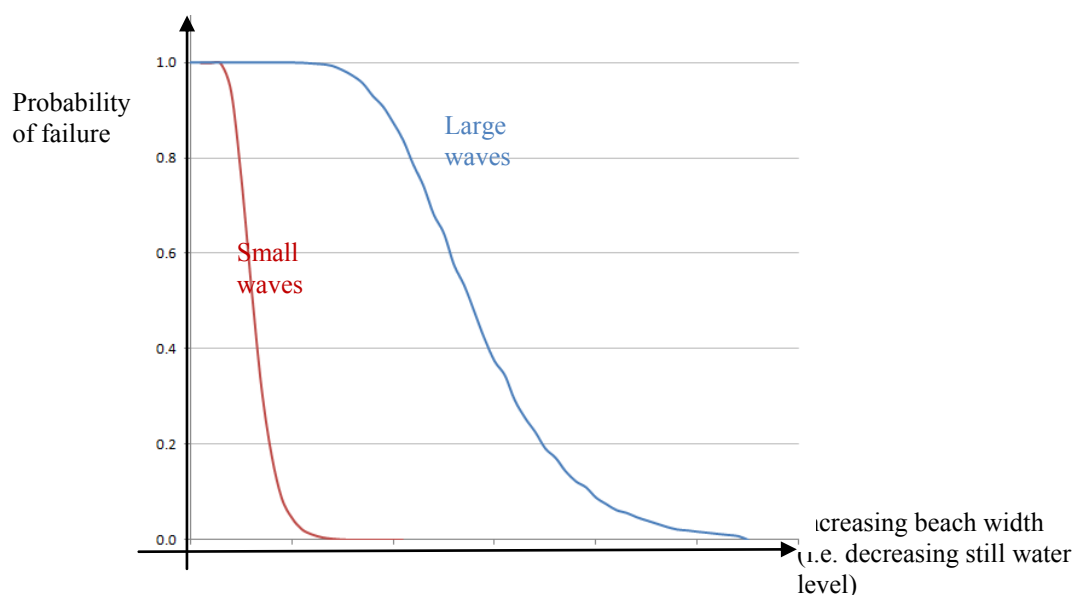


Figure C6. Example fragility curve for beach retreat during a storm

Appendix D – Evaluation of the 10 March flood event photo data set

In Chapter 5, a collation of flood event observations is described to assess the storm surge and coastal Solent flood event of 10 March 2008, and validate coastal inundation simulations. This section summarises the role of the photos alone, to delimit the 10 March 2008 observation polygons; by reviewing the photos and applying measuring tools in ArcGIS. The annotated metadata in the following figures includes a summary of the areas of the polygon considered as the observed flood, interpreted from the combined methods (DEM, descriptive information, local water level etc.) and referred to in Table 5.2 to compare with the numerical simulations.

As shown the largest area for which photos provide visual evidence and quantification of flooding is at Selsey (Location 28); where the breach and overtopping of a shingle beach flooded a caravan park and surrounding land. The visual coverage of inundation was also relatively high at Calshot and Langstone; although at the former of these locations the impact upon buildings was low. In terms of visual coverage relative to the interpreted observation of the polygons, the visual coverage was high at locations 36 and 37, where the polygon was almost entirely reconstructed by the photos – although this is partly attributed to the reliance upon photos to reconstruct the flood outline (in the absence of more detailed descriptive data).

Section 7.3.2 and 8.2 make recommendations for further developments in these areas. It is clear that photos are also benefited by descriptive information and knowledge of previous floods. For example at Location 27, Bosham, the report by West (2010) is highly informative; whilst at Location 37 (overtopping at Yaverland) the photo source verified that the water outside the building affected was indeed sea water. Future flood event research should attempt to gather and rate images for flood event analysis, including methods that can more accurately use images to quantify flood event uncertainty. For example in most cases, despite that photos constrain some of the flood extent edges, it cannot be definitively stated whether the actual flood extent is actually smaller or larger than the polygon interpretation, unless full spatial and temporal coverage is available.

A selection of photos is subsequently shown. The full selection has been archived and is available upon request from the Channel Coastal Observatory (the data management centre for the Regional Coastal Monitoring Programmes: [www. channelcoast.org](http://www.channelcoast.org)).

Table D1. Summary of the photos and their role in the validation polygons

Table D1: Summary of the photos and their role in the validation polygons									
Number of photos (sum by sub-region)	Location number (Figure 5.7)	Number of photos available	Polygon area (km ²)	Visual coverage (km ²)	% of polygon verified by photo	Flood area: rank by polygon	Visual coverage: rank (by actual area)	Visual coverage: rank (by % area of polygon verified)	Visual coverage (km ²) / Polygon area (km ²)
88	1	19	0.0020	0.0010	50	21	21	11	0.50
	2	12	0.0310	0.0295	95	5	5	3	0.95
	3	8	0.0025	0.0005	20	23	23	16	0.20
	4	19	0.0420	0.0399	95	3	3	3	0.95
	5	2	0.0690	0.0007	1	22	22	28	0.01
	6	10	0.0011	0.0001	5	28	28	24	0.09
	7	0	0.0170	0.0000	0	29	29	29	0.00
	8	7	0.0011	0.0001	8	27	27	22	0.09
	9	11	0.0210	0.0071	34	9	9	14	0.34
	10	0	0.0070	0.0000	0	29	29	29	0.00
22	11	0	0.0040	0.0000	0	29	29	29	0.00
	12	20	0.0040	0.0038	95	15	15	3	0.95
	13	1	0.0280	0.0064	23	12	12	15	0.23
	14	1	0.0250	0.0015	6	20	20	23	0.06
1	15	1	0.0050	0.0018	35	18	18	13	0.36
	16	0	0.0260	0.0000	0	29	29	29	0.00
3	17	1	0.0020	0.0002	12	25	25	18	0.10
	18	0	0.0000	0.0000	0	29	29	29	N/A
	19	2	0.0140	0.0015	11	19	19	19	0.11
4	20	3	0.0160	0.0130	81	8	8	7	0.81
	21	1	0.0000	0.0000	0	29	29	29	N/A
	22	0	0.0000	0.0000	0	29	29	29	N/A
81	23	2	0.0220	0.0020	9	17	17	20	0.09
	24	3	0.0480	0.0365	76	4	4	8	0.76
	25	33	0.0094	0.007	76	6	6	8	0.74
	26	43	0.0690	0.0614	89	2	2	6	0.89
23	27	12	0.0770	0.0069	9	11	11	20	0.09
	28	11	4.7000	0.2350	5	1	1	24	0.05
98	29	9	0.0270	0.0041	15	14	14	17	0.15
	30	3	0.0120	0.0060	50	13	13	11	0.50
	31	6	0.0600	0.0030	5	16	16	24	0.05
	32	0	0.0260	0.0000	0	29	29	29	0.00
	33	0	0.0040	0.0000	0	29	29	29	0.00
	34	2	0.0160	0.0005	3	24	24	27	0.03
	35	38	0.0300	0.0204	68	7	7	10	0.68
	36	5	0.0001	0.0001	100	26	26	1	1.00
	37	35	0.0070	0.0070	100	10	10	1	1.00
Excluding Selsey (L28)	Total area (km ²)	320	0.75	0.28					
Incl. Selsey			5.45	0.52					

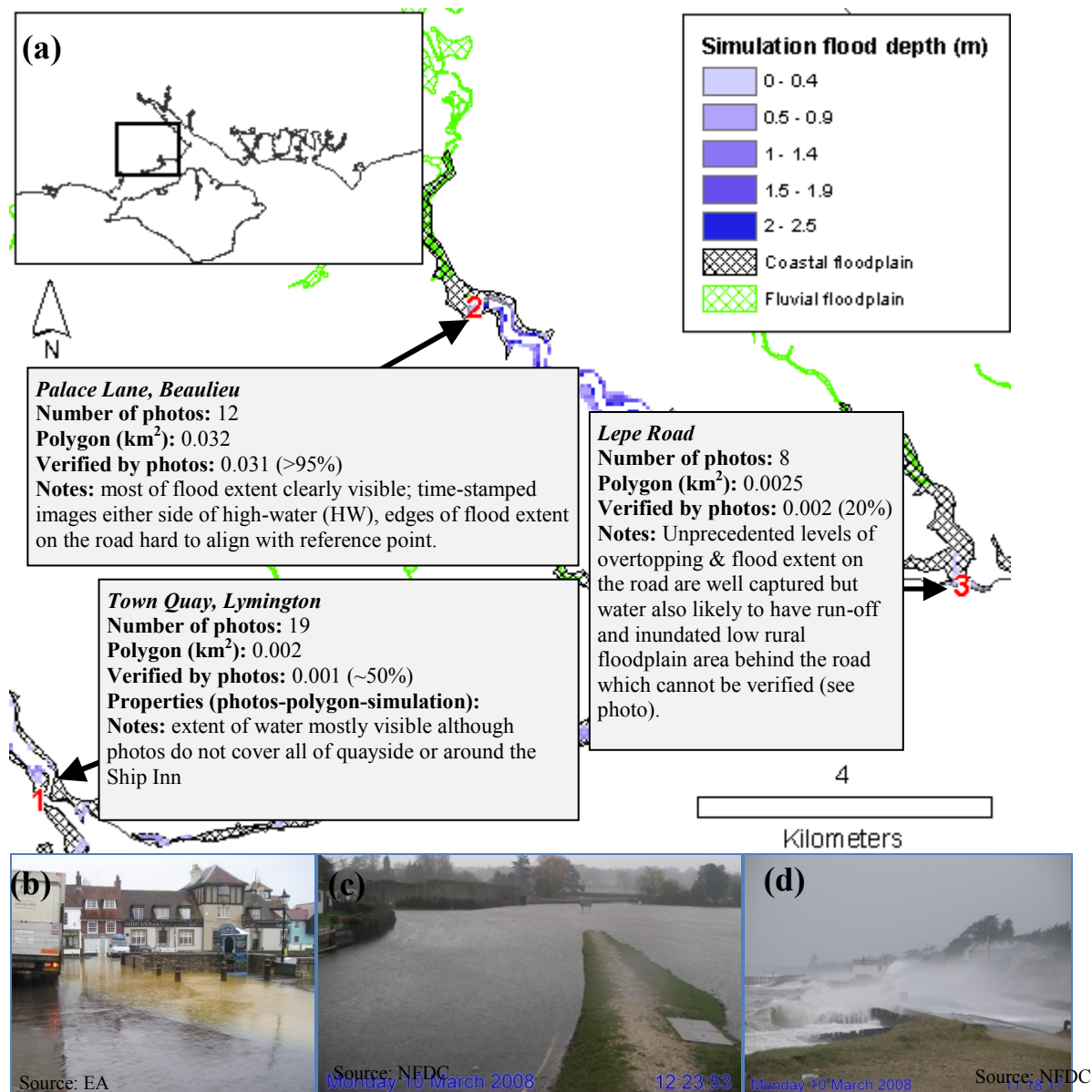


Figure D1. (a) Map showing floodplain, event simulation, and metadata summary, (b) Location 1 (Lymington, looking towards the ‘Ship Inn’), (c) Location 2 (Beaulieu, facing north on Palace Lane), (d) Location 3 (Lepe, viewed from car park entrance at Lepe Country Park, facing west)

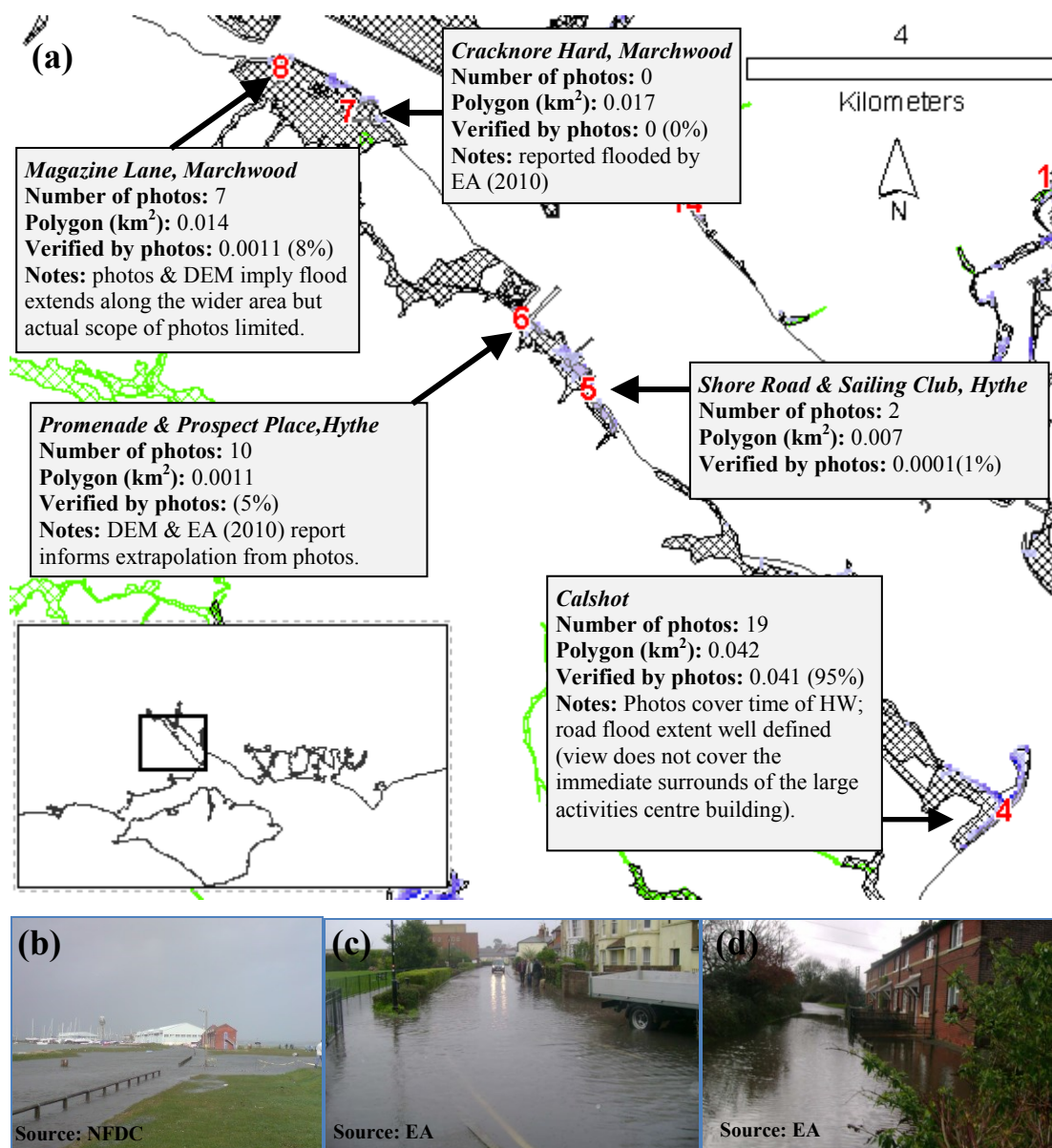


Figure D2. (a) Map showing flood floodplain, simulation of event and annotated with photo metadata, (b) Location 4 (facing north towards the activities centre on Calshot Road), (c) Location 6 (facing southeast, Prospect Place, Hythe), (d) Location 8 (Magazine Lane, Marchwood).

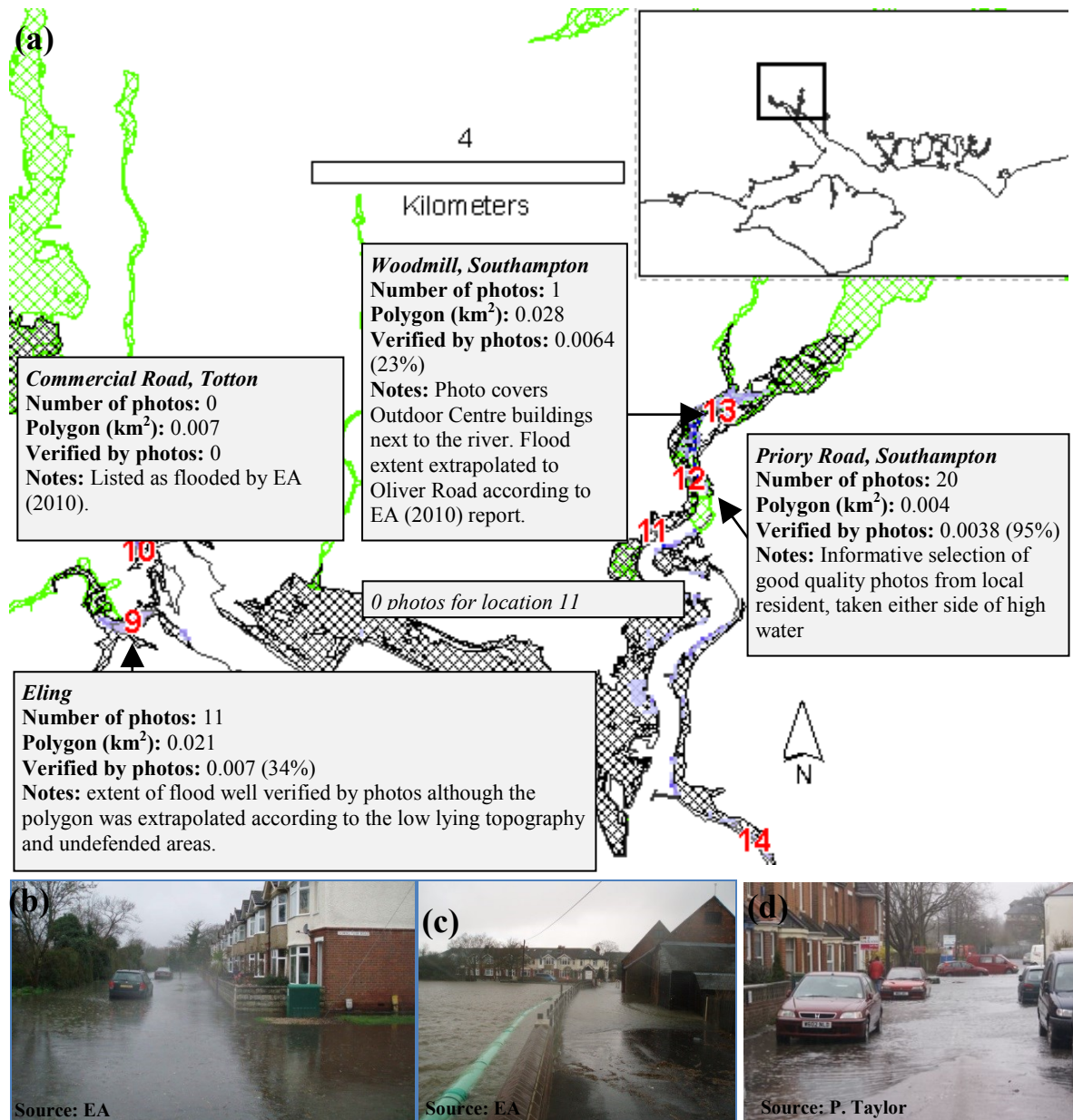


Figure D3. (a) Map showing floodplain, event simulation, and metadata summary, (b) Location 9 (intersection Down's Park Crescent and Down's Park Road), (c) Location 9 (Eling Hill and Lexby Road); and (d) looking south towards Priory Road (St Denys, Southampton).

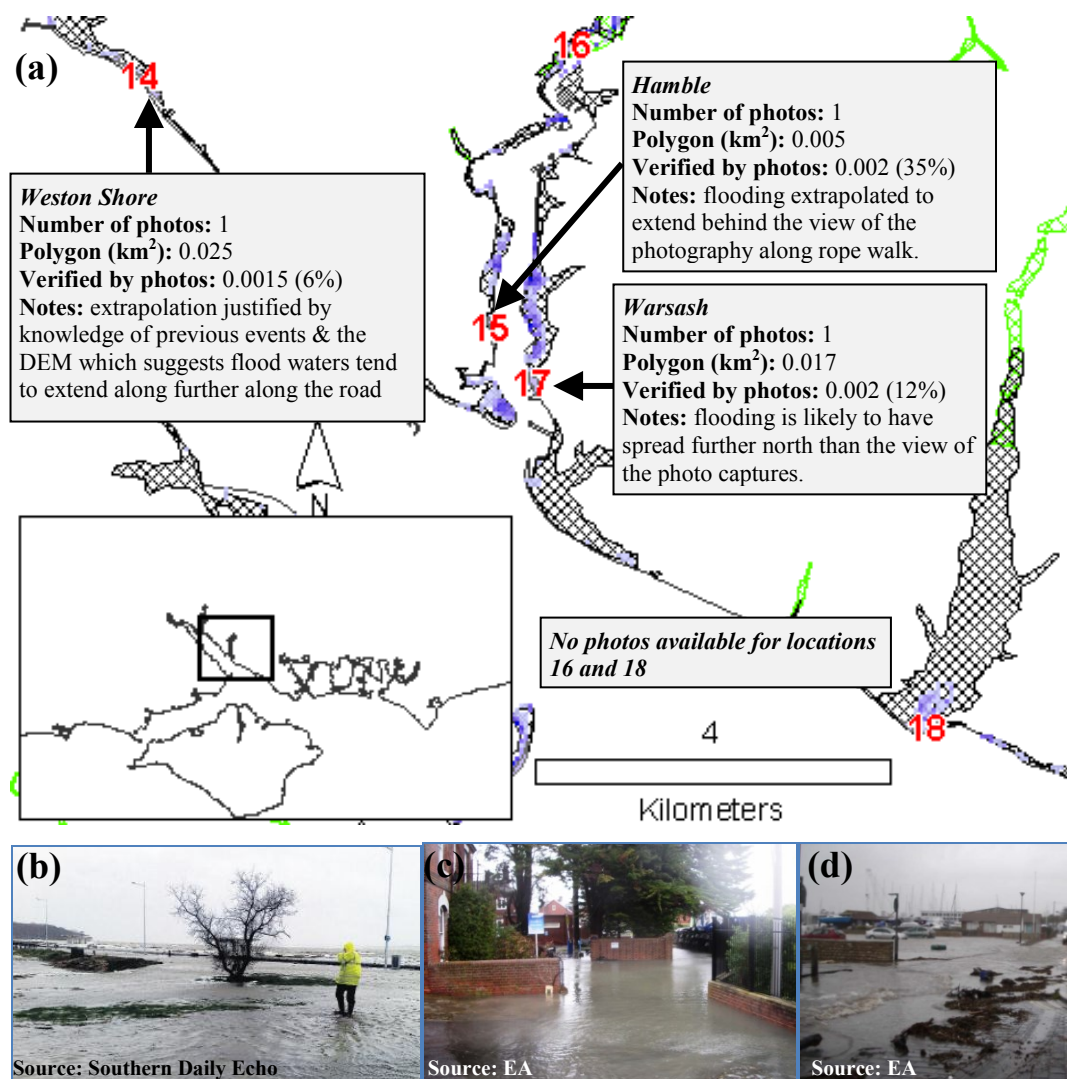


Figure D4. (a) Map showing floodplain, event simulation, and metadata summary, (b) Location 14 (Weston Road), (c) Location 15 (Rope Walk, Hamble), and (d) Location 17 (near the Rising Sun pub, Warsash).

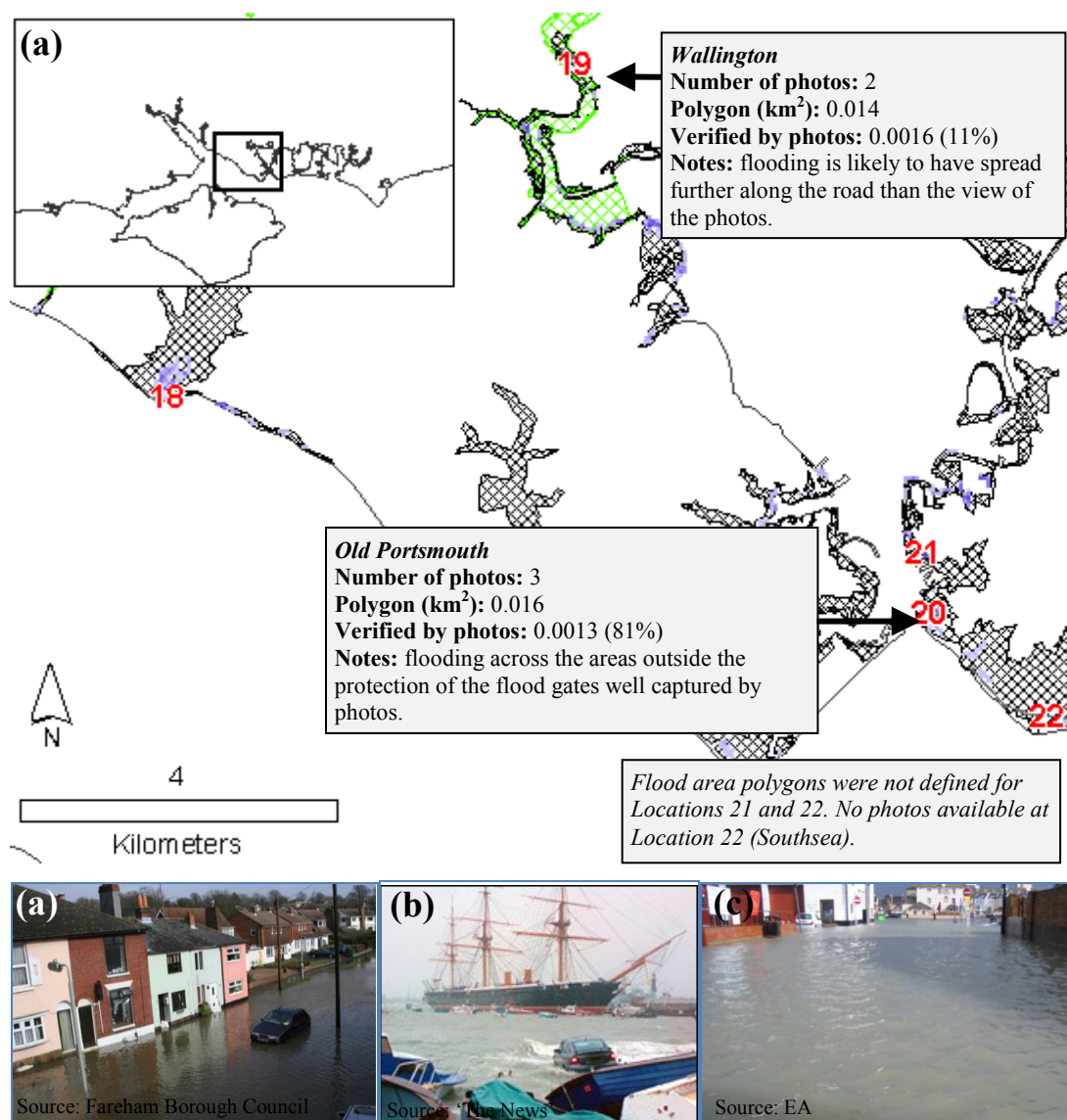


Figure D5. (a) Map showing floodplain, event simulation, and metadata summary, (b) Location 10 (Wallington, Fareham), (c) Location 21 (outside the Ship Ansom pub, Portsmouth), and (d) Location 20 (Old Portsmouth).

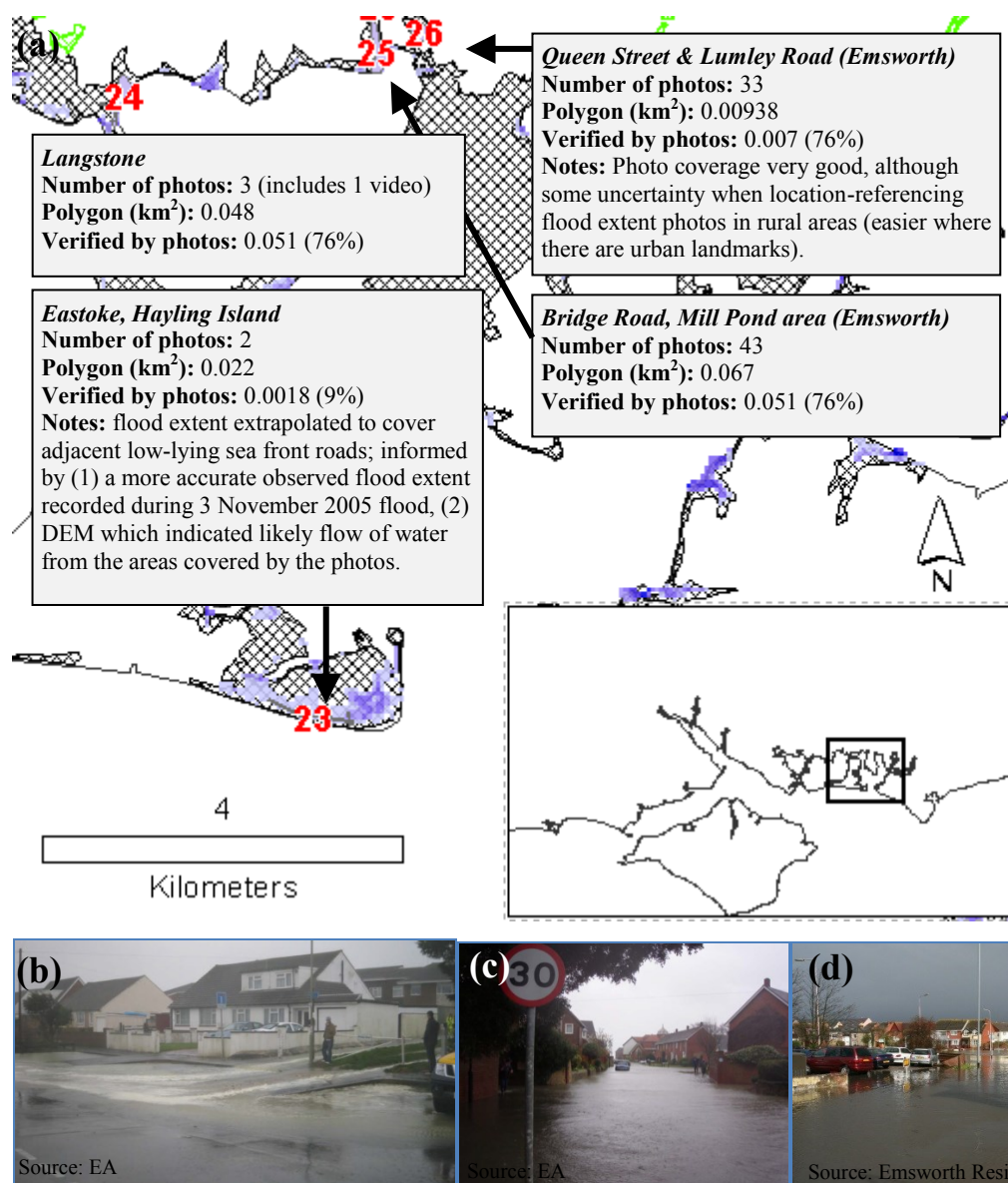


Figure D6. (a) Map showing floodplain, event simulation, and metadata summary, (b) Location 23 (Junction of Bosmere Road and Southwood Road, Eastoke, Hayling Island), (c) Location 23 (Langstone), and (d) Location 25 (Emsworth).

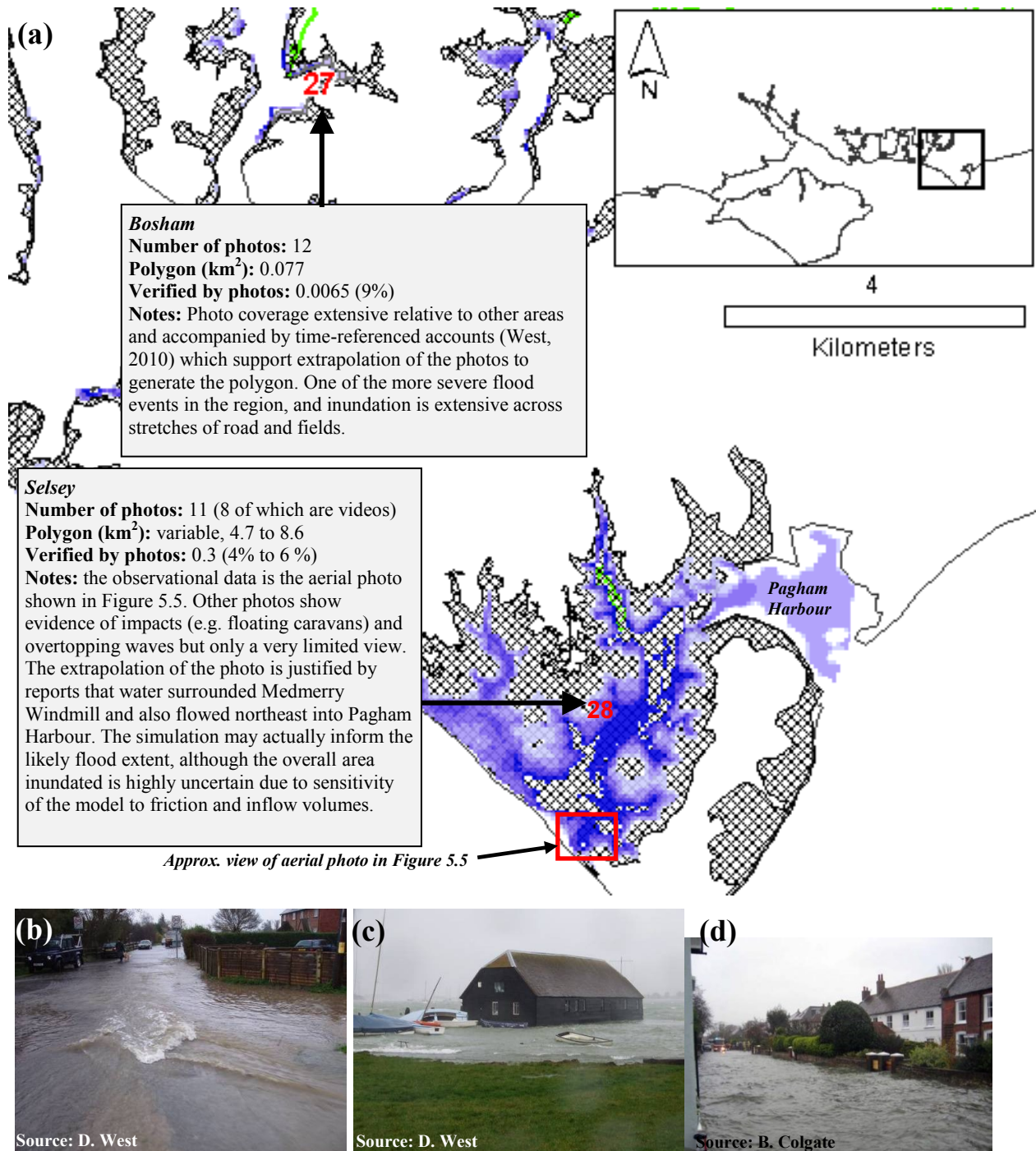


Figure D7. (a) Map showing floodplain, event simulation, and metadata summary. The photos show flooding at Location 27 (Bosham), (b) sea water had been ‘flowing across field garden and down access track into Stumps Lane’ (West, 2010), (c) water surrounds the Sailing Club and (d) floods in Bosham Lane.

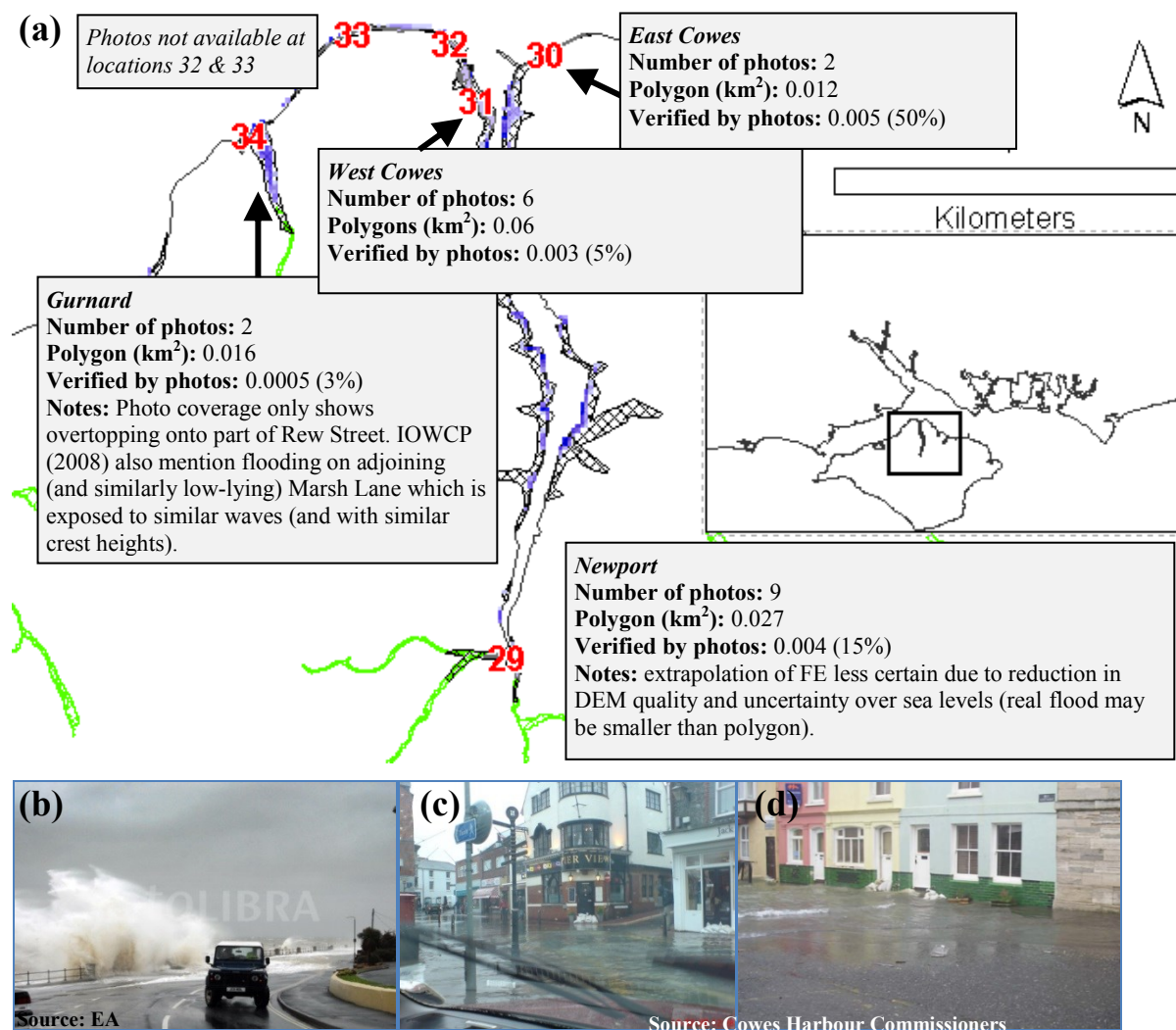


Figure D7. (a) Map showing floodplain, event simulation, and metadata summary, (b) waves overtopping and flooding at Location 34 (Gurnard), (c) flooding at Location 31 (facing the 'Pier View' Pub in Cowes High Street), (d) Location 30 (adjacent to the floating bridge, East Cowes).

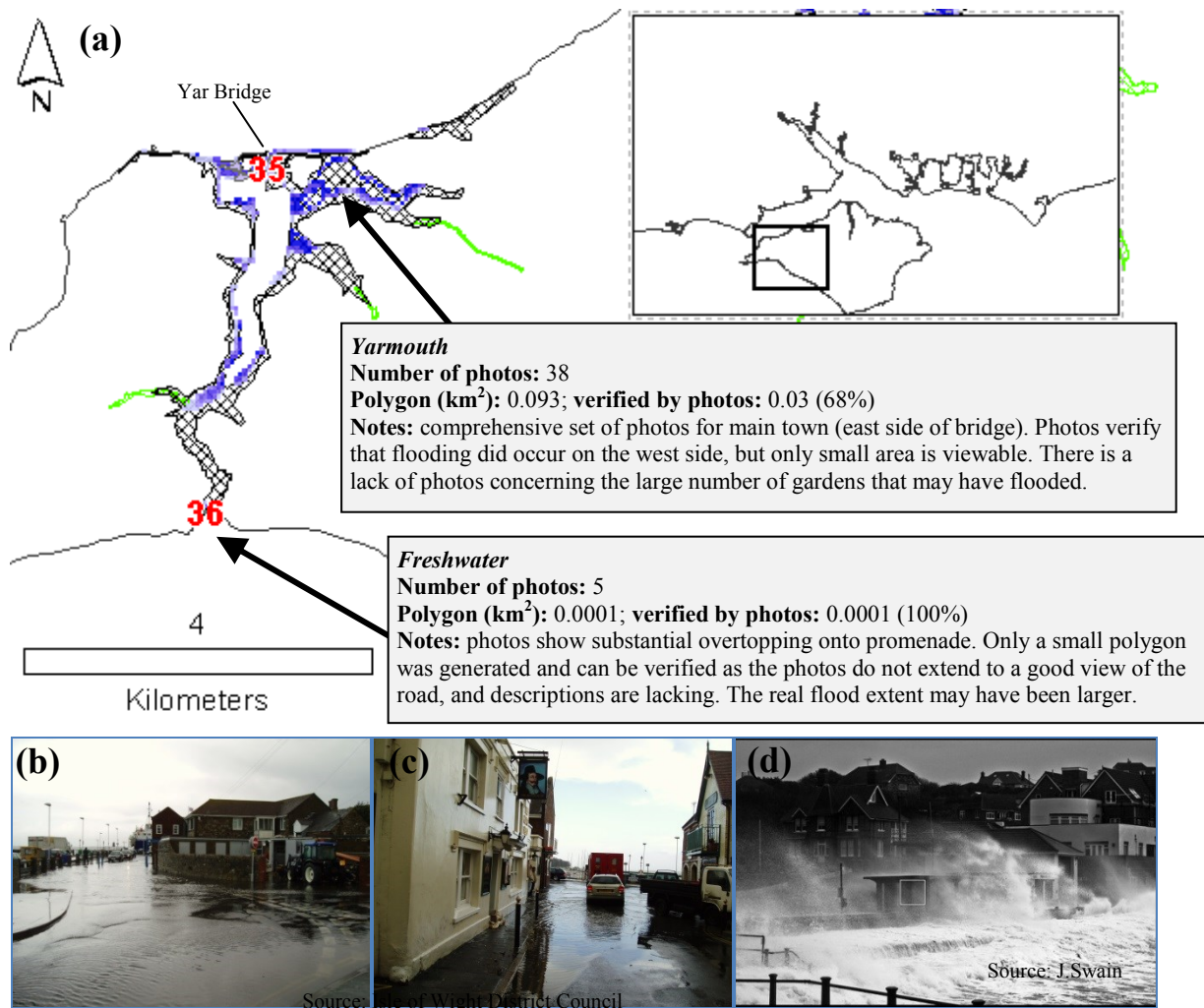


Figure D8. (a) Map showing floodplain, event simulation, and metadata summary, (b) and (c) flooding at Location 35 (Yarmouth), (d) Location 36 (Freshwater Bay)

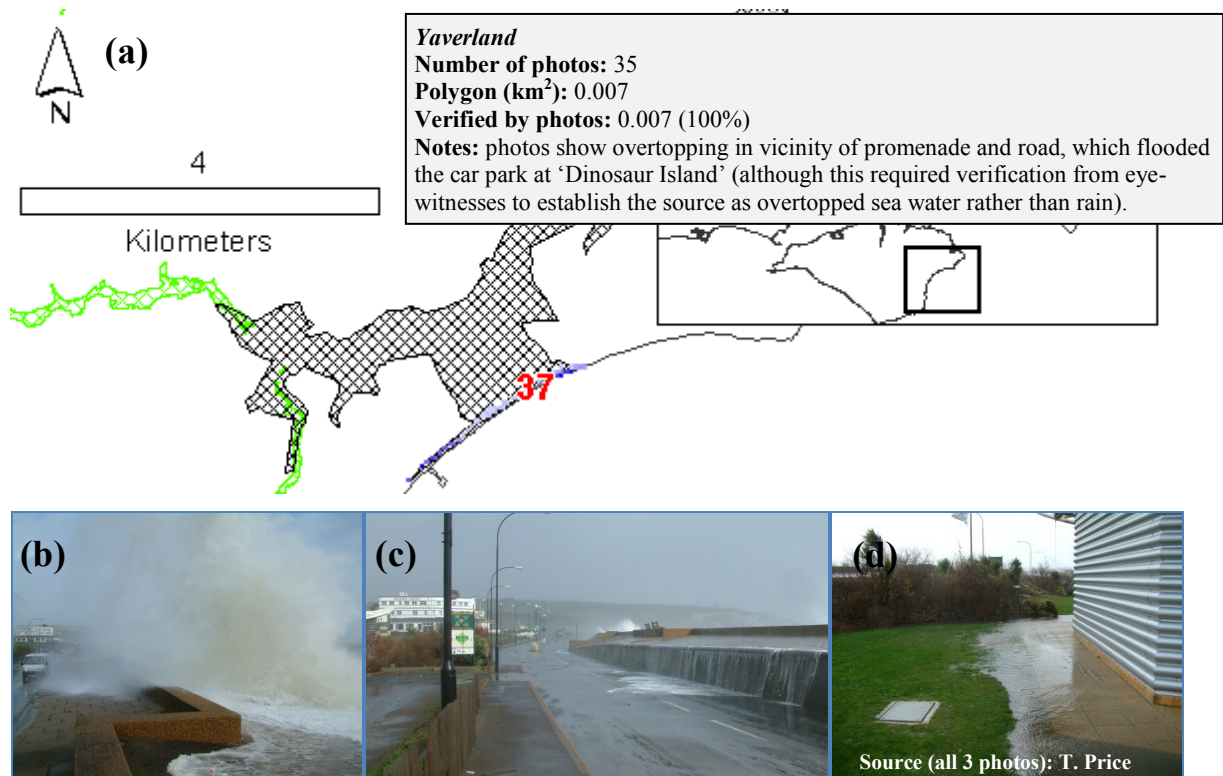


Figure D9. (a) Map showing floodplain, event simulation, and metadata summary, (b) waves overtopping at Location 35 (Yaverland), which caused (c) water to flow across the road, and then (d) accumulate around a building ('Dinosaur Island')

Appendix E – Wave Overtopping

As noted in Chapter 6, hypothetical simulations were used to assess whether coastal flooding can occur during more severe than previously seen still water level conditions. The empirical formulae incorporated the relationship between overtopping and flooding, and the validation analyses (Chapter 5) verified the fundamental method. However, in addition, a relatively straightforward rule by FEMA (2007) in flood hazard mapping guidelines describes a relationship between the freeboard (between SWL and crest), significant wave heights (H_s), and significant overtopping events – and portrays the variability expected as a function of structure slope.

Applied to loads and structures in the Solent, this relationship was found to be commensurate with predictions from high overtopping generated by EurOtop formulae and flood event simulations. For example as highlighted in Tables E1a and E1b, the onset of ‘waveform’ overtopping (and hence volumes likely to cause flooding) at the two detailed case studies is indicated as likely at extreme present day water levels, whilst less likely for the 10 March 2008.

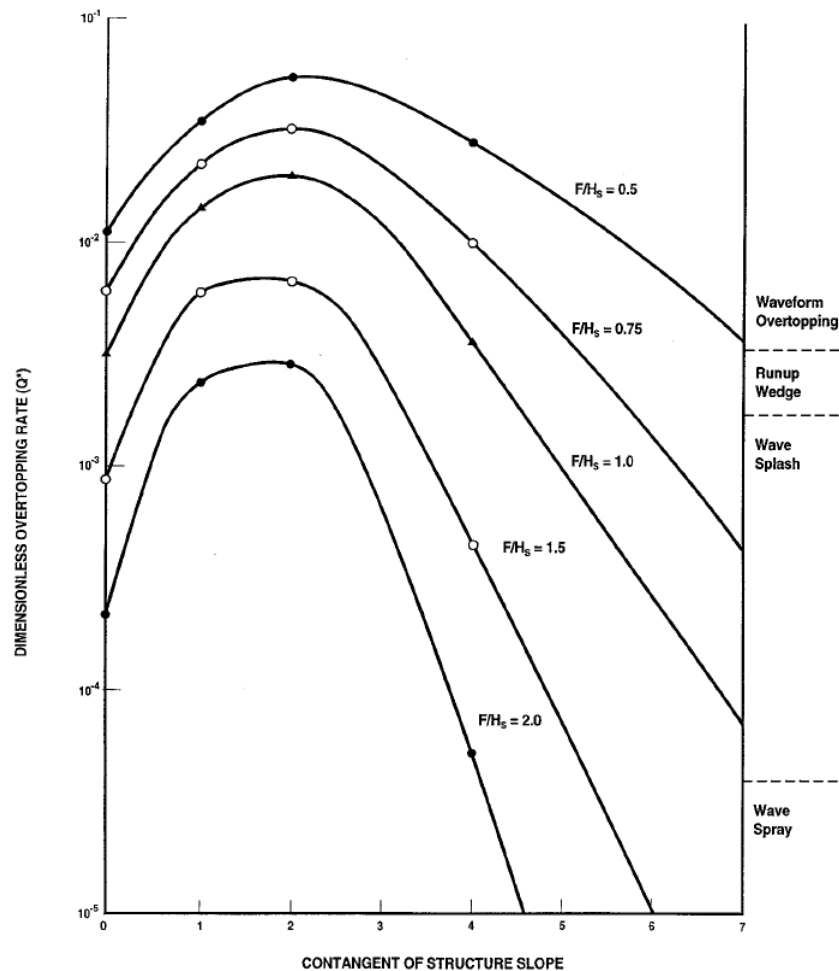


Figure E1. Schematic summary of storm-wave overtopping at structures of various slopes and freeboards (source: FEMA, 2007)

Table E1(a) A typical situation at east Pennington (crest heights in the region 3 mODN, and fetch-limited wave reach 1-2 m) and **(b)** Southsea, Portsmouth (crest heights in the region 4 mODN, fetch-limited wave reach 1-2 m)

Crest = 3mODN				
SWL (mODN)	Rc	Hs=1m	Hs=2m	
		Rc/Hs	Rc/Hs	
2.0	1.0	1.0	0.5	Approx. 10 March 2008 SWL
2.1	0.9	0.9	0.5	
2.2	0.8	0.8	0.4	
2.3	0.7	0.7	0.4	Approx. 1 in 200 SWL
2.4	0.6	0.6	0.3	
2.5	0.5	0.5	0.3	
2.6	0.4	0.4	0.2	
2.7	0.3	0.3	0.2	
2.8	0.2	0.2	0.1	
2.9	0.1	0.1	0.1	
3.0	0.0	0.0	0.0	
3.1	-0.1	-0.1	-0.1	
3.2	-0.2	-0.2	-0.1	
3.3	-0.3	-0.3	-0.2	

Crest = 4mODN				
SWL (mODN)	Rc	Hs=1m	Hs=2m	
		Rc/Hs	Rc/Hs	
2.0	2.0	2.0	1.0	
2.1	1.9	1.9	1.0	
2.2	1.8	1.8	0.9	
2.3	1.7	1.7	0.9	
2.4	1.6	1.6	0.8	
2.5	1.5	1.5	0.8	
2.6	1.4	1.4	0.7	Approx. 10 March 2008 SWL
2.7	1.3	1.3	0.7	
2.8	1.2	1.2	0.6	
2.9	1.1	1.1	0.6	Approx. 1 in 200 SWL
3.0	1.0	1.0	0.5	
3.1	0.9	0.9	0.5	
3.2	0.8	0.8	0.4	
3.3	0.7	0.7	0.4	